“Altered cell surface glycosylation and organ specific metastasis”

By
Shyam Kailashrao More
(LIFE09201004004)

Tata Memorial Centre
Mumbai

A thesis submitted to the
Board of Studies in Life Sciences
In partial fulfillment of requirements
for the Degree of

DOCTOR OF PHILOSOPHY
of
HOMI BHABHA NATIONAL INSTITUTE

September, 2016

Homi Bhabha National Institute

Recommendations of the Viva Voce Committee

As members of the Viva Voce Committee, we certify that we have read the dissertation prepared by Mr. Shyam Kailashrao More entitled "Altered cell surface glycosylation and organ specific metastasis" and recommend that it may be accepted as fulfilling the thesis requirement for the award of Degree of Doctor of Philosophy.

S. N. Dalal — 27/9/16

Chairman – Dr. Sorab N. Dalal — Date:

S. V. Chiplunkar — 27/9/2016

Guide/Convener – Dr. Shubhada V. Chiplunkar — Date:

M. V. Vaidya — 27/09/2016

Member 1 – Dr. Milind Vaidya — Date:

Rukmini Govekar — 27/09/16

Member 2 – Dr. Rukmini Govekar — Date:

Neeta Singh. — 27-9-16

External Examiner – Dr. Neeta Singh — Date:

Final approval and acceptance of this thesis is contingent upon the candidate's submission of the final copies of the thesis to HBNI.

I/We hereby certify that I/we have read this thesis prepared under my/our direction and recommend that it may be accepted as fulfilling the thesis requirement.

Date: 27/09/2016
Place: Navi Mumbai

S. V. Chiplunkar 27/9/16

Dr. Shubhada V. Chiplunkar
Guide

STATEMENT BY AUTHOR

This dissertation has been submitted in partial fulfillment of requirements for an advanced degree at Homi Bhabha National Institute (HBNI) and is deposited in the library to be made available to borrowers under rules of the HBNI.

Brief quotations from this dissertation are allowable without special permission, provided that accurate acknowledgement of source is made. Requests for permission for extended quotation from or reproduction of this manuscript in whole or in part may be granted by the Competent Authority of HBNI when in his or her judgment, the proposed use of the material is in the interests of scholarship. In all the other instances, however, permission must be obtained from the author.

Navi Mumbai

Date: 27/09/2016 Shyam Kailashrao More

DECLARATION

I, hereby declare that the investigation presented in the thesis has been carried out by me. The work is original and has not been submitted earlier as a whole or in part for a degree/diploma at this or any other Institution or University.

Navi Mumbai

Date: 27/09/2016 Shyam Kailashrao More

LIST OF PUBLICATIONS ARISING FROM THE THESIS

Journal

1) **S.K. More**, S.V. Chiplunkar, R.D. Kalraiya, *Galectin-3 induced cell spreading and motility relies on distinct signaling mechanisms compared to fibronectin,* Molecular and Cellular Biochemistry, 416(2016)179-91.
2) **S.K. More**[*], N. Srinivasan[*], S. Budnar, S.M. Bane, A. Upadhya, R.A. Thorat, A.D. Ingle, S.V. Chiplunkar, R.D. Kalraiya, *N-glycans and metastasis in galectin-3 transgenic mice*, Biochemical and biophysical research communications, 460 (2015) 302-307 (*Equal Contribution).
3) A.K. Agarwal, N. Srinivasan, R. Godbole, **S.K. More**, S. Budnar, R.P. Gude, R.D. Kalraiya, *Role of tumor cell surface lysosome-associated membrane protein 1 (LAMP1) and its associated carbohydrates in lung metastasis*, Journal of cancer research and clinical oncology, 141(9) (2015) 1563-74.
4) M.C. Dange[*], N. Srinivasan[*], **S.K. More**, S.M. Bane, A. Upadhya, A.D. Ingle, R.P. Gude, R. Mukhopadhyaya, R.D. Kalraiya, *Galectin-3 expressed on different lung compartments promotes organ specific metastasis by facilitating arrest, extravasation and organ colonization via high affinity ligands on melanoma cells*, Clinical & experimental metastasis, 31 (2014) 661-673 (*Equal Contribution).

Conferences (Abstracts published)

1) Galectin-3 mediated cell spreading and movement utilizes distinct molecular mechanisms compared to those used on fibronectin. S.K. More, R.D. Kalraiya, Journal of Carcinogenesis 2015.

Presentation at conferences

1) Presented poster titled Galectin-3 mediated cell spreading and movement utilizes distinct molecular mechanisms compared to those used on fibronectin in "*Molecular Pathways to Therapeutics: Paradigms and Challenges in Oncology*", Carcinogenesis 2015, International conference organized by Carcinogenesis Foundation, USA and TMC-ACTREC, India on Feb-2015, TMC-ACTREC, Navi Mumbai.
2) Presented poster titled Identification of galectin-3 binding proteins carrying poly-*N*-acetyllactosamine (polyLacNAc) substituted β1, 6 branched N-oligosaccharides on melanoma cells to elucidate their role in lung specific metastasis in National Conference on "*Glycobiology of Cancer; Lectins as tools and Targets*", Nov 2013, Karnatak University.
3) Presented poster titled Galectin-3 on the lungs and melanoma metastasis in National Conference on "*Glycobiology of Cancer; Lectins as tools and Targets*", Nov 2013, Karnatak University.

Navi Mumbai

Date: 27/09/2016 Shyam Kailashrao More

Dedicated to

My Parents

ACKNOWLEDGEMENTS

I would like to acknowledge Late Dr. Rajiv D. Kalraiya who was my former PhD guide, for giving me an opportunity to join his lab and work on one of the most interesting project in the lab. His expertise in the scientific research helped me to achieve my scientific goal. I am very grateful to Dr. Shubhada V. Chiplunkar who is my current PhD guide. Because of her support and valuable suggestions, it is possible to me to communicate the second paper, got the acceptance on the day of thesis submission and to write the entire thesis in stipulated time period. I am very thankful to Dr. Robin Mukhopadhya who was always there for me for any problem related to writing the synopsis and thesis corrections.

I am very thankful to the ACTREC Director Dr. Shubhada V. Chiplunkar, and Deputy Director Dr. Sudip Gupta for infrastructure and facilities.

I am very thankful to the Doctoral committee (DC) members: Dr. Shubhada V. Chiplunkar (former chairperson), Dr. Sorab N. Dalal (former DC member and current chairperson), Dr. Robin Mukhopadhya, Dr. Rajiv P. Gude (former DC members), Dr. Rukmini Govekar and Dr. Millind M. Vaidya (current DC members) for their timely valuable suggestions and comments which helped me to complete my objectives of thesis project.

I would like to thank ACTREC Principal Investigators Dr. Tanuja Teni (Office-In-Charge of Kalraiya lab), Dr. Sorab Dalal and Dr. Milind M. Vaidya for their help and support.

I am extremely thankful to common instrument facilities of ACTREC especially Microscopy facility: Vaishali, Tanuja and Jairaj; Genomics, proteomics and flow cytometry.

I am very thankful to Kalraiya lab members; Students: Venu, Nithya, Srikanth, Amit, Akhil, Manohar, Poonam, Rajeshri, Preeti, Rashmi, Zenab, Azhar, Anupama, Suhas, Shivkumar,; Staff: Sanjay Bane, D. S. Chavan, Anand Pawar, Prema mam and Poonam mam; Trainees: Shruti, Shreya, Parnika, Mitan, Abdul, Urjita, Khushbu, Nikhil, Sanika who helped me in one or more way during my PhD work and making Kalraiya lab environment cheerful.

I would like to thank ACTREC students, Student Council of ACTREC (SCA) and especially Batchmates – 2010 who supported me during all the time in the Institute.

I am very thankful to CSIR for fellowship and Homi Bhabha National Institute (HBNI).

Finally, I am very grateful to my parents who always supported and encouraged me. I am very thankful to my elder brother Kishor and his wife Anuja for being kind with me and nephews Asawari and little Raghav for the fun. I am very thankful to my wife Amruta who is with me all the time.

Thank you everyone *Shyam Kailashrao More*

CONTENTS

Page No.

Homi Bhabha National Institute

Ph. D. PROGRAMME

1. Name of the Student:	Shyam Kailashrao More
2. Name of the Constituent Institution:	Tata Memorial Centre**,** Advanced Centre for Treatment, Research and Education in Cancer
3. Enrolment No. :	LIFE09201004004
4. Title of the Thesis:	**"**Altered cell surface glycosylation and organ specific metastasis"
5. Board of Studies:	Life Sciences

SYNOPSIS

Introduction

Cancer is a group of diseases which leads to abnormal growth of cells. The high death rate in cancer patients is due to metastasis, which is still poorly understood because of its complexity and multistep nature. Dissemination of cells from primary tumor to secondary non-contagious sites is called metastasis. To successfully colonize at secondary sites, a cancer cell must complete a series of sequential steps. These steps typically include detachment from the primary tumor, invasion through surrounding tissues and basement membranes, entry and survival in the circulation and arrest & establishment in a distant target organ [1].

Tumor cells show several cell surface modifications associated with metastatic phenotype, including changes in cell surface glycosylation. One of the frequently observed modifications is altered expression of β1, 6 branched N-oligosaccharides on cell surface glycoproteins [2,3]. These oligosaccharides have been strongly associated with invasive and metastatic phenotype of tumor cells. Another interesting feature of these oligosaccharides is that majority of the cell lines expressing them metastasize to either lungs or to liver [4].

Previous work in this lab has shown that poly-*N*-acetyllactosamine (polyLacNAc) substituted β1, 6 branched N-oligosaccharides, expressed on B16F10 (a murine lung metastatic cell line) cells, promote lung specific metastasis via galectin-3, which is expressed in highest amounts on the lungs. Galectin-3/polyLacNAc interaction promotes adhesion to vascular endothelium, spreading, degradation of vascular basement membrane and movement into organ parenchyma. Inhibition of these oligosaccharides by down regulating enzymes responsible for polyLacNAc substitutions inhibited all these processes and metastasis [5,6,7].

In order to investigate the role of galectin-3, it is also important to know galectin-3 binding proteins. Mass spectrometric screen was performed to find out galectin-3 binding proteins. It was found that along with many other cell surface glycoproteins, CD147 is a major carrier of β1, 6 branched N-oligosaccharides. It is reported that glycol-deficient CD147 fails to induce matrix metalloproteases by tumor cells [8,9]. It is interesting to study the role of CD147 and its glycosylation in galectin-3 mediated metastatic processes of B16F10 cells.

Galectin-3 is a nucleo-cytoplasmic protein which is secreted out in a non-classical manner and often gets incorporated into the extracellular matrix (ECM) and basement membrane (BM). It is a member of large family of galactose binding lectins and polyLacNAc on N-glycans and Thomson Freudenreich (TF) antigens present in large number on mucinous proteins have been shown to

serve as ligands. As a result galectin-3 influences functions of myriad classes of cell surface receptors/glycoproteins. The functions of galectin-3 are largely dependent on its sub-cellular localization. Galectin-3 has been shown to regulate cellular motility in many different ways. The secreted extracellular galectin-3 exerts its cellular effects on motility related processes both in soluble form and as immobilized component on cells, ECM and BM [10,11]. However, it is not clear how immobilized galectin-3 promotes such complex cellular processes. The present study aims to investigate the following;

Key Questions

- How crucial is the galectin-3/polyLacNAc interaction for lung metastasis?
- What is the precise role of carriers of β1, 6 branched N-glycoproteins during metastatic progression?
- Which of the signaling pathways regulate galectin-3 induced cell adhesion, spreading and motility?

Objectives

The following objectives were proposed to answer these questions:

1. To confirm the role of galectin-3 on the lungs in organ specific metastasis
2. Role of CD147, a carrier of β1,6 branched N-oligosaccharides, in metastasis
3. To investigate the role of galectin-3 in processes like adhesion, spreading and movement critical for metastasis

Methodology

Cell culture

B16F1 and B16F10 murine melanoma cells were routinely cultured in DMEM containing 10% serum at 37^{o}C with 5% CO_2.

Preparation of modified citrus pectin (MCP) from citrus pectin (CP)

MCP powder was prepared from CP as exactly described in Ref. [12]

Expression and purification of recombinant human (rh) galectin-3

Purification of galectin-3 was carried out using *E. coli* BL star 21 containing pET3c plasmid coding for rh galectin-3 [7]. The expression of galectin-3 was induced by IPTG and purified by using Lactose-Sepharose column.

Cloning, expression and purification of human and mouse truncated galectin-3 (htGal-3 and mtGal-3)

Coding DNA sequence (CDS) of C-terminal carbohydrate recognition domain (CRD) of galectin-3 (human and mouse origin) was cloned into pET3a bacterial expression vector. These constructs were transformed into *E. coli BL21 (DE3)* and expression of ht and mtGal-3 was induced by IPTG. The tGal-3 protein was purified using Lactose-Sepharose column.

Experimental metastasis assay

B16F10 cells ($0.1x10^6$) treated with tGal-3 were pre-incubated with 0.1 ml of 500 µg/ml of tGal-3 for 1 h on ice. Mice that received these pre-treated cells also received injections of tGal-3 (250 µg in 0.1 ml, via intra muscular injection) on day 1 (2 h before and after injection of cells) and once on day 2. This experiment was done with ht and mtGal-3. In another set, B16F10 cells treated with MCP, B16F10 cells ($0.1x10^6$) were resuspended in medium with and without MCP (0.05%). Mice which received cells with MCP were kept on drinking water containing 1.5% MCP that was started 5 days prior to injection till the day of sacrifice. On day 17^{th} mice were sacrificed, lungs were collected and colonies were counted.

Generation of bone marrow chimeric mice

The bone marrow of irradiated gal-$3^{-/-}$ (null) mice was replaced with that from gal-$3^{-/-}$ mice which served as control (Group 1). Bone marrow of irradiated galectin-$3^{-/-}$ mice was replaced with that from gal-$3^{+/+}$ (wild-type) mice (Group 2). Chimerism was confirmed by genotyping of these mice using tail and blood genomic DNA by PCR. Experimental metastasis assay was performed using B16F10 cells in these chimeric mice.

Cloning and expression of wild type and glyco-deficient CD147 in B16F10 cells

CDS of CD147 was successfully cloned into the pmGFPN1 vector. Five glycosylation sites in CD147 were independently (N44Q, N154Q, N159Q, N190Q and N193Q) and in combinations (N44,154,159,190,193Q-Glyco-deficient (GM); N44,154,190Q-Typical glycomutant (TGM) present on consensus sequence N-X-S/T, X= any amino acid except proline; N159,193Q Atypical glycomutant (ATGM) present on non-consensus sequence) was mutated from aspargine (N) to glutamine (Q) by site directed mutagenesis. Wild type (Wt) and all CD147 glycomutants were transfected in B16F10 cells and expressed as a fusion protein with green fluorescent protein (GFP) and its localization were analysed using confocal microscopy.

Cell spreading assay

B16F10 cells ($0.5x10^6$) were seeded on galectin-3 and fibronectin coated coverslips in serum free medium and incubated for 15, 30, 45 and 60 minutes. Adhered cells were fixed with paraformaldehyde and permeabilized with Triton X-100. Phalloidin-TRITC was used for F-actin (Filamentous actin) staining and DAPI for staining nuclei. The images of stained cells were acquired by confocal microscopy.

Treatment with pharmacological inhibitor

For studying cell spreading and activation of Akt and Erk, B16F10 cells were pre-incubated with pharmacological inhibitor wortmannin (Wm) and PD98059 (PD) for 1 hour. In case of wound

healing assay, treatment was for 2 hour. The concentrations were 500 nM Wm or 25 µm PD in 0.1% DMSO. Cells incubated in 0.1% DMSO served as a vehicle control (VC). Later cells were harvested to perform cell spreading assay and activation of Akt and Erk. In wound healing assays after treatment wound was made and cell migration was monitored.

Live cell imaging and Fluorescence recovery after photobleaching (FRAP)

B16F10 cell line expressing green fluorescent actin (GFP-Actin) was successfully generated. These cells were seeded on glass bottom culture dishes either coated with galectin-3 and fibronectin in serum free DMEM devoid of phenol red. Live cell imaging was performed for 1 hour using spinning disc microscope at 60x magnification. To measure actin turnover in the lamellipodial region of these cells FRAP experiments were performed. Cells were seeded on glass bottom tissue culture dishes either coated with galectin-3 or fibronectin in serum free DMEM devoid of phenol red. After incubating for 4 hours lamellipodial region was bleached and recovery was traced using confocal microscopy.

Preparation of cell lysates and Immunoblotting

The 24 hour serum starved cells were harvested and seeded on galectin-3 or fibronectin coated plates for 15, 30 and 60 min time interval. At respective time points, non-adherent cells in each plate were removed and lysis buffer was added to prepare cell lysate. Cells lysed at 0 min time point served as control. Equal amount of protein in each cell lysate was loaded on SDS-PAGE, transferred on PVDF and immunoblotted using anti- Akt, pAkt, Erk and pErk antibodies.

Rac1 activation assay

Glutathione-Sepharose beads conjugated with GST-PAK1 were used for pull-down of activated GTP coupled Rac1. For Rac1 activation assay, cell lysate was prepared as exactly described in above section. Equal amount of Sepharose-PAK1 beads were incubated with 2 mg protein cell

lysates at each time point on rocker for 1 h at 4^{o}C. Beads were washed and bound protein was eluted using 4x Lamelli buffer at 100^{o}C for 10 min. Western blotted total cell lysates and respective PAK1 bound proteins were analysed using anti-Rac1 antibody.

Wound healing assay

Wound healing assays were performed on galectin-3 or fibronectin coated plates. Non-specific sites on the plates were blocked with 2% BSA. Uncoated culture dishes, blocked only with BSA served as control. Melanoma cells were seeded on coated plates incubated at 37^{o}C for 24 hours in a CO_2 incubator. The cells were washed free of serum and grown under serum free conditions for 24 hours for cell synchronization. A straight, uniform wound was made and wound closure of cells was measured for 16 hours by time lapse video imaging.

Results

***Objective 1*: To confirm the role of galectin-3 on the lungs in organ specific metastasis**

a) Effect of competitive inhibitor modified citrus pectin (MCP) on metastatic processes

MCP powder was in the form of shorter, non-branched, galactose-rich, carbohydrate chains. These shorter chains dissolve more readily in water and are better absorbed and utilized by the body than ordinary, long-chain pectin. It is believed that shorter polysaccharide units afford MCP its ability to access and bind tightly to galectin-3. Inhibitory effect of MCP was observed in vitro on cell spreading of B16F10 cells on galectin-3. In presence of MCP, metastatic lung colonies of B16F10 cells were decreased in experimental mice.

b) Cloning, expression and purification of htGal-3 and mtGal-3 and its effect on metastatic processes

CRD of human galectin-3 was successfully cloned, expressed and purified by using Lactose-Sepharose column. The purity and identity was confirmed by coomassiae brilliant blue (CBB)

staining and mass spectroscopy (MS) respectively. As truncated galectin-3 (only CRD) is devoid of N-terminal oligomerization domain, it is not able to form galectin-3 lattice on cell membrane. B16F10 cells incubated with htgal-3 showed reduced spreading on galectin-3 and even significantly reduced metastatic colonies on the lungs of mice.

Human galectin-3 CRD shares 87% identity with mouse galectin-3 CRD. In order to rule out possibility that htGal-3 may generate antibody response in mice which may block its function, CRD of mouse galectin-3 to be used in these experiments. It was cloned, expressed and purified using Lactose-Sepharose column. Purity and identity was confirmed by SDS-PAGE CBB staining and MS respectively. Results obtained with mtGal-3 were comparable to htGal-3.

c) Experimental metastasis assay in galectin-3 transgenic and bone marrow chimeric mice

Galectin-3 knockout mice were used to prove that polyLacNAc on tumor cells indeed brings about these effects via galectin-3. It was shown using galectin-3 transgenic mice that decreased metastasis of B16F10 cells correlates with galectin-3 expression on the lungs in galectin-$3^{+/+}$ and galectin-$3^{+/-}$ (hemizygous) mice. However, galectin-$3^{-/-}$ mice showed comparable number of colonies to galectin-$3^{+/+}$ mice. Even after inhibition of sugars on B16F10 cells, metastasis was observed in galectin-$3^{-/-}$ mice. It could be because of compromised immune status in these mice, as galectin-3 regulates several immune functions. However, generation of chimeric mice by replacing the bone marrow in galectin-$3^{-/-}$ mice with that from galectin-$3^{+/+}$ mice did not have any effect on B16F10 melanoma metastasis. This points towards the possibility that galectin-3 is involved even during immune cell maturation.

<u>Objective 2</u>: Role of CD147, a carrier of ß1, 6 branched N-oligosaccharides, in metastasis

a) CD147 Glycomutant failed to express on the cell surface

Wt CD147 and GM CD147 were transfected in the B16F10 cells using lipofectamine. It was observed that Wt CD147 localizes on the cell membrane while GM CD147 was localized in the cytoplasm. It suggests that glycosylation plays important role in the localization and targeting of CD147 to the cell membrane.

b) N154, N190 and N193 are the critical glycosylation sites on CD147 for its targeting to the cell surface

TGM and ATGM CD147 were generated and expressed in B16F10 cells using lipofectamine. It was found that both CD147 mutants show cytoplasmic localization. Finally all the five glycosylation sites in CD147 were independently mutated and expressed in B16F10 cells. N154Q, N190Q and N193Q CD147 mutants accumulated inside the cell cytoplasm while N44Q, N159Q CD147 glycomutant showed cell surface localization. Wild type CD147 was expressed on the cell surface while CD147 deficient with all glycosylation sites accumulated in the cytoplasm. Under these conditions it was not possible to investigate the functions of glyco-deficient CD147 as these were not seen on the membrane.

<u>Objective 3</u>: To investigate the role of galectin-3 in processes like adhesion, spreading, and movement critical for metastasis

a) B16F10 cells show distinct cytoskeletal organization, spreading kinetics and actin dynamics when allowed to spread on galectin-3 as compared to fibronectin

The cell spreading on fibronectin showed stellate morphology with abundant stress fibers traversing across the cell body. Galectin-3 induced cell spreading showed rounded morphology and intensity of actin bundles are more along the periphery of the cells. These differences are also reflected during motility of cells on galectin-3 and fibronectin.

Cell spreading kinetics using fixed cell imaging showed that B16F10 cells on immobilized galectin-3 show frill-like lamellipodial morphology even at initial (15 min) time point. Lamellipodial structures at 15 min time point in cells plated on fibronectin were very different in appearance to those seen on galectin-3, which progressively increases with time up to 60 min. Live cell imaging with stable B16F10 cells expressing GFP-Actin showed that lamellipodial dynamics in cells plated on galectin-3 is very high as compared to cells plated on fibronectin. Actin dynamics in the lamellipodial region was assessed using FRAP in B16F10 cells expressing GFP-Actin spread on immobilized galectin-3 was significantly higher (68% recovery) as compared to cells spread on fibronectin (55% recovery).

b) Akt phosphorylation is inversely regulated while Erk is positively regulated in cells spread on galectin-3 and fibronectin

In order to investigate the signalling pathways induced by galectin-3 and fibronectin, time dependent activation of Akt and Erk was studied. Increase in Akt phosphorylation was observed in cells plated on galectin-3 while inverse correlation was observed in case of cells plated on fibronectin in a time dependent manner. Phosphoryation of Akt could be completely abrogated by wortmannin in cells spread on both galectin-3 and fibronectin, however, PD98059 had no effect on Akt phosphorylation. Comparison of Erk phosphorylation in cells spread on galectin-3 and fibronectin showed that there is a time dependent decrease in phosphorylation of Erk in both. Treatment with wortmannin only partially affected Erk phosphorylation in cells spread on galectin-3 as well as fibronectin while PD98059 completely inhibited phosphorylation of Erk in these cells. These differences in regulation of signalling pathways in cells plated on substrates like galectin-3 and fibronectin could be because of activation through different cell surface receptors, which in turn ultimately modulate RhoGTPases, especially Rac1.

c) Rac1 activation is inversely regulated in cells spread on galectin-3 and fibronectin

The levels of activated Rac1 assessed in cells plated on galectin-3 was highest at 15 min time point, which gradually decreased with time up to 60 min. However, in case of cells spread on fibronectin it was reversed. Activated Rac1 levels were lowest at 15 min and kept increasing with time, highest being at 60 min. Activation pattern of Rac1 appears to correlate with their time dependent spreading and lamellipodial organization on these substrates. Activation of Rac1 inversely correlated with activation of Akt on both substrates.

d) Inhibitors of Akt and Erk pathway inhibit cellular spreading and migration on galectin-3 but have no effect on fibronectin

Cell spreading and wound healing assays results showed that as compared to untreated cells, the cells treated with wortmanin and PD98059 significantly inhibit spreading and migration of cells on galectin-3 coated plates, whereas, treatment of cells with these inhibitors marginally affect the spreading and movement of cells on fibronectin. The results suggest that distinct signalling mechanisms dictate the microfilament organization, formation of lamellipodial structures, spreading and movement of cells on galectin-3 and fibronectin.

Summary and Conclusion

The role of galectin-3/polyLacNAc interaction in lung specific metastasis was strengthened or proved by using competitive and dominant negative inhibitors, MCP and truncated galectin-3 respectively. It was established that this interaction is indeed important for lung specific metastasis by using galectin-3 transgenic mice (galectin-$3^{+/-}$ mice). Surprisingly the reversal of metastasis in galectin-$3^{-/-}$ mice possibly suggests compromised status of host anti-tumor immunity in these mice. The glycosylation sites on galectin-3 binding protein CD147, required for its targeting to the cell membrane, were identified. The present study successfully dissected the molecular mechanisms

involved in galectin-3 mediated cellular spreading and motility. It demonstrates that the dynamics and organization of lamellipodial structures and signalling events on galectin-3 are very distinct as compared to those observed on very well studied extracellular matrix component such as fibronectin.

References

[1] G.P. Gupta, J. Massague, Cancer metastasis: building a framework, Cell 127 (2006) 679-695.

[2] S. Hakomori, Tumor malignancy defined by aberrant glycosylation and sphingo(glyco)lipid metabolism, Cancer Res 56 (1996) 5309-5318.

[3] H. Ponta, J. Sleeman, P. Herrlich, Tumor metastasis formation: cell-surface proteins confer metastasis-promoting or -suppressing properties, Biochim Biophys Acta 1198 (1994) 1-10.

[4] J.W. Dennis, M. Granovsky, C.E. Warren, Glycoprotein glycosylation and cancer progression, Biochim Biophys Acta 1473 (1999) 21-34.

[5] M.C. Dange, N. Srinivasan, S.K. More, S.M. Bane, A. Upadhya, A.D. Ingle, R.P. Gude, R. Mukhopadhyaya, R.D. Kalraiya, Galectin-3 expressed on different lung compartments promotes organ specific metastasis by facilitating arrest, extravasation and organ colonization via high affinity ligands on melanoma cells, Clin Exp Metastasis 31 (2014) 661-673.

[6] V. Krishnan, S.M. Bane, P.D. Kawle, K.N. Naresh, R.D. Kalraiya, Altered melanoma cell surface glycosylation mediates organ specific adhesion and metastasis via lectin receptors on the lung vascular endothelium, Clin Exp Metastasis 22 (2005) 11-24.

[7] N. Srinivasan, S.M. Bane, S.D. Ahire, A.D. Ingle, R.D. Kalraiya, Poly N-acetyllactosamine substitutions on N- and not O-oligosaccharides or Thomsen-Friedenreich antigen facilitate lung specific metastasis of melanoma cells via galectin-3, Glycoconj J 26 (2009) 445-456.

[8] Y. Bai, W. Huang, L.T. Ma, J.L. Jiang, Z.N. Chen, Importance of N-glycosylation on CD147 for its biological functions, Int J Mol Sci 15 (2014) 6356-6377.

[9] L. Xiong, C.K. Edwards, 3rd, L. Zhou, The biological function and clinical utilization of CD147 in human diseases: a review of the current scientific literature, Int J Mol Sci 15 (2014) 17411-17441.

[10] J. Dumic, S. Dabelic, M. Flogel, Galectin-3: an open-ended story, Biochim Biophys Acta 1760 (2006) 616-635.

[11] A. Fortuna-Costa, A.M. Gomes, E.O. Kozlowski, M.P. Stelling, M.S. Pavao, Extracellular galectin-3 in tumor progression and metastasis, Front Oncol 4 (2014) 138.

[12] P. Nangia-Makker, V. Hogan, Y. Honjo, S. Baccarini, L. Tait, R. Bresalier, A. Raz, Inhibition of human cancer cell growth and metastasis in nude mice by oral intake of modified citrus pectin, J Natl Cancer Inst 94 (2002) 1854-1862.

Publications in Refereed Journal

a) Published manuscripts

- **S.K. More**, N. Srinivasan, S. Budnar, S.M. Bane, A. Upadhya, R.A. Thorat, A.D. Ingle, S.V. Chiplunkar, R.D. Kalraiya, N-glycans and metastasis in galectin-3 transgenic mice, Biochemical and Biophysical Research Communications, 460 (2015) 302-307.
- A.K. Agarwal, N. Srinivasan, R. Godbole, **S.K. More**, S. Budnar, R.P. Gude, R.D. Kalraiya, Role of tumor cell surface lysosome-associated membrane protein-1 (LAMP1) and its associated carbohydrates in lung metastasis, Journal of Cancer Research and Clinical Oncology, 141 (2015) 1563-74.
- M.C. Dange, N. Srinivasan, **S.K. More**, S.M. Bane, A. Upadhya, A.D. Ingle, R.P. Gude, R. Mukhopadhyaya, R.D. Kalraiya, Galectin-3 expressed on different lung compartments promotes organ specific metastasis by facilitating arrest, extravasation and organ colonization via high affinity ligands on melanoma cells, Clinical & Experimental Metastasis, 31 (2014) 661-673.

b) Communicated Manuscript

- **S.K. More**, R.D. Kalraiya, S.V. Chiplunkar, Galectin-3 mediated cell spreading and movement utilizes distinct molecular mechanisms compared to that on fibronectin (Molecular and Cellular Biochemistry, Under Review).

c) Manuscripts in preparation

- M.C. Dange, H.S. Bhonsle, R.K. Godbole, **S.K. More**, S.M. Bane, M.J. Kulkarni, R.D. Kalraiya, Identification of galectin-3 receptors carrying poly-*N*-acetyllactosamine substituted β1, 6 branched N-glycans involved in lung specific metastasis by mass spectrometry.

d) Other Publications / Conference Presentations

- "*Molecular Pathways to Therapeutics: Paradigms and Challenges in Oncology*", Carcinogenesis 2015, International conference organized by Carcinogenesis Foundation, USA and TMC-ACTREC, India on Feb-2015, TMC-ACTREC, Navi Mumbai. S.K. More et al, Galectin-3 mediated cell spreading and movement utilizes distinct molecular mechanisms compared to those used on fibronectin.
  Abstract published in "Journal of Carcinogenesis 2015, Abstract No. S65, Page No. S36S.K. More, R.D. Kalraiya".
- National Conference on "*Glycobiology of Cancer; Lectins as tools and Targets*", Nov 2013, Karnatak University, India, S.K. More et al, Identification of galectin-3 binding proteins carrying poly-*N*-acetyllactosamine (polyLacNAc) substituted β1, 6 branched N-oligosaccharides on melanoma cells to elucidate their role in lung specific metastasis.

Signature of Student: Skmore

Date: 11/1/2016

Doctoral Committee:

S. No.	Name	Designation	Signature	Date
1	Dr. S. N. Dalal	Chairperson	S.N Dalal	12/1/2016
2	Dr. S. V. Chiplunkar	Guide/Convener	S.Chiplunkar	18/1/2016
3	Dr. Rukmini Govekar	Member		12/01/2016
4	Dr. M. M. Vaidya	Member	M M Vaidya	12/01/2016

Forwarded through:

S.Chiplunkar 18/1/16

Dr. S.V. Chiplunkar
Director, ACTREC
Chairperson,
Academics and Training Program,
ACTREC

Dr. S. V. Chiplunkar
Director
Advanced Centre for Treatment, Research & Education in Cancer (ACTREC)
Tata Memorial Centre
Kharghar, Navi Mumbai 410210.

Prof. K. Sharma
Director, Academics,
Tata Memorial Centre

PROF. K. S. SHARMA
DIRECTOR (ACADEMICS)
TATA MEMORIAL CENTRE,
PAREL, MUMBAI

LIST OF ILLUSTRATIONS

LIST OF FIGURES

LIST OF TABLES

Chapter 1

Introduction

The high death rate in cancer patients is due to metastasis. However, it is poorly understood because of its complexity and multistep nature. Dissemination of cells from primary tumor to secondary non-contagious site is called metastasis. Metastasis is essential phenomenon in pathogenesis of cancer. To successfully colonize at secondary site a cancer cell must complete a sequential series of steps. Cell surface molecules and its associated post-translational modification play a crucial role in all the steps of metastatic cascade. One of the frequently observed modifications is the altered expression of β1, 6 branched N-oligosaccharides on cell surface glycoproteins. These oligosaccharides have been strongly associated with the invasive and metastatic phenotype of tumor cells. Another interesting feature of these oligosaccharides is that majority of the cell lines expressing them metastasize either to lungs or liver.

Previous work from our laboratory has shown that poly-*N*-acetyllactosamine (polyLacNAc) substituted β1, 6 branched N-oligosaccharides expressed on B16F10 cells promote lung specific metastasis via galectin-3, which is expressed in highest amounts on the lungs [6]. Galectin-3 is a nucleo-cytoplasmic protein that is secreted out in a non-classical manner and often gets incorporated onto the cell surface, extracellular matrix (ECM) and basement membrane (BM) [10]. It was shown to be expressed on almost all the compartments of the lungs and constitutively on the surface of vascular endothelium. Galectin-3/polyLacNAc interaction forms first adhesive anchor in the lung vasculature and subsequently it promotes spreading of cells, degradation of vascular basement membrane and movement into organ parenchyma [5]. The polyLacNAc, on N- and not on O-linked glycoproteins, facilitates the lung specific metastasis [7]. Inhibition of these oligosaccharides by down regulating the enzymes responsible for polyLacNAc substitutions or specific N-glycosylation inhibitors like swainsonine inhibited all these processes and metastasis [5,6,7].

In addition, it has been shown that the lysosome-associated membrane glycoprotein 1 (LAMP1) and β1 integrins are the major carriers of polyLacNAc substituted β1, 6 branched N-linked oligosaccharides. The inhibition of LAMP1 by down regulating it or by using antibody against LAMP1 inhibits the lung specific metastasis of B16F10 cells [6,13,14]. The β1, 6 branched N-linked oligosaccharides carrying glycoproteins were identified by mass spectrometric method from B16F10 murine melanoma cells, in which LAMP1 and β1 integrins, and other 28 glycoproteins were identified. However, one of them, the CD147, is found to be a potential major player in mediating the lung specific metastasis of B16F10 cells

Galectin-3 is a nucleo-cytoplasmic protein which is secreted out in a non-classical manner and often gets incorporated into the ECM and BM. It is a member of a large family of galactose binding lectins and polyLacNAc on N-glycans and Thomson Freudenreich antigens (T/Tn) present in large number on mucinous proteins have been shown to serve as the ligands [10]. As a result, galectin-3 influences the functions of myriad classes of cell surface receptors/glycoproteins, which include growth factor receptors, receptor tyrosine kinases, integrin family receptors, immunoglobulin superfamily proteins, LAMPs and several others. The functions of galectin-3 are largely dependent on its sub-cellular localization. Galectin-3 has been shown to regulate cellular motility in many different ways and is dependent on the sub-cellular localization of galectin-3. Silencing the endogenous galectin-3 in pancreatic, gastric, osteosarcoma, human tongue and murine melanoma cancer cells decreases migration and invasion or the overexpression of galectin-3 increases the migration of colon cancer cells [11,15]. The secreted extracellular galectin-3 exerts its cellular effects on motility related processes both in the soluble form and as immobilized component on cells, ECM and BM. Galectin-3 on the ECM, BM and even on the cell surface may participate in cellular processes important from metastasis point of view [10,11,15,16]. However, it is not clear

how immobilized galectin-3 as a component of ECM/BM promote such complex cellular processes like spreading and movement critical for cancer cell metastasis. The downstream signaling events that regulate spreading and movement on galectin-3 and how they are different to those seen on classical substrates like fibronectin is still not known.

Based on the these previous findings, the key questions raised are,

1) How crucial is the galectin-3/polyLacNAc interaction for lung metastasis?
2) What is the precise role of carriers of β1, 6 branched N-glycoproteins during metastatic progression?
3) Which of the signaling pathways regulate galectin-3 induced cell adhesion, spreading and motility?

1.1 Objectives

The following objectives were proposed to address these questions.

1) **To confirm the role of galectin-3 on the lungs in organ specific metastasis**
2) **Role of CD147, a carrier of β1, 6 branched N-oligosaccharides, in metastasis**
3) **To investigate the role of galectin-3 in processes like adhesion, spreading and movement critical for metastasis**

1.2 Plan of work

1) **To confirm the role of galectin-3 on the lungs in organ specific metastasis**

To confirm the role galectin-3/polyLacNAc interaction in lung specific metastasis, the competitive inhibitor to galectin-3 (Modified citrus pectin (MCP)) which competes with polyLacNAc to bind to the endogenous galectin-3 and dominant negative inhibitor of galectin-3 (Truncated galectin-3 (tGal-3)) which competes with endogenous galectin-3 to bind to the polyLacNAc on the cell surface were used. Galectin-3 transgenic mice were used to prove the importance of galectin-

3/polyLacNAc interaction in lung specific metastasis. To prove the importance of galectin-3 in regulation of anti-tumor immune response, it was planned to generate bone marrow chimeric mice to perform experimental metastasis assay using B16F10 murine melanoma cells.

2) **Role of CD147, a carrier of β1, 6 branched N-oligosaccharides, in metastasis**

The mass spectrometric screen identified CD147 as a galectin-3 binding protein. Wild type and glycodeficient CD147 were cloned and expressed as a fusion protein with green fluorescent protein. The effect of glycosylation on CD147 in the metastatic processes was investigated using these cell lines.

3) **To investigate the role of galectin-3 in processes like adhesion, spreading and movement critical for metastasis**

It has been shown that immobilized galectin-3 is able to promote melanoma cell adhesion, spreading, matrix degradation by secreting matrix metalloproteinase-9 (MMP-9) and movement. Galectin-3 supported cell spreading is found to be unique. The organization of microfilament and lamellipodial morphology was seen to be very different from that seen on cells spread on fibronectin, a very well-studied ECM component. Underlying mechanism and cellular signaling behind cell spreading and movement induced by galectin-3 was planned to investigate using various approaches.

Chapter 2

Review of Literature

2.1 Cancer

Cancer is one of the leading cause of deaths in the world, which surpasses the deaths caused due to all types of coronary heart diseases and strokes, according to 2011 World Health Organization (WHO) estimation [17]. It is observed that approximately 14 million new cases and 8.2 million cancer related deaths occurred worldwide in 2012. Among the men, lung cancer while in women, breast cancer cases were highly diagnosed worldwide in 2012. In India, oral cancer is the leading cause of death in men while in woman major cause of death is due to cervical cancer. According to WHO 2014 report, one third cancer deaths are due to behavioral and dietary risks while infections from some types of viruses, bacteria or parasites are among the other risk factors of cancers. Genetic and environmental risk factors contribute to 5-10% of cause of cancer related deaths [18,19,20,21,22].

Cancer is a group of disease caused due to sequential accumulation of mutations in the genome and results in abnormal cell growth homeostasis. The uncontrolled growth of cells beyond the limited divisions result in the mass of benign tumor. In some cases, it start to detach and spread from primary site to another site, this phenomenon is called metastasis and these are the malignant type of tumors. The acquisition of cancerous phenotype or transformation in the normal cells is the result of dominant gain-of-function mutations in proto-oncogenes and the recessive loss-of-function mutations in tumor suppressor genes [23]. The products of oncogenes are transcription factors, chromatic remodelers, growth factors, growth factor receptors, signal transducers and apoptosis regulators. Gain of functions in these proteins which regulate the key cellular processes including cell cycle regulation, cell proliferation and regulators of apoptosis result in transformation [24]. Tumor suppressor genes regulate the cellular functions such as cell cycle checkpoint responses, detection and repair of DNA damage, protein ubiquitination and

degradation, mitogenic signaling, cell specification, differentiation and migration, angiogenesis. The loss-of-functions in genes involved in these cellular processes result in the cellular transformation [23,25,26].

The sequential accumulation of mutations in these key cellular driver genes such as proto-oncogenes and tumor suppressor genes results in acquisition of cancerous phenotype. These transformed cells acquired the capabilities of sustaining proliferative signaling, evading growth suppressors, resisting cell death, enabling replicative immortality, inducing angiogenesis, deregulating cellular energetics, avoiding immune destructions, activating invasion and metastasis. These are especially called as hallmarks of cancers [27,28].

2.1.1 Self-sufficiency in growth signals

The growth signals are required for proliferation of cells to break the quiescent state. Cancer cells become self-sufficient to these growth signals for proliferation by adapting the various strategies. They themselves produce growth factors to drive the proliferative signals by autocrine manner. They can also stimulate the normal neighboring cells in tumor-associated stroma to produce growth factors which act in paracrine manner [29,30]. Over expression of receptors in some types of cancer is observed. In these cases cancer cells become hyper responsive to even limited growth factors. Sustained proliferation in cancer cells are also because of structural alterations in receptors results in ligand independent activation. Constitutive activation of downstream pathways of receptors is also one of the way adapted by cancer cell. Somatic mutations in proteins like B-Raf in human melanoma and phosphoinositide 3-kinase (PI3K) in many tumor types results in gain-of-function in turn constitutively active the downstream pathways [31,32]. Disruption of negative feedback loop mechanism by loss-of-function mutations in PTEN, RAS and mTOR results in unchecked proliferative signals [32,33]. Cancer cells also adapted to hyper proliferative signals

which cause senescence state by deactivating senescence circuitry or by maintaining relative mitogenic signaling [34].

2.1.2 Insensitivity to antigrowth signals

Cancer cells achieve limitless proliferation and growth signals by counteracting the antigrowth signals. The tumor suppressor genes are mainly involved in counteracting the proliferative signals. These genes are activated and arrest the cell growth until the repair. If damage to the cell is unrepairable, these gatekeeper genes send the cell to the senescence and apoptosis [26]. The RB and TP53 tumor suppressor genes are the classical examples which regulate the anti-proliferative signals in the cells. RB is a central regulator of extracellular and intracellular signals which integrate and regulate cell proliferation. P53 is a stress and abnormality sensor inside the cell. The loss-of-function mutations in these tumor suppressor genes results in unchecked antigrowth signals which leads to proliferation [23,25,26].

2.1.3 Evading apoptosis

Programmed cell death is a natural way of barrier to cancer. Apoptotic signals are originated from physiological stresses in hyper proliferative cells, DNA damaged cells. Apoptosis is highly regulated by pro- and anti-apoptotic Bcl-2 family proteins. Bcl-X_L, Bcl-W, Mcl-1, A1 are the antiapoptotic proteins which inhibit apoptosis while Bax and Bak are the proapoptotic proteins which promote apoptosis [35]. Tumor cells counteract this process by upregulating the levels of antiapoptotic proteins survival signal or by deregulating the signals generated from TP53 or alternatively by limiting the expressions of proapoptotic proteins [23,25,26].

2.1.4 Limitless replicative potential

The cells normally divide up to certain limit, there after enter into the viable non proliferative state, senescence followed by cell death. Limitless replicative potential is required for cancer cells to

proliferate and form macroscopic tumor. Shortening of ends of chromosomes with each division is the principal factor of control of cell proliferation and immortalization and this shortening is protected by telomeres [36]. With each division telomeres are degraded and lose their protective capabilities. Cancer cells expresses telomerase which has capability to add the telomeric deoxyribonucleic acid (DNA) sequences to the ends of the chromosomes. Cancer cells achieve limitless replicative potential by protecting the ends of chromosomes which avoids chromosome fusion and subsequent damage to the DNA [37].

2.1.5 Sustained angiogenesis

The growing tumor demands more nutrients and oxygen and simultaneously want to dispose metabolic waste and carbon dioxide. Tumor cells cause the sprouting of existing vasculature and form network of blood vessels is angiogenesis. Angiogenic switch remains on during tumor growth [38]. Angiogenesis is regulated by signaling molecules which either inhibit or promote the angiogenesis. Vascular endothelial growth factor-A (VEGF-A) is promoter of angiogenesis while Thrombospondin-1(TSP-1) is an inhibitor of angiogenesis. These signaling molecules bind to the cell surface receptors of vascular endothelial cells and exerts their effects [39,40].

2.1.6 Tissue invasion and metastasis

During cancer progression local tissue invasion and distant metastasis is feature of advancement of the disease. The primary tumor sheds the cells in local tissue and in circulation after reaching its maximum size. The breakdown of cell to cell and cell to ECM interaction results in local invasion of cancer cells [1,41,42,43,44]. The deregulated expression of cell adhesion molecules is the prime reason for cell detachment. These cells steadily undergo epithelial to mesenchymal transition (EMT). Tumor cells after acquiring mesenchymal phenotype successfully metastasize at distant organ site and give rise to a secondary tumor [45,46].

2.1.7 Deregulation of cellular energetics

Reprogramming the energy metabolism is one of the enabling hallmark of cancer [28]. During limitless proliferation cancer cells adjust the energy need by deregulating the metabolic pathways. During aerobic conditions pyruvate generated from glycolysis was dispatched to mitochondria for generation of energy while in anaerobic conditions glycolysis is favored and very few pyruvate is utilized by mitochondria. Cancer cells favor glycolysis even in aerobic conditions 'aerobic glycolysis', despite lower yield of energy as compared to aerobic oxidation in the mitochondria [47]. Increased glycolysis in cancer cells allows glycolytic intermediate utilized for biosynthetic processes of macromolecules and organelles [48].

2.1.8 Avoidance of immune destruction

Second most enabling hallmark of cancer cells is evading the immune destruction [28]. Immune surveillance mechanism operating in the body constantly keep check on cancer cells and growing tumors. Both adaptive and innate immunity play a role of immune surveillance in eradicating the cancer. Functional deficiency in $CD8^+$ cytotoxic T lymphocytes (CTLs), $CD4^+$ T_H1 helper T cells or natural killer (NK) cells leads to tumor formation in mice [49]. To counter host anti-tumor immune response, cancer cells adapt various strategies. Cancer cells show less immune response because of absence of strong antigen or loss of major histocompatibility class (MHC) I or class I like, or co-stimulatory molecules. Development of immune suppressive tumor microenvironment also results in tumor growth. Recruitment of inflammatory cells such as regulatory T cells (Tregs) and myeloid-derived suppressor cells (MDSCs) which can suppress the cytotoxic lymphocytes in order to promote the tumor growth [50,51].

2.2 Metastasis

Metastasis is the major cause of deaths in cancer patients, yet underlying molecular mechanisms are poorly understood, possibly, because of complexity and multistep nature of the disease [52]. To successfully metastasize, cancer cells must complete a sequential series of events which include separation from the primary tumor, invasion through surrounding tissues and basement membranes, entry and survival in the circulation and arrest in a distant target organ vasculature, extravasation and adaptation to the new organ growth environment [1,41,53].

Tumors often metastasize regionally to the organs in anatomic vicinity like those receiving afferent blood vessel from the primary or the draining lymph nodes. As these organs receive maximum number of cells, some of these cells may get mechanically trapped in fine vasculature and get adapted to new organ environment and give rise to metastatic colonies [54]. Colon cancers metastasizing to liver and several tumors colonizing lymph nodes are classical examples of this pattern of metastasis proposed by Ewing in 1927 [43]. However, many tumor cells bypass several organs in their blood flow path and metastasize to very specific distant organ sites. The 'Seed and Soil' hypothesis was proposed by Dr. Stephen Paget in 1889 to explain the phenomenon of organ specificity of metastasis based on the autopsy studies of >900 breast cancer patients. He compared organ microenvironment with soil and tumor cells with seeds and explained that like seeds cancer cells although get dispersed to all the organs but survive and give rise to metastatic colonies only in the organs that can support their growth [43,55]. Apart from the organ microenvironment, adhesive interactions, chemokines and their receptors have also been shown to be the key participants in organ specific metastasis [43,56,57].

2.2.1 Mechanisms of organ specific metastasis

The organ specific metastasis is mainly governed by 3 major contributing factors which includes organ microenvironment, adhesive interaction and chemokines and their receptors.

2.2.1.1 Organ microenvironment

Once the tumor cells reaches the target organ, it grows as secondary tumor only when target organ microenvironment is suitable for its growth. The organ specific pattern of some cancers is indication of survival advantage at the secondary sites. Prostate cancer frequently metastasize to the bone marrow while breast cancer metastasize to the brain, lung and bone marrow [44]. The factors present in the organ microenvironment contribute in the regulation of metastasis related genes. For instance the TGF-α produced by liver for its regeneration through EGFR also activate the genes of metastatic human colon cancer cells and support its growth and proliferation in the liver [58,59,60].

2.2.1.2 Adhesive interactions

The tumor cell expresses cell surface molecules act as a ligand for endogenous receptors expressed by the target organ endothelium. These receptor-ligand interaction acts as a first adhesive anchor in organ specific metastasis. These interaction between tumor cells and target organ endothelium is the first crucial step in organ specific metastasis. These adhesive interactions further strengthened by facilitating cell spreading which avoid cancer cells flown away with the blood flow [44]. Lung colonizing cancer cells have been shown to get redirected to liver upon forced expression of ligands for E-selectin on liver [61]. Constitutive expression of E-selectin on vessels of the bones or on inflamed organ endothelium has been shown to facilitate organ homing of cells expressing specific E-selectin ligands [62,63]. In breast cancer metastasis to the lung, metadhrin expressed by breast cancer cells has specific affinity to the lung vasculature [64]. Also interaction between α3β1 integrin on breast cancer cells and laminin 5 on lung capillary basement membranes favours lung specific metastasis [65].

2.2.1.3 Chemokines and their receptors

Involvement of chemokines and their receptors in organ specific metastasis is an emerging phenomenon. Certain organs secrete chemokines and tumor cells express receptors for those chemokines and lodge organ specifically. C-X-C motif chemokine ligand 12 (CXCL12) (also known as stromal cell derived factor 1; SDF1) expressed by residential mesenchymal cells of bone marrow attract the breast cancer cells expressing its receptors C-X-C motif chemokine receptor 4 (CXCR4). Expression of CXCR4 in the breast cancer cells is the marker of bone metastasis [66,67]. C-C motif chemokine ligand 5 (CCL5) released by bone marrow cells cause the metastasis of breast cancers to the lung [68].

2.2.2 Basic steps involved in organ specific metastasis

2.2.2.1 Detachment of the cells from the primary site

Due to the limitless proliferation in genetically unstable cell forms a mass of tumor. It grows up to 1-2 mm^3 with intense vascularization around it. At this stage the cancer cells start to detach from their primary sites. Alterations in expression of cell adhesion molecules leads to disruption of cell to cell desmosomal and cell-ECM hemidesmosomal contacts [41,43,53,57,69].

2.2.2.2 Invasion into the surrounding tissue and tumor cell motility

The cells that have broken free from primary tumors need to be motile and are able to create space for movement. The surrounding matrix is used as traction for movement of cells. Integrin receptors together cover all the major collagen and noncollagenous glycoproteins and thus serve as a major class of molecules involved in movement of cells. Modulation of integrin receptor expression, post translational modifications (PTMs) on them or their association with membrane microdomains all regulate cellular movement. The tumor cells utilize all these mechanisms to achieve a motile state. Most of the enzymes secreted by tumor cells are in zymogenic form and their activation occurs in a cascade in space and time dependent manner. The urokinase plasminogen activator / urokinase

plasminogen activator receptor (uPA/uPAR) system and membrane tethered forms of MMPs (MT1-MMP) that get activated during transport to cell surface and associated with motility receptors together with uPAR are the major regulators that couple matrix degradation and cellular movement. The other components that participate in tumor cell invasion include the lysosomal enzymes cathepsins, ADAM (A Disintegrin and Matrix metalloproteinase) family of proteins, glycosaminoglycanases like heparanases and several others [70].

During invasive processes various factors affects the tumor cell motility. Almost all the ECM and BM component are shown to regulate motility processes. ECM (interstitial matrix) is present in between the cells which gives tissue architecture and integrity. It is made up of fibrillar collagen, proteoglycans and various glycoproteins such as fibronectin and tenascin C etc [71,72]. While the BM separate the epithelium or endothelium from stroma. BM contains laminin, type IV collagen, fibronectin, linker proteins nidogen and entactin. It is more compact and less porous than ECM [73]. These matrix component either positively or negatively regulate the cellular adhesion, spreading and motility [72,74].

Fibronectin is major component of ECM but is also present in the basement membrane, although, proportions in the two may vary. Fibronectin appears to play a major role in stabilizing cellular interaction with matrix via integrin receptors on the cells. Although, α5β1 integrin is the major integrin receptor, several other receptor like αMβ2, αvβ3 and αIIbβ3 have also been shown to serve as receptors for fibronectin [75,76,77]. While α5β1 and αvβ3 have been shown to serve as the major fibronectin receptors on invading tumor cells others show cell type specific expression like αMβ2 on leukocytes and αIIbβ3 on platelets. These receptors promote adhesion, spreading and movement of cells in response to external cues [78]. The fibronectin mediated cellular effects and downstream molecular events have been thoroughly researched over last three decades, and serve

as a model to explore and understand the possible mechanisms utilized for similar cellular processes on other substrates [76].

Fibronectin activates integrin receptors on cells which come in its contact. The activated integrin receptor(s) recruits focal adhesion kinase (FAK). FAK itself gets activated on integrin binding by auto-phosphorylation at Tyr327 site which acts as docking site for Src and PI3K. Docking of these proteins on FAK leads to its phosphorylation at multiple sites. Both Src and PI3K also get activated on binding to FAK. Activation of FAK-Src complex results in further activation and phosphorylation of scaffolding proteins, p130Cas and paxillin. These proteins further activate guanine nucleotide exchange factors (GEFs) for Rac1 and CDC42 which are the key regulators of lamellipodia and filopodia, respectively.

Activation of Rac1 is also brought about by PI3K. Activation of PI3K results in activation of Akt which in turn activates several Rac-GEFs and phosphorylates numerous other proteins which regulate actin cytoskeletal or microfilament organization [79,80]. Microfilaments are also organized via integrin through an alternate mechanism. The Ser925 site on activated FAK recruits Grb2-SOS which in turn activates extracellular signal regulated kinase-mitogen-activated protein kinase (Erk-MAPK) cascade. This leads to phosphorylation of myosin light chain kinase (MLCK1). This pathway is believed to be used to release the rear end of the motile cell for efficient movement [79,80,81,82,83,84,85].

In addition to integrin receptors, growth factor receptors (GFRs) also participate in cellular motility. The matrix which acts as a sink provides a rich source of growth factors (GFs) [72]. GFRs independently or in combination with integrins, activate downstream signaling required for cell migration. GFRs regulate motility by influencing microfilament organization by activating GEFs via PI3K and ERK-MAPK pathways [86,87].

2.2.2.3 Intravasation and survival in the circulation

The process of entry of tumor cells into the lumen of lymphatic or blood vessels is termed as intravasation. Intact vascular BM lining the blood vessels acts as obstacle for entry of tumor cells in the circulation. For intravasation metastatic cells either produces degradative enzymes that disrupt the vascular BM or induces the process of angiogenesis. Tumors do not grow beyond a certain size unless well vascularized. Metastatic tumors are generally highly angiogenic. The newly formed blood vessels around tumors however, are poorly formed. They lack BM and even the endothelial lining is often discontinuous. This offers an easy escape route for tumor cells to get into circulation. The process of intravasation can also be facilitated by molecular alteration that supports ability of tumor cell to cross the endothelial barrier and pericyte [88].

Once the tumor cells have successfully intravasated into the lumen of blood vessels, they can easily disseminate through venous and arterial circulation. During circulation tumor cells must survive variety of stresses in order to reach distant sites. For example anoikis, a form of apoptosis induced in absence of adhesion to substratum, they also seem to be deprived of integrin-ECM interaction dependent survival signals, to overcome that tumor cells show increased expression of tyrosine receptor kinase expression that prevents anoikis and promotes their survival [89]. Tumor cells also must overcome the damage sustained by shear forces of blood flow, predation by natural killer cells, a component of innate immune system, and also the toxicity induced by high level of oxygen. In order to overcome these, tumor cells form large emboli by their interaction with platelets. This not only aids in evading immune surveillance but also acts as shock absorber [90].

2.2.2.4 Organ colonization

Once in circulation tumor cells are able to reach almost all organ sites. However, some tumors metastasize only regionally either to the lymph nodes or to the organs in the anatomic vicinity,

while several others metastasize to very specific distant organ sites [43,44,56,57]. At the target site these tumor cells colonize and establish as secondary metastatic colonies.

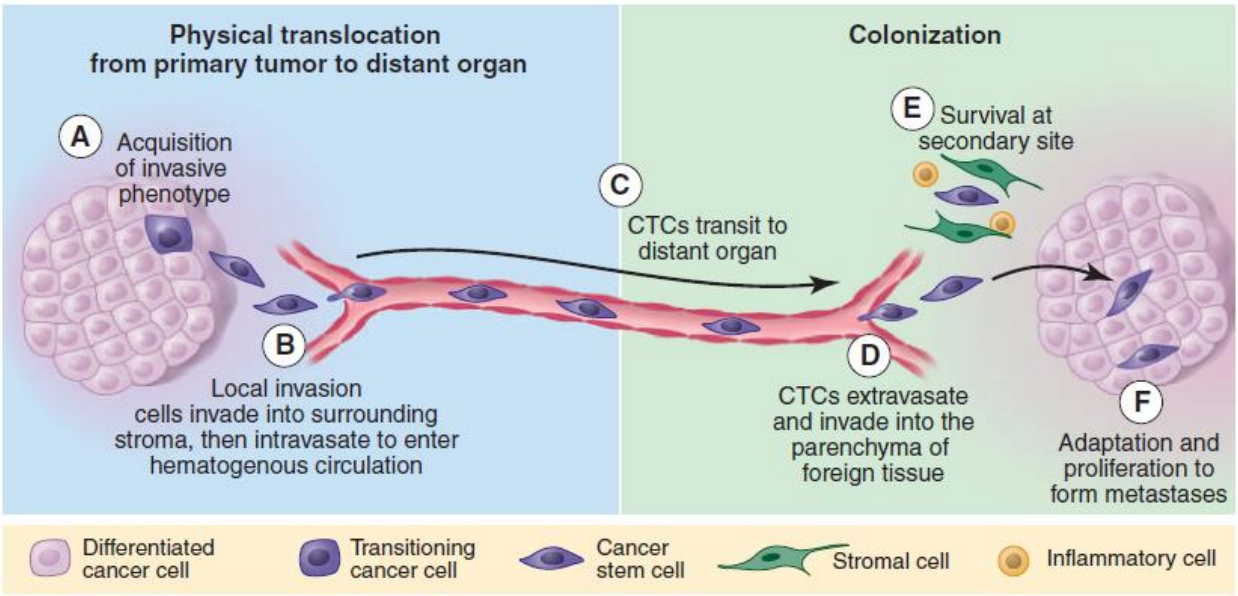

Illustration 1: Metastatic cascade (Source: Christine L. *et al*., Science 331 (2011) 1559)

2.3 Glycosylation and Cancer

Altered or aberrant cell surface glycosylation is an emerging concept of abnormalities in the cell physiology and homeostasis in cancer. Changes in glycosylation include loss or excess of expression of certain structures, incomplete or truncated structures, accumulation of precursors or presence of novel structures. These modifications in the normal glycosylation patterns are correlated with cancer progression [91]. Altered expressions of various types of glycosylations are observed in the transformed cells such as,

2.3.1 Mucin glycosylation

Mucins are the MUC family proteins overexpressed in various cancers. The Muc proteins carry various O-glycosylation sites in tandem repeat regions. In carcinoma incomplete mucin glycosylation is observed. The incomplete glycosylation results in more frequent T/Tn and sialylated Tn antigens on mucins during cancers. These antigens acts as anti-adhesion molecules because of heavy negative charge and also provoke immune response in the patient [92].

2.3.2 Sialic acids

The net increase in content of sialic acid is a feature of transformed cells. Heavy negative charge due to sialic acids on the cancer cell surface results in weaker adhesions to the cell and/or ECM and also protects from alternate complement system. α 2,6 sialic acid linkage on either N- or O-glycans and sialyl Tn antigen on O-glycans is a form of aberrant expression of sialic acid on the cancer cells. Also the modifications on gangliosides and changes in N-Acetylneuraminic acid (NANA) observed in cancers. Moreover, changes in the sialic acids results in changes in binding of sialic acid binding lectin (SIGLECS) which gives advantage to the cancer cells [93,94].

2.3.3 Sialylated lewis structures and selectin ligands

Lewis^{x} and Lewis^{a} structures on N-, O-glycans, and glycospingolipids are found to be overexpressed in carcinomas. These sialylated and fucosylated structures forms ligand for endogenous selectins [94]. These receptor ligand interactions promote the organ specific metastasis of certain cancer types. Constitutive expression of E-selectin on vessels of the bones or on inflammed organ endothelium has been shown to facilitate organ homing of cells expressing specific E-selectin ligands lewis antigens.

2.3.4 Glycosphingolipids and Blood group related structures

Glycosphingolipids such as gangliosides are shown to be highly expressed in neuroectodermal cancers like neuroblastoma and melanoma [95]. Complete loss of glycosylphosphatidylinositol

(GPI) anchored glycophospholipids are observed in cancers of hematopoietic systems. Altered or loss of blood group related antigens are also observed in some forms of cancers. For example Sda (Cad) antigen expressed in colon completely lost in colon carcinoma [2].

2.3.5 Hyaluronan

Hyaluronic acid (HA) is a polysachharide made up of repeating units of disachharides. It is nonsulfated and exist in free form. It is the only glycosaminoglycan (GAG) which does not bind to any core protein. It is synthesised in the cytoplasm and plasma membrane and secreted outside. Many cancer types express high levels of hyaluronan. CD44 is the known receptor for hyaluronan. Hyaluronan-CD44 interactions are implicated in various cancers. Hyaluronan-CD44 signalling is hyperactivated in cancer state which regulates the cell proliferation, survival, migration and invasion.

2.3.6 Sulphated glycosaminoglycans

Proteoglycans are composed of a core protein which is covalently attached to the GAG chain. Choindroitin sulphate, dermatan sulphate, keratan sulphate and heparan sulphate (HS) are the GAG chains. The content and distribution of the proteoglycans varies in pathogenesis of cancer. The role of heparin sulphate proteoglycan is demonstrated in various cancers. It modulates cancer either in a positive or negative manner. For example HS side chain of perlecan promotes angiogenesis while core C-terminal domain of the core protein endorepellin has anti-angiogenic activity [96].

2.3.7 N-glycans and poly-*N*-acetyllactosamine (polyLacNAc)

During cancer progression changes in the N-glycan structures are more often observed and are most studied phenomenon. One of the frequently observed cell surface modifications on glycoproteins is β1, 6 branched N-glycans [97]. This aspect is further discussed in section 1.4.

2.4 N-glycans

2.4.1 Biosynthesis of N-glycans

Synthesis of N-glycans on proteins is the co-translation modifications occurred in the endoplasmic reticulum (ER) and processed and matured in the golgi complex (GC). The amide group of asparagine (Asp) is the modification site from a consensus sequence Asp-X-Ser/Thr, X is any amino acid except proline. The basic steps of N-glycans biosynthesis are,

1) Dolichol phosphate (Dol-P) a polyisoprenol lipid is located on cytoplasmic face of ER receives first sugar GlcNAc further it extends and forms Dol-P-P-$GlcNAc_2Man_5$.
2) It is then flipped on the luminal side of the ER and grows into mature glycan precursor and results in formation of $Glc_3Man_9GlcNAc_2$-P-P-Dol.
3) This glycan precursor is next transferred from (Dol-P) to Asp of nascent protein in lumen of the rough ER and results in formation of $Glc_3Man_9GlcNAc_2$Asn.
4) Trimming of this precursor takes place in the ER and cis-golgi by various glycosidases and results in formation of $Man_5GlcNAc_2$Asn
5) Actions of N-acetylglucosaminyltransferase (GnTs) biosynthesis of hybrid and complex sugars begins in the medial golgi.
6) Maturation of these sugars are completed in the trans-golgi.

N-glycans are matured into 3 major common forms viz. Oligomannose, Hybrid or Complex. In the oligomannose structures mannose (man) is attached to the core. In complex structures antennae is initiated by the actions of GnTs. In hybrid structures mannose is attached to the core and one or two antennae structures are attached to this core.

During maturation of these structures various modifications take place due to the action of GnTs. Usually the complex structures are of bi-antennary nature. Most of the time these branches are

elongated and substituted with sialic acid, fucose, galactose, *N*-acetylgalactosamine (GlucNAc) residues. The complex structures may further mature into the tri-, and tetra- antennary structures due to the actions of GnTs. These tri- and tetra- antennary structures are further elongated and form polyLacNAc structures. These substitutions on the antennary structures serve as the binding sites for endogenous lectins. Action of GnT-V enzymes coded by mannoside acetyl- glucosaminyltransferase 5 (*MGAT5*) gene results in the formation of β1, 6 branch which is a favoured site for further elongation. The bi-antennary structures are seen in the normal cells while tri- and tetra- antennary structures are observed in the cell involved in invasive functions [97,98].

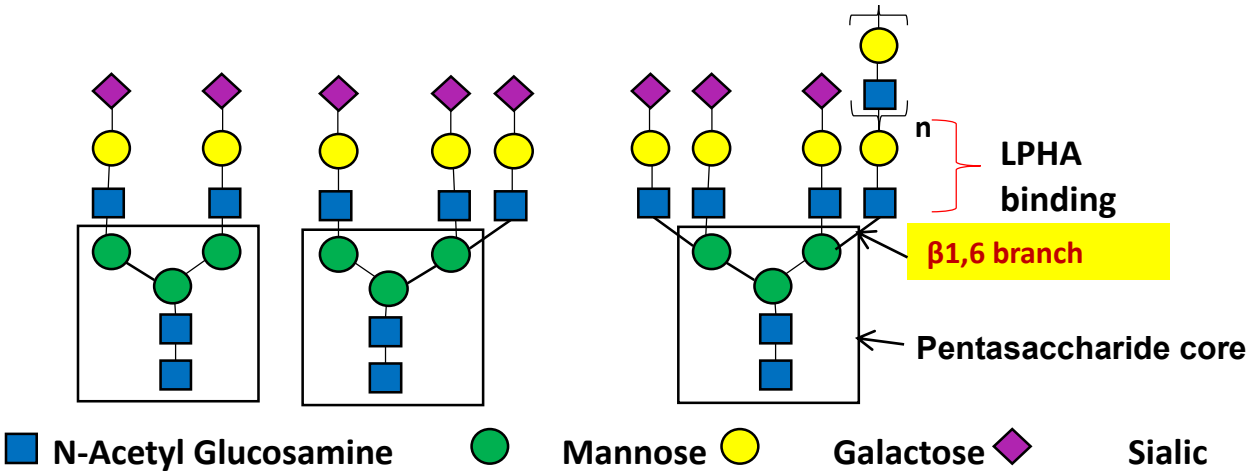

Illustration 2: Types of N-glycans

2.4.2 β1, 6 branched N-glycans and metastasis

Tumor cells show several cell surface modifications associated with the metastatic phenotype, including changes in cell surface glycosylation [2,3]. The *MGAT5* gene code for GnT-V enzyme responsible for addition of β1, 6 branched N-linked glycans. This site is act as site for further

substitution for lactosamine, sialic acid and fucose. Leuco-phytohaemagglutinin (LPHA) lectin has binding affinity to β1, 6 branch while galectins have affinity to bind elongated polyLacNAc structures [99,100]. Terminal sugars like sialic acid and fucose form lewis antigens detected by selectins. α 2,6 and α 2,3 linked sialic acids forms the binding sites for SIGLECS. One of the frequently observed modifications is the altered expression of β1, 6 branched N-oligosaccharides on cell surface glycoproteins [101,102].

The increased β1, 6 branched N-oligosaccharides on proteins may affect the structure and function of the proteins which carry them and also they may provide several novel ligands for endogenous lectins. These oligosaccharides have been strongly associated with invasive and metastatic phenotype of tumor cells [99,100]. Its expression has been shown to correlate with disease progression in several human tumors such as breast, colon, oesophagus, endometrium and gliomas and with metastatic potential of several human and murine cancer cell lines [4,103,104,105]. Induction or inhibition of the β1, 6 branch in various cell lines using different strategies has been found to result in a corresponding induction or abrogation of metastatic potential [101,106,107,108]. They are expressed on invasive cancers and invasive normal cells like trophoblast cells during embryo implantation , activated endothelial cells, granulocytes and macrophages which indicates their role in invasion, although the mechanism is poorly understood [105,109,110]. Recently, the role of β1, 6 branched N-glycans has also been implicated in providing resistance against anoikis in hepatoma cells. Another unique feature is that majority of the cell lines expressing these oligosaccharides metastasize either to the lungs or to the liver [101,111,112]. It is known that the β1, 6 branched N-glycans carrying sialyl lewis antigen metastasize to the liver [61,113,114]. However, the mechanisms of lung specific metastasis is not known.

The action of GnT-V is countered by GnT-III enzyme by adding bisecting GlcNAc N-glycans in β1, 4 linkage and suppresses the additional maturation of N-glycan branching which results in suppression of the cancer cell metastasis [108,115].

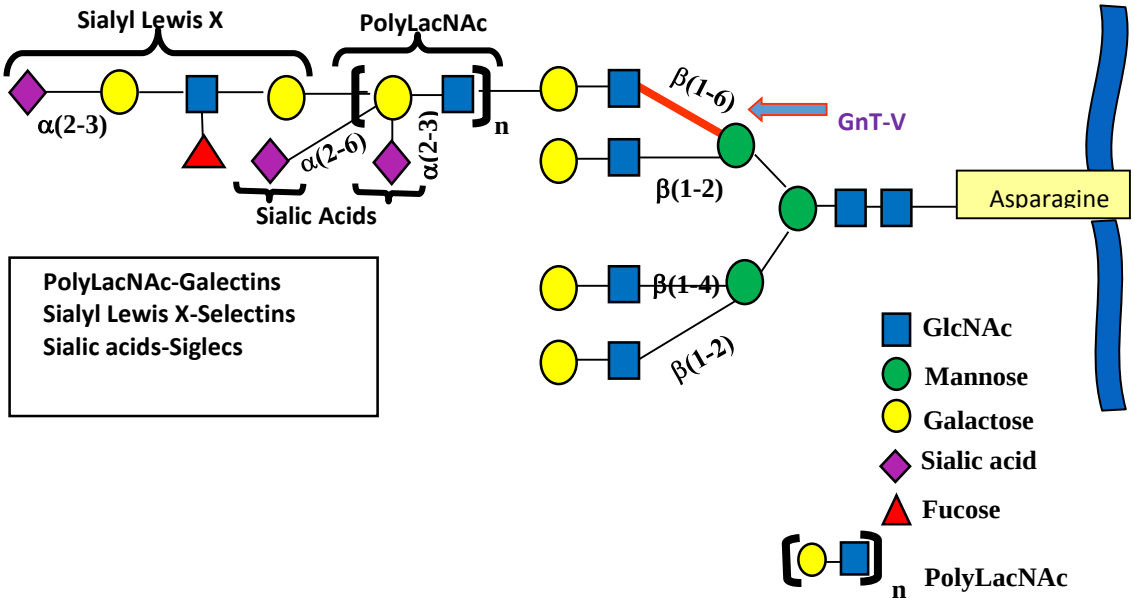

Illustration 3: β1, 6 branched N-oligosaccharides acts as preferred site for substitution of various sugars

2.5 Lectins

Lectins are the group of family proteins which have carbohydrate recognition domain (CRD). Lectin term is derived from Latin word 'legere' meaning 'To select'. Lectins recognize and bind to the sugars with diverse affinity and avidity. Initially, lectins were discovered in the plants but they are also found to be present in the microbes and animals [10,116,117].

Lectin family members include,

i. R-type lectins: CRD structurally similar to ricin's CRD

ii. L-type lectins: discovered firstly in leguminous plants

iii. P-type lectins: Recognizes mannose-6-phosphate (M6P)

iv. C-type lectins: Ca^{2+} dependent

v. I-type lectins: belongs to immunoglobulin superfamily proteins (IgSF)

vi. Galectins: sulfhydryl-dependent (S-type) β-galactoside binding lectin

vii. Microbial lectins: present in viruses, bacteria, protozoa, fungi etc

2.5.1 Galectins

Galectins are the β-galactoside binding lectins. They were previously known as S-type lectins. CRD of the galectin family proteins are highly evolutionary conserved region. They are the most studied and widely present in variety of organisms. In the vertebrate, galectin-1 is the first lectin discovered in 1976 from extracts of calf heart and lung. CRD of the galectin is made up of approximately 130 amino acids [116].

2.5.2 Classification of the galectins

A) Based on sequence homology

i. **Galectin-1 subgroup:** includes galectin-1 and -2

ii. **Galectin-3 subgroup:** includes all remaining galectins

B) Based on structure

i. **Prototypical:** includes galectin-1, -2, -7, -10, -13, -14; Single CRD that may associate and form homodimer

ii. **Chimeric:** includes galectin-3; Contain single CRD, N-terminal oligomerization domain

iii. **Tandem-repeat:** includes galectin-4, -8, -9, -12; Two CRD in a single polypeptide linked by small peptide domain

2.6 Galectin-3

Galectin-3 (Gal-3) is 29 to 35 kDa protein. It was firstly identified as Mac-2 32 kDa protein in murine macrophages. Afterwards it was discovered as CBP-35 (carbohydrate binding protein) 35 kDa in mouse fibroblasts, εbp (ε binding protein) in rat basophilic leukemia cells, RL-29 29 kDa in rat lung tissue, HL-29 in human lung tissue, L-34 34 kDa in rat fibroblasts, non-integrin laminin binding protein (LBP) in macrophages [10].

Among galectins, galectin-3 is the most studied only member of chimera type galectin. It is a nucleo-cytoplasmic protein which is secreted out in a non-classical manner often gets incorporated onto the cell surface, ECM and BM [10,11,15,16]. It is widely expressed in various tissue types. It is a member of a large family of galactose binding lectins and recognise [-3Galβ1-4GlcNAcβ1-$]_n$ or polyLacNAc on N-glycans and Thomson Freudenreich antigens are the major carbohydrate ligands present on glycoproteins present on the cell surface, ECM and BM [116]. As a result galectin-3 influences the functions of myriad classes of cell surface receptors/glycoproteins, which include growth factor receptors, receptor tyrosine kinases, integrin family receptors, immunoglobulin superfamily proteins, LAMPs and several others [118]. The affinity of galectin-3 increases with LacNAc units.

2.6.1 Galectin-3 structure

Galectin-3 consists of N-terminal domain (ND) for multimerization and approximately 130 amino acids C-terminal CRD domain. The ND consists of 7–14 repeats of a 9-amino acid sequence: Pro-Gly-Ala-Tyr-Pro-Gly-X-X-X. This sequence is also called as collagen-like ND due to its homology with collagen α1 (II) chain. ND is sensitive to proteolytic cleavage by MMP-2 and MMP-9. The first 12 amino acids of ND are required for secretion and nuclear localization. Highly conserved ser6 residue is required for anti-apoptotic activity. Tyr102 residue of the ND may also participate in the carbohydrate binding activity. CRD consists of NWGR (Asp-Trp-Gly-Arg) motif

essential for binding to β-galactoside. This motif is also seen in Bcl-2 family proteins and involved in anti-apoptotic related properties of galectin-3.

Galectin-3 exists in monomeric form in solution while in the absence of its ligand it is in homodimeric form by self-association with CRD. In presence of ligand, galectin-3 can multimerize through ND up to pentameric form and able to form lattice with cell surface glycoproteins [10,16].

2.6.2 Galectin-3 functions

The functions of galectin-3 are largely dependent on its sub-cellular localization. Depending on its localization the intracellular and extracellular functions of galectin-3 varies. The intracellular functions depends on endogenously expressed galectin-3 in the cytoplasm and/or nucleus while extracellular galectin-3 may be a secreted soluble or exogenously added in the form of soluble or immobilized form. However, galectin-3 on the ECM, BM and even on the cell surface may participate in cellular processes important from metastasis point of view. Galectin-3 regulates the wide variety of cellular functions including cell growth, differentiation, transformation and immune responses etc. The galectin-3 knock-out mice are viable, there is no embryonic lethality suggesting the functional redundancy [10,11,15].

The key functions of galectin-3 related to involvement in cancer metastasis and immune response are discussed below.

2.6.2.1 Galectin-3 and cancer

Galectin-3 is found to be involved in the various cancer associated processes including transformation, tumor growth, anoikis resistance, apoptosis, angiogenesis, cell adhesion, cell motility and cell invasion.

Over expressed galectin-3 induces cellular transformation in normal human fetal thyroid follicular cell line TAD-2. Galectin-3 controls the activity of Ras required for transformation. Galectin-3

expression is necessary for maintenance of transformed and tumorigenic phenotype of MDA-MB-435 breast carcinoma cells. It is also an a critical determinant in adhesion independent cell survival in human breast cancer cells as well as being an antiapoptotic protein, exerts its effect by influencing mitochondrial homeostasis. Ser6 phosphorylation regulates galectin-3 translocation from nucleus to cytoplasm and its antiapoptotic activity. Galectin-3 induces endothelial cell morphogenesis and angiogenesis, while its cleavage at ND by MMPs induces angiogenesis in breast cancer. The homo and heterotypic adhesion of MDA-MB-435 breast cells is mediated by galectin-3 and T/Tn-antigen interactions under flow conditions [10,16].

Galctin-3 has been shown to regulate cellular motility in many different ways and is dependent on the sub-cellular localization of galectin-3. Silencing the endogenous galectin-3 in pancreatic, gastric, osteosarcoma, human tongue, esophageal and murine melanoma cancer cells decreases migration and invasion [119,120,121,122,123,124] or the overexpression of galectin-3 increases the migration of colon cancer cells [125].

The secreted extracellular galectin-3 exerts its cellular effects on motility related processes both in the soluble form and as immobilized component on cells, ECM and BM. The soluble galectin-3 promotes fibronectin dependent cell spreading and motility of mammary carcinoma cells by interacting with *MGAT5*-modified N-linked oligosaccharides [126]. Interaction of integrin receptors on the cell surface, with their ligand fibronectin in presence of galectin-3, leads to phosphorylation of caveolin-1. This stabilizes FAK in the focal adhesions (FAs) which induces its disassembly and turnover required for cell migration [127]. Galectin-3 also regulates motogenic response of epidermal growth factor (EGF) in mammary cell lines [128]. Exogenously added soluble galectin-3 has also been shown to induce lamellipodial formation in corneal epithelial cells by interacting with integrins [129]. Moreover, extracellular galectin-3 facilitates PI3K dependent

migration of sarcoma derived cell line on laminin 111 [130]. Down regulation of galectin-3 in intestinal epithelial cells affects the stability of desmosomal cadherins and intercellular adhesion [131]. Binding of galectin-3 to N-cadherins has been shown to destabilize cell-cell junctions in murine mammary cancer cells which might favor cell migration [132]. From the other members of galectin family, galectin-8 has very similar oligosaccharide specificity [133]. It has been shown to act as a matricellular protein and modulator of cell adhesion by interacting with integrins [134,135].

2.6.2.2 Galcetin-3 and immune response

Accumulating evidence suggests the importance of galectin-3 in functionally regulating the host immune response. The galectin-3 null mice have distinct phenotypes, including inflammatory responses. Galectin-3 is important in development and activation of cells involved in innate and adaptive immune responses [136,137,138,139]. It is also expressed by activated monocytes and macrophages, professional antigen presenting cells (APCs) like dendritic cells (DCs), neutrophils, several mast cell lines, eosinophiles and activated B- and T-cells [136].

Galectin-3 influences innate immunity by mediating macrophage migration and acts as a chemo-attractant for monocytes, and modulates adhesion and migration of DCs in parasitic infection [140,141]. It promotes adhesion of human neutrophils to laminin in a dose dependent manner and regulates traversing of neutrophils through BM at sites of inflammation [142,143] and plays an important role in controlling APC function [144]. Galectin-3 has also been shown to be expressed in medulla and in lesser extent in cortex of the thymus [145], intra-thymically produced galectin-3 acts as de-adhesion molecule to modulate thymocytes/ micro-environmental interaction [145,146]. In the thymic region it induces apoptosis of double-negative ($CD4^-CD8^-$) or double positive ($CD4^+CD8^+$) thymocytes [147].

Galectin-3 helps in developing memory B-cells. Inhibition of endogenous galectin-3 expression blocked T-cell proliferation suggesting role of galectin-3 in proliferation of activated T-cells [148]. It regulates T-cell signaling, activation, apoptosis, cytokine secretion, regulatory T-cell expansion [149]. Galectin-3 released by accessory cells such as macrophages may also participate in Ca^{2+} signaling during T-cell activation and its deficiency results in increased frequency of $CD4^{+}CD25^{+}FOXP3^{+}$Treg cells [131,143,150,151]. In contrast, galectin-3 induces apoptosis in tumor reactive $CD8^{+}$ T cells in a mouse model of colorectal cancer [152]. Expression of galectin-3 correlates with apoptosis of tumor associated lymphocytes in human melanoma biopsies [153]. In summary, galectin-3 regulate the host anti-tumor immune response either in a positive or negative way.

2.7 CD147 highly glycosylated galectin-3 binding protein

Cluster of differentiation 147 (CD147) or basigin (BSG), encoded by *basigin* gene, is a glycosylated transmembrane protein. It is also known as HAb18G in human, gp42 in mice, 5A11, HT7 or neurothelin in chickens. Initially, it was referred as tumor cell-mediated collagen enzyme activation factor (tumor cell collagenase stimulatory factor, TCSF) and then renamed EMMPRIN (Extracellular MMP inducer). In mice (*Mus musculus)* there are two isoforms of CD147, isoform I and isoform II. Isoform I is a long, 389 amino acid protein comprising three immunoglobulin like domains, specifically expressed in retina. Isoform II is widely expressed and is also known as basigin-2 or 5A11. It is a shorter isoform made up of 273 amino acids contains two immunoglobulin like domains [8,9,154,155].

2.7.1 Structure of CD147

CD147 is a single-pass type I membrane protein. Widely expressed mouse CD147 consists of 21 amino acids signal peptide, 40 amino acids cytoplasmic tail, 24 amino acid transmembrane

domain, 188 amino acid extracellular domain. The cytoplasmic tail contains two phosphorylation sites. There are three N-glycosylation sites reported on CD147 extracellular domain at 44th, 154th and 190th asparagine which follow the consensus sequence rule (Asg-X-Ser/Thr; X = any amino acid except proline) [156]. Recently, two more N-glycosylation sites were discovered on CD147 at 159th and 193rd asparagine. These two glycosylation sites are referred as atypical glycosylation sites because it does not follow consensus sequence rule [157,158]. Molecular weight of CD147 is 29.674 kDa while on SDS-PAGE it occurs at ~32 kDa as low glycosylated form (LG, Core glycosylated) and ~40-60 kDa region as high glycosylated (HG) form depending on the level of glycosylation. Mutations in three conserved Asg confirms the glycosylation on CD147. Up till now the type of sugars on atypical sites and its functional importance is not reported. HG-CD147 consists of complex carbohydrate structures while LG-CD147 consists of high mannose carbohydrate structures [159]. Addition of sugars occurs in ER on LG-CD147, which acts as a precursor for HG-CD147, and further processing takes place in GC. It has been reported that CD147 contains high mannose type bi-antennary complex-type oligosachharides, also presence of β1, 6 branched N-oligosachharides on CD147 was confirmed [156].

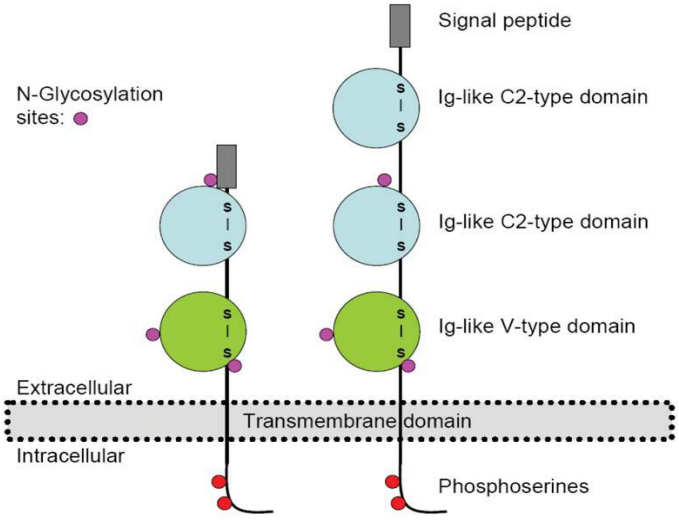

Illustration 4: CD147 architecture

(Source: Weidle UH *et al*., Cancer Genomics & Proteomics, 7 (2010) 157-170)

2.7.2 Functions of CD147

CD147 plays an important role in both healthy tissues and disease conditions involving regulation of the immune response, cancer chemoresistance, cellular proliferation, anoikis, tumor cell migration, metastasis and differentiation. It is found to be expressed in various tumors and its expression is correlated with tumor histological type and clinical stage of the disease. CD147 induces MMP secretion from adjacent fibroblast to promote the invasion of the cancer cells. CD147 always associate with other proteins in pathogenesis of cancer such as monocarboxylate transporter 1 (MCT1), CD44, insulin like growth factor I, cyclophilin, ubiquitin C, annexin A2 etc [8,9,154,155,160]. The association of CD147 and β1 integrin in retinal pigment epithelial (RPE) cell surface is induced by galectin-3 clustering [161]. CD147 along with CD44 and EGF receptor (EGFR) promotes invadopodia activity and invasiveness in breast epithelial cells. It directly regulate the invadopodia formation and activity along with MT1-MMP complexes in lipid rafts [162,163]. The down regulation of Let-7b miRNA to the CD147 inhibits metastasis in mouse melanoma cells [164]. Overexpression of CD147 promotes tumor growth in Chinese hamster ovary cells [165]. CD147 may be a potential therapeutic target for treating various cancers and other diseases. Using monoclonal antibody against CD147 clinical trials are on the way in hepatocellular carcinoma [9,166].

Glycosylation on CD147 is essential for functioning of CD147. The glycosylated form of CD147 induces strong MMP secretion than deglycosylated form [167]. The glycosylation of CD147 is essential for interacting with other proteins. Huang *et al*. has shown that deglycosylated human CD147 fails to target on the cell surface it was degraded by ERAD pathway. The Asg152 site was

found to be crucial for targeting human CD147 to the cell surface [156]. However, atypical glycosylation sites discovered in mice CD147 were until now not reported in human CD147. Also the role of typical versus atypical glycosylation sites remains unexplored in invasive and metastatic processes.

Chapter 3

Materials and Methods

3.1 Materials

3.1.1 Cell lines and reagents

High metastatic B16F10 and low metastatic B16F1 murine melanoma cell lines were obtained from National Centre for Cell Science (NCCS), Pune, India. It is an adherent cell line routinely cultured in DMEM containing 10% fetal bovine serum (FBS).

FBS, DMEM (Dulbecco's Modified Eagle Medium) powder, Antibiotic-Antimycotic solution, L-Glutamine, Trizol, Calcein-AM were obtained from GIBCO, Invitrogen Corporation, USA. Aprotinin, Leupeptin, Pepstatin, PMSF, Trypsin, Dextrose, Tween-20, Bovine Serum Albumin (BSA), TEMED (N,N,N',N'-Tetramethyl-ethylenediamine), β-mercaptoethanol, Glycine, Paraformaldehyde, Coomassie Brilliant Blue, Ponceau-S, Lactose, Divinyl Sulphone (DVS), Dialysis tubing, Lysolecithin, Phalloidin-TRITC (Tetramethylrhodamine), DAPI (4',6-Diamidino-2-Phenylindole, Dihydrochloride), Trypan Blue, PIPES, Lysozyme, RNase A, Ethidium Bromide, Agarose, Diethyl Pyrocarbonate (DEPC), Polybrene, Puromycin, Doxycycline, Lipofectamine 2000 Transfection reagent, Pectin from citrus peel and Primers for PCR were obtained from Sigma Chemical Co, USA. Ampicillin, Kanamycin, Yeast Extract, Tryptone, Luria-Bertani broth and Agar powder were obtained from HIMEDIA, India. Tris, NP-40, Sodium Deoxycholate, Sodium Dodecyl Sulphate (SDS), Bisacrylamide, Isopropyl β-D-1-thiogalactopyranoside (IPTG), Neomycin (G418) and Triton X-100 were obtained from USB, USA. Taq DNA polymerase, Phusion high-fidelity DNA polymerase, T4 DNA ligase buffer, ATP, dNTP mixture, T4 DNA ligase enzyme, Klenow Fragment enzyme and restriction enzymes were obtained from either New England Biolabs (NEB), USA or Fermentas, USA. Protoscript first strand cDNA synthesis kit was obtained from NEB, USA. Plasmid DNA extraction and DNA gel extraction kits were obtained from either Sigma or Qiagen, USA. Acrylamide, PVDF membrane

and ECL plus kit were acquired from Amersham-Pharmacia Biotech Ltd., England. WesternBright ECL Western blotting detection kit was from Advansta, USA. Glutathione Sepharose^{TM} 4B beads were obtained from Amersham Biosciences. Folin & Ciocalteu's phenol (FCP) Reagent and Ammonium persulphate (APS) was obtained from SRL Pvt. Ltd. India. Fibronectin was purchased from BD Pharmingen, USA. Vectashield with or without DAPI mounting medium were from Vector Labs, USA. Proteinase K, Protease Inhibitor cocktail, Phosphatase Inhibitor cocktail, Wortmannin and PD98059 were procured from Calbiochem, USA. Sepharose 4B beads and Cyanogen bromide activated Sepharose 4B beads were procured from Pharmacia Fine Chemicals, Sweden AB. Inbred strains of C57BL/6 mice were used for the metastatic assays and for other experiments. All other fine chemicals were obtained locally and were of Analytical (AR) or better grade. Water used to prepare all the reagents was of Milli-Q grade.

3.1.2 Antibodies

Rabbit Anti-Akt antibody, Rabbit Anti-Phospho-Akt (Ser473) monoclonal antibody (Clone 193H12), Rabbit Anti-p44/42 MAPK (Erk1/2) monoclonal antibody (Clone 137F5), Rabbit Anti-phospho-p44/42 MAPK (Thr202/Tyr204) (Phospho-Erk1/2) XP^{TM} monoclonal antibody (Clone D13.14.4E) was obtained from Cell Signaling Technology, Inc., USA. Monoclonal Anti-β-Actin antibody produced in mouse (Clone AC-74), Rabbit Anti-GFP (N-terminal) antibody, Anti-Mouse HRP antibody was acquired from Sigma Chemical Co., USA. Rabbit Anti-CD147 monoclonal antibody (Clone EPR4052) from Abcam Inc., USA. Mouse Anti-Rac1 monoclonal antibody (Clone 23A8) from Merck Millipore Corporation, Germany. Anti-Rabbit HRP from Santacruz Biotechnology Inc., USA, while Rabbit Anti-galectin-3 polyclonal antibody was raised in in-house animal facility, ACTREC, India.

3.2 Methods

3.2.1 Cell revival, passaging and preservation

Cell lines preserved in FBS containing 10% DMSO in liquid nitrogen revived by snap thawing at 37ºC followed by adding 10 ml complete DMEM (contains 10% FBS). Further the cell pellet was obtained by centrifuging at 1200 rpm at room temperature (RT) for 10 minutes. The supernatant was discarded and cell pellet was gently resuspended in complete DMEM. This suspension was dispensed in tissue culture dishes or flasks and cultured at 37ºC, 5% CO_2 in the humidified incubator.

For sub-culturing or passaging the adherent cells were washed 2 times with autoclaved sterile PBS, pH 7.4 to remove the serum. Adherent cells were incubated with TPEG solution (contains 0.25% Trypsin, 0.02% EDTA, 0.05% Glucose prepared in autoclaved sterile PBS, pH 7.4 and filtered using 0.1 µm filter) for 60 seconds to break the contacts of these cells with surfaces of culture plates. After this double the volume of complete DMEM was added to inhibit trypsin action. The cells were flushed, collected and centrifuged at 1200 rpm at RT for 10 minutes. The supernatant was discarded and cell pellet was gently resuspended in complete DMEM. This suspension was dispensed in tissue culture dishes or flasks and cultured at 37ºC, 5% CO_2 in the humidified incubator. Alternatively, these cells were used for experimental purpose or the cell pellet was resuspended in FBS containing 10% DMSO (cell density was adjusted approximately $2.5x10^6$/ml) and subjected for serial cooling and finally stored or preserved in liquid nitrogen.

3.2.2 Preparation of total cell lysate

The total cell lysate was prepared by harvesting the cells. The harvested cells were washed with PBS, pH 7.4 for three times by resuspending the pellet and centrifuging at 1200 rpm at 4ºC for 10 minutes. Approximately for the $15x10^6$ cells, 1 ml of lysis buffer (20 mM Tris pH 7.5, 150 mM Nacl, 1% NP40, 0.5% Sodium deoxycholate, 1 mM $CaCl_2$, 1 mM $MgCl_2$ and 1x protease inhibitor

cocktail) was added. The lysed cells were sonicated using sonicator at 50% output for 3 cycles at 5 minutes time interval between each cycle in cold conditions. Cell lysate was centrifuged at 16000 rpm, 4^{o}C for 30 minutes. The supernatant was collected and the amount of the protein was estimated.

3.2.3 Preparation of cell lysate for probing phosphorylated proteins (pAkt and pErk)

B16F10 cells were grown for 24 hour in serum free conditions and harvested using 0.01% EDTA and 0.05% glucose. To study the effect of pharmacological inhibitors the cells were incubated for 1 hour either with 500 nM wortmannin (Wm), 25 µm PD98059 (PD) or 0.1% DMSO (vehicle control (VC)) before harvesting them. The harvested cells were washed and 4x10^{6} cells were seeded on galectin-3 or fibronectin coated 90 mm plates for 15, 30 and 60 min time interval. At respective time points, non-adherent cells in each plate were removed and 1 ml lysis buffer (50 mM Tris·Cl pH 7.4, 150 mM NaCl, 1% NP40, 1% sodium deoxycholate, 0.1% SDS, 1 mM EDTA, 1 mM EGTA, 1x phosphatase and protease inhibitor cocktail) was added to the plate. The cells were collected, sonicated and centrifuged at 15000 rpm, for 30 min at 4^{o}C. The protein content in these cell lysates was estimated. The cell lysed at 0 min time point served as control. An equal amount of protein in each cell lysate was loaded on SDS-PAGE, transferred on PVDF membrane and immunoblotted for Akt, pAkt, Erk and pErk.

3.2.4 Protein estimation using modified Peterson Lowry method

Modified Peterson's Lowry method was used to estimate the protein content [168]. 1 mg/ml BSA stock solution was used to prepare the standards of range 5-30 µg to obtain the standard curve. In 1 ml of distilled water, mix the appropriate volume protein samples. Then add the CTC regent [equal volumes of Solution A (0.1% Copper Sulphate, 0.2% Sodium Potassium Tartarate and 10% Sodium Carbonate), 10% SDS, 0.8 N NaOH, and distilled water] and incubate for 10 minutes. 0.5

ml of six times diluted Folin and Ciocalteau's reagent was then added to each tube and mixed by vortexing. The samples were incubated for 30 minutes at room temperature in dark and the absorbance was measured at 750 nm using a UV Spectrophotometer.

3.2.5 Sodium Dodecyl Sulphate Polyacrylamide Gel Electrophoresis (SDS-PAGE)

SDS-PAGE was performed to resolve the proteins based on the molecular size. It was performed exactly as described in Ref. [169]. 30% Acrylamide (29.2% acrylamide and 0.8% N,N'-methylene-bisacrylamide) was mixed with 1 M Tris base (pH 8.8) and 20% SDS, in order to obtain the desired resolving gel concentration containing 0.37 M Tris-Base and 0.1% SDS. Fifty micro litres each of ammonium persulphate (20% w/v) and TEMED (Tetraethylmethyl ethylene diamine) 10% (v/v) were added and the gel was poured between sealed glass plates with spacers. A stacking gel (4.5% Acrylamide, 0.0625 M Tris pH 6.8, 0.2% SDS), was overlaid on the polymerized resolving gel. The protein samples were boiled for 5 minutes with or without β-mercaptoethanol in sample buffer (0.0625 M Tris pH 6.8, 2% SDS, 10% glycerol (w/v), 750 mM β-mercaptoethanol and 0.05% Bromo Phenol blue) and loaded into wells. Electrophoresis was done using electrode buffer (0.025 M Tris.chloride, 0.2% SDS (w/v) and 0.192 M glycine) at 100 Volts (constant voltage). Finally, protein bands on the gels were detected by staining with either 0.2% Coomassie Brilliant Blue (CBB, in 50% methanol, 10% acetic acid and 40% distilled water), or by silver staining or proteins were transferred to polyvinylidene diflouride (PVDF) membrane for blotting.

3.2.6 Western Blotting

The transfer of proteins from the gel to a PVDF membrane was done as per Towbin H. *et al*. [169] The resolving gel was equilibrated in chilled transfer buffer (0.025 M Tris, 0.192 M Glycine, and 20% Methanol) for 15 minutes. The membrane was pretreated with methanol for activation, super-imposed on the gel and the transfer apparatus was set as per manufacturer's instructions. Transfer

of proteins to the membrane was carried out with chilled transfer buffer using a constant voltage of 70 Volts for 3 hours. Extent of protein transferred to the membrane was checked by soaking in 0.2% (v/v) Ponceau–S stain in 3% trichloroacetic and 3% sulphosalicylic acid, for 2 minutes. The stain was later washed off with Tris Buffered Solution (TBS-20 mM Tris and 500 mM NaCl).

3.2.7 Probing of PVDF membrane/western blots with specific antibodies

The PVDF membranes blotted with protein were blocked with either 3% BSA or 5% milk and probed with their specific primary antibodies and secondary HRP conjugated antibody. Concentration of primary antibodies and their respective secondary HRP conjugated antibody is listed in Table 1. The blots were developed using Enhanced Chemiluminiscent (ECL plus) reagent.

Table 1: Lists of specific antibodies used for the study, their concentration and incubation time

Name of Antibody	Blocking (1 hour at room temperature)	Primary Antibody	Secondary Antibody (1 hour at room temperature)
Akt	5% BSA	1:8000 in 5% BSA for overnight at 4^{o}C	1 µg/ml Anti-Rabbit HRP in 1% BSA
phospho-Akt	5% BSA	1:1000 in 5% BSA for overnight at 4^{o}C	1 µg/ml Anti-Rabbit HRP in 1% BSA
Erk	5% BSA	1:5000 in 5% BSA for overnight at 4^{o}C	1 µg/ml Anti-Rabbit HRP in 1% BSA
phospho-Erk	5% BSA	1:1000 in 5% BSA for overnight at 4^{o}C	1 µg/ml Anti-Rabbit HRP in 1% BSA
Rac1	5% Skimmed milk	1:2000 in 3% Skimmed milk for overnight at 4^{o}C	0.5 µg/ml Anti-mouse HRP in 3% Skimmed milk
CD147	3% BSA	1:3000 in 1% BSA for 1 hour at room temperature	1 µg/ml Anti-Rabbit HRP in 1% BSA
β-Actin	3% BSA	0.1 µg/ml in 1% BSA for 1 hour at room temperature	0.5 µg/ml Anti-mouse HRP in 1% BSA
GFP	5% Skimmed milk	0.5 µg/ml in 2.5% Skimmed milk for 1 hour at room temperature	1 µg/ml Anti-Rabbit HRP in 1.5% Skimmed milk

3.2.8 Extraction, purification and characterization of recombinant human galectin-3

Purification of galectin-3 was carried out using *E. coli* BL star 21 (containing pET3c plasmid coding for recombinant human (rh) Galectin-3). *E. coli* BL star 21 expressing full length human recombinant galectin-3 has a kind gift from Dr. Hakon Leffler. The steps involved in purification of galectin-3 are as follows;

3.2.8.1 Cultivation of *E. coli* BL star 21 and induction of galectin-3

E.coli BL star 21 which has preserved as 30% glycerol stock culture at -80°C was thawed and a loopful inoculated on Luria-Bertanii (LB) Ampicillin (amp) agar plate containing 100 µg/ml Ampicillin by streak plate method. Isolated colonies growing on this plate after incubation at 37ºC for 24 h were used as starter culture for galectin-3 production. 100 ml of LB broth containing 100 µg/ml ampicillin was inoculated with a single isolated colony from the culture grown on LB-amp agar. The broth was incubated at 37ºC overnight in shaker incubator. A firm cell pellet was obtained by centrifuging the entire volume of the overnight grown culture at 5000 rpm for 10 minutes. The pellet was then washed twice using sterile physiological saline (0.85% NaCl), following which a saline suspension of the culture (~50 ml) was prepared its optical density (OD) at 600 nm was determined spectrophotometrically. This was used as the inoculum for the next step. An appropriate volume of washed saline culture was calculated and inoculated in 1 litre of LB broth containing ampicillin and its OD at 600 nm adjusted between 0.05-0.1.This ensured that cells remain in the exponential phase during protein production. The 1 litre broth culture was distributed into five (2 litre) flasks each containing 200 ml culture and incubated at 37ºC for 4 hours on shaker incubator to circumvent the lag phase. After 4 hours, Isopropyl Thio D-Galactopyranoside (IPTG) was added to the flasks at a concentration of 50 mg/litre to induce the production of galectin-3 and incubated at 37ºC for 3 hours under shaking conditions. 10 ml of

broth (5 ml from each flask) was removed in a sterile 100 ml flask before addition of IPTG. This un-induced sample was grown separately at 37ºC for 3 hours and further analyzed according to the protocol.

3.2.8.2 Preparation of bacterial cell lysate

The bacterial cell pellet was obtained by centrifuging the cells at 5000 rpm at 4ºC for 20 minutes. The pellet obtained from the total 1 litre broth was resuspended in 50 ml MEPBS lysis buffer (PBS containing 0.2 M EDTA and 4 mM β-mercaptoethanol) with 50 µl of protease inhibitor mix (1 µg/ml of each of pepstatin, leupeptin, aprotinin) and 0.3 mM PMSF made in DMSO. Bacterial cell lysate was prepared by sonication of 5 ml cell suspension by giving three cycles of 30 pulses using a 0.95 cm sonicator probe with a power output between 25-30 watts. Cell debris was removed by ultracentrifugation at 15000 rpm at 4ºC for 20 minutes. The supernatant cell lysate were collected for both the induced and un-induced samples.

3.2.8.3 Purification of galectin-3 using Lactose-Sepharose column

Lactose was coupled to Sepharose 4B beads by employing the bivalent reagent; Divinylsulfone (DVS) as per Ref. (Page 88-90, Immobilized Affinity Ligand Techniques, Academic Press). The Sepharose was cross-linked and activated with excess divinyl sulfone whose free reactive end binds to the hydroxyl group of lactose. The lactose Sepharose beads were de-gassed and resuspended in MEPBS buffer, following which it was packed into a column with glass wool packing at the bottom. Care was taken to avoid trapping of air bubbles between the beads. The column was washed with 2-3 column volumes of MEPBS containing 1 mM NaCl and 150 mM lactose and equilibrated with MEPBS buffer before use. The cell lysate was then loaded onto the column at a constant flow rate of 10-12 ml/hour and unbound fractions were collected. The column was washed extensively with MEPBS till the OD at 280 nm of the unbound fractions stabilized at

a value close to that of MEPBS buffer. Bound galectin-3 was then eluted as 1 ml fractions using MEPBS buffer containing 150 mM lactose at a flow rate of 15 ml/hour. Absorbance of the eluted fractions was then measured at 280 nm. The eluted fractions showing peak OD values were loaded on a 15% polyacrylamide gel and stained with Coomassie Brilliant blue.

3.2.8.4 Dialysis and lyophilization

The specific fractions which showed presence of galectin-3 were pooled and dialyzed overnight against 25 mM ammonium bicarbonate buffer at 4ºC to remove the excess lactose bound to galectin-3. The dialyzed protein was aliquoted, dried by lyophilization and stored at -80°C.

3.2.8.5 Characterization of purified galectin-3

The extent of induction and yield of galectin-3 in un-induced, induced, unbound and affinity purified fractions was estimated by Peterson and Lowry method. The concentration of purified galectin-3 was compared and normalized with the previous batch of pure galectin-3 by Coomassie staining of various concentrations of the two batches. The purity of galectin-3 was also confirmed by Western blotting using anti-galectin-3 antibody.

3.2.9 Methods used during all types of molecular cloning

3.2.9.1 Preparation of ultra-competent *E. coli* DH5α cells

Reagents required: SOB (300 ml) (Composition: Tryptone 6 g, Yeast extract 1.5 g, NaCl 0.15 g, KCl 5.6 g). The pH of the SOB medium was adjusted to pH 7 with 1 N NaOH, followed by the addition of 4 ml of 1 M glucose and 1 ml of 2 mM $MgCl_2$, just prior to inoculation of bacteria.

Transformation Buffer (200 ml) (Composition: PIPES 0.6 g, $CaCl_2$ 0.4 g, KCl 3.7 g). The pH was adjusted to pH 6.7 with 10 N KOH and 2.18 g $MnCl_2$ and sterilized by filtering it through 0.22 µm filter.

Ultra competent *E. coli* DH5α cells were prepared as described in. A single colony of DH5α strain of *E. coli*, from an overnight grown LB agar plate was inoculated into 250 ml of SOB medium and incubated at 18°C with mild shaking till the OD at 600 nm reached about 0.3 to 0.5. The culture was incubated on ice for 10 min followed by centrifugation at 2500 g for 10 min at 4°C to pellet the bacterial culture. The culture supernatant was discarded and the bacterial cell pellet was gently resuspended in 80 ml of ice cold transformation buffer. The cell suspension was incubated on ice for 10 min followed by centrifugation at 2500 g for 10 min at 4°C. The supernatant was discarded and the bacterial cell pellet was resuspended in 20 ml of ice cold transformation buffer containing 7% DMSO. This suspension of cells was incubated on ice for 10 min and subsequently aliquoted into nearly 200 µl aliquots in 1.5 ml micro centrifuge tubes, snap freezed into liquid nitrogen and immediately stored at -80°C until further use.

3.2.9.2 Transformation

Ultra-competent cells were transformed with different plasmid vectors. Competent cells transformed with linearized vector alone, served as negative control. Briefly, competent cells were thawed, added to the ligation mixture and kept on ice for 30 minutes. The cells were placed at 42 ºC (water bath) for exactly 90 seconds and subjected to cold shock on ice for 2-5 min. The cells were then mixed with 1 ml of sterile LB broth and incubated at 37ºC for 30 minutes in a shaker incubator. The cells were spun at 5000 rpm for 5 minutes, pellet was resuspended in 200 µl of LB broth and spread on to LB agar plate with or without containing either 100 µg/ml ampicillin or 50 µg/ml kanamycin and incubated for 24 hours at 37ºC.

3.2.9.3 Plasmid extraction using alkaline lysis method (Mini-Prep)

Individual colony has picked up and inoculated in 1 ml LB broth for plasmid extraction and was allowed to grow overnight at 37°C. Plasmid isolation from the overnight grown culture was carried

out by the alkaline lysis method. The overnight grown 1.5 ml bacterial cultures were centrifuged at 5000 rpm at 4°C for 5 min, the medium was removed and the pellets were dried. To the dried bacterial pellets, 100 µl of alkaline lysis solution I (GTE buffer: 50 mM Glucose, 25 mM Tris pH 8.0 and 10 mM EDTA) was added and vortexed till the pellets were completely dissolved. Then, 200 µl of alkaline lysis solution II (0.2 N NaOH and 1% SDS) was added, mixed gently by inverting and kept for 2 min 150 µl of ice-cold alkaline lysis solution III (3 M potassium acetate pH 4.8 in glacial acetic acid) was then added to each tube and kept on ice for 10 min. The tubes were then centrifuged at 13000 rpm, 4°C for 15 min and the supernatants containing the renatured plasmids were transferred to fresh tubes. Equal volume of phenol: chloroform: isoamylalcohol (25:24:1) was added to supernatant for removal of proteins and saccharides, mixed by vortexing and centrifuged as above for 5 min. The aqueous phase was transferred to a fresh microcentrifuge tube and double the volume of absolute alcohol was added and mixed well for precipitation of plasmid DNA. Tubes were kept on ice for 15 min and centrifuged at the above conditions for 20 min. The ethanol was removed and the pellets were washed with 70% chilled ethanol to remove salts, centrifuged as above for 5 min and all the traces of ethanol were removed. The pellets were completely dried at 37°C for 30 min. The dried pellets were reconstituted in 20 µl of autoclaved distilled water. 0.3 µl of RNase (1 µg/ml) was added to each tube and incubated at 37°C for 45 min to degrade RNA molecules.

3.2.9.4 Maxiprep for large scale plasmid DNA extraction

Maxiprep is different from that of Miniprep as the starting *E. coli* culture volume is 100-200 ml LB broth. Maxiprep was performed using kit based method from Sigma Aldrich. 200 ml of overnight grown culture was pelleted by centrifugation at 5000 g for 10 min. The pellet was resuspended in 12 ml resuspension solution and vortexed until the pellets were completely

dissolved. Cells were lysed by adding 12 ml of lysis solution and mixed thoroughly by gently inverting the tubes for 6-8 times and the tubes were kept at room temperature for 3 min. 12 ml of chilled neutralization solution was added to neutralize the lysed cells resulting in the formation of a white aggregate (cell debris, proteins, lipids, SDS and chromosomal DNA). Then 9 ml of binding solution was added to the pellet and poured into the barrel of the filter syringe and were incubated for 5 min at room temperature so that the white aggregate floated to the top. During incubation, the binding column was prepared by adding 12 ml of column preparation solution and was centrifuged at 5000 g for 5 min. By holding the filter syringe barrel over binding column, the plunger was gently inserted to expel the clear lysate into the column. The binding column was then spun in a swinging bucket rotor at 3000 g for 2 min and the eluent was discarded. The column was then washed with wash solution 1 and 2 and centrifuged at 5000 g for 2 min and 5 min respectively. The column was then transferred to a fresh 50 ml collection tube and 3 ml of elution solution was added and was kept at room temperature for 20 min and was then centrifuged at 5000 g for 5 min for the elution of DNA.

3.2.9.5 Screening of recombinant clones

Individual colonies that were grown on LB agar plates after transformation were picked up and inoculated into 1 ml LB broth and allowed to grow overnight at 37°C. Plasmids were extracted from them by alkaline lysis method and recombinant clones were screened by restriction digestion.

3.2.10 Cloning, expression and purification of human and mouse origin truncated galectin-3

3.2.10.1 Human truncated galectin-3 (htGal-3)

E. coli BL star 21 expressing full length human recombinant galectin-3 is a kind gift from Dr. Hakon Leffler. The full length coding DNA sequence (CDS) of galectin-3 is in pET3c bacterial expression plasmid vector. This plasmid was isolated using Miniprep and acts as template for

amplifying CDS of truncated galectin-3. The CDS of galectin-3 is 753 bp. Galectin-3 consists of 250 amino acids in which N-terminal oligomerization domain, middle collagen like repeating sequence and C-terminal carbohydrate recognition domain (CRD). Towards the C-terminal region 135 amino acids compromise the CRD of galectin-3 [170]. This region was amplified and cloned in pET3a bacterial expression vector using following primers.

Forward primer with SalI and NdeI restriction site

5' ATAGTCGACCATATGGTGCCTTATAACCTGCCT 3'

Reverse primer with BamHI site

5' GGCGGATCCTTATATCATGGTATATGAAGC 3'

Initially, using PCR the CRD region (408 bp) was amplified using above mentioned primers and template. The amplified product was resolved on agarose gel electrophoresis and cut purified using Gel Extraction kit according to manufacturer's protocol. The purified amplified 408 bp product (Insert) and pET3c plasmid (Vector) was independently double digested with NdeI and BamHI at 37^{o}C overnight. After digestion insert was again purified using PCR Cleanup kit according to manufacturer's protocol while vector was resolved on agarose gel electrophoresis and cut purified using Gel Extraction kit according to manufacturer's protocol. The ligation was carried out using double digested, purified insert and vector at 22^{o}C, overnight. The ligated product was transformed in ultra-competent *E. coli* DH5α strain and screen was performed for positive plasmid clone.

The positive clone was sequenced and its DNA sequence confirmed using In-house sequencing facility. This positive clone was then transformed in *E. coli BL21 (DE3)* bacterial expression strain. The recombinant human truncated galectin-3 (containing CRD region only) was purified using freshly prepared Lactose-Sepharose column. The methodology is same as for the purification of full length human recombinant galectin-3 expect the IPTG concentration. IPTG concentration used

in this case was 1 mM. Finally, the identity and sequence of the protein was confirmed by mass spectrometry and purity and quality was confirmed by coomassie staining and Western blot.

The pET3a vector map used for cloning of tgal-3:

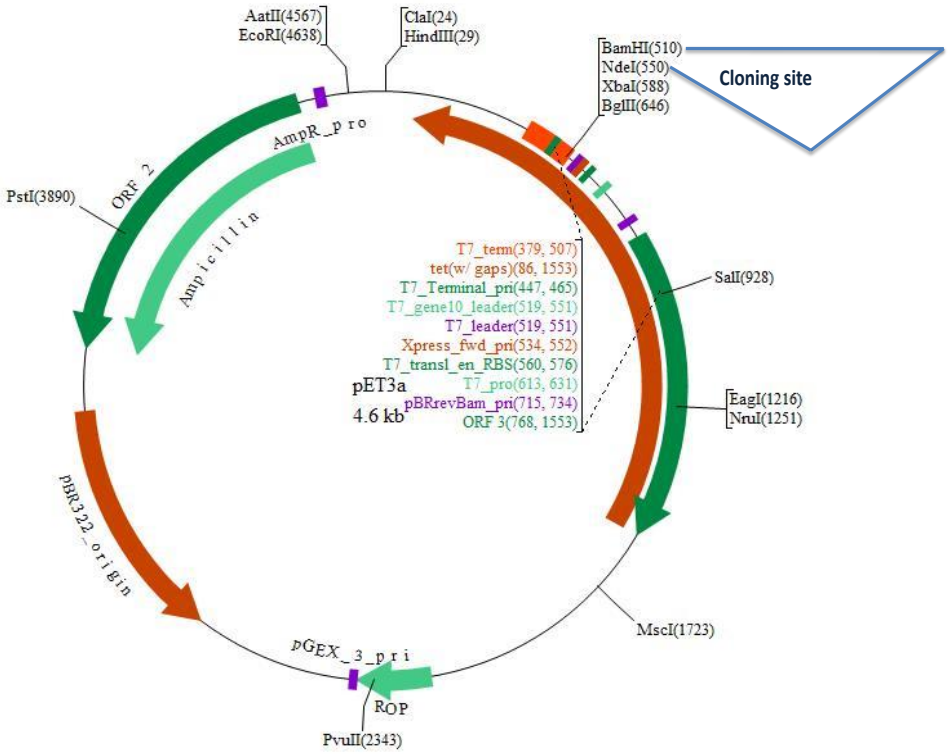

Table 2. PCR conditions used for amplification of htGal-3 from pET3c plasmid

Step	Temperature (^{o}C)	Time (min)	Components	Volume (µl)
1. Initial denaturation	95	5	10x PCR buffer	2.5
2. Denaturation	95	0.5	10 mM dNTPs	0.5
3. Annealing	56	0.5	25 mM $MgCl_2$	1.5

4. Extension	72	0.5	Forward primer (10 þmol/µl)	1
5. No. of cycles	Go to step 2 for 34 times		Reverse primer (10 þmol/µl)	1
6. Final extension	72	10	Taq polymerase (5 U/µl)	0.25
7. End			Distilled water	15.25
			DNA template	2

3.2.10.2 Mouse truncated galectin-3 (mtGal-3)

The coding DNA sequence of C-terminal CRD of mouse origin of galectin-3 was cloned into the pET3a bacterial expression vector using forward 5'ATAGTCATCATATCATCATAGTCGATCATATGGTGCCC3' and reverse 5'GGTGGATCCTTAGATCATGGCGTGGTTAGC3' primers. The total RNA was extracted from B16F10 murine melanoma cells and converted it into cDNA using first strand cDNA synthesis kit according to manufacturer's protocol. This cDNA served as a template for PCR reaction to amplify CRD.

The strategy of cloning including PCR conditions, expression, purification and characterization was same as for human truncated galectin-3. The expressed protein was of 15.4 kDa (Mouse origin galectin-3 comprised with 264 amino acids, in which CRD is 130^{th} - 264^{th} amino acid of full length galectin-3 (408 bp)). The mtGal-3 protein was purified using lactose sepharose column.

3.2.11 Mass spectrometry for identification of galectin-3

The molecular weight and identity of purified truncated galectin-3 was confirmed by mass spectrometry (MS) and MS/MS respectively. The purified truncated galectin-3 protein was loaded on SDS-PAGE. After coomassie staining of the gel, band at the region of ~17 kDa was cut into 1 mm cube pieces and transferred to a 1.5 ml eppendorf tube. Washing of gel pieces was done with 50 mM NH_4HCO_3 and acetonitrile to destain the gel pieces. After the gel pieces had shrunken and destained it was dried in a speedvac centrifuge.

In next step of reduction and alkylation, gel pieces were swelled in freshly prepared 10 mM dithiotreitol/50 mM NH_4HCO_3 and incubated for 45 min at 56^oC. The excess of liquid was removed and replaced with freshly prepared 55 mM iodoacetamide (light sensitive) in 50 mM NH_4HCO_3 and incubated for 30 min at room temperature. After incubation iodoacetamide solution removed and gel pieces were washed with 50 mM NH_4HCO_3 and acetonitrile (1+1, v/v) twice for 15 minutes each time. After gel pieces have shrunk, acetonitrile was removed and gel pieces were dried in speedvac.

In gel digestion was performed using trypsin. Trypsin enzyme (prepared in 25 mM NH_4HCO_3) was added to gel pieces and incubated at 37^oC for 30 minutes. After incubation, excess trypsin was removed and then incubated at 37^oC overnight approximately 2-3 µl of 25 mM NH_4HCO_3 solution was added to keep gel wet overnight. The overnight trypsin digested protein peptides were extracted from gel pieces using extraction buffer (equal volumes of acetonitrile (ACN) and trifluroacetate (TFA)) and ultrasonicated for 30 minutes and then vacuum dried.

After the sample was vaccume dried, 10% ACN and 0.1 % TFA solution was added and centrifuged for 2 minutes and then kept on ice. This sample was mixed with matrix and subjected to mass spectrometry. Sample was ready for mass spectrometric peptide analysis and was analyzed by mass spectrometry using MASCOT software. To identify the molecular weight the whole

protein spectra (undigested protein) was obtained by directly mixing the purified protein with the matrix and subjected for mass spectrometry

3.2.12 Preparation of modified citrus pectin (MCP) from citrus pectin (CP)

MCP was prepared exactly as described in Ref. [12]. Briefly, CP was solubilized as a 1.5% solution in distilled water, and its pH was increased to 10.0 with NaOH (3 N) for 1 hour at 50–60°C. The solution was then cooled to room temperature while its pH was adjusted to 3.0 with 3 N HCl and stored overnight. Samples were precipitated the next day with 95% ethanol and incubated at –20 °C for 2 hours, filtered, washed with acetone, and dried on Whatmann filters. For oral feeding of the mice, 1-1.5% solution of MCP was prepared in autoclaved water, its pH was adjusted to approximately 7.0.

3.2.13 Generation of bone marrow chimeric mice

Bone marrow chimeric mice were generated exactly as described by Mace K.A. *et al*. [171]. Briefly, the 8-10 week old galectin-$3^{-/-}$ (galectin-3 null) female mice were lethally irradiated (10 Gy). The bone marrow cells were harvested from 8-10 week old galectin-$3^{+/+}$ (galectin-3 wild type) mice and galectin-$3^{-/-}$ female mice by flushing the femur and tibia with DMEM. The bone marrow in irradiated galectin-$3^{-/-}$ mice was replaced, in group 1 with that from galectin-$3^{-/-}$ mice which served as control, while in group 2 with that from galectin-$3^{+/+}$ mice by injecting $1x10^6$ cells through retro-orbital plexus after 6 h of irradiation. Mice were treated with antibiotics for 2 week to establish the bone marrow. The lethally irradiated 2 mice were kept as a control, died in 10 days due to lack of bone marrow cells. Chimerism was confirmed by genotyping of these mice using tail and blood genomic DNA by PCR as described by Hsu D.K. *et al*. [172]. These bone marrow chimeric mice were used to perform experimental metastasis assay using B16F10 cells.

3.2.14 Genotyping

Genomic DNA for genotyping was prepared from either tail or blood of adult mice as per. Hsu D.K. *et al*. [171,172]. Galectin-3 status of the littermates was determined by PCR using genomic DNA obtained from the tails of the 3-4 week mice. PCR was performed using 1 μg genomic DNA and primers: PRIMER 1 (a primer annealing to the neo cassette region) 5'GGCTGACCGCTTCCTCGTGCTTTACGG3', PRIMER 2 (a primer annealing to the non-disrupted region of intron 4 of intact galectin-3 gene) 5'GTAGGTGAGAGTCACAAGCTG GAGGCC3' and PRIMER 3 (a common downstream primer annealing to EXON 5) 5'CAC TCTCAAAGGGGAAGGCTGACTGTC3'. The PCR was carried out and the PCR product was analyzed on 2% agarose gel by electrophoresis followed by ethidium bromide staining. galectin-$3^{+/+}$ mice give an amplicon of 450 bp, galectin-$3^{+/-}$ (galectin-3 hemizygous/heterozygous) mice give 2 amplicons of 450 bp and 300 bp while galectin-$3^{-/-}$ mice give an amplicon of 300 bp.

3.2.15 Experimental metastasis assay using B16F10 cells

Experimental metastasis assay was performed as described in Ref. [173]. Briefly, experimental metastasis assay was performed by injecting serum free 0.1 million B16F10 in plain DMEM through tail vein. The lungs were harvested after scarifying mice on either 17^{th} or 19^{th} day after injection of the cells. The lung metastatic colonies were counted using dissecting microscope.

For treatment of cells with glycosylation inhibitors, melanoma cells were allowed to grow to 50% confluency before adding swainsonine (2 μg/ml) [111]. The cells were harvested after 24 h, washed once in DMEM containing 10% FBS, and twice in DMEM. These cells were further used for experimental metastasis assay.

For injecting B16F10 cells treated with htGal-3 or mtGal-3, 0.1 million B16F10 cells were pre-incubated with 0.1 ml of 500 μg/ml of htGal-3 or mtGal-3 for 1 h on ice. The mice that received

pre-treated cells also received injections of htGal-3 or mtGal-3 (250 µg in 0.1 ml, via intra muscular injection) on day 1 (2 h before and after injection of cells) and once on day 2.

For injecting B16F10 cells treated with MCP, 0.1 million B16F10 cells were resuspended in medium with and without MCP (0.05%) and mice which received cells with MCP were on drinking water containing 1% or 1.5% MCP from 5 days prior to injection till the day of sacrifice.

In bone marrow chimeric mice B16F10 cells were injected in both group 1 and group 2 through tail vein.

3.2.16 Cell spreading assay

Cell spreading assay was done exactly as described in Ref [174]. Briefly, Melanoma cells were harvested and washed thrice with serum free DMEM. 1 ml of melanoma cell suspension containing 0.5 X 10^6 /ml in serum free DMEM were seeded on uncoated or precoated coverslips either with 75 µg/ml galectin-3 or 10 µg/ml fibronectin incubated overnight at 4ºC. (For all the experiments same concentration of galectin-3 and fibronectin was used. The volumes used for coating was 1 ml for 35 mm, 2 ml for 60 mm and 4 ml for 90 mm plates). The cells were then incubated at 37ºC for 15, 30, 45 and 60 minutes time points in a CO_2 incubator. Cells were seeded on uncoated coverslip incubated for either 45 min or 60 min served as control. After each time points, the non-adherent cells were removed by gentle washing 3-4 times with 1 ml PBS (pre-warmed to 37ºC). The adherent cells were fixed in 1 ml of 4% paraformaldehyde solution (pre-warmed to 37ºC) for 5 minutes in a CO_2 incubator. The 4% paraformaldehyde fixative solution was prepared as follows- 4 g of paraformaldehyde was dissolved in 80 ml PBS and kept for boiling. A drop of 1 N NaOH was added to aid in dissolution. After cooling, the pH of the solution was checked, adjusted to 7 and the volume was made up to 100 ml with PBS. The solution was filtered and kept at 37ºC. The fixative was removed by giving 4 gentle washes with pre-warmed PBS for 5 minutes following

which the cells were permeabilized with 1 ml of 0.5% Triton-X 100 in PBS at room temperature for 15 minutes. The cells were gently washed to remove Triton-X 100 using PBS (4-5 washes) for 5 minutes. Further staining was performed in dark to avoid quenching of fluorescent dyes. The Phalloidin staining solution was prepared just before use.

Preparation of Phalloidin staining solution: The following solutions were added in the order given below (For 100 µl solution) and kept at 37^{o}C in dark. Lysolecithin (10 µg/µl) 1 µl, Methanol (AR Grade) 10 µl, BSA (Stock 4% in PBS) 1.25 µl, Phalloidin-TRITC (2 mg/ml stock, in methanol) 1 µl, PBS (pH 7.4) 86.75 µl.

The coverslips was placed in a moist chamber on a parafilm and the Phalloidin staining solution was added either on the coverslips (15 µl staining solution). Alternatively, the coverslips were inverted on 10 µl of staining solution and incubated at 37^{o}C for 15 min. The coverslips were then overlaid with 4 % BSA without removing staining solution (final BSA conc. 2 %) or were inverted on 10 µl 2% BSA solution, and incubated at room temperature for 10 min. The cells were washed with PBS at room temperature for four times for 5 min. The nuclei of the cells were stained by inverting the coverslips on 10 µls of 5 µg/ml of DAPI in PBS (4', 6'- Diamidino-2-Phenylindole Dihydrochloride) for 1-2 minutes followed by 3-4 washes with PBS. The stained cells were mounted on glass slides by inverting the coverslips on 10 µls of Anti-fading agent such as Vectashield. The excess mountant was removed by pressing the inverted glass slide on tissue paper and the edges of the coverslips were sealed with nail paint to prevent drying. The images were acquired using a Carl Ziess Laser confocal Microscope at 63x magnification.

To assess the effect of tgal-3 and MCP cell spreading assay was performed by treating the B16F10 cells in presence of tGal-3 (75 µg/ml, 1 h incubated on ice) or MCP (0.5%) on galectin-3 coated coverslips.

To assess the effect of pharmacological inhibitors on cell spreading, adherent murine melanoma cells were pre-incubated for 1 hour either with 500 nM Wm or 25 µm PD98059 (PD) in 0.1% DMSO. Cells incubated in 0.1% DMSO served as a vehicle control (VC). Later the cells were harvested and cell spreading assay as described above was performed.

3.2.17 Generation of stable B16F10 cell line expressing green fluorescent actin (GFP-Actin)

The total RNA was extracted from B16F10 murine melanoma cells using TriZol reagent. The total RNA was converted into the total cDNA using first strand cDNA synthesis kit according to the manufacturer's protocol. The coding DNA sequence (CDS) of actin (375 aa acid protein) was specifically PCR amplified from total cDNA using forward primer with EcoRI and reverse primer with BamHI site. This amplified 1.128 kb actin CDS (Insert) was resolved on agarose gel and cut purified using Gel extraction kit. The insert and pmGFPC1 vector was independently double digested with EcoRI and BamHI restriction enzymes. After digestion insert was again purified using PCR Cleanup kit while vector was resolved on agarose gel electrophoresis and cut purified using Gel Extraction kit according to manufacturer's protocol. The ligation was carried out using double digested, purified insert and vector at 22^{o}C, overnight. The ligated product was transformed in ultra-competent *E. coli* DH5α strain and screen was performed for positive plasmid clone. The positive clone was sequenced and its DNA sequence confirmed using In-house sequencing facility. In order to clone florescent actin into the lentiviral vector, the CMV-GFP-Actin was amplified from pmGFPC1 vector using forward primer (with no restriction site) and reverse primer with NotI site. The amplified 2.487 kb product was digested with NotI while pTRIPz lentiviral vector was sequentially digested with XbaI, blunting enzyme DNA polymerase I (large klenow fragment) and Not1. This digested insert and vector was ligated and obtained colonies after transformation were

screened. The positive plasmid clone was sequenced and its DNA sequence confirmed using In-house sequencing facility.

Primers used for amplifying and cloning CDS of actin into pmGFPC1:

Forward primer 5'GCGGAATTCTATGGATGACGATATCGCTGCG3'

Reverse primer 5'TATGGATCCCTAGAAGCACTTGCGGTGCAC3'

Primers used for amplification and cloning of CMV-GFP-Actin from pmGFPC1 vector into pTRIPz:

Forward primer 5'CGGGACGCGTTAGTTATTAATAGTAATCAATTACGGGG3'

Reverse primer 5'AATAATAGCGGCCGCCTAGAAGCACTTGCGGTGCA3'

This pTRIPz lentiviral vector constitutively expressing GFP-Actin under CMV promoter was co-transfected with helper plasmids (pMD2.G and psPAX2) in HEK293FT cells for generating virus particles which were used for transduction of B16F10 cells. The transduced B16F10 cells selected using puromycin (1 µg/ml). The mixed population of stable B16F10 cells expressing GFP-Actin maintained in DMEM containing 0.5 µg/ml puromycin.

Vector maps used for cloning of Actin:

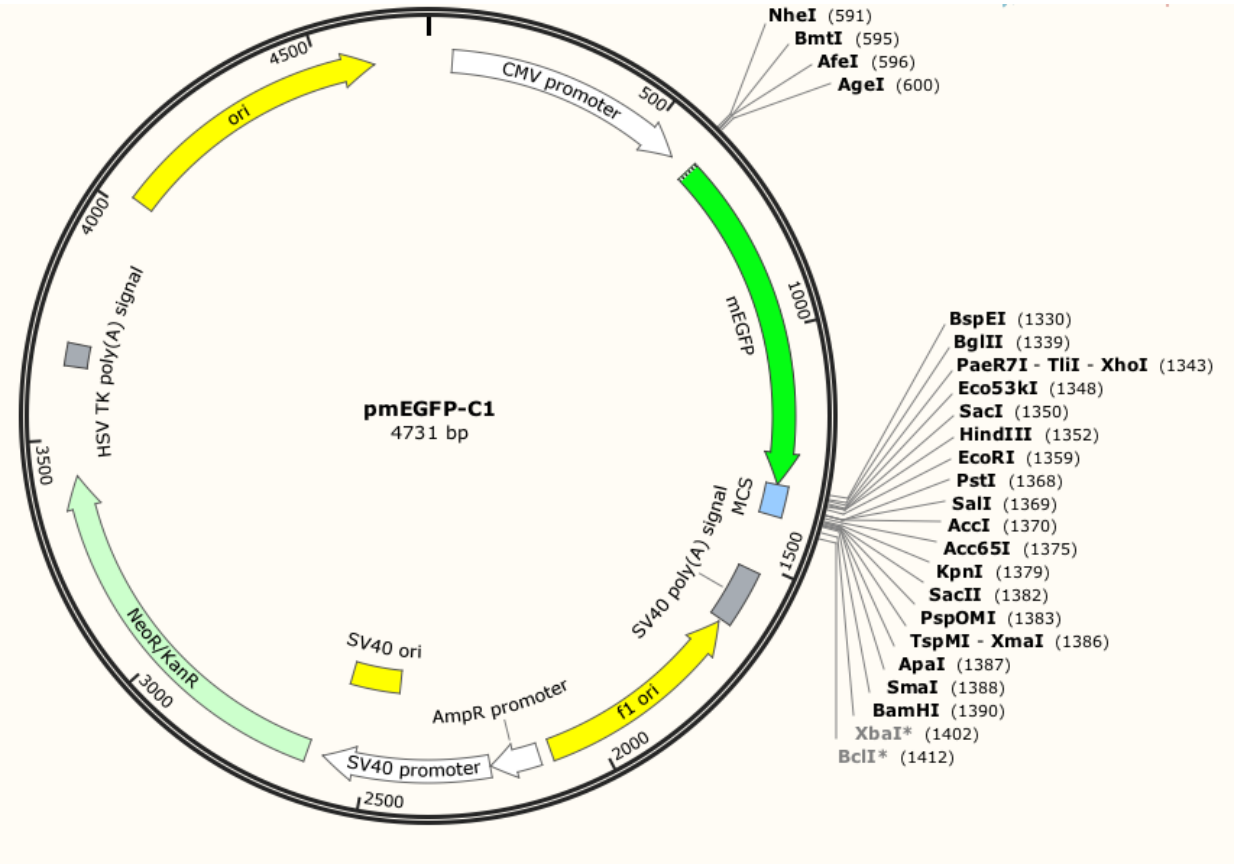
pmEGFP-C1
4731 bp
CMV promoter
mEGFP
MCS
SV40 poly(A) signal
f1 ori
SV40 promoter
AmpR promoter
SV40 ori
NeoR/KanR
HSV TK poly(A) signal
ori
500
1000
1500
2000
2500
3000
3500
4000
4500
NheI (591)
BmtI (595)
AfeI (596)
AgeI (600)
BspEI (1330)
BglII (1339)
PaeR7I - TliI - XhoI (1343)
Eco53kI (1348)
SacI (1350)
HindIII (1352)
EcoRI (1359)
PstI (1368)
SalI (1369)
AccI (1370)
Acc65I (1375)
KpnI (1379)
SacII (1382)
PspOMI (1383)
TspMI - XmaI (1386)
ApaI (1387)
SmaI (1388)
BamHI (1390)
XbaI* (1402)
BclI* (1412)

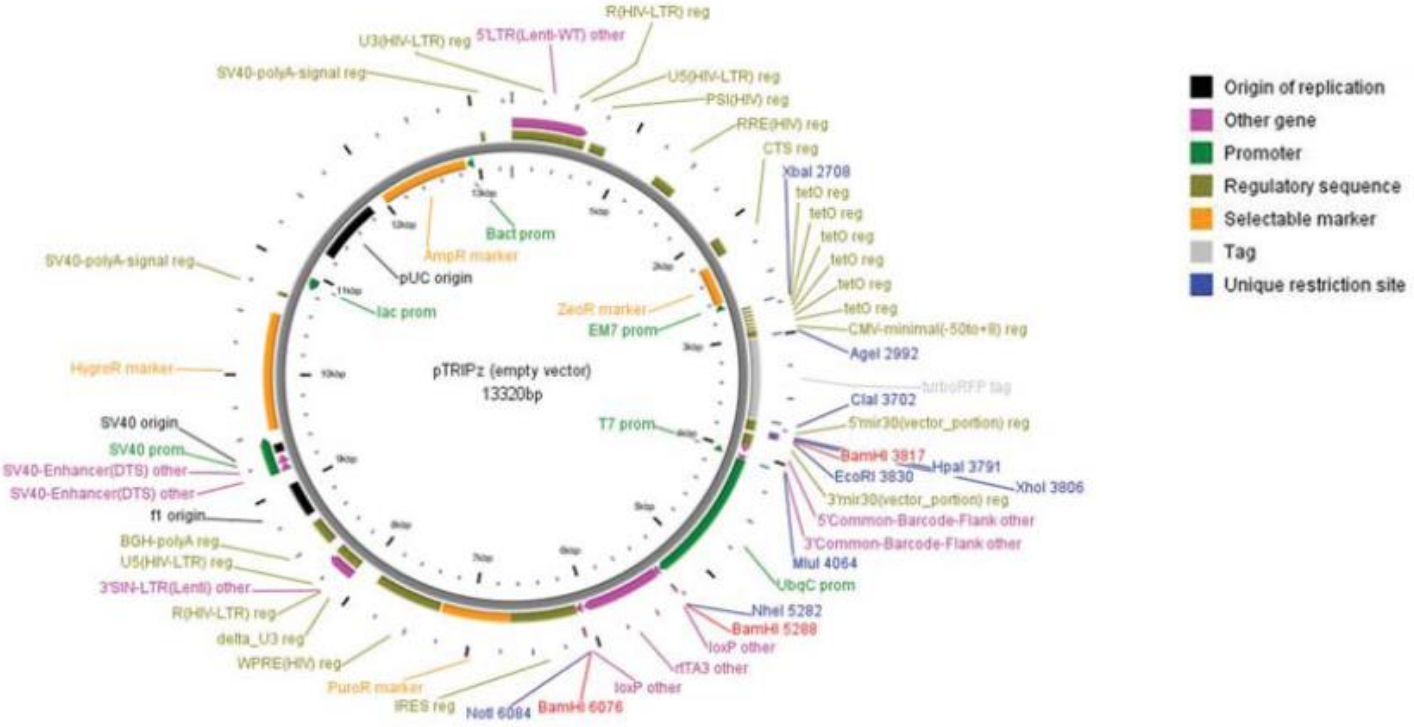

Strategy for cloning of actin into the lentiviral vector:

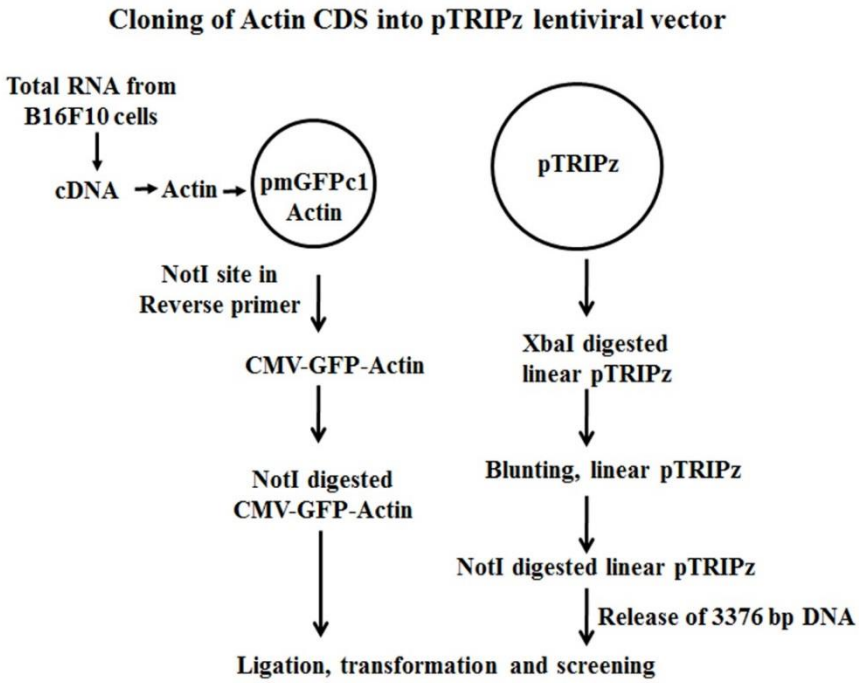

Table 3. PCR conditions for amplification of Actin and CMV-GFP-Actin

Step	Temperature (°C)		Time (sec)		Components	Volume (µl)	
	Actin	CMV-GFP-Actin	Actin	CMV-GFP-Actin		Actin	CMV-GFP-Actin
1. Initial denaturation	94	94	45	180	5x phusion PCR buffer	4	4
2. Denaturation	94	94	15	30	10 mM dNTPs	0.4	0.4
3. Annealing	56	56	15	20	Distilled water	11.4	12.6
4. Extension	72	72	60	45	Forward primer (10 þmol/µl)	1	1
5. No. of cycles	Go to step 2 for 34 times				Reverse primer (10 þmol/µl)	1	1
6. Final extension	72	72	900	600	DNA polymerase	0.2	0.2 (phusion)
7. End					DNA template	cDNA from	0.8 (Actin

		B16F10	pmGFP C1)

3.2.18 Live cell imaging

Live cell imaging was performed to study the kinetics of cell spreading on immobilized galectin-3 and fibronectin. The 35 mm glass bottom tissue culture dishes were coated either with 75 µg galectin-3 or 10 µg of fibronectin in 1 ml PBS and incubated overnight at 4ºC. B16F10 cells stably expressing GFP-Actin were harvested and washed thrice with serum free DMEM devoid of phenol red and density was adjusted to $5x10^4$ cells /ml in serum and phenol red free DMEM. The coating solution was removed and 1 ml of melanoma cell suspension was seeded on these coated plates. Live cell imaging was performed for 1 hour and the images were acquired in a single plane at 1 min time interval on these cells maintained at 37ºC in a 5% CO_2 incubator, using Olympus 3i spinning disc microscope at 60x magnification.

The live cell imaging of B16F10 cells during wound closure (as per wound healing assay) grown on galectin-3 and fibronectin coated coverslips was performed for 16 h at 37ºc in CO_2 incubator and the cells were fixed and stained with phalloidin-TRITC for F-actin and DAPI to stain the nucleus. Images were acquired using Leica STED confocal microscope at 40x magnification.

3.2.19 Fluorescence Recovery After Photo-bleaching (FRAP)

Actin turnover in the lamellipodial region was assessed using FRAP. As mentioned above for live cell imaging, the melanoma cells stably expressing GFP-Actin were seeded on uncoated and galectin-3 or fibronectin coated petri dishes in serum and phenol red free DMEM and incubated for 4 hours at 37ºC in a 5% CO_2 incubator. The bleaching is performed at the lamellipodial region using 488 nm laser at 100% laser power and 100% iterations in order to achieve at least 85% bleaching. The 4 pre-bleached images were acquired and after bleaching images were acquired at

1 second time interval for up to 4 minute in the bleached region using LSM780 Carl Zeiss confocal microscope at 63x magnification. Three independent FRAP experiments were performed for each substrate. In each experiment at least 10 cells were bleached. The percent recovery was calculated as described in Ref. [175] and plotted using Graphpad software.

3.2.20 Wound healing assay

Wound healing assays were performed in 6 well plates either on BSA or coated with galectin-3 or fibronectin. Uncoated culture dishes, coated only with BSA served as control. Non-specific sites on the plates were blocked with 2% BSA in PBS for 1 hour at 37ºC. Melanoma cells were harvested and seeded on coated plates at a density of 0.6 X 10^6 cells in 2 ml of complete DMEM and incubated at 37ºC for 24 hours in a CO_2 incubator. The cells were washed free of serum and grown under serum free conditions for 24 hours for cell synchronization and to reach 95% confluency. A straight, uniform wound was made using a 2 µl micropipette tip. The dislodged cells were washed off and cells were maintained in serum free DMEM. Uncoated culture dishes, blocked only with BSA served as control. Wound closure of cells was measured for 16 hours by time lapse video imaging of at least three different positions across the length of the wound using a Carl Zeiss Inverted Microscope. Mean values of triplicate wound for each data set were analyzed using Image J software. To assess the effect of pharmacological inhibitors on cell motility, adherent murine melanoma cells were pre-incubated for 2 hour before making the wound, either with 500 nM Wm or 25 µm PD98059 in 0.1% DMSO. Cells incubated in 0.1% DMSO served as a vehicle control (VC).

3.2.21 RhoGTPase assay

GST-PAK1 protein was purified using *E. coli* containing pGEX plasmid having coding DNA sequence (CDS) for GST-PAK1. The purified GST-PAK1 was coupled to Glutathione-Sepharose

beads. These coupled beads (Glutathione-Sepharose-GST-PAK1 that is Sepharose-PAK1) were further used for the detection of activated Rac1 (GTP-Rac1). The method for the expression, purification, coupling of GST-PAK1 to Glutathione Sepharose beads and RhoGTPase assay for Rac was exactly done as described in Ref. [176].

Briefly, the overnight grown culture of *E. coli* streaked on LB agar plate containing ampicillin was inoculated in 10 ml LB broth and incubated for 6 hour at 37^{o}C, 180 rpm. This starter culture was further inoculated in 1 litre LB broth containing ampicillin and incubated for 4 hour at 37^{o}C, 180 rpm (OD at 600 nm reached up to 0.7 to 0.8). After this 100 µM IPTG was added to induce the expression of GST-PAK1 and culture was grown overnight at 18^{o}C, 180 rpm. The overnight grown culture was pelleted and resuspended in 30 ml lysis buffer A (50 mM Tris pH 7.5, 150 mM Nacl, 5 mM $Mgcl_2$,10 mM DTT, 0.1% Triton-X-100 and 1x protease inhibitor cocktail) and sonicated for 3 cycles of 30 pulse for 30 sec, output set at 30% . The supernatant was collected after centrifuging at 15000 rpm, 4^{o}C for 30 min. The purification of GST-PAK1 was carried out using Glutathione-Sepharose beads. The 1 ml beads (v/v) (washed with lysis buffer to remove the preservatives) were suspended in 15 ml supernatant in 15 ml falcon tube and kept for 1 hour on rotor shaker at 4^{o}C. Later the beads were pelleted by centrifuging at 1000 rpm, 4^{o}C for 4 minutes. The beads were washed four times with 15 ml Tris wash buffer (50 mM Tris.Cl pH 7.5 ,0.5% (w/v) Triton X-100, 150 mM NaCl, 5 mM MgCl2, 1 mM DTT and 1x protease inhibitor cocktail) by centrifuging at 1000 rpm, 4^{o}C for 4 minutes to remove the unbound protein. The washed pelleted beads were resuspended in storage buffer (Tris wash buffer A + 10% glycerol), aliquoted and stored at -80^{o}C. Before use of these Sepharose-Glutathione the-GST-PAK1 (Sepharose-PAK1) beads, storage buffer was removed by washing beads with lysis buffer A.

The Pak1 domain has ability to bind the activated Rac1 and/or CDC42 that is GTP-Rac1 and/or GTP-CDC42. To study the activation status of Rac1 in cells plated on galectin-3 and fibronectin, Sepharose-PAK1 beads were used. For Rac1 activation assay, 24 hour serum starved cells were harvested, washed and $4x10^6$ cells were seeded on galectin-3/fibronectin coated 90 mm plates for 15, 30 and 60 min time interval. At respective time points, non-adherent cells in each plate were removed and 1 ml lysis buffer (50 mM Tris·Cl, pH 7.2, 1% (w/v) Triton X-100, 500 mM NaCl, 10 mM $MgCl_2$, and protease inhibitor cocktail) was added to the plate. The cells were collected, sonicated and centrifuged at 15000 rpm, for 30 min at 4^{o}C. The protein content in these cell lysates was estimated. The cell lysed at 0 min time point served as control. Equal amount of Sepharose-PAK1 beads were incubated with 2 mg (in 1 ml of lysis buffer) protein in lysates of cells harvested at each time point on rocker for 1 h at 4^{o}C. The beads were washed 3 times with Tris wash buffer and the bound protein was eluted using 4x Lamelli buffer at 100^{o}C for 10 min. Western blotted total cell lysates and respective PAK1 bound proteins were analyzed using anti-Rac1 antibody.

3.2.22 Cloning of wild type CD147 in pmGFP-N1 mammalian expression plasmid vector

The total RNA was extracted from B16F10 murine melanoma cells and converted it into cDNA using first strand cDNA synthesis kit according to manufacturer's protocol. This cDNA served as a template for PCR reaction to amplify 822 bp CDS of CD147 (273 amino acid protein). The forward and reverse primers consist of EcoRI and BamHI sites.

Forward primer 5'ATACTTAGAATTCGCCACCATGGCGGCGGCGCTGCTGCTG3'

Reverse primer 5'ACTAGTTGGATCCGCGGTGGCGTTCCTCTGGCGTAC3'

Using these primers the CDS of CD147 was amplified. The amplified product was resolved on agarose gel electrophoresis and cut purified using Gel Extraction kit according to manufacturer's protocol. The purified amplified 822 bp product (Insert) and pmGFP-N1 plasmid (Vector) was

independently double digested with EcoRI and BamHI at 37°C overnight. After digestion insert was again purified using PCR Cleanup kit according while vector was resolved on agarose gel electrophoresis and cut purified using Gel Extraction kit according to manufacturer's protocol. The ligation was carried out using double digested, purified insert and vector at 22°C, overnight. The ligated product was transformed in ultra-competent *E. coli* DH5α strain and screen was performed for positive plasmid clone. The positive clone was sequenced and its DNA sequence confirmed using In-house sequencing facility. From this positive clone, plasmid was extracted and used for further studies.

pmGFP-N1 vector map used for cloning of CD147:

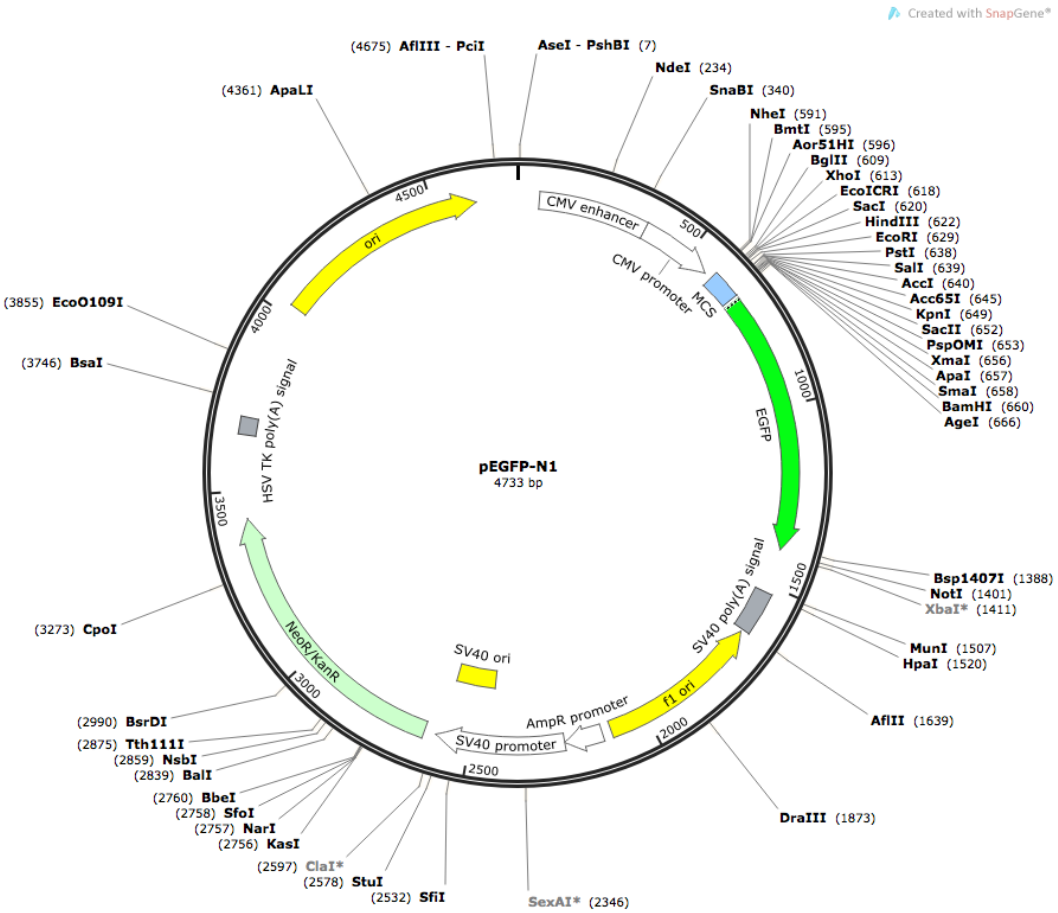

Table 4. PCR conditions for amplification of CD147 from cDNA

Step	Temperature (^{O}C)	Time (min)	Components	Volume (µl)
1. Initial denaturation	95	5	5x PCR buffer	5
2. Denaturation	95	0.5	10 mM dNTPs	0.5
3. Annealing	56	0.5	Distilled water	10.75
4. Extension	72	0.5	Forward primer (10 þmol/µl)	1
5. No. of cycles	Go to step 2 for 34 times		Reverse primer (10 þmol/µl)	1
6. Final extension	72	10	Phusion polymerase (2 U/µl)	0.25
7. End			DNA template	2 (100 ng)

3.2.23 Generation of CD147 glycomutant by site directed mutagenesis (SDM)

To obtain glycomutant CD147, site-directed mutagenesis was performed in the wild type CD147 cloned in pmGFP-N1. There are 5 N-glycosylation sites on CD147 viz. N44, N154, N159, N190 and N193. To generate the various glycomutant of all these sites were sequentially mutated using following primers.

The Aspargine (N/Asp) AAC / AAT was replaced with Glutamine (Q/Gln) CAA / CAG

1) N44Q

F 5'GCTTACCTGCTCTTTGAACAGCAGTGGCGTTGAC3'

R 5'GTCAACGCCACTGCTGTTCAAAGAGCAGGTAAGC3'

2) N154, 159Q

F 5’GGCAATCACCCAGAGCACTGAAGCCCAGGGCAAGTATGTGGTGGTATCC3’

R 5’CATACTTGCCCTGGGCTTCAGTGCTCTGGGTGATTGCCTCTTCTTCCCC3’

3) N190, 193Q

F 5’CCTACGTGTGTCAAGCCACCCAAGCCCAGGGCACTACTCGGG3’

R 5’AGTGCCCTGGGCTTGGGTGGCTTGACACACGTAGGTGCCAGGGTC3’

4) N154Q

F 5’GAAGAGGCAATCACCCAGAGCACTGAAGCCAATG3’

R 5’CATTGGCTTCAGTGCTCTGGGTGATTGCCTCTTC3’

5) N159Q

F 5’CAATAGCACTGAAGCCCAAGGCAAGTATGTGGTGG3’

R 5’CAATAGCACTGAAGCCCAAGGCAAGTATGTGGTGG3’

6) N190Q

F 5’CTGGCACCTACGTGTGTCAAGCCACCAACGCCCAG3’

R 5’CTGGGCGTTGGTGGCTTGACACACGTAGGTGCCAG3’

7) N193Q

F 5’GTGTGTAATGCCACCCAAGCCCAGGGCACTACTC3’

R 5’GAGTAGTGCCCTGGGCTTGGGTGGCATTACACAC3’

The various CD147 glycomutants were generated by site directed mutagenesis using above mentioned primers.

- Individual site specific CD147 glycomutants: N44Q, N154Q, N159Q, N190Q and N193Q
- Typical CD147 glycomutant (TGM): N44,154,190Q
- Atypical CD147 glycomutant (ATGM): N159,193Q
- CD147 glycomutant (GM): N44,154,159,190,193Q

The glycosylation sites in wild type CD147 were sequentially mutated. At first N44, then combinely N154, 159 and lastly N190, 193 were mutated to glutamine to get the glycomutant N44Q (44^{th} N mutated to Q) and GM (All 5 N mutated to Q). Individual site specific glycomutants (N154Q, N159Q, N190Q and N193Q) were prepared using respective primers. The 3 typical glycosylation sites (N44, N154 and N190) were mutated using primer set number 1, 4 and 6 while atypical glycomutant was generated using primer set number 5 and 7 sequentially.

The forward and reverse oligonucleotides were procured, reconstituted in sterile distilled water to obtain 100 µM concentrations. Equal volumes (10 µl of 10 µM) of both the oligonucleotides were mixed with PCR master mix containing wild type pmGFP-N1 CD147 plasmid clone as a template and PCR amplified. The PCR product was DpnI digested and the digested plasmid was used for transformation of ultra-competent *E. coli* DH5α cells and spread plated on LB agar plates. Colonies growing on ligation test plate were counted and subjected to Mini prep based plasmid extraction by alkaline lysis method. The screening of colonies containing the mutant CD147 cDNA was done in purified plasmids by checking release of an insert of 822 base pairs on double digestion with restriction enzymes EcoRI and BamHI. The positive colony showing the presence of mutant CD147 after the sequencing, was used for transfection.

Table 5. PCR conditions for SDM in wild type CD147 cloned in pmGFP-N1

Step	Temperature (^oC)	Time (min)	Components	Volume (µl)
1. Initial denaturation	95	2	5x PCR buffer	5
2. Denaturation	95	0.5	10 mM dNTPs	1
3. Annealing	62	0.5	DMSO	0.75
4. Extension	72	10	Forward primer (10 þmol/µl)	1

5. No. of cycles	Go to step 2 for 16 times	Reverse primer (10 þmol/µl)	1
6. End		Phusion polymerase (2 U/ µl)	0.5
		Distilled water	10.75
		DNA template (2 ng/µl)	5

3.2.24 Transfection and Confocal microscopy to observe the expression of CD147

Exponentially growing culture of B16F10 cells were harvested and seeded on 35 mm culture dishes and grown up to approximately 80% confluency. Typically 1.5 µg of plasmid DNA and 6 µl of lipofectamine™ 2000 solution, each was diluted in 0.1 ml plain DMEM in sterile microcentrifuge tube and incubated for 5 min at room temperature. The DNA and lipofectamine solution was gently mixed with pipette and after 30 min incubation at room temperature added to the 35 mm culture dishes drop wise. The final volume in this plate was adjusted to 1 ml by adding plain DMEM. The plate was gently swirled and incubated overnight at 37°C. The medium was removed and culture was rinsed twice with PBS or plain DMEM. The cells were then grown for 24 h in complete medium.

After 48 h of transfections the cells were fixed with 4% paraformaldehyde at 37^{o}C for 5 minutes and stained with DAPI for nucleus and observed under confocal microscope to study the localization of wild type and glycomutant CD147. Images were taken at 63x magnification using Leica STED confocal microscope.

3.2.25 Statistics

All the statistical analysis was done by using Graphpad prism 5 or 6 software. For comparison of two groups, student's t test was performed and for multiple comparison either one way ANOVA or two way ANOVA was performed. All the error bars represent mean $\pm$ s.e.m.

Chapter 4

Results

Objective I: To confirm the role of galectin-3 on the lungs in organ specific metastasis

Model system used for the study of phenomenon of organ specific metastasis is the B16 murine melanoma cells. This model was developed by I. J. Fidler in 1973 from spontaneous tumor in the mice [177].

Key features of this model are as follows.

- ❑ Availability of cell lines with varying metastatic potentials
    - B16F1 is low metastatic, while
    - B16F10 is high metastatic
- ❑ Shows lung specific metastasis irrespective of route of administration (Tail vein-lung is the last organ, subcutaneous, intra-aortic-lung is the first organ)
- ❑ Expresses β1, 6 branched N-oligosaccharides
- ❑ Melanin produced by melanoma cells helps in quantitation/visualization

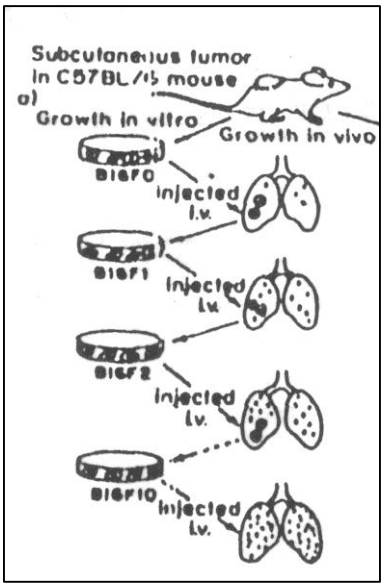

Illustration 5: B16 murine melanoma model (right panel) and lungs showing metastatic colonies after experimental metastasis assay by injecting 0.1 million cells (Left panel)

Galectin-3/polyLacNAc interaction aids in lung specific metastasis of B16F10 cells. It is possible to block this interaction by using galactose rich sugars or by decreasing the availability of polyLacNAc to bind to the galectin-3. To fulfill these two goals, modified citrus pectin (MCP) and truncated galectin-3 (tGal-3) may be helpful.

4.1 Effect of MCP on metastatic potential of B16F10 cells

MCP powder is shorter, non-branched, galactose-rich, carbohydrate chains. These shorter chains dissolve more readily in water and are better absorbed and utilized by the body than ordinary, long-chain pectin. It is supposed that the shorter polysaccharide units afford MCP its ability to access and bind tightly to galactose-binding lectins like galectin-3.

In *in vitro* assays, the inhibitory effect of MCP was tested on cell spreading. Cell spreading is a post adhesive event required for cell migration during successful metastasis [178]. The cells incubated with MCP at 0.1% concentration show immature actin organization, lamellopodial formation and statistically significant decrease in cytoplasm to nucleus (C/N) ratio on galectin-3 as compared to that of cells untreated with MCP (Fig. 1). Cell spreading on uncoated coverslips served as control (Fig. 1A) where cells are not able to spread and develop a mature lamellipodia (Fig. 1B).

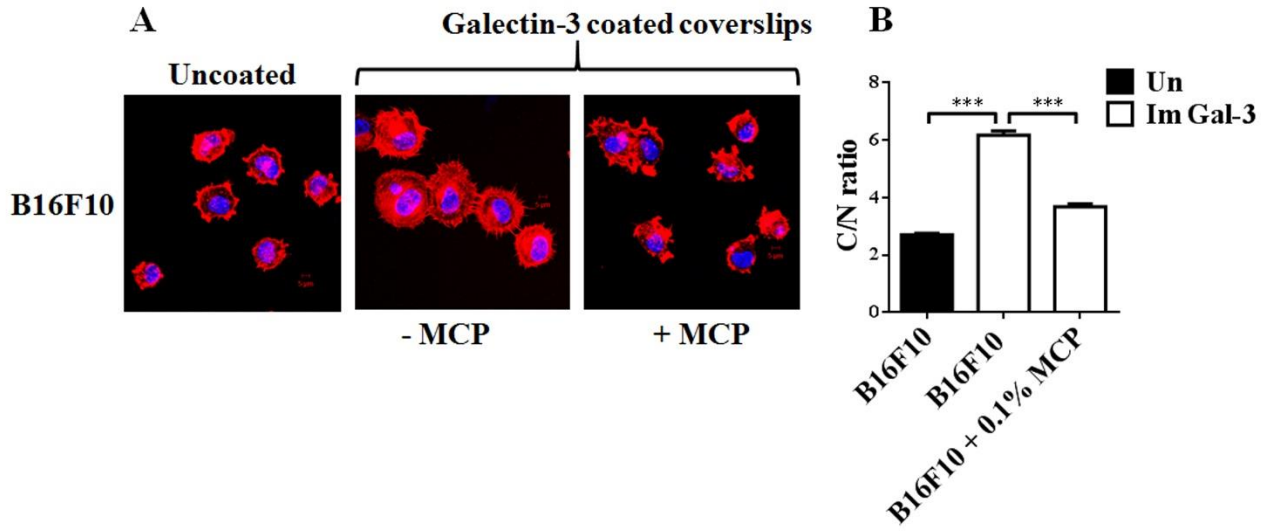

Fig. 1. MCP treatment inhibit the cell spreading of B16F10 cells on immobilized (Im) galectin-3. (A) Confocal microscopy images of spreading of cells on uncoated (Un) and on galectin-3 (Gal-3) coated coverslips in absence and presence of 0.1% MCP. The cells were stained with phalloidin-TRITC for filamentous actin (Red) and DAPI for nucleus (Blue); 63x magnification; scale bar = 5 µm. (B) Quantitation of cell spreading assay in which the images of at least 50 cells of each type from three independent experiments were analyzed to calculate the area of cytoplasm and nucleus (C/N ratio). Data is mean ± SE of three independent experiments. ***p<0.001.

The effect of MCP was further tested on experimental metastasis assay using B16F10 cells. 1% MCP was fed through drinking water to the mice, one week prior to the injection of cells. It was necessary to build up the desired concentration of MCP in the circulation. Subsequently, B16F10 cells along with 0.05% MCP was injected through tail vein. Mice were sacrificed after 17 days of injection and the lung metastatic colonies were observed (Fig. 2A). The lung metastatic colonies were found to be decreased in the mice fed with MCP compared to that of mice fed only drinking water (Fig. 2B & C).

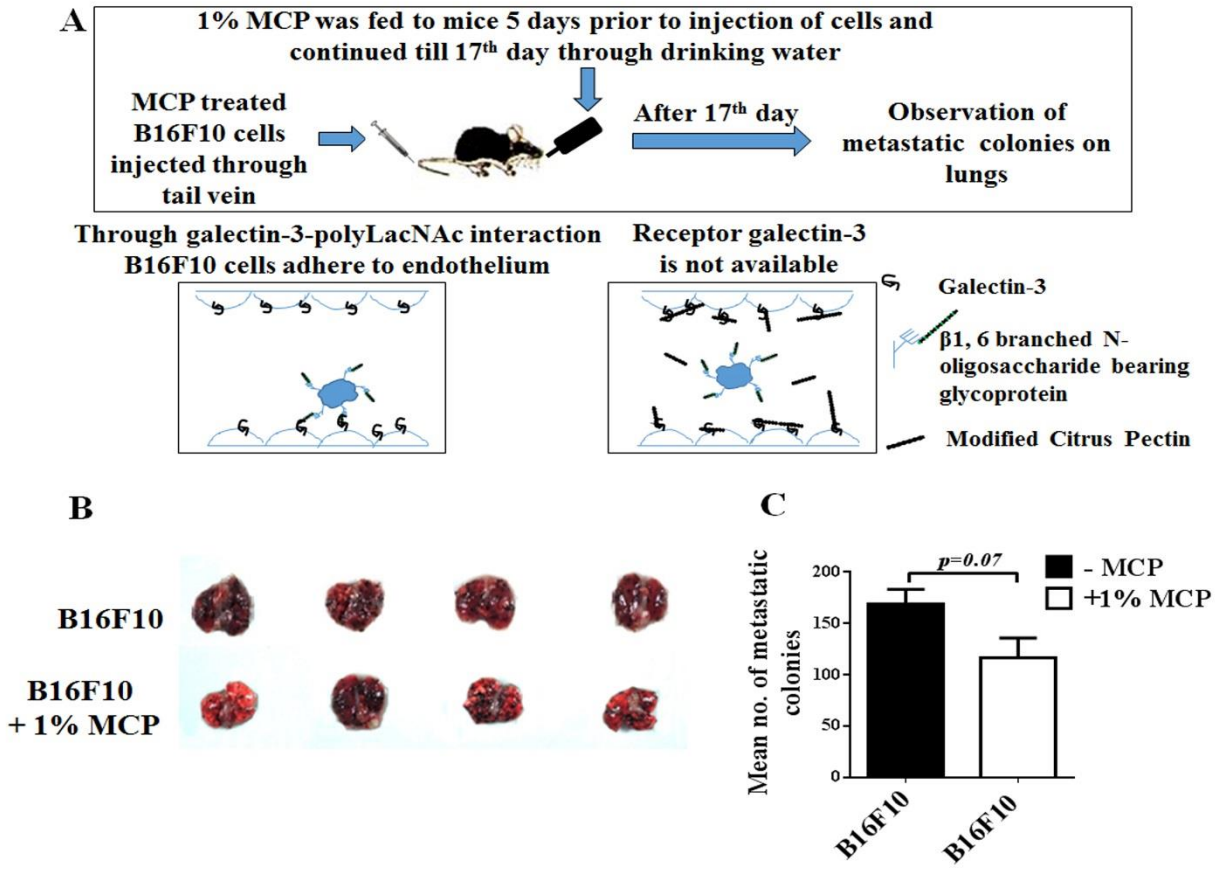

Fig. 2. MCP treatment affects the metastatic potential of B16F10 cells. (A) Schematic representation of work flow of experimental metastasis assay using MCP. (B) Comparison of melanoma colonies in lungs of C57BL/6 mice in absence and presence of 1% MCP, after injection of 0.1 million B16F10 cells under experimental metastasis assay conditions. (C) Quantitation of number of lung colonies of the two groups of mice in (B). Significance obtained by performing student's T-test is denoted by p value.

4.2 Cloning, expression and purification of human truncated galectin (htGal-3)

Galectin-3/polyLacNAc interaction can be interfered using truncated galectin-3, which lacks N-terminal oligomerization domain and has only CRD. This tGal-3 has capacity to bind to its ligand lactose. To block the polyLacNAc of B16F10 cells tGal-3 can be used. In the beginning, for cloning the coding DNA sequence (CDS) of truncated galectin-3, it was amplified using forward

and reverse primers containing NdeI and BamHI site (Fig. 3A). The amplified CDS was successfully cloned, expressed, purified using freshly prepared Lactose-Sepharose column. The coomassie stained SDS-PAGE showing the single band at 17 kDa region of htGal-3 confirms the purity of the protein while western blot confirms the intactness (no degraded protein products) (Fig. 3B-D). The identity of the purified protein was confirmed by whole protein spectra by MS showing the major peak at 15 kDa region of monomer while minor peak at 30 kDa region of dimer (Fig. 4A). In the solution galectin-3 exists in monomer as a major fraction while dimer as a minor fraction in the absence of ligand lactose. Also the sequence coverage of amino acids of htGal-3 was matched with the C-terminal region of the human origin galectin-3 as confirmed by MS/MS (Fig. 4B & C). The large scale batch purification of htGal-3 carried out and the expression and purification was confirmed by loading different fractions on SDS-PAGE stained with coomassie (Fig. 4D).

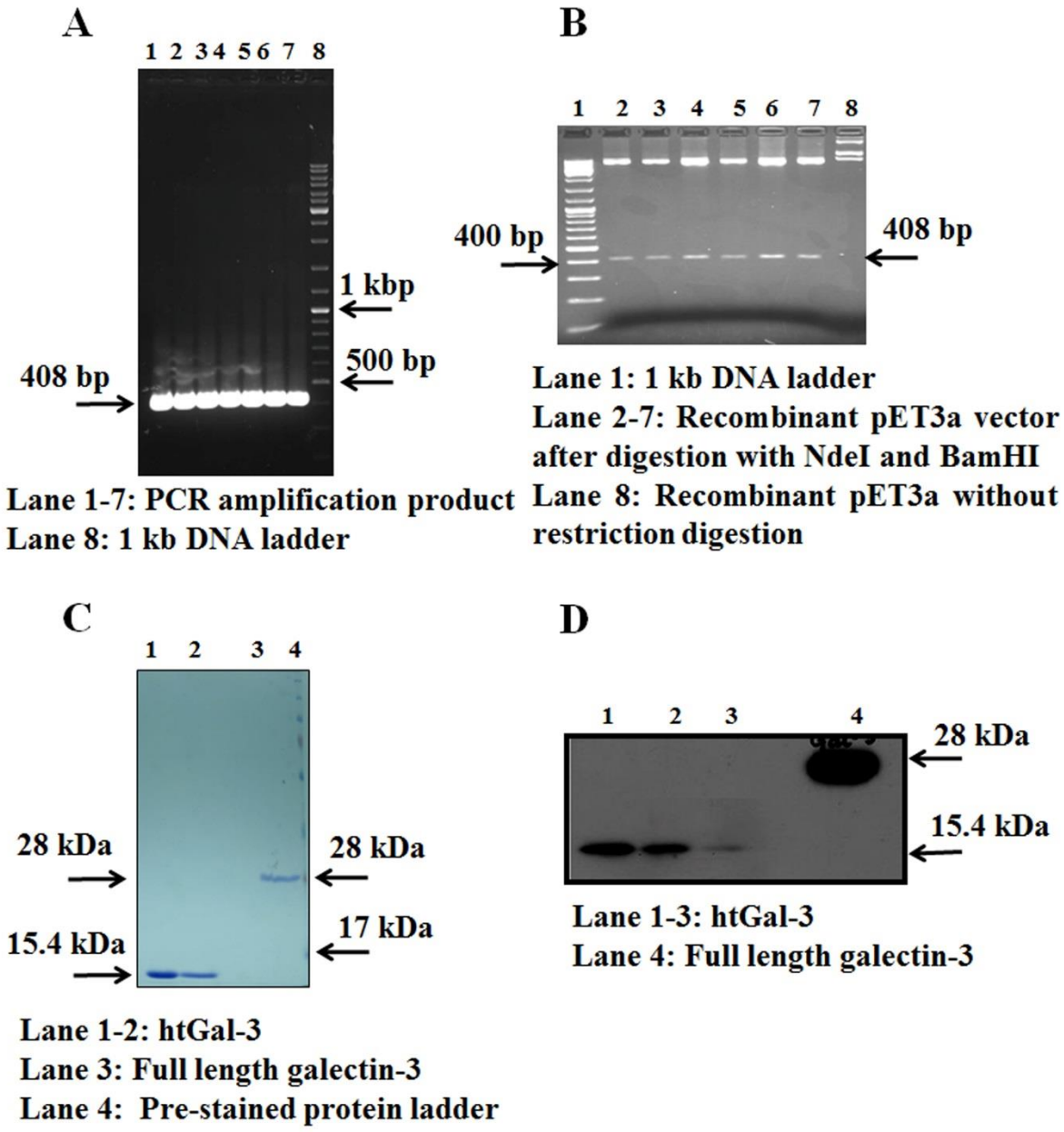

Fig. 3. Human truncated galectin-3 was cloned, expressed and purified using Lactose-Sepharose column. (A) Agarose gel image showing the PCR amplification product at 400 bp region of CDS of human truncated galectin-3 containing CRD. (B) Agarose gel image showing the band release at approximately 400 bp after screening of 7 colonies using restriction digestion with NdeI and BamHI. (C) Coomassie blue stained SDS-PAGE showing purified fractions of truncated galectin-3 and full length galectin-3. (D) Western blotting showing bands at 15 kDa region of human truncated galectin-3 corresponding to full length galectin-3 after probing with anti-galectin-3 antibody.

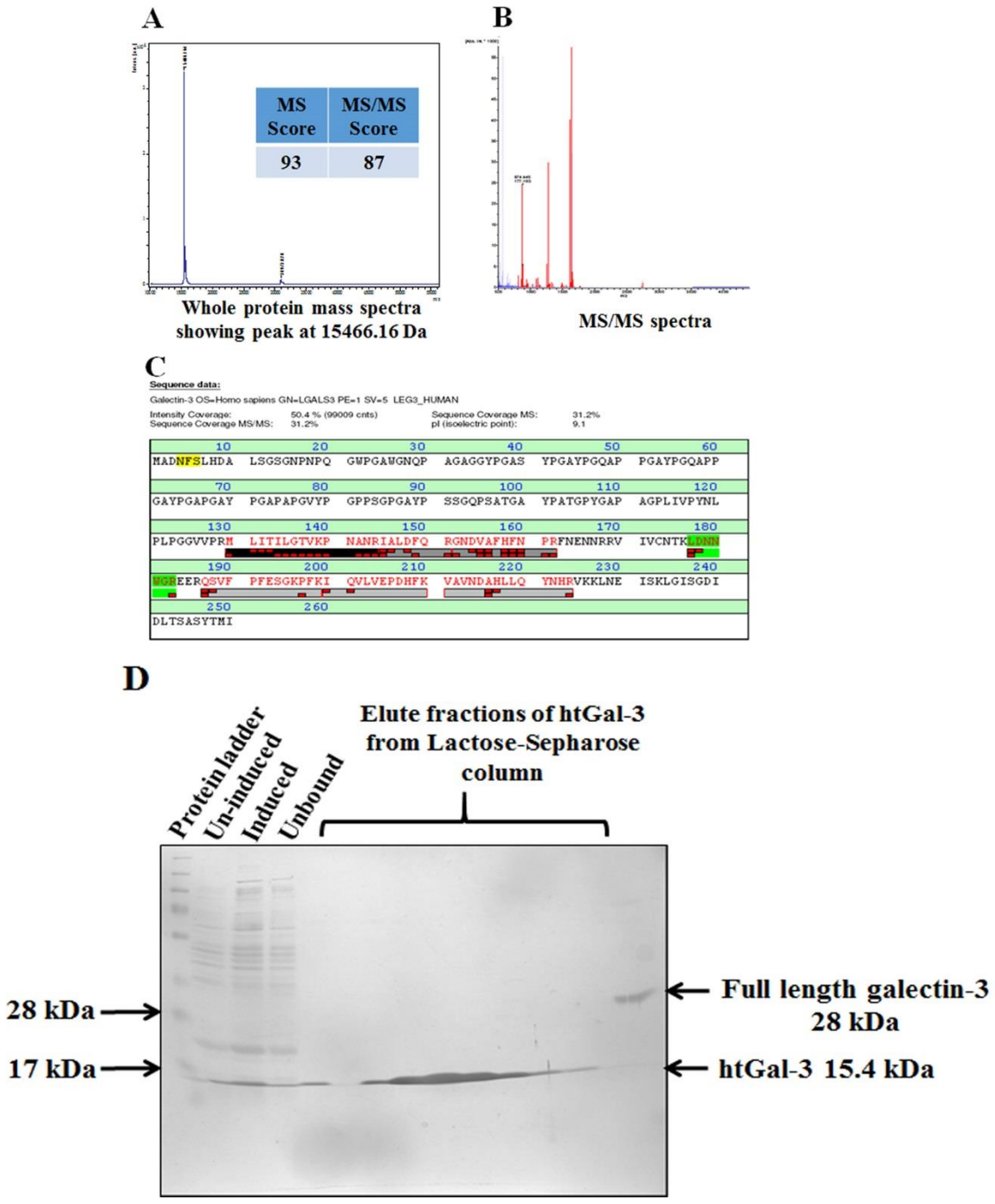

Fig. 4. Protein identity and sequence coverage was confirmed using mass spectroscopy and MS/MS. (A) Whole protein mass spectra showing major peak at 15466.16 Da region while minor peak at 30000 Da region. (B) MS/MS spectra of the truncated galectin-3 showing the fragmentation pattern. (C) **S**equence in red was the matched sequence with human truncated galectin-3. (D) Coomassie stained SDS-PAGE showing various fractions of batch purification of human truncated galectin-3.

4.3 Effect of htGal-3 on metastatic potential of B16F10 cells

The effect of purified htGal-3 on viability of the cells was tested and concentration was selected that was not toxic to the cells. The cells were allowed to spread on galectin-3 coated coverslips in absence and presence of 75 µg htGal-3. The cells were spread and formed the well-organized actin bundles and lamellipodia on immobilized galectin-3, while in presence of htGal-3, cells were not able to spread and there was poor actin organization and lamellipodia formation. The cell spreading on uncoated surfaces served as a control, which showed immature actin organization and lamellipodia formation (Fig. 5A). These results were also reflected in C/N ratios where there is statistically significant decrease in their area when they are treated with htGal-3 (Fig. 5B).

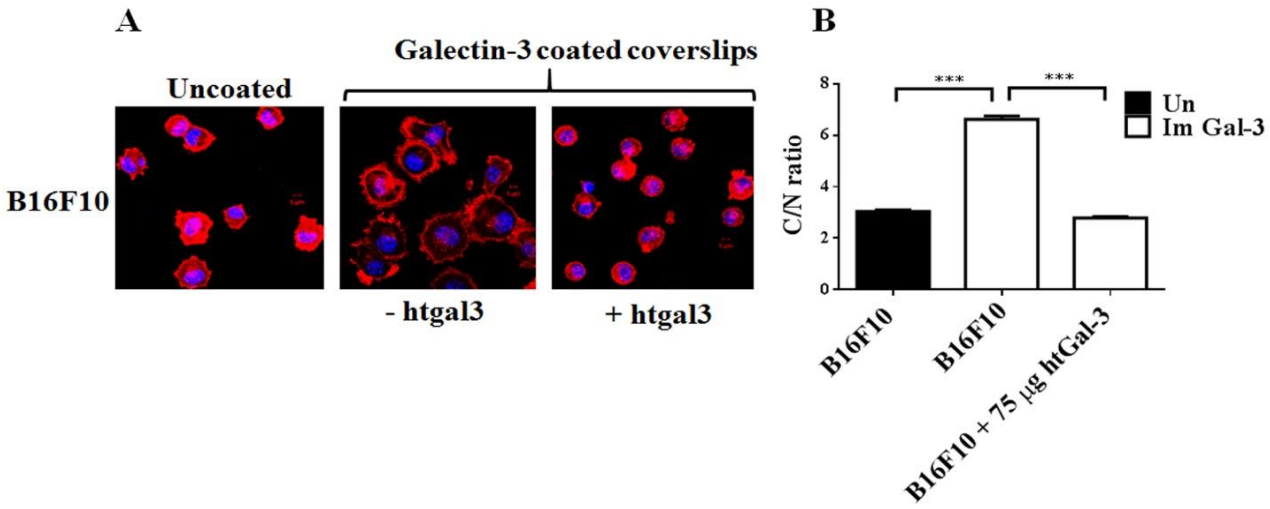

Fig. 5. Truncated galectin-3 treatment inhibit the cell spreading of B16F10 cells on immobilized galectin-3. (A) Confocal microscopy images of spreading of cells on uncoated (Un) and on galectin-3 coated coverslip in absence and presence of truncated galectin-3. The cells were stained with phalloidin-TRITC for filamentous actin (Red) and DAPI for nucleus (Blue); 63x magnification, Scale bar = 5 µm. (B) Quantitation of cell spreading assay in which the images of at least 50 cells of each type from three independent experiments were analyzed to calculate the area of cytoplasm and nucleus (C/N ratio). Data is mean ± SE of three independent experiments. ***p<0.001.

Under experimental metastasis assay conditions, B16F10 cells alone injected into the mice were showing the lung metastatic colonies while decreased lung metastatic colonies were observed when treated with htGal-3 (Fig. 6A & B). It was found that there was statistically significant decrease in lung metastatic colonies in htGal-3 treated group compared to that of untreated group (Fig. 6C).

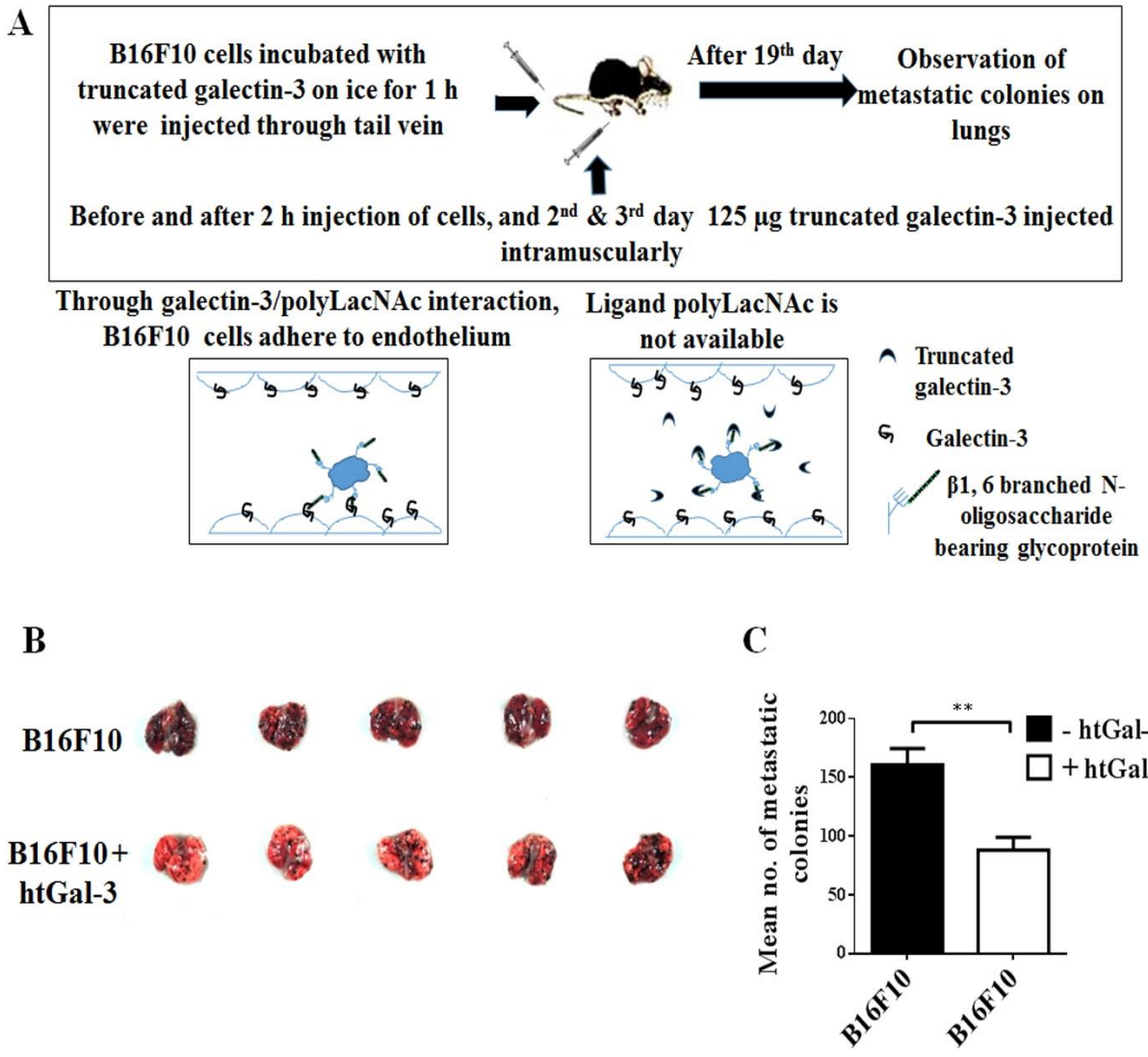

Fig. 6. Truncated galectin-3 treatment affects the metastatic potential of B16F10 cells. (A) Schematic representation of work flow of experimental metastasis assay using truncated galectin-3. (B) Comparison of melanoma colonies in lungs of C57BL/6 mice in absence and presence of truncated galectin-3, after injection of 0.1 million B16F10 cells under experimental metastasis assay conditions. (C) Quantitation of number of lung colonies of the two groups of mice in (B). Significance is obtained denoted by *. **$p<0.01$.

4.4 Effect of mouse truncated galectin-3 (mtGal-3) on metastatic potential of B16F10 cells

Human galectin-3 CRD shares 87% identity with mouse galectin-3 CRD. In order to rule out possibility that htGal-3 may generate antibody response in mice which may block its function, CRD of mouse galectin-3 has used in these experiments. The CRD of mouse galectin-3 (mtgal-3) was cloned, expressed and purified.

The total RNA extracted from B16F10 cells was converted into cDNA. This cDNA was used to amplify CDS of CRD of galectin-3 using forward and reverse primers containing NdeI and BamHI restriction sites (Fig. 7A). Amplified CDS successfully cloned and the positive clone was screened using restriction digestion strategy (Fig. 7B). The mtGal-3 was expressed, purified using Lactose-Sepharose column (Fig. 7C). The identity and sequence was validated using MS and MS/MS (Fig. 7D & E).

The experimental metastasis assay was performed by treating cells with mtGal-3 exactly as described for htGal-3. Results obtained with mtGal-3 were comparable to htGal-3. The lung metastatic colonies of B16F10 cells was found to be significantly decreased in presence of mtGal-3 (Fig. 7F & G).

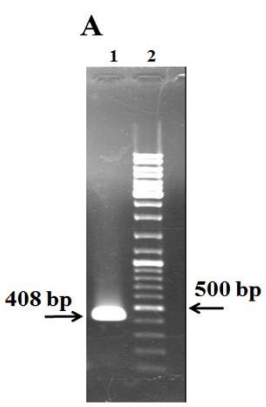

Lane 1: PCR amplification product
Lane 2: 1 kb DNA ladder

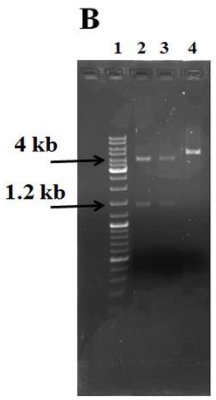

Lane 1: 1 kb DNA ladder
Lane 2-3: Recombinant pET3a vector after digestion with PstI
Lane 4: pET3a empty vector after digestion with PstI

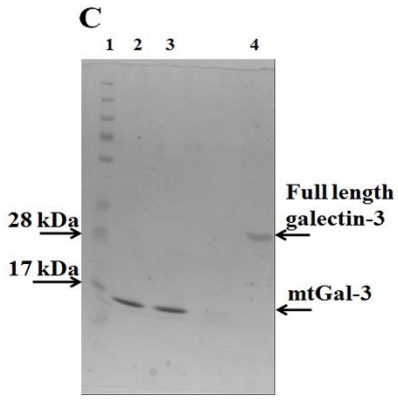

Coomassie BB stained SDS-PAGE
Lane 1: Pre-stained protein ladder
Lane 2-3: mtGal-3
Lane 4: Full length galectin-3

D

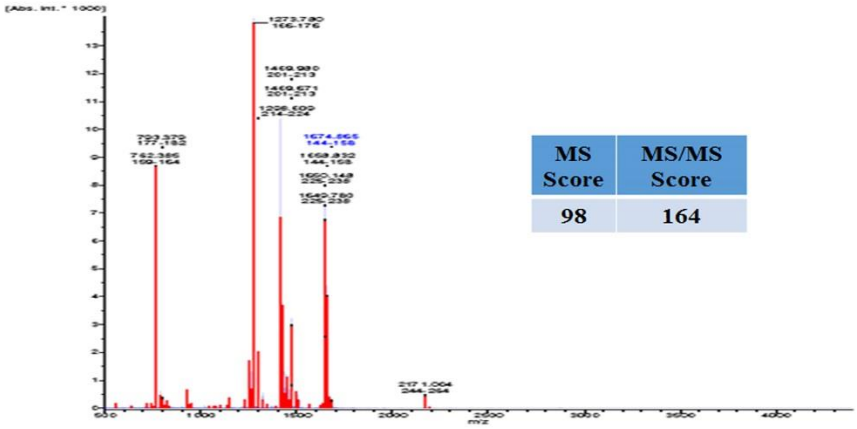

MS Score	MS/MS Score
98	164

E

Sequence data:

Galectin-3 OS=Mus musculus GN=Lgals3 PE=1 SV=3 LEG3_MOUSE

Intensity Coverage: 40.9 % (31712 cnts) Sequence Coverage MS: 36.7%
Sequence Coverage MS/MS: 22.3% pI (isoelectric point): 9.1

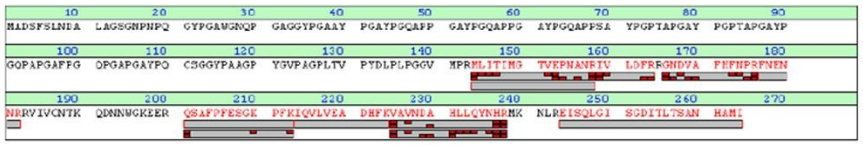

F

G

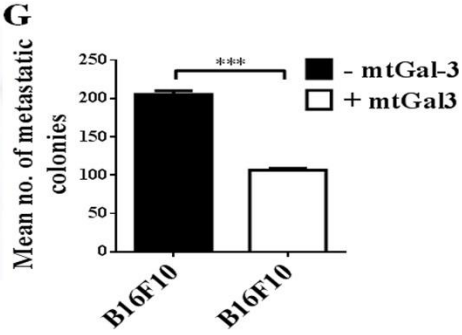

Fig. 7. Mouse truncated galectin-3 was cloned, expressed, purified and its effect was assessed on metastatic potential of B16F10 cells. (A) PCR amplification product at 400 bp region of CDS of mouse truncated galectin-3 containing CRD. (B) Agarose gel image showing the band release at 1.2 kb after screening of 7 colonies using restriction digestion with PstI. (C) Coomassiae stained SDS-PAGE showing the purified fractions of truncated galectin-3 and full length galectin-3. (D) MS/MS spectra of the truncated galectin-3 showing the fragmentation pattern. (E) Sequence in red was the matched sequence with mouse truncated galectin-3. (F) Comparison of melanoma colonies in lungs of C57BL/6 mice in absence and presence of truncated galectin-3, after injection of 0.1 million B16F10 cells under experimental metastasis assay conditions. (G) Quantitation of number of lung colonies of the two groups of mice in (F). Significance is obtained denoted by *. ***$p<0.001$.

4.5 Lung metastatic potential of B16F10 cells in galectin-3 transgenic mice

The role of galectin-3/polyLacNAc interaction in lung specific metastasis of B16F10 cells was established. To prove that polyLacNAc on tumor cells indeed brings about these effects via galectin-3 we used galectin- 3 transgenic mice.

Galectin-3 transgenic mice were characterized using tail genomic DNA as template for PCR. The amplicon size for galectin-$3^{+/+}$ and galectin-$3^{-/-}$ mice was 450 bp and 300 bp, respectively. However, the two amplicons 450 bp and 300 bp were obtained for galectin-$3^{+/-}$ mice (Fig. 8A). These results indicate that the mice were successfully propagated and maintained. The experimental metastasis assay was performed using B16F10 cells in galectin-3 transgenic mice. B16F10 cells ($0.1x10^6$) were injected through tail vein in galectin-$3^{+/+}$, galectin-$3^{+/-}$ and galectin-$3^{-/-}$ mice. The decreased lung metastatic colonies of B16F10 cells were observed in galectin-$3^{+/-}$ mice as compared to galectin-$3^{+/+}$ mice. However, surprisingly galectin-$3^{-/-}$ mice showed comparable number of colonies to galectin-$3^{+/+}$ mice (Fig. 8B). The N-glycosylation inhibitor swansonine treated B16F10 cells were injected in galectin-$3^{-/-}$ mice to assess the importance of sugars. The comparable number of lung metastatic colonies were obtained either in presence or absence of swainsonine suggesting the irrelevance of sugars of B16F10 cells (Fig. 8C). The lung

metastatic colonies of B16F10 cells in galectin-3$^{-/-}$ mice even absence of galectin-3, warrants further confirmation of involvement of galectin-3/polyLacNAc interaction in lung specific metastasis.

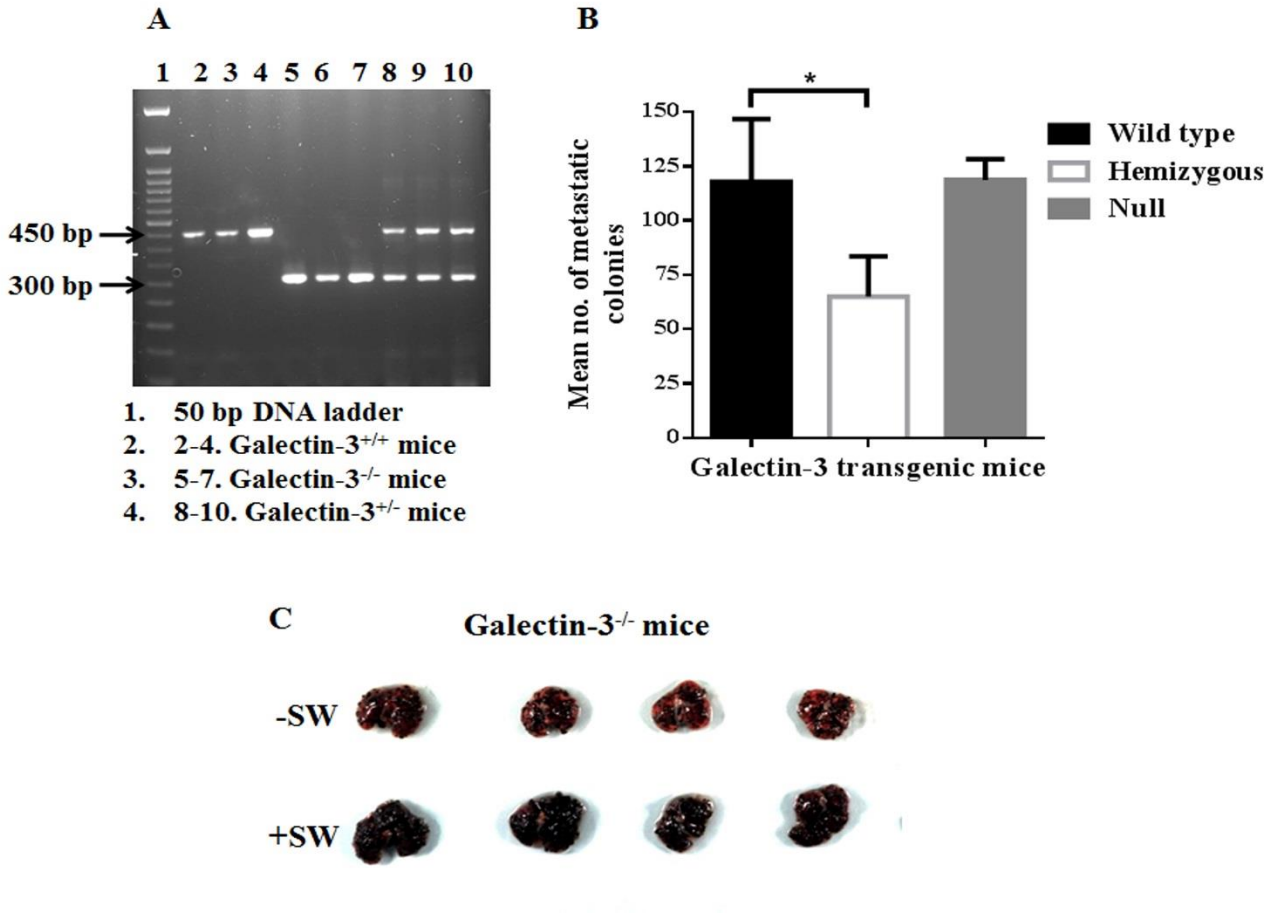

Fig. 8. Lung metastatic potential of B16F10 cells were comparable in galectin-3$^{+/+}$ galectin-3$^{-/-}$ mice. (A) Assessment of galectin-3 status of mouse using PCR and utilizing genomic DNA as template extracted from tail and primers specific for galectin-3 gene. (B) Quantitation of number of lung colonies of the three groups of (galectin-3$^{+/+}$, galectin-3$^{+/-}$ and galectin-3$^{-/-}$) mice under experimental metastasis assay conditions. Significance is obtained denoted by *, $p<0.05$. (C) Comparison of melanoma colonies in lungs of galectin-3$^{-/-}$ mice after injecting 0.15 million untreated and swainsonine treated B16F10 cells, under experimental metastasis assay conditions.

4.6 Effect on metastatic potential of B16F10 cells in bone marrow chimeric mice

The involvement of galectin-3/polyLacNAc interaction in lung specific metastasis of B16F10 cells was confirmed by using MCP, a competitive inhibitor to LacNAc which blocks endogenous galectin-3 and truncated galectin-3, a dominant negative inhibitor that compete with endogenous galectin-3. To test if absence of galectin-3 in some way alters the anti-tumor immunity and thus metastatic outcome of cells in galectin-$3^{-/-}$ mice, bone marrow chimeric mice were generated. Replacement of bone marrow of galectin-$3^{-/-}$ mice with that from galectin-$3^{+/+}$ mice was confirmed by analyzing the tail and blood genomic DNA as a template for PCR. The bands at 300 bp in both groups obtained with the tail genomic DNA confirmed their galectin-$3^{-/-}$ phenotype (Fig. 9A). Further, the appearance of only 300 bp band in group 1 and bands of both 300 and 450 bp obtained with blood genomic DNA in group 2 confirms galectin-$3^{-/-}$ phenotype in group 1 and successful chimerism in group 2 (Fig. 9B). Experimental metastasis assay was performed in these mice using B16F10 cells. The comparable lung metastatic colonies were obtained in both the groups. The generation of bone marrow chimeric mice had no effect on the metastatic outcome of B16F10 cells in the lungs (Fig. 9C).

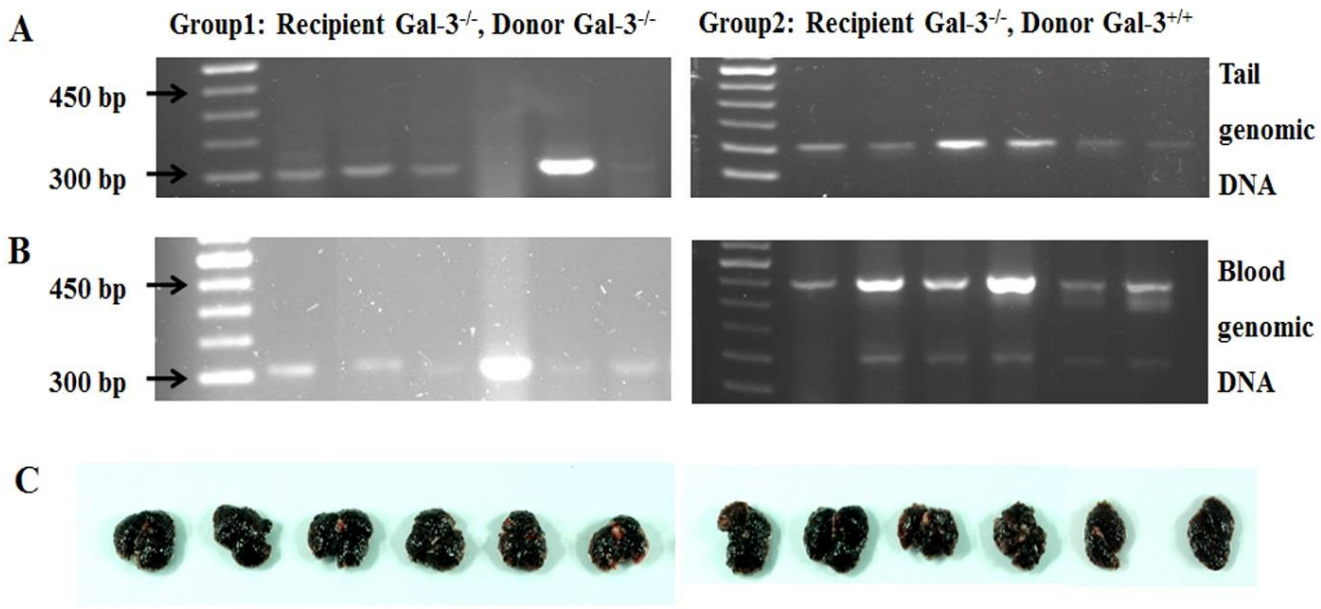

Fig. 9. Experimental metastasis assay using bone marrow chimeric mice. (A) Agarose gel image showing PCR amplification band at 300 bp using tail genomic DNA as a template. (B) Agarose gel image showing the PCR amplification band at 300 bp and 450 bp using blood genomic DNA as a template. (C) Lung images taken after experimental metastasis assay.

Objective II: Role of CD147, a carrier of β1, 6 branched N-oligosaccharides, in metastasis

In order to investigate the role of galectin-3, it is also important to know galectin-3 binding proteins. Mass spectrometric screen was performed to find out galectin-3 binding proteins. It was found that along with many other cell surface glycoproteins, CD147 is a major carrier of β1, 6 branched N-oligosaccharides. It is reported that glyco-deficient CD147 fails to induce matrix metalloproteases by tumor cells. Hence we studied the role of CD147 and its glycosylation in galectin-3 mediated metastatic processes of B16F10 cells.

4.7 Analysis of expression levels of CD147 in B16F1 and B16F10 cell lines

CD147 is a highly glycosylated galectin-3 binding protein that has two isoforms. B16F10 cell line abundantly expresses isoform 2 but no Isoform 1 (Fig. 10A). The expression levels of CD147 was found to be higher in B16F10 cells as compared to that of B16F1 cells. Also both the cell lines express high and low glycosylated forms of the CD147 (Fig. 10B).

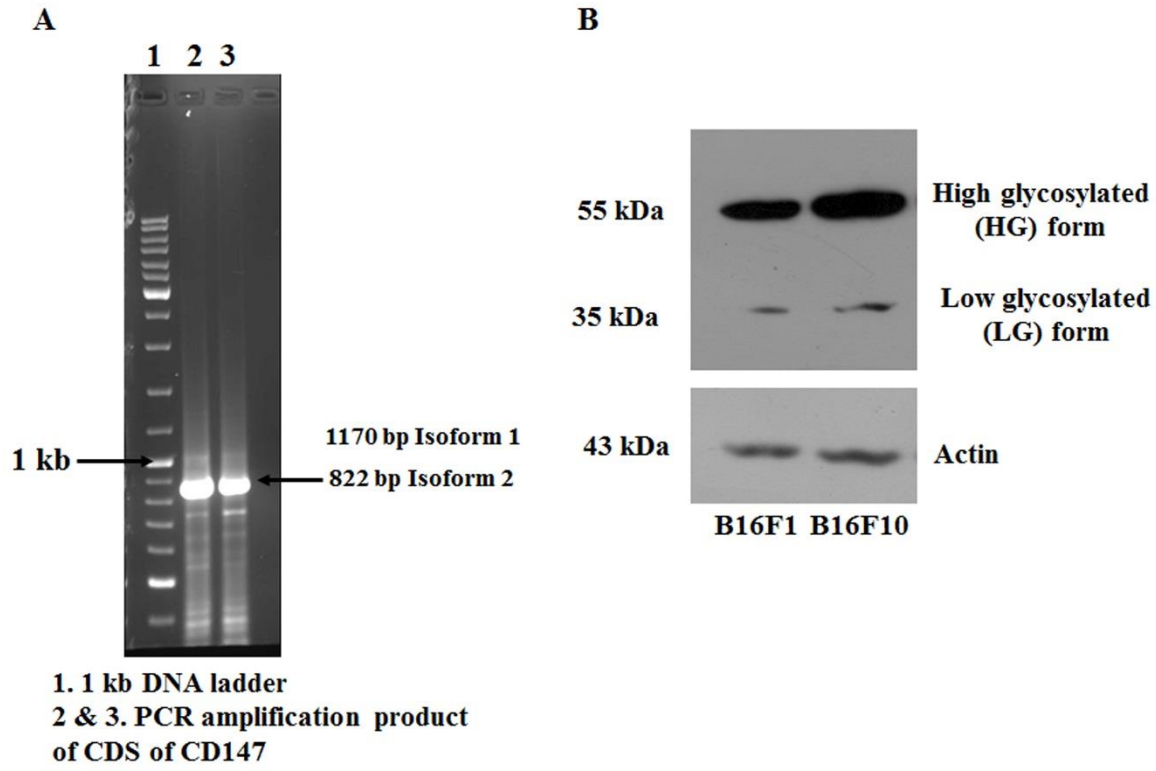

Fig. 10. Expression levels of CD147 correlates with the metastatic potential. (A) Agarose gel image showing the PCR amplification product of CD147. (B) Western blotting using lysates of B16F10 and B16F1 cells with anti-CD147 antibody. Actin served as a loading control.

4.8 Expression of glycomutant CD147 in B16F10 cells

To study the role of CD147 in galectin-3 mediated metastatic progression, wild type (Wt) CD147 was successfully cloned into the pmGFPN1 plasmid vector. All the five glycosylation sites in CD147 was successfully mutated using site directed mutagenesis (SDM) to generate the

glycodeficient CD147 (N44,154,159,190,193Q-Glyco-deficient GM). The wild type and glycomutant CD147 were expressed as a fusion proteins with green fluorescent protein (GFP).

Wt CD147 and GM CD147 were transfected in the B16F10 cells. The expression of Wt and GM CD147 was analyzed by confocal microscopy. Wt CD147 was shown to be expressed on the cell surface while CD147 deficient with all glycosylation sites was found to be accumulated in the cell cytoplasm (Fig. 11A). It suggests that glycosylation plays important role in the localization and targeting of CD147 to the cell membrane.

4.9 Screening of glycosylation site/s required for localization of CD147 to the membrane

To investigate the crucial site required for targeting of CD147 to the membrane, combinations of CD147 mutants were generated. CD147 glycosylation sites were mutated independently (N44Q, N154Q, N159Q, N190Q and N193Q) and in combinations (N44,154,190Q - typical glycomutant TGM observed on consensus sequence; N159,193Q atypical glycomutant ATGM observed on non-consensus sequence) and expressed in B16F10 cells by transfection.

TGM and ATGM CD147 were expressed in B16F10 cells showed cytoplasmic localization. N154Q, N190Q and N193Q CD147 mutants accumulated inside the cell cytoplasm while N44Q, N159Q CD147 glycomutant showed cell surface localization (Fig. 11). Wild type CD147 was expressed on the cell surface while CD147 deficient with all glycosylation sites accumulated in the cytoplasm. Under these conditions it was not possible to investigate the functions of glyco-deficient CD147 as these were not seen on the membrane.

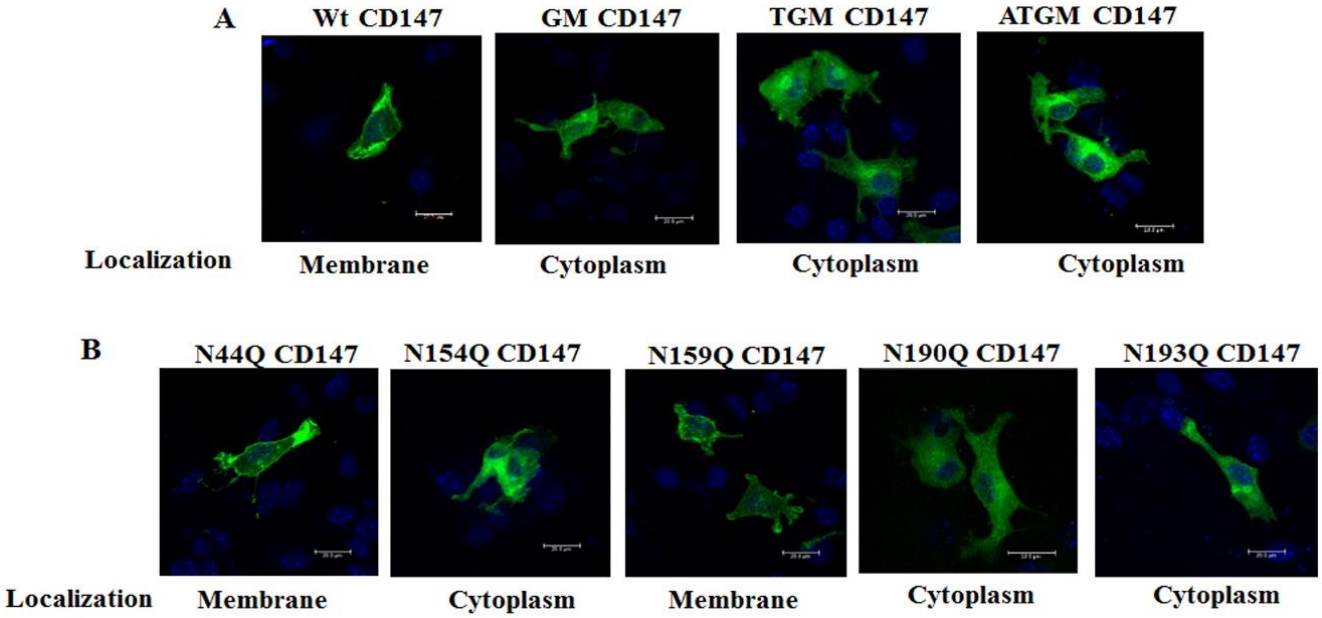

Fig. 11. Localization of CD147 mutants after transfection in B16F10 cells. (A) Wild type, GM, TGM and ATGM CD147 were expressed in B16F10 cells. (B) Independent glycomutants of CD147 were expressed in B16F10 cells; 63x magnification; Scale bar= 20 µm.

Objective III: To investigate the role of galectin-3 in processes like adhesion, spreading and movement critical for metastasis

Galectin-3 is a nucleo-cytoplasmic protein which is secreted out in a non-classical manner and often gets incorporated into the ECM and BM. Galectin-3 has been shown to regulate cellular motility in many different ways and is dependent on the sub-cellular localization of galectin-3. The secreted extracellular galectin-3 exerts its cellular effects on motility related processes both in the soluble form and as immobilized component on cells, ECM and BM. However, it is not clear how immobilized galectin-3 as a component of ECM/BM promotes such complex cellular processes like spreading and movement critical for cancer cell metastasis.

4.10 Cytoskeletal organization during spreading of cells on galectin-3 and fibronectin

Cells utilize extracellular matrix component (ECM) as the substrate for their spreading and movement. Different ECM components determine the type of cytoskeletal organization during spreading and movement of the cells. Here we compared the cell spreading pattern and cytoskeletal organization on galectin-3 with that of very well studied ECM component fibronectin. It was observed that the spreading of B16F10 melanoma cells on galectin-3 was very different from that seen on fibronectin (Fig. 12). The cell spreading on fibronectin showed stretched and mesenchymal cell-like morphology with abundant stress fibers traversing across the cell body (Fig. 12C & F). Galectin-3 induced cell spreading showed rounded morphology and the intensity of the actin bundles was more along the periphery of the cells (Fig. 12B & E). The arborate or stellate morphology of cell spreading was more prominent on fibronectin while flat and rounded cell spreading was seen on galectin-3. These morphological differences were also reflected during motility of the cells on galectin-3 (Fig. 12G) and fibronectin (Fig. 12H). Fixed and live cell imaging on immobilized galectin-3 and fibronectin was performed to see if differences in spreading kinetics are evident even at early time points. Cell spreading on uncoated coverslips served as a control (Fig. 12A & D).

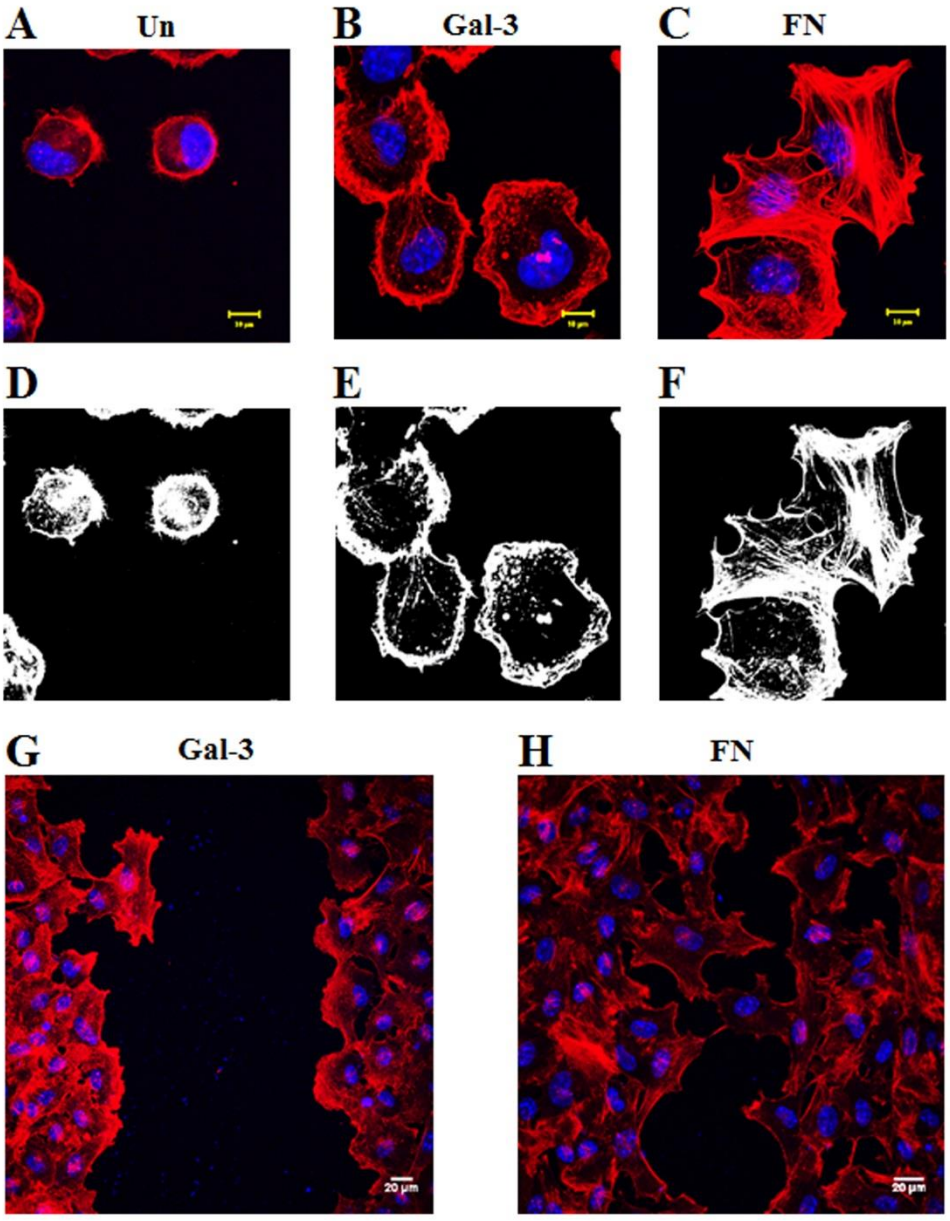

Fig. 12. Spreading pattern and actin cytoskeletal organization of cells on immobilized galectin-3 and fibronectin (FN). Images represent the spreading pattern of cells on uncoated (Un) (A) and (D), galectin-3 (Gal-3) (B) and (E), and fibronectin (FN) (C) and (F) coated coverslips. (A), (B) and (C) are the colored confocal images while the (D), (E) and (F) are the threshold images of the same, respectively. The cells were fixed and stained with phalloidin-TRITC for filamentous actin and DAPI for nucleus; 63x magnification, Scan zoom 1.5x; Scale bar: 10 µm. The differences in lamellipodial structures in cells migrating on coverslips coated with galectin-3 (G) and fibronectin (H) to close the wound created 16 hour prior. The cells were fixed and stained with phalloidin-TRITC for filamentous actin and DAPI for nucleus; 40x magnification; Scale bar: 20 µm.

4.11 Generation of stable B16F10 cell line expressing GFP-Actin

To study the microfilament organization in live B16F10 cells in response to immobilized gaelctin-3 and fibronectin, GFP-Actin was stably expressed in these cells. To express GFP-Actin in B16F10 cells, total RNA was extracted from B16F10 cells and converted into cDNA. By using this cDNA as a template, full length 1.1 kb CDS of actin was amplified by using forward and reverse primers containing EcoRI and BamHI sites respectively (Fig. 13A). The amplified CDS and pmGFPC1 were independently double digested using EcoRI and BamHI restriction enzymes, purified, ligated and transformed. The colonies were screened using EcoRI and BamHI (Fig. 13B) and the positive clones were confirmed by sequencing. The whole cassette of CMV-GFP-Actin (Insert) from pmGFPC1 was amplified using forward primer with no restriction site and the reverse primer containing NotI restriction site (Fig. 13C). The pTRIPz lentiviral plasmid vector was digested with XbaI, purified, and blunted. After blunting it was digested with NotI and resolved on agarose gel where 3.3 kb release was seen with 9.9 kb backbone of pTRIPz (Fig. 13D). This 9.9 kb vector backbone was purified and ligated with insert, already digested with NotI, and transformed. The positive clone was screened by restriction digestion (Fig. 13E) and confirmed by DNA sequencing. The lentiviral particles were generated and transduced in B16F10 cells. Cells were selected using puromycin (Fig. 13F). The expression of GFP-actin was confirmed by observing green fluorescent cells and actin filament network (Fig. 13G & H). The lysates prepared from this cell line were probed with anti-GFP antibody showing the shift in molecular weight of GFP (Fig. 13I).

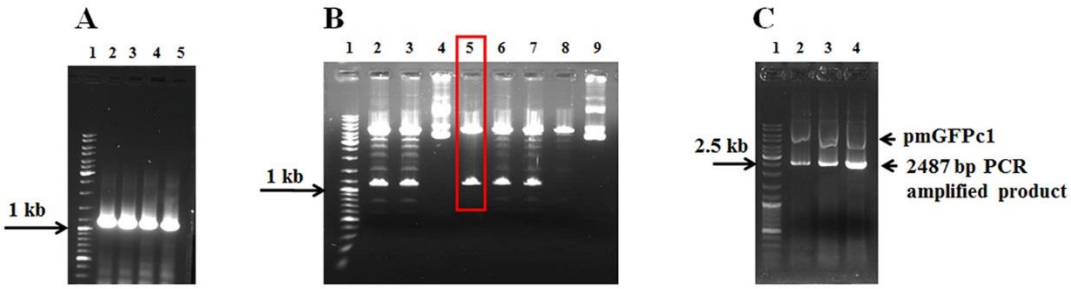

1: 1 kb DNA ladder
2-5: 1.1 kb PCR amplified product

1: 1 kb DNA ladder,
2-9. Recombinant pmGFPc1 after digestion with EcoRI & BamHI

1: 1 kb DNA ladder
2-4: 2.48 kb PCR amplified product

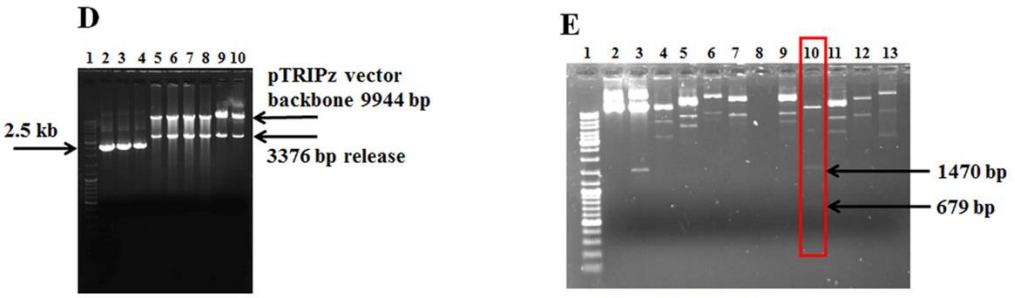

1: 1 kb DNA ladder
2-4: Amplified & digested CMV-GFP-Actin with NotI
5-10: Empty pTRIPz after digestion with NotI

1: 1 kb DNA ladder
2-13: Recombinant pTRIPz after digestion

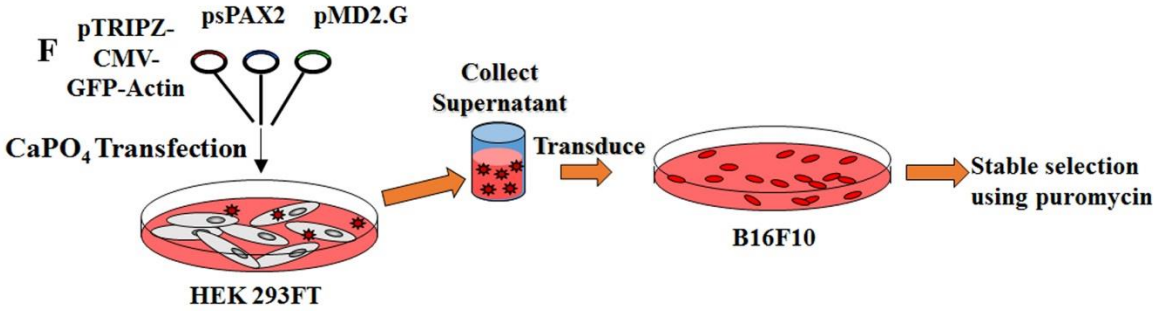

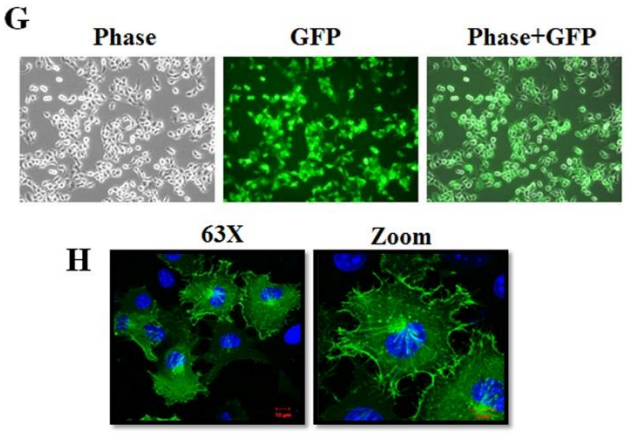

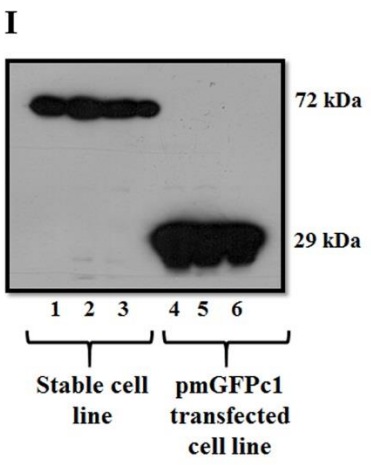

Fig. 13. Generation of B16F10 cell line stably expressing green fluorescent actin. (A) PCR amplification of 1.1 kb CDS of actin. (B) 1.1 kb band release of actin CDS from recombinant pmGFPc1 after restriction digestion with EcoRI and BamHI. (C) PCR amplification of CMV-GFP-Actin cassette from pmGFPc1. (D) Amplified CMV-GFP-Actin cassette and empty pTRIPz independently digested with NotI. (E) The 1470 bp and 679 bp band release after digestion with KpnI for screening of positive clone. (F) Schematic representation of preparation of viral particles and transduction of B16F10 cells. (G) Represent the images of B16F10 cells expressing green fluorescent actin acquired at 10x magnification and (H) at 63x magnification. Scale: 10 µM. (I) Immunoblots showing expression of GFP-actin and GFP.

4.12 Spreading kinetics of B16F10 cells on galectin-3 and fibronectin

The cell spreading kinetics was studied on immobilized galectin-3 and fibronectin. Fixed cell imaging showed that B16F10 cells on immobilized galectin-3 start spreading early showing frill-like lamellipodial morphology even at initial (15 min) time point, keeps increasing up to 30 min which was similar to that seen at 60 min (Fig. 14A). Lamellipodial structures at 15 min in cells plated on fibronectin were very different in appearance to those seen on galectin-3, which progressively increase up to 60 min (Fig. 14B). Cell spreading on uncoated coverslips for 60 min served as a control (Fig. 14C)

Live cell imaging was performed using B16F10 cells stably expressing GFP-Actin. The lamellipodial dynamics in cells plated on galectin-3 is very high even at very initial time points and the spreading of cells is stabilized by 30 min (Fig. 14D). However, in case of cells plated on fibronectin the lamellipodial dynamics is low and keeps increasing at constant rate to 60 min (Fig. 14E). The differences in cell spreading kinetics, microfilament architecture and lamellipodial organization on immobilized galectin-3 and fibronectin could be due to differential actin turn-over in the lamellipodial region.

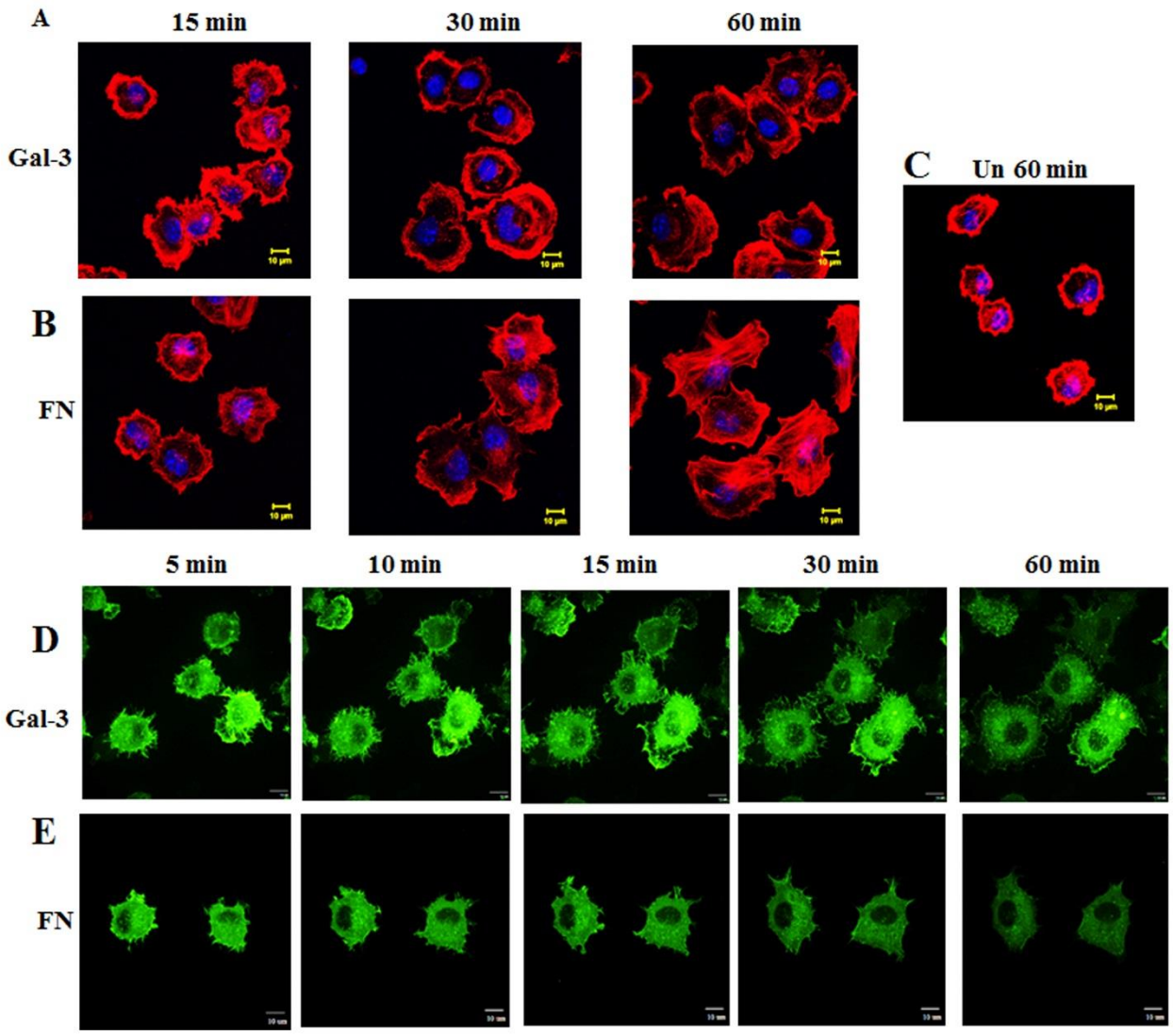

Fig. 14. Spreading kinetics of cells on galectin-3 and fibronectin assessed using fixed and live cell imaging. (A) and (B) represent the images of the cell spreading on immobilized galectin-3 and fibronectin respectively fixed at 15, 30 and 60 min, and (C) images of cell spreading on uncoated coverslips for 60 min. The cells were stained with phalloidin-TRITC for filamentous actin and DAPI for nucleus; 63x magnification. (D) and (E) represent the images extracted at time points 5, 15, 30 and 60 min from live cell imaging experiment performed using B16F10 cells expressing GFP-actin on immobilized galectin-3 and fibronectin respectively. Scale bar: 10 µm.

4.13 Turnover of filamentous actin in the lamellipodial region in cells spread on galectin-3 and fibronectin

Actin dynamics in the lamellipodial region was assessed using fluorescence recovery after photo-bleaching in B16F10 cells spread on immobilized galectin-3 and fibronectin. Percent recovery of the bleached area was significantly higher (68%) in the cells spread on galectin-3 as compared to those spread on fibronectin (54%). The cells spread on uncoated surfaces show lower recovery in the bleached region (46%) (Fig. 15). These results suggest actin dynamics in the lamellipodial region in the cells spread on galectin-3 is significantly higher as compared to that seen in cells plated on fibronectin. Differences in the morphological changes and actin recovery in this region could be due to the differential regulation of molecular signaling induced by galectin-3 and fibronectin.

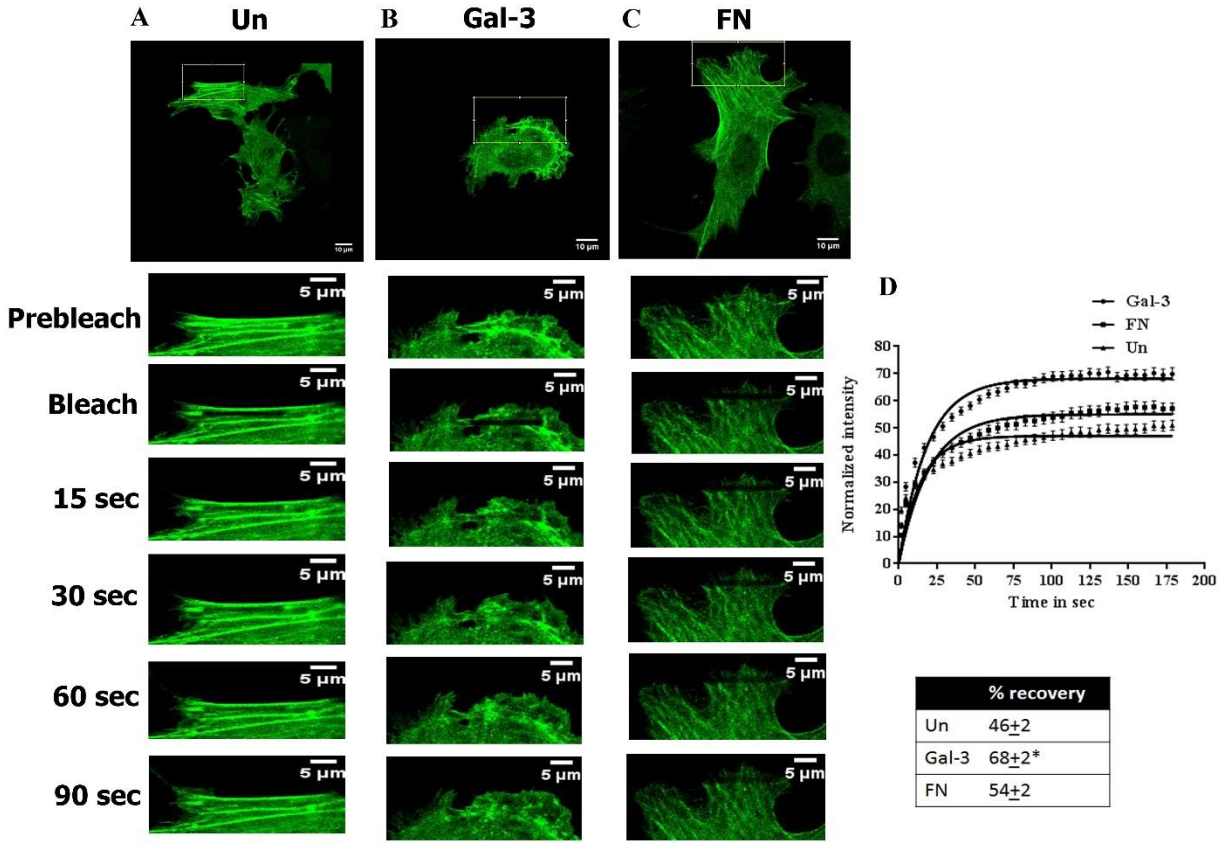

	% recovery
Un	46±2
Gal-3	68±2*
FN	54±2

Fig. 15. Actin turnover in the lamellipodial region of cells spread on galectin-3 and fibronectin. **(**A), (B) and (C) represent the images of FRAP analysis of GFP-actin in the lamellipodial region of B16F10 cells on uncoated, galectin-3 and fibronectin coated surfaces respectively. (D) Graphical representation of percent fluorescence recovery over time of GFP-actin in the lamellipodial region of cells on uncoated, galectin-3 and fibronectin coated surfaces. FRAP values obtained from 30 cells were used to calculate the percent recovery. Data is mean ± SE of three independent experiments *$p<0.05$.

4.14 Profile of Akt and Erk phosphorylation in cells spread on galectin-3 and fibronectin

In order to investigate the signaling pathways induced by galectin-3 and fibronectin, the time dependent activation of Akt and Erk was studied. Increase in Akt phosphorylation was observed in cells plated on galectin-3 while inverse correlation was observed in case of cells plated on fibronectin in a time dependent manner. Maximum phosphorylation of Akt is observed at 60 min on galectin-3 plated cells while fibronectin plated cells show maximum phosphorylation at 15 min (Fig. 16A & D). Phosphoryation of Akt could be completely abrogated by PI3K inhibitor wortmannin (Wm) in cells spread on both galectin-3 and fibronectin. However, PD98059, an inhibitor of MEK1/2 had no effect on Akt phosphorylation (Fig. 16B, E, C, F). Comparison of Erk phosphorylation in cells spread on galectin-3 and fibronectin showed that there is a time dependent decrease in phosphorylation of Erk in cells spread on both the substrates (Fig. 17A & D). Treatment with Wm only partially affected Erk phosphorylation while PD98059 completely inhibited phosphorylation of Erk in cells spread on both the substrates (Fig. 17B, E, C, F).

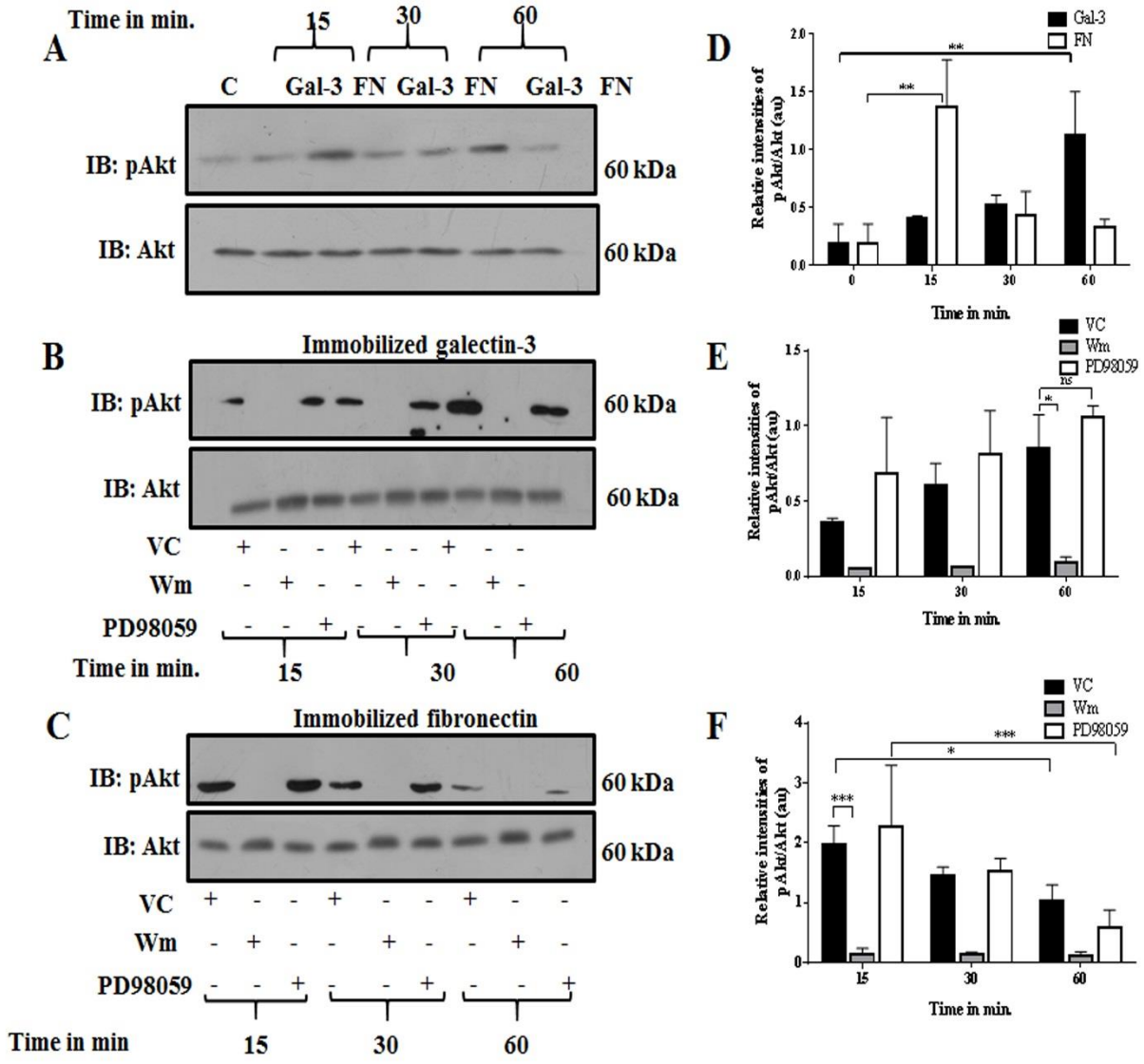

Fig. 16. Spreading of cells increases Akt phosphorylation with time on galectin-3 while decreases it on fibronectin**. (**A), (B) and (C) represent immunoblots of lysates of B16F10 cells spread on a immobilized galectin-3 and fibronectin for 0, 15, 30 and 60 min time points, C=0 min control. (B) and (C) represents immunoblots of lysates of B16F10 cells grown in presence of vehicle control (VC), Wm and PD98059, on (B) immobilized galectin-3 and (C) fibronectin. Each bar in the graphs (D), (E) and (F) represents the mean ratio of staining intensities with pAkt and Akt antibodies, in (A), (B) and (C) respectively. Data are mean ± SE of three independent experiments. *p<0.05, **p<0.01 and ***p<0.001.

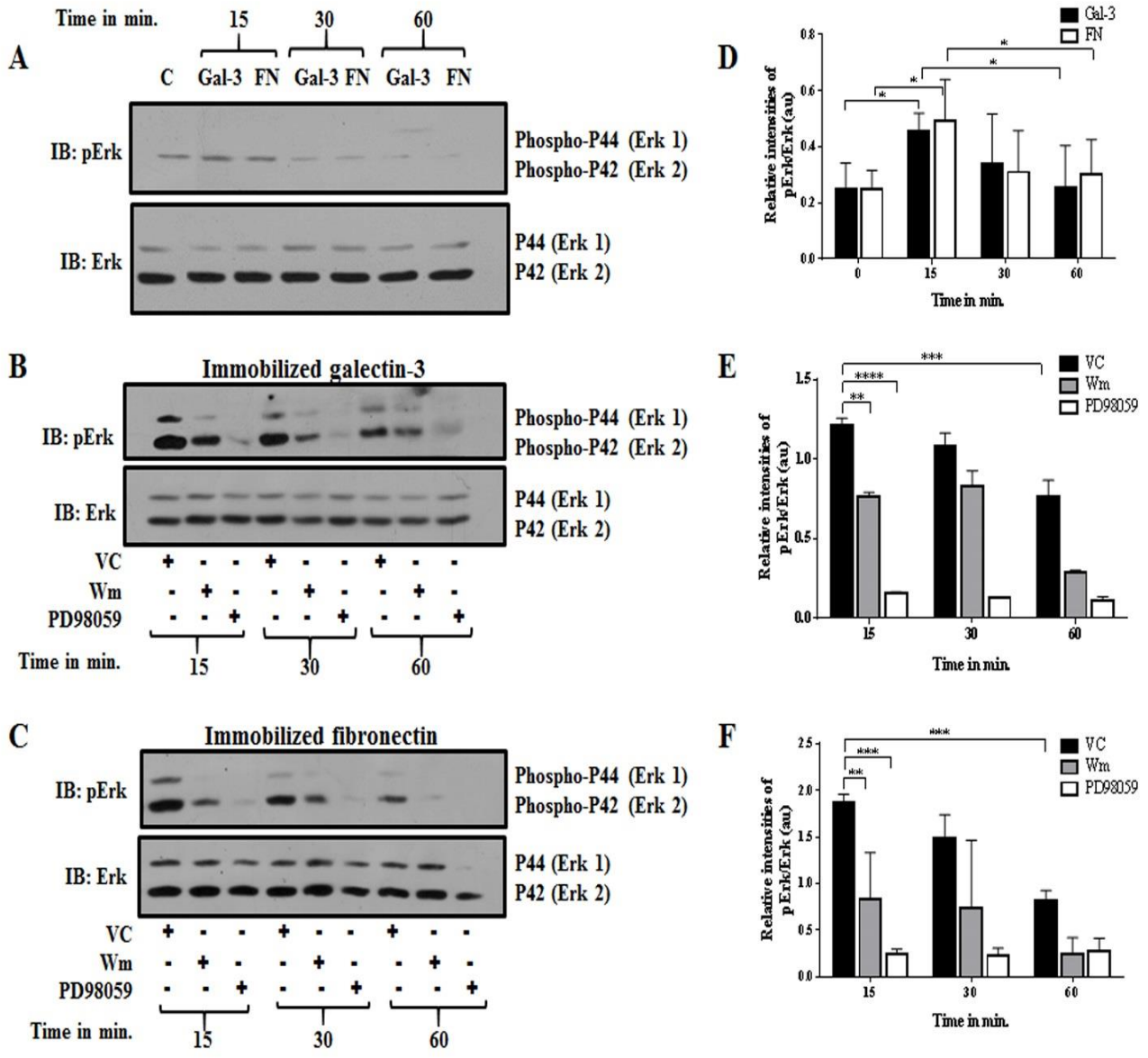

Fig. 17. Spreading of cells on galectin-3 and fibronectin decreases Erk phosphorylation with time**.** **(**A), (B) and (C) represent immunoblots of lysates of B16F10 cells spread on a immobilized galectin-3 and fibronectin for 0, 15, 30 and 60 min time points, C=0 min control. (B) & (C) represent immunoblots of lysates of B16F10 cells grown in presence of vehicle control (VC), Wm and PD98059, on (B) immobilized galectin-3 and (C) fibronectin. Each bar in the graphs (D), (E) and (F) represents the mean ratio of staining intensities with pErk and Erk antibodies, in (A), (B) and (C) respectively. Data are mean $\pm$ SE of three independent experiments. *p<0.05, **p<0.01 and ***p<0.001. (Erk1/p44 is 44 kDa, Erk2/p42 is 42 kDa protein)

4.15 Profile of Rac1 activation in cells spread on galectin-3 and fibronectin

Cyclic activation and deactivation of Rac1 plays an important role in organization of actin in the lamellipodial region which in turn dictates the cell motility [179]. The levels of activated GTP coupled Rac1 in cells spread on galectin-3 and fibronectin for different time points was assessed using Sepharose-PAK1 beads which bind to Rac1-GTP. The levels of activated Rac1 in cells plated on galectin-3 was highest at 15 min that kept on going down with time up to 60 min (Fig. 18A & C). However, in case of cells spread on fibronectin it was reverse. Activated Rac1 levels were lowest at 15 min and kept increasing with time, highest being at 60 min (Fig. 18B & D). The pattern of time dependent Rac1 activation in cells spread on both the substrates (Fig. 18) is opposite to each other however it appears to correlate with their time dependent spreading and lamellipodial organization (Figs. 12 and 14) on these substrates.

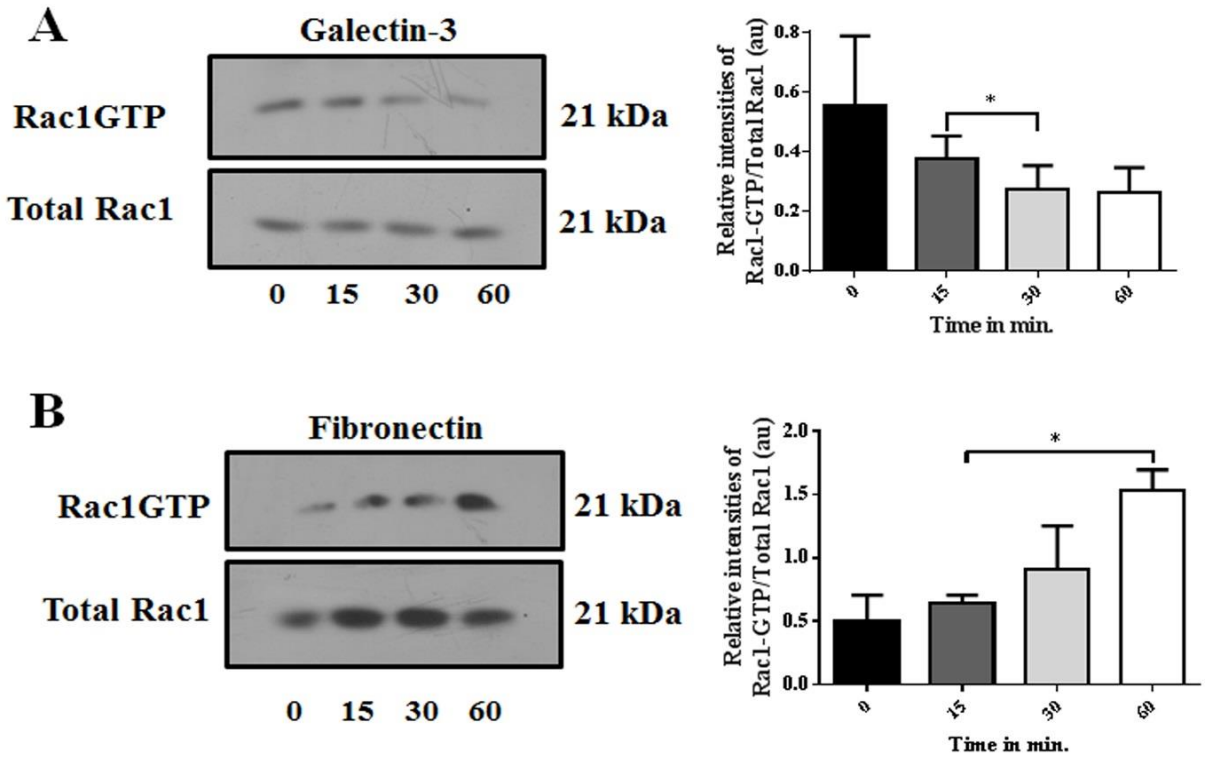

Fig. 18. Differential activation of Rac1 on immobilized galectin-3 and fibronectin. Western blotted purified activated Rac1 (as described in Materials and Methods) from lysates of cells allowed to spread for 0, 15, 30 and 60 min on (A) immobilized galectin-3 and (B) fibronectin, probed with anti-Rac1 antibody. Levels of total Rac1 in the cell lysates served as loading control. (C) and (D) represent the graphical quantitation of (A) and (B) respectively. Data are mean ± SE of three independent experiments. *$p<0.05$.

4.16 Effect of inhibitors of Akt and Erk pathway on cellular spreading and migration on galectin-3 and fibronectin

Standard spreading assay of B16F10 cells treated only with the vehicle (0.1% DMSO) (VC), Wm and PD98059 was performed on uncoated and galectin-3 or fibronectin coated coverslips for 45 min at 37ºC and 5% CO_2. Results showed that in comparison to cells plated on uncoated coverslips (Fig. 19A), those on galectin-3 (Fig. 19B) and fibronectin (Fig. 19C) spread well and show very well organized microfilament architecture, although distinct for each substrate. This is also very evident in significantly higher ratio of cytoplasmic to nuclear area in these cells as compared to those on uncoated coverslips (Fig. 19D). However, treatment of cells with Wm and PD98059 significantly inhibited the spreading, lamellipodial structures and microfilament organization in cells plated on galectin-3, however, those plated on fibronectin largely remain unaffected (Fig. 19D).

Spreading is an initial event that influences cellular motility. Wound healing assay was performed on cells plated on BSA, galectin-3 and fibronectin coated plates in absence or presence of vehicle, Wm and PD98059. Results showed that as compared to vehicle control, Wm and PD98059 significantly inhibit migration of cells on galectin-3 coated plates (Fig. 19E & H), whereas, these inhibitors very marginally affect movement of cells on fibronectin (Fig. 19F & H). The lowest wound closure was observed on uncoated surfaces blocked with BSA (Fig. 19G & H).

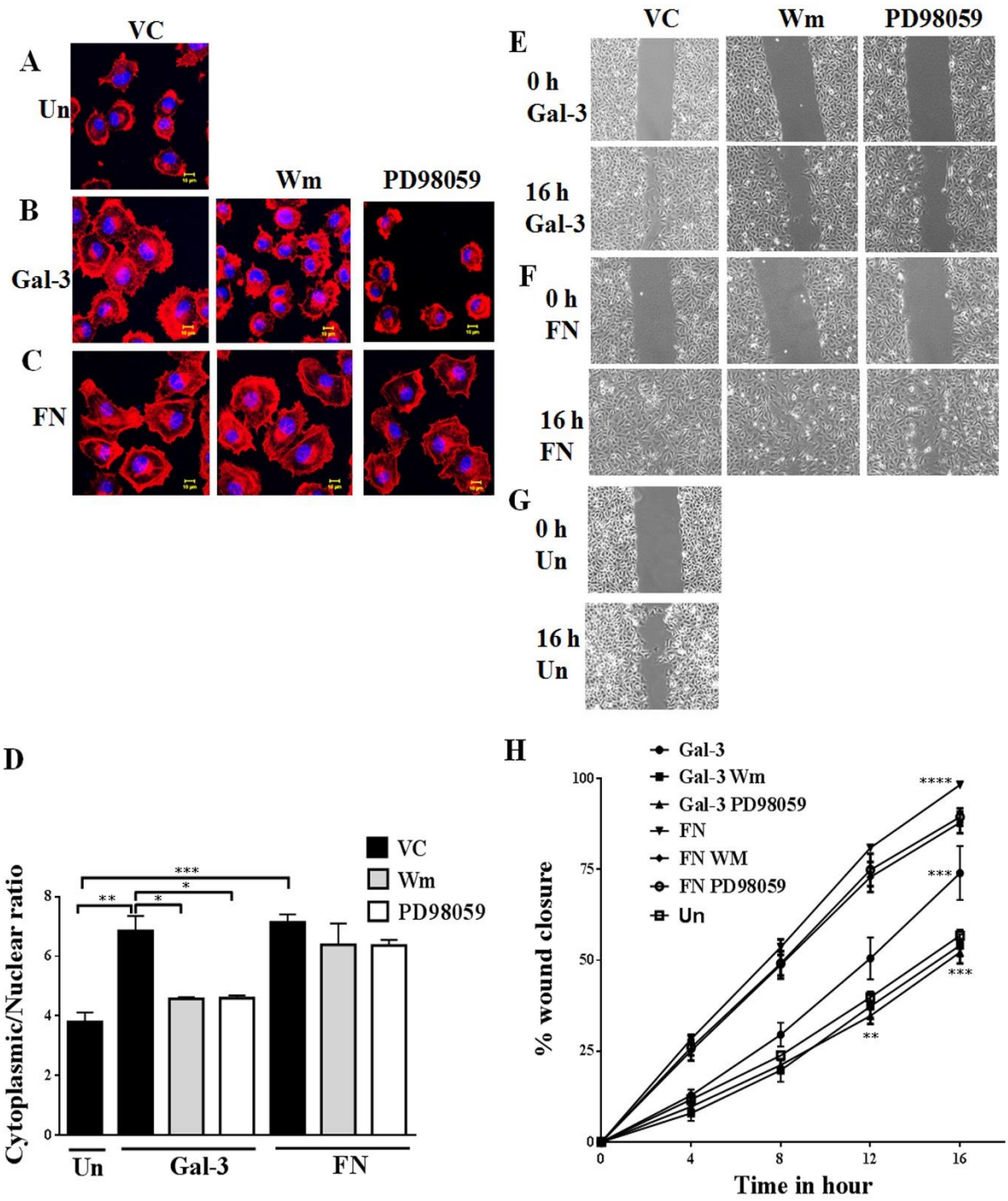

Fig. 19. Effect of Wm and PD98059 on cell spreading and migration. **(**A), (B) and (C) represent images of the cell spreading of B16F10 cells treated with vehicle control (VC), Wm and PD98059, on uncoated (Un), immobilized galectin-3 and fibronectin respectively. The cells were fixed and stained with phalloidin-TRITC for filamentous actin and DAPI for nucleus; 63x magnification.

Scale bar: 10 μm. Each bar in (D) represents the mean ratio of cytoplasmic/nuclear area of at least 50 cells in (A), (B) and (C) of three independent experiments *p<0.05, **p<0.01 and ***p<0.001. (E), (F) and (G) are representative images of wound healing assay at 0 and 16 hour, on galectin-3 coated, fibronectin coated and uncoated surfaces respectively, of B16F10 cells treated with VC, Wm and PD98059. (H) Represents mean percent wound closure of cells in (E), (F) and (G), at 4 hour interval up to 16 hour. Area of wound closure was measured at three different positions from three different experiments. Two-way analysis of variance followed by Bonferroni's multiple comparison test was performed to compare significance. *p<0.05, **p<0.01 and ***p<0.001; All error bars represent mean $\pm$ s.e.m.

Chapter 5

Discussion

Dissemination of cells from primary tumor to secondary non-contiguous organ site is called metastasis. Metastasis is an essential phenomenon in pathogenesis of cancer. It is a complex, multistep process. To successfully colonize at secondary site a cancer cell must complete a sequential series of steps. These steps typically include detachment from the primary tumor, invasion through surrounding tissues and basement membranes, entry and survival in the circulation and arrest & establishment in a distant target organ [1,41,53].

Cell surface molecules play a crucial role in all the steps of metastatic cascade. Tumor cells show several cell surface modifications associated with the metastatic phenotype, including changes in the cell surface glycosylation [180,181]. One of the frequently observed modifications is the altered expression of β1, 6 branched N-oligosaccharides on cell surface glycoproteins. These oligosaccharides have been strongly associated with the invasive and metastatic phenotype of tumor cells [4,101,105,182]. The increased β1, 6 branched N-oligosaccharides on proteins may affect the structure and function of the proteins which carry them and also they may provide several novel ligands for endogenous lectins [4,111,183,184]. Another interesting feature of these oligosaccharides is that majority of the cell lines expressing them metastasize either to the lungs or liver [101,111,112].

Previous work in our lab has shown that polyLacNAc substituted β1, 6 branched N-oligosaccharides expressed on B16F10 cells promote lung specific metastasis via galectin-3 which is expressed in highest amounts on the lungs. It was shown to be expressed on almost all the compartments of the lungs and constitutively on the surface of vascular endothelium. Galectin-3/polyLacNAc interaction promotes adhesion to vascular endothelium, spreading, degradation of vascular basement membrane and movement into organ parenchyma. Inhibition of these

oligosaccharides by down regulating the enzymes, responsible for polyLacNAc substitutions, inhibited all these processes and metastasis [5,6].

The importance of galectin-3/polyLacNAc interaction in lung specific metastasis of B16F10 cells was further proved by alternative approaches. Galectin-3 is a monomeric lectin that forms oligomers on binding to its ligand via its N-terminal domain [10]. Truncated galectin-3, devoid of the N-terminal domain, has been shown to act as a dominant negative inhibitor of galectin-3, affect growth and lymph node metastasis of breast cancer cell line on sustained treatment [185]. Pre-incubation of B16F10 cells with purified truncated galectin-3 (Figs. 3 and 4) inhibited lung metastasis apparently by blocking polyLacNAc on melanoma cells making it unavailable for binding to galectin-3 on the lung vascular endothelial cells (Figs. 5-7). MCP has been shown to affect several galectin-3 mediated processes including metastasis [12,186,187]. Inhibition of experimental metastasis in mice fed with MCP indicated that MCP in circulation possibly competes with polyLacNAc on melanoma cells for binding to endothelial cells (Figs. 1 and 2).

The three subpopulations of galectin-3 transgenic mice, successfully genotyped and characterized, provide an important tool to investigate the role of galectin-3 in metastatic process. The galectin-$3^{+/-}$ mice in which the expression of galectin-3 was <50% as compared to galectin-$3^{+/+}$ mice, also showed correspondingly reduced lung metastasis, indicating that galectin-3 on the lungs is indeed an important determinant of metastatic outcome. Surprisingly, however, the galectin-$3^{-/-}$ mice which lacked galectin-3 on the lungs showed almost similar extent of metastasis as the galectin-$3^{+/+}$ mice (Fig. 8A and B).

Galectins are a family of β-galactoside binding lectins which often exhibit functional redundancy. Besides galectin-3, other members including galectin-1, -8 and -9 have been shown to be expressed on the lungs and have very similar oligosaccharide specificity [10,133]. However, analysis of the

transcripts of these galectins, or comparison of the lactose binding proteins in the lungs from galectin-$3^{+/+}$ and galectin-$3^{-/-}$ mice did not show any significant difference. Although, the results do not completely rule out the possibility of some other galectin taking over the function of galectin-3, it weakens this possibility [188]. An alternative approach was devised to test this. While inhibition of N-oligosaccharides significantly inhibits metastasis of B16F10 cells in galectin-$3^{+/+}$ mice [7], their inhibition should also inhibit metastasis in the galectin-$3^{-/-}$ mice, in case other galectins take over galectin-3 function. However, swainsonine treatment failed to have any effect on the metastatic properties of these cells in galectin-$3^{-/-}$ mice (Fig. 8C), pointing towards possible alternate mechanism(s).

Almost a million tumor cells are believed to be in circulation in a patient diagnosed with cancer, however, only a few of them metastasize. Experimentally it has been shown that, although, > 95% of the B16F10 cells injected via tail vein can be recovered from the lungs of mice within 2 minutes of injection, majority of them are cleared by 24 hours. Only about 2% of the injected cells remain in the lungs by 24 hours [189]. Even of these 2% arrested cells, only those that are able to interact with the host organ environment are possibly able to survive and grow as 100-150 metastatic colonies. Interactions between molecules like polyLacNAc on cancer cells and galectin-3 on the organs like lungs would assume importance at this stage. However, host immune competence would play a key role in clearing majority of the cells from the target organ. Agents which augment NK cell activity in mice have indeed been shown to be very efficient in inhibiting metastasis, which was ineffective in beige mice which lack NK cells or in mice where NK cells were depleted [189]. With this information background the question arose - "are galectin-$3^{-/-}$ mice not competent enough immunologically?"

Galectin-3 plays an important role in regulating different functions of innate and adaptive immune systems [136,137,138,139]. Almost all types of immune cells express galectin-3. As galectin-3 is present in the nucleus, cytoplasm and on the cells surface and as part of ECM, its function varies depending on its subcellular localization. Galectin-3 in the cytoplasm is anti-apoptotic while nuclear galectin-3 is pro-apoptotic whereas that on the cell surface or on ECM/BM performs very different functions. As a result galectin-3 influences immune response in a variety of ways which are often conflicting [15,136,139].

Galectin-3 influences innate immunity by modulating adhesion and migration of monocytes [140], macrophages and dendritic cells [141]. It promotes adhesion of neutrophils to laminin and regulates neutrophil traversing through BM at sites of inflammation [142,143]. Galectin-3 also, regulates T-cell signaling, activation, cytokine secretion, apoptosis and regulatory T-cell proliferation. Galectin-3 deficiency results in increased frequency of immune suppressor cells such as $CD4^{+}CD25^{+}FOXP3^{+}T_{reg}$ cells [143,150,151,190]. In contrast, galectin-3 induces apoptosis in $CD8^{+}$T cells in mouse model of colorectal cancer [152]. Although, galectin-$3^{-/-}$ mice are viable, they have a distinct phenotype in terms of their immune functions related to autoimmunity, and responses to allergy, inflammation and infectious diseases [172]. However, unified picture of galectin-3 mediated effects on host immunity and metastasis is yet to emerge clearly. It is very likely that galectin-$3^{-/-}$ mice are defective in their critical immune function which may positively or negatively influence metastatic outcome.

In such a scenario, analogous to the beige mice which lack NK cell activity, the galectin-$3^{-/-}$ mice would also have much higher burden of mechanically arrested melanoma cells in the lungs. If they are not cleared efficiently, some of these possibly give rise to metastatic colonies, especially because the high metastatic B16F10 cells have been selected specifically for lung colonization by

serial *in vitro* and *in vivo* passaging of B16F1 cells. Some of these would be able to adapt to the growth environment of the lungs even in absence of polyLacNAc and galectin-3. This would be very similar to what is proposed for anatomical/mechanical mode of metastatic spread. However, a recent report on experiments with B16F1 cells using galectin-$3^{+/+}$ and galectin-$3^{-/-}$ mice has suggested that the galectin-$3^{-/-}$ mice may be more competent in terms of their anti-tumor immunity as compared to galectin-$3^{+/+}$ mice via their enhanced NK-cell activity [191]. In contrast to these, our preliminary experiments with B16F1 cells in these mice did not give statistically significant variation in the number of metastatic colonies, mainly because the total number of metastatic colonies of B16F1 cells in the lungs as such, was very low.

Generating chimeric mice by replacing the bone marrow of galectin-$3^{-/-}$ mice with that of galectin-$3^{+/+}$ type mice may possibly restore immunity and thus should inhibit metastasis. Although, chimeric mice could be successfully generated, metastasis of B16F10 cells in the lungs could not be inhibited in these mice (Fig. 9). Galectin-3 also appears to be required for maturation of several immune cells like the maturation of plasma cells into memory B cells and the selection of $CD4^{+}$T and $CD8^{+}$T cells in the thymus [147]. These results suggest that in the absence of galectin-3, even after replacing the bone marrow, the galectin-$3^{-/-}$ mice may not achieve an effective anti-tumor immunity.

By employing galectin-$3^{+/+}$ and galectin-$3^{+/-}$ transgenic mice and lung homing high metastatic B16F10 cells, the present investigation very clearly demonstrates that specific interactions between molecules on the tumor cells and on the target organ indeed play an important role in facilitating organ specific metastasis. By utilizing galectin-$3^{-/-}$ mice, it also demonstrates the importance of host immunity in controlling metastasis and the complex manner in which it is regulated. This warrants a thorough investigation. Recently, Choudary *et al*. showed that the

galectin-3$^{-/-}$ mice lack the active immune response. It is mainly because of decreased NK cell cytotoxicity, disturbed serum Th1, Th2 and Th17 cytokine milieu, reduced serum IFN-γ levels and attenuation of splenic STAT1 mediated IFN-γ signaling [192].

In order to investigate the role of galectin-3, it is also important to know about the galectin-3 binding proteins. Mass spectrometric screen was performed to find out galectin-3 binding proteins. It was found that along with many other cell surface glycoproteins, CD147 is a major carrier of β1, 6 branched N-oligosaccharides. It is reported that glyco-deficient CD147 fails to induce matrix metalloproteases by tumor cells [156,167]. Hence we studied the role of CD147 and its glycosylation in galectin-3 mediated metastatic processes of B16F10 cells.

CD147 is a highly glycosylated galectin-3 binding protein that has two isoforms [8,9]. B16F10 cells abundantly expresses isoform 2 but no isoform 1. The expression levels of CD147 was found to be higher in B16F10 cells as compared to that of B16F1 cells. Also both the cell lines express high and low glycosylated forms of the CD147 (Fig. 10).

Wt CD147 was shown to be expressed on the cell surface while CD147 deficient with all glycosylation sites was found to be accumulated in the cell cytoplasm (Fig. 11A). It suggests that glycosylation plays important role in the localization and targeting of CD147 to the cell membrane. To investigate the crucial site required for targeting of CD147 to the membrane combinations of CD147, mutants were generated. TGM and ATGM CD147 were expressed in B16F10 cells show cytoplasmic localization. N154Q, N190Q and N193Q CD147 mutants accumulated inside the cell cytoplasm while N44Q, N159Q CD147 glycomutants showed cell surface localization (Fig. 11). Wild type CD147 was expressed on the cell surface while CD147 deficient with all glycosylation sites accumulated in the cytoplasm. Under these conditions it was not possible to investigate the functions of glyco-deficient CD147 as these were not seen on the membrane.

Motility of cancer cells is critical for their invasiveness and metastasis. Cellular adhesion followed by spreading are crucial events that determine the pattern of cellular movement [87,193,194,195,196,197]. The effect of galectin-3 on metastatic processes and downstream signaling induced by it was poorly understood. The present investigation explores the molecular mechanisms involved in galectin-3 mediated processes, especially cellular spreading and motility by comparing it with that on ECM component fibronectin which is very well studied.

The lamellipodial organization in the cells spread on galectin-3 is very different from that seen in cells spread on fibronectin. The cells on fibronectin show features of mesenchymal-like cells with classical stress fibers traversing throughout the cell body, whereas those on galectin-3 display broad and rounded lamellipodia with parallel actin bundles along the cell periphery. The cells appear to maintain their distinct morphology even during migration on these substrates (Fig. 12). Further, the kinetics of cell spreading and lamellipodial organization on each of these substrates was markedly different. The cells on galectin-3 attain the morphology and lamellipodial organization at an early time point. However, the mesenchymal morphology, the lamellipodial structures and the stress fibers keep growing steadily and get stabilized at a later time point in cells on fibronectin (Fig. 14).

Organization of microfilaments is the major determinant of the type of lamellipodial structures, which in turn depends on the actin dynamics [178,198,199,200]. The actin dynamics in the lamellipodial region of cells on galectin-3 was significantly higher as compared to that on fibronectin as analyzed using FRAP (Fig. 15). This suggests that very distinct signaling mechanisms operate in the cells spread on galectin-3 and on fibronectin which regulate microfilaments, lamellipodia formation and spreading morphology.

The two major pathways which are known to regulate cellular spreading and motility are PI3K/Akt and Erk-MAPK. Both Akt and Erk are activated in response to extracellular cues [80,82,201]. Here we compared the activation status of these two regulators in cells spread on galectin-3 and fibronectin. Fibronectin being one of the best studied ECM component acts as a substrate for various normal as well as cancer cell lines and support their adhesion dependent motility. Fibronectin induces out-side in signaling through integrin receptors while galectin-3 has myriad of cell surface receptors. Most studies have investigated the activation of signaling pathways in cells plated on fibronectin coated plates. Chinese Hamster Ovary (CHO-P) cells [135] and transformed cell lines like murine hepatocellular carcinoma cells CBO140C12 [202], Cos7 cells [203] and human non-small cell lung carcinoma H1792 cells [204] plated on fibronectin show activation of both Akt and Erk.

The secreted extracellular galectin-3 exerts its cellular effects on motility related processes both in the soluble form and as immobilized component on cells, ECM and BM. The soluble galectin-3 promotes fibronectin dependent cell spreading and motility of mammary carcinoma cells by interacting with β1, 6 branched N-linked oligosaccharides [126]. Interaction of integrin receptors with fibronectin in presence of galectin-3 leads to phosphorylation of caveolin-1 which stabilizes FAK in the focal adhesions (FAs) and induces its disassembly, required for cell migration [127]. Galectin-3 also regulates motogenic response of epidermal growth factor in mammary cell lines [128]. Exogenously added soluble galectin-3 has also been shown to induce lamellipodial formation in corneal epithelial cells by interacting with integrins [129]. Moreover, extracellular galectin-3 facilitates PI3K dependent migration of sarcoma derived cell line on laminin 111 [130]. Down regulation of galectin-3 in intestinal epithelial cells affects the stability of desmosomal cadherins and intercellular adhesion [131]. Binding of galectin-3 to N-cadherins has been shown

to destabilize cell-cell junctions in murine mammary cancer cells which might favor cell migration [132]. Galectin-8 which has oligosaccharide specificity very similar to galectin-3 [133] has been shown to act as a matricellular protein and modulator of cell adhesion by interacting with integrins [134,135]. The Erk phosphorylation in response to EGF was activated only in galectin-3 expressing and not galectin-3 null keratinocytes [205]. However, there is no study that investigates the signaling mechanisms in cells that use galectin-3 as the substratum for their adhesion, spreading, movement and possibly their growth. Further, although there are a few studies that have explored the time dependent signaling mechanisms during spreading of cells on fibronectin [84], there are no reports about the signals induced during cellular spreading mediated by immobilized galectin-3.

Comparison of the signaling pathways activated during spreading of B16F10 cells that express high levels of polyLacNAc, on fibronectin and galectin-3 showed distinct pattern. The cells showed sustained time dependent activation of Akt when spread on galectin-3, however, it was only transient in cells on fibronectin (Fig. 16A). The receptors for fibronectin are well defined integrin receptors. However, all the surface proteins that carry polyLacNAc substituted β1, 6 branched N-oligosaccharides can be receptors for galectin-3, which include integrins, cell adhesion molecules (CAMs), receptor tyrosine kinases (RTKs), growth factor receptors (GFRs) and lysosome-associated membrane proteins (LAMPs) [118] (Unpublished data). The differential activation of Akt in cells on galectin-3 and fibronectin is possibly due to the different set of receptors for each substrate which follow different pathway(s) for activation of Akt. The activation of Erk is generally transient in a migrating cell, and sustained activation leads to cellular differentiation [206]. The activation of Erk in B16F10 cells was indeed transient during spreading irrespective of the substrate used, galectin-3 or fibronectin (Fig. 17A).

Pharmacological inhibition of PI3K/Akt and Erk-MAPK signaling pathways using wortmannin and PD98059 respectively, showed that wortmannin significantly inhibits phosphorylation of Akt while Erk phosphorylation was affected only partially, on both the substrates. However, PD98059, inhibitor of MEK1/2 inhibits phosphorylation of Erk but not Akt on both the substrates (Figs. 16 and 17). These results suggest that the Akt is activated independently of Erk-MAPK pathway while Erk activation depends on both PI3K/Akt and Erk-MAPK pathways.

Akt activation results in the regulation of the activity of RhoGTPases which play an important role in microfilament organization. RhoGTPases, Rac1, CDC42 and RhoA are the major players that control cellular migration by regulating formation of cellular structures like lamellipodia, filopodia and stress fibers, respectively. Formation of lamellipodia is an important step in cellular spreading and substrate dependent motility (haptotaxis). Rac1 is the major regulator of the lamellipodial organization and activation of Rac1 is required for its formation [79,179,200,207,208]. The time dependent increase in the levels of activated Rac1 correlated with the lamellipodial organization in cells plated on fibronectin (Fig. 18B). Both Rac1 activation and formation of lamellipodia keep increasing with time (Figs. 18B and 14B & E). The time dependent increase in Rac1 activation was accompanied with a corresponding decrease in Akt activation (Figs. 18B and 16A).

However, in cells plated on galectin-3 where well-formed lamellipodial structures get organized even at an early time point (15 min) the levels of activated Rac1 is highest, and keeps decreasing with time (Figs. 18A and 14A & C). Although, Akt activation in cells on galectin-3 follow the same inverse trend in comparison to Rac1 activation (Figs. 16A and 18A) as seen in fibronectin, it keeps increasing with time. GTP binding activity of Rac1 is critical for the formation of lamellipodial structures and activated Akt has been shown to inhibit this activity by phosphorylating Rac1 at Ser 71 [209,210]. This explains the changes in the lamellipodial structures

and inverse correlation of Akt and Rac1 activation in cells on galectin-3 and fibronectin which was opposite to each other on these substrates.

Although, activated Rac1 is the major regulator of lamellipodia formation and cellular spreading, it can be activated by multiple mechanisms. Spreading and motility in presence of inhibitors of PI3K/Akt (wortmannin) and Erk-MAPK (PD98059) showed that both these pathways operate for spreading and movement on galectin-3. However, none of these inhibitors had any significant effect on these processes on fibronectin (Fig. 19), suggesting that Rac1 activation in these cells occurs via some other mechanism. FAK on activated integrin receptor for fibronectin often gets auto-phosphorylated at Tyr397 which serves as docking site for Src and PI3K resulting in their activation. Activated FAK-Src complex activates scaffolding proteins like p130Cas and paxillin which in turn activate GEFs for Rac1 and CDC42, the key regulators of lamellipodia and filopodia, respectively [83,211]. The Rac1 activation and lamellipodia formation in B16F10 cells plated on fibronectin possibly act via FAK-Src/p130Cas pathway, explaining the absence of any effect of wortmannin or PD98059 on cellular spreading and motility on this substrate.

These studies clearly demonstrate that immobilized galectin-3 like other components of ECM and BM also supports spreading and movement of cells. By way of multiple receptors on the cell surface expressing high affinity ligands like polyLacNAc, galectin-3 signals distinct pathways that modulate microfilament dynamics and promote lamellipodial organization that supports spreading and movement. We demonstrate that each of these characteristics including, lamellipodial organization, actin dynamics, signaling pathways, spreading and movement on galectin-3 are very distinct from that seen on the classical ECM component, fibronectin.

While fibronectin supports directional motility of cells with mesenchymal phenotype which is required for almost all the stages of metastatic cascade. However, the cells do not need directional

long distance motility once they reach the target organ. The cells adopt themselves to random movement required to explore the microenvironment of the target organ. The spreading and motility pattern of cells seen on immobilized galectin-3 are typical features of random movement [212,213]. Lungs which express highest levels of galectin-3 on almost all the tissue compartment [5,6] is utilized by B16F10 melanoma cells for random movement and in their establishment in the target organ. These observations together with earlier reports about the participation of galectin-3 in the initial arrest and processes involved in extravasation, clearly demonstrate its critical role in organ (lung) specific metastasis.

Chapter 6

Summary and Conclusion

Summary

- Modified citrus pectin and truncated galectin-3 affects the metastatic potential of B16F10 cells
- Lung metastatic potential of B16F10 cells were comparable in galectin-$3^{+/+}$ and galectin-$3^{-/-}$ mice
- B16F10 murine melanoma metastasis was unaffected in bone marrow chimeric mice
- Expression levels of CD147 correlates with the metastatic potential of the cell lines
- CD147 glycomutant failed to express on the cell surface
- N154, N190 and N193 are the critical glycosylation sites on CD147 for its targeting to the cell surface
- B16F10 cells show distinct cytoskeletal organization when allowed to spread on galectin-3 as opposed to fibronectin
- Spreading kinetics of B16F10 cells on galectin-3 is more dynamic
- Turnover of filamentous actin at the lamellipodial region is high in cells spread on galectin-3 as compared to those on fibronectin
- Akt phosphorylation is inversely regulated in cells spread on galectin-3 and fibronectin while Erk is regulated similarly in both
- Rac1 activation is inversely regulated in cells spread on galectin-3 and fibronectin
- Inhibitors of Akt and Erk pathway inhibit cellular spreading and migration on galectin-3 but have no effect on fibronectin

Conclusion

The role of galectin-3/polyLacNAc interaction in lung specific metastasis was strengthened or proved by using competitive and dominant negative inhibitors, MCP and truncated galectin-3 respectively. It was established that this interaction is indeed important for lung specific metastasis by using galectin-3 transgenic mice (galectin-$3^{+/-}$ mice). Surprisingly, the reversal of metastasis in galectin-$3^{-/-}$ mice possibly suggests compromised status of host anti-tumor immunity in these mice. The glycosylation sites on galectin-3 binding protein CD147, required for its targeting to the cell membrane, were identified. The present study successfully dissected the molecular mechanisms involved in galectin-3 mediated cellular spreading and motility. It demonstrates that the dynamics and organization of lamellipodial structures and signaling events on galectin-3 are very distinct as compared to those observed on very well studied extracellular matrix component such as fibronectin.

References

[1] G.P. Gupta, J. Massague, Cancer metastasis: building a framework, Cell 127 (2006) 679-695.
[2] S. Hakomori, Tumor malignancy defined by aberrant glycosylation and sphingo(glyco)lipid metabolism, Cancer Res 56 (1996) 5309-5318.
[3] H. Ponta, J. Sleeman, P. Herrlich, Tumor metastasis formation: cell-surface proteins confer metastasis-promoting or -suppressing properties, Biochim Biophys Acta 1198 (1994) 1-10.
[4] J.W. Dennis, M. Granovsky, C.E. Warren, Glycoprotein glycosylation and cancer progression, Biochim Biophys Acta 1473 (1999) 21-34.
[5] M.C. Dange, N. Srinivasan, S.K. More, S.M. Bane, A. Upadhya, A.D. Ingle, R.P. Gude, R. Mukhopadhyaya, R.D. Kalraiya, Galectin-3 expressed on different lung compartments promotes organ specific metastasis by facilitating arrest, extravasation and organ colonization via high affinity ligands on melanoma cells, Clin Exp Metastasis 31 (2014) 661-673.
[6] V. Krishnan, S.M. Bane, P.D. Kawle, K.N. Naresh, R.D. Kalraiya, Altered melanoma cell surface glycosylation mediates organ specific adhesion and metastasis via lectin receptors on the lung vascular endothelium, Clin Exp Metastasis 22 (2005) 11-24.
[7] N. Srinivasan, S.M. Bane, S.D. Ahire, A.D. Ingle, R.D. Kalraiya, Poly N-acetyllactosamine substitutions on N- and not O-oligosaccharides or Thomsen-Friedenreich antigen facilitate lung specific metastasis of melanoma cells via galectin-3, Glycoconj J 26 (2009) 445-456.
[8] Y. Bai, W. Huang, L.T. Ma, J.L. Jiang, Z.N. Chen, Importance of N-glycosylation on CD147 for its biological functions, Int J Mol Sci 15 (2014) 6356-6377.
[9] L. Xiong, C.K. Edwards, 3rd, L. Zhou, The biological function and clinical utilization of CD147 in human diseases: a review of the current scientific literature, Int J Mol Sci 15 (2014) 17411-17441.
[10] J. Dumic, S. Dabelic, M. Flogel, Galectin-3: an open-ended story, Biochim Biophys Acta 1760 (2006) 616-635.
[11] A. Fortuna-Costa, A.M. Gomes, E.O. Kozlowski, M.P. Stelling, M.S. Pavao, Extracellular galectin-3 in tumor progression and metastasis, Front Oncol 4 (2014) 138.
[12] P. Nangia-Makker, V. Hogan, Y. Honjo, S. Baccarini, L. Tait, R. Bresalier, A. Raz, Inhibition of human cancer cell growth and metastasis in nude mice by oral intake of modified citrus pectin, J Natl Cancer Inst 94 (2002) 1854-1862.
[13] A.K. Agarwal, R.P. Gude, R.D. Kalraiya, Regulation of melanoma metastasis to lungs by cell surface Lysosome Associated Membrane Protein-1 (LAMP1) via galectin-3, Biochem Biophys Res Commun 449 (2014) 332-337.
[14] M.C. Dange, A.K. Agarwal, R.D. Kalraiya, Extracellular galectin-3 induces MMP9 expression by activating p38 MAPK pathway via lysosome-associated membrane protein-1 (LAMP1), Mol Cell Biochem 404 (2015) 79-86.
[15] S. Califice, V. Castronovo, F. Van Den Brule, Galectin-3 and cancer (Review), Int J Oncol 25 (2004) 983-992.
[16] A.U. Newlaczyl, L.G. Yu, Galectin-3--a jack-of-all-trades in cancer, Cancer Lett 313 (2011) 123-128.
[17] J. Ferlay, I. Soerjomataram, R. Dikshit, S. Eser, C. Mathers, M. Rebelo, D.M. Parkin, D. Forman, F. Bray, Cancer incidence and mortality worldwide: sources, methods and major patterns in GLOBOCAN 2012, Int J Cancer 136 (2015) E359-386.

[18] P. Anand, A.B. Kunnumakkara, C. Sundaram, K.B. Harikumar, S.T. Tharakan, O.S. Lai, B. Sung, B.B. Aggarwal, Cancer is a preventable disease that requires major lifestyle changes, Pharm Res 25 (2008) 2097-2116.
[19] A. Jemal, F. Bray, M.M. Center, J. Ferlay, E. Ward, D. Forman, Global cancer statistics, CA Cancer J Clin 61 (2011) 69-90.
[20] A. Jemal, M.M. Center, C. DeSantis, E.M. Ward, Global patterns of cancer incidence and mortality rates and trends, Cancer Epidemiol Biomarkers Prev 19 (2010) 1893-1907.
[21] R. Siegel, J. Ma, Z. Zou, A. Jemal, Cancer statistics, 2014, CA Cancer J Clin 64 (2014) 9-29.
[22] M.J. Thun, J.O. DeLancey, M.M. Center, A. Jemal, E.M. Ward, The global burden of cancer: priorities for prevention, Carcinogenesis 31 (2010) 100-110.
[23] E.Y. Lee, W.J. Muller, Oncogenes and tumor suppressor genes, Cold Spring Harb Perspect Biol 2 (2010) a003236.
[24] C.M. Croce, Oncogenes and cancer, N Engl J Med 358 (2008) 502-511.
[25] S.R. Payne, C.J. Kemp, Tumor suppressor genetics, Carcinogenesis 26 (2005) 2031-2045.
[26] C.J. Sherr, Principles of tumor suppression, Cell 116 (2004) 235-246.
[27] D. Hanahan, R.A. Weinberg, The hallmarks of cancer, Cell 100 (2000) 57-70.
[28] D. Hanahan, R.A. Weinberg, Hallmarks of cancer: the next generation, Cell 144 (2011) 646-674.
[29] N.A. Bhowmick, E.G. Neilson, H.L. Moses, Stromal fibroblasts in cancer initiation and progression, Nature 432 (2004) 332-337.
[30] N. Cheng, A. Chytil, Y. Shyr, A. Joly, H.L. Moses, Transforming growth factor-beta signaling-deficient fibroblasts enhance hepatocyte growth factor signaling in mammary carcinoma cells to promote scattering and invasion, Mol Cancer Res 6 (2008) 1521-1533.
[31] M.A. Davies, Y. Samuels, Analysis of the genome to personalize therapy for melanoma, Oncogene 29 (2010) 5545-5555.
[32] B.H. Jiang, L.Z. Liu, PI3K/PTEN signaling in angiogenesis and tumorigenesis, Adv Cancer Res 102 (2009) 19-65.
[33] T.L. Yuan, L.C. Cantley, PI3K pathway alterations in cancer: variations on a theme, Oncogene 27 (2008) 5497-5510.
[34] M. Collado, M. Serrano, Senescence in tumours: evidence from mice and humans, Nat Rev Cancer 10 (2010) 51-57.
[35] J.M. Adams, S. Cory, The Bcl-2 apoptotic switch in cancer development and therapy, Oncogene 26 (2007) 1324-1337.
[36] M.A. Blasco, Telomeres and human disease: ageing, cancer and beyond, Nat Rev Genet 6 (2005) 611-622.
[37] D.E. Hansel, A.K. Meeker, J. Hicks, A.M. De Marzo, K.D. Lillemoe, R. Schulick, R.H. Hruban, A. Maitra, P. Argani, Telomere length variation in biliary tract metaplasia, dysplasia, and carcinoma, Mod Pathol 19 (2006) 772-779.
[38] D. Hanahan, J. Folkman, Patterns and emerging mechanisms of the angiogenic switch during tumorigenesis, Cell 86 (1996) 353-364.
[39] S. Kazerounian, K.O. Yee, J. Lawler, Thrombospondins in cancer, Cell Mol Life Sci 65 (2008) 700-712.
[40] F. Mac Gabhann, A.S. Popel, Systems biology of vascular endothelial growth factors, Microcirculation 15 (2008) 715-738.
[41] M. Bacac, I. Stamenkovic, Metastatic cancer cell, Annu Rev Pathol 3 (2008) 221-247.

[42] A.F. Chambers, A.C. Groom, I.C. MacDonald, Dissemination and growth of cancer cells in metastatic sites, Nat Rev Cancer 2 (2002) 563-572.
[43] I.J. Fidler, The pathogenesis of cancer metastasis: the 'seed and soil' hypothesis revisited, Nat Rev Cancer 3 (2003) 453-458.
[44] D.X. Nguyen, P.D. Bos, J. Massague, Metastasis: from dissemination to organ-specific colonization, Nat Rev Cancer 9 (2009) 274-284.
[45] C.L. Chaffer, R.A. Weinberg, A perspective on cancer cell metastasis, Science 331 (2011) 1559-1564.
[46] M.W. Klymkowsky, P. Savagner, Epithelial-mesenchymal transition: a cancer researcher's conceptual friend and foe, Am J Pathol 174 (2009) 1588-1593.
[47] O. Warburg, On respiratory impairment in cancer cells, Science 124 (1956) 269-270.
[48] M.G. Vander Heiden, L.C. Cantley, C.B. Thompson, Understanding the Warburg effect: the metabolic requirements of cell proliferation, Science 324 (2009) 1029-1033.
[49] R. Kim, M. Emi, K. Tanabe, Cancer immunoediting from immune surveillance to immune escape, Immunology 121 (2007) 1-14.
[50] D. Mittal, M.M. Gubin, R.D. Schreiber, M.J. Smyth, New insights into cancer immunoediting and its three component phases--elimination, equilibrium and escape, Curr Opin Immunol 27 (2014) 16-25.
[51] R.D. Schreiber, L.J. Old, M.J. Smyth, Cancer immunoediting: integrating immunity's roles in cancer suppression and promotion, Science 331 (2011) 1565-1570.
[52] C.A. Klein, Cancer. The metastasis cascade, Science 321 (2008) 1785-1787.
[53] A.C. Chiang, J. Massague, Molecular basis of metastasis, N Engl J Med 359 (2008) 2814-2823.
[54] E.V. Sugarbaker, Cancer metastasis: a product of tumor-host interactions, Curr Probl Cancer 3 (1979) 1-59.
[55] S. Paget, The distribution of secondary growths in cancer of the breast. 1889, Cancer Metastasis Rev 8 (1989) 98-101.
[56] A. Ben-Baruch, Organ selectivity in metastasis: regulation by chemokines and their receptors, Clin Exp Metastasis 25 (2008) 345-356.
[57] I.J. Fidler, Modulation of the organ microenvironment for treatment of cancer metastasis, J Natl Cancer Inst 87 (1995) 1588-1592.
[58] I.J. Fidler, The organ microenvironment and cancer metastasis, Differentiation 70 (2002) 498-505.
[59] P. Friedl, S. Alexander, Cancer invasion and the microenvironment: plasticity and reciprocity, Cell 147 (2011) 992-1009.
[60] R. Radinsky, S. Risin, D. Fan, Z. Dong, D. Bielenberg, C.D. Bucana, I.J. Fidler, Level and function of epidermal growth factor receptor predict the metastatic potential of human colon carcinoma cells, Clin Cancer Res 1 (1995) 19-31.
[61] L. Biancone, M. Araki, K. Araki, P. Vassalli, I. Stamenkovic, Redirection of tumor metastasis by expression of E-selectin in vivo, J Exp Med 183 (1996) 581-587.
[62] C.J. Dimitroff, M. Lechpammer, D. Long-Woodward, J.L. Kutok, Rolling of human bone-metastatic prostate tumor cells on human bone marrow endothelium under shear flow is mediated by E-selectin, Cancer Res 64 (2004) 5261-5269.
[63] C. Strell, F. Entschladen, Extravasation of leukocytes in comparison to tumor cells, Cell Commun Signal 6 (2008) 10.

[64] D.M. Brown, E. Ruoslahti, Metadherin, a cell surface protein in breast tumors that mediates lung metastasis, Cancer Cell 5 (2004) 365-374.
[65] H. Wang, W. Fu, J.H. Im, Z. Zhou, S.A. Santoro, V. Iyer, C.M. DiPersio, Q.C. Yu, V. Quaranta, A. Al-Mehdi, R.J. Muschel, Tumor cell alpha3beta1 integrin and vascular laminin-5 mediate pulmonary arrest and metastasis, J Cell Biol 164 (2004) 935-941.
[66] Y. Kang, P.M. Siegel, W. Shu, M. Drobnjak, S.M. Kakonen, C. Cordon-Cardo, T.A. Guise, J. Massague, A multigenic program mediating breast cancer metastasis to bone, Cancer Cell 3 (2003) 537-549.
[67] L.J. Ling, S. Wang, X.A. Liu, E.C. Shen, Q. Ding, C. Lu, J. Xu, Q.H. Cao, H.Q. Zhu, F. Wang, A novel mouse model of human breast cancer stem-like cells with high CD44+CD24-/lower phenotype metastasis to human bone, Chin Med J (Engl) 121 (2008) 1980-1986.
[68] A.E. Karnoub, A.B. Dash, A.P. Vo, A. Sullivan, M.W. Brooks, G.W. Bell, A.L. Richardson, K. Polyak, R. Tubo, R.A. Weinberg, Mesenchymal stem cells within tumour stroma promote breast cancer metastasis, Nature 449 (2007) 557-563.
[69] S.A. Brooks, H.J. Lomax-Browne, T.M. Carter, C.E. Kinch, D.M. Hall, Molecular interactions in cancer cell metastasis, Acta Histochem 112 (2010) 3-25.
[70] J.K. Woodward, I. Holen, R.E. Coleman, D.J. Buttle, The roles of proteolytic enzymes in the development of tumour-induced bone disease in breast and prostate cancer, Bone 41 (2007) 912-927.
[71] C. Frantz, K.M. Stewart, V.M. Weaver, The extracellular matrix at a glance, J Cell Sci 123 (2010) 4195-4200.
[72] P. Lu, V.M. Weaver, Z. Werb, The extracellular matrix: a dynamic niche in cancer progression, J Cell Biol 196 (2012) 395-406.
[73] W. Halfter, J. Candiello, H. Hu, P. Zhang, E. Schreiber, M. Balasubramani, Protein composition and biomechanical properties of in vivo-derived basement membranes, Cell Adh Migr 7 (2013) 64-71.
[74] S.H. Kim, J. Turnbull, S. Guimond, Extracellular matrix and cell signalling: the dynamic cooperation of integrin, proteoglycan and growth factor receptor, J Endocrinol 209 (2011) 139-151.
[75] J.D. Humphries, A. Byron, M.J. Humphries, Integrin ligands at a glance, J Cell Sci 119 (2006) 3901-3903.
[76] R. Pankov, K.M. Yamada, Fibronectin at a glance, J Cell Sci 115 (2002) 3861-3863.
[77] E.F. Plow, T.A. Haas, L. Zhang, J. Loftus, J.W. Smith, Ligand binding to integrins, J Biol Chem 275 (2000) 21785-21788.
[78] R.O. Hynes, Integrins: bidirectional, allosteric signaling machines, Cell 110 (2002) 673-687.
[79] H.C. Welch, W.J. Coadwell, L.R. Stephens, P.T. Hawkins, Phosphoinositide 3-kinase-dependent activation of Rac, FEBS Lett 546 (2003) 93-97.
[80] G. Xue, B.A. Hemmings, PKB/Akt-dependent regulation of cell motility, J Natl Cancer Inst 105 (2013) 393-404.
[81] D.S. Harburger, D.A. Calderwood, Integrin signalling at a glance, J Cell Sci 122 (2009) 159-163.
[82] J.D. Hood, D.A. Cheresh, Role of integrins in cell invasion and migration, Nat Rev Cancer 2 (2002) 91-100.
[83] S. Huveneers, E.H. Danen, Adhesion signaling - crosstalk between integrins, Src and Rho, J Cell Sci 122 (2009) 1059-1069.

[84] D.D. Schlaepfer, K.C. Jones, T. Hunter, Multiple Grb2-mediated integrin-stimulated signaling pathways to ERK2/mitogen-activated protein kinase: summation of both c-Src- and focal adhesion kinase-initiated tyrosine phosphorylation events, Mol Cell Biol 18 (1998) 2571-2585.
[85] D.D. Schlaepfer, S.K. Mitra, Multiple connections link FAK to cell motility and invasion, Curr Opin Genet Dev 14 (2004) 92-101.
[86] D.J. Sieg, C.R. Hauck, D. Ilic, C.K. Klingbeil, E. Schaefer, C.H. Damsky, D.D. Schlaepfer, FAK integrates growth-factor and integrin signals to promote cell migration, Nat Cell Biol 2 (2000) 249-256.
[87] A. Wells, Tumor invasion: role of growth factor-induced cell motility, Adv Cancer Res 78 (2000) 31-101.
[88] A.C. Dudley, Tumor endothelial cells, Cold Spring Harb Perspect Med 2 (2012) a006536.
[89] T.R. Geiger, D.S. Peeper, Critical role for TrkB kinase function in anoikis suppression, tumorigenesis, and metastasis, Cancer Res 67 (2007) 6221-6229.
[90] L.J. Gay, B. Felding-Habermann, Contribution of platelets to tumour metastasis, Nat Rev Cancer 11 (2011) 123-134.
[91] A. Varki, R. Kannagi, B.P. Toole, Glycosylation Changes in Cancer, in: A. Varki, R.D. Cummings, J.D. Esko, H.H. Freeze, P. Stanley, C.R. Bertozzi, G.W. Hart, M.E. Etzler (Eds.), Essentials of Glycobiology, Cold Spring Harbor (NY), 2009.
[92] Y.S. Kim, J. Gum, Jr., I. Brockhausen, Mucin glycoproteins in neoplasia, Glycoconj J 13 (1996) 693-707.
[93] P. Fredman, K. Hedberg, T. Brezicka, Gangliosides as therapeutic targets for cancer, BioDrugs 17 (2003) 155-167.
[94] Y.J. Kim, A. Varki, Perspectives on the significance of altered glycosylation of glycoproteins in cancer, Glycoconj J 14 (1997) 569-576.
[95] K. Mujoo, D.A. Cheresh, H.M. Yang, R.A. Reisfeld, Disialoganglioside GD2 on human neuroblastoma cells: target antigen for monoclonal antibody-mediated cytolysis and suppression of tumor growth, Cancer Res 47 (1987) 1098-1104.
[96] R.V. Iozzo, R.D. Sanderson, Proteoglycans in cancer biology, tumour microenvironment and angiogenesis, J Cell Mol Med 15 (2011) 1013-1031.
[97] K.S. Lau, J.W. Dennis, N-Glycans in cancer progression, Glycobiology 18 (2008) 750-760.
[98] P. Stanley, H. Schachter, N. Taniguchi, N-Glycans, in: A. Varki, R.D. Cummings, J.D. Esko, H.H. Freeze, P. Stanley, C.R. Bertozzi, G.W. Hart, M.E. Etzler (Eds.), Essentials of Glycobiology, Cold Spring Harbor (NY), 2009.
[99] R.D. Cummings, S. Kornfeld, Characterization of the structural determinants required for the high affinity interaction of asparagine-linked oligosaccharides with immobilized Phaseolus vulgaris leukoagglutinating and erythroagglutinating lectins, J Biol Chem 257 (1982) 11230-11234.
[100] R.D. Cummings, I.S. Trowbridge, S. Kornfeld, A mouse lymphoma cell line resistant to the leukoagglutinating lectin from Phaseolus vulgaris is deficient in UDP-GlcNAc: alpha-D-mannoside beta 1,6 N-acetylglucosaminyltransferase, J Biol Chem 257 (1982) 13421-13427.
[101] J.W. Dennis, S. Laferte, C. Waghorne, M.L. Breitman, R.S. Kerbel, Beta 1-6 branching of Asn-linked oligosaccharides is directly associated with metastasis, Science 236 (1987) 582-585.

[102] S. Hiraizumi, S. Takasaki, N. Ohuchi, Y. Harada, M. Nose, S. Mori, A. Kobata, Altered glycosylation of membrane glycoproteins associated with human mammary carcinoma, Jpn J Cancer Res 83 (1992) 1063-1072.
[103] B. Fernandes, U. Sagman, M. Auger, M. Demetrio, J.W. Dennis, Beta 1-6 branched oligosaccharides as a marker of tumor progression in human breast and colon neoplasia, Cancer Res 51 (1991) 718-723.
[104] R. Takano, M. Nose, T. Nishihira, M. Kyogoku, Increase of beta 1-6-branched oligosaccharides in human esophageal carcinomas invasive against surrounding tissue in vivo and in vitro, Am J Pathol 137 (1990) 1007-1011.
[105] H. Yamamoto, J. Swoger, S. Greene, T. Saito, J. Hurh, C. Sweeley, J. Leestma, E. Mkrdichian, L. Cerullo, A. Nishikawa, Y. Ihara, N. Taniguchi, J.R. Moskal, Beta1,6-N-acetylglucosamine-bearing N-glycans in human gliomas: implications for a role in regulating invasivity, Cancer Res 60 (2000) 134-142.
[106] A.K. Chakraborty, J. Pawelek, Y. Ikeda, E. Miyoshi, N. Kolesnikova, Y. Funasaka, M. Ichihashi, N. Taniguchi, Fusion hybrids with macrophage and melanoma cells up-regulate N-acetylglucosaminyltransferase V, beta1-6 branching, and metastasis, Cell Growth Differ 12 (2001) 623-630.
[107] Y. Lu, J.C. Pelling, W.G. Chaney, Tumor cell surface beta 1-6 branched oligosaccharides and lung metastasis, Clin Exp Metastasis 12 (1994) 47-54.
[108] M. Yoshimura, A. Nishikawa, Y. Ihara, S. Taniguchi, N. Taniguchi, Suppression of lung metastasis of B16 mouse melanoma by N-acetylglucosaminyltransferase III gene transfection, Proc Natl Acad Sci U S A 92 (1995) 8754-8758.
[109] R. Pili, J. Chang, R.A. Partis, R.A. Mueller, F.J. Chrest, A. Passaniti, The alpha-glucosidase I inhibitor castanospermine alters endothelial cell glycosylation, prevents angiogenesis, and inhibits tumor growth, Cancer Res 55 (1995) 2920-2926.
[110] M. Tomiie, S. Isaka, E. Miyoshi, N. Taniguchi, T. Kimura, K. Ogita, T. Tsutsui, K. Shimoya, T. Nakagawa, A. Kondo, M. Koyama, Y. Murata, Elevated expression of N-acetylglucosaminyltransferase V in first trimester human placenta, Biochem Biophys Res Commun 330 (2005) 999-1004.
[111] M.J. Humphries, K. Matsumoto, S.L. White, K. Olden, Oligosaccharide modification by swainsonine treatment inhibits pulmonary colonization by B16-F10 murine melanoma cells, Proc Natl Acad Sci U S A 83 (1986) 1752-1756.
[112] P.J. Seberger, W.G. Chaney, Control of metastasis by Asn-linked, beta1-6 branched oligosaccharides in mouse mammary cancer cells, Glycobiology 9 (1999) 235-241.
[113] B.W. Weston, K.M. Hiller, J.P. Mayben, G.A. Manousos, K.M. Bendt, R. Liu, J.C. Cusack, Jr., Expression of human alpha(1,3)fucosyltransferase antisense sequences inhibits selectin-mediated adhesion and liver metastasis of colon carcinoma cells, Cancer Res 59 (1999) 2127-2135.
[114] N. Yamada, Y.S. Chung, S. Takatsuka, Y. Arimoto, T. Sawada, T. Dohi, M. Sowa, Increased sialyl Lewis A expression and fucosyltransferase activity with acquisition of a high metastatic capacity in a colon cancer cell line, Br J Cancer 76 (1997) 582-587.
[115] J. Gu, N. Taniguchi, Potential of N-glycan in cell adhesion and migration as either a positive or negative regulator, Cell Adh Migr 2 (2008) 243-245.
[116] S.H. Barondes, D.N. Cooper, M.A. Gitt, H. Leffler, Galectins. Structure and function of a large family of animal lectins, J Biol Chem 269 (1994) 20807-20810.

[117] A. Varki, M.E. Etzler, R.D. Cummings, J.D. Esko, Discovery and Classification of Glycan-Binding Proteins, in: A. Varki, R.D. Cummings, J.D. Esko, H.H. Freeze, P. Stanley, C.R. Bertozzi, G.W. Hart, M.E. Etzler (Eds.), Essentials of Glycobiology, Cold Spring Harbor (NY), 2009.
[118] M. Przybylo, D. Martuszewska, E. Pochec, D. Hoja-Lukowicz, A. Litynska, Identification of proteins bearing beta1-6 branched N-glycans in human melanoma cell lines from different progression stages by tandem mass spectrometry analysis, Biochim Biophys Acta 1770 (2007) 1427-1435.
[119] S.J. Kim, I.J. Choi, T.C. Cheong, S.J. Lee, R. Lotan, S.H. Park, K.H. Chun, Galectin-3 increases gastric cancer cell motility by up-regulating fascin-1 expression, Gastroenterology 138 (2010) 1035-1045 e1031-1032.
[120] G.B. Park, D.J. Kim, Y.S. Kim, H.K. Lee, C.W. Kim, D.Y. Hur, Silencing of galectin-3 represses osteosarcoma cell migration and invasion through inhibition of FAK/Src/Lyn activation and beta-catenin expression and increases susceptibility to chemotherapeutic agents, Int J Oncol 46 (2015) 185-194.
[121] S. Song, B. Ji, V. Ramachandran, H. Wang, M. Hafley, C. Logsdon, R.S. Bresalier, Overexpressed galectin-3 in pancreatic cancer induces cell proliferation and invasion by binding Ras and activating Ras signaling, PLoS One 7 (2012) e42699.
[122] Y.G. Wang, S.J. Kim, J.H. Baek, H.W. Lee, S.Y. Jeong, K.H. Chun, Galectin-3 increases the motility of mouse melanoma cells by regulating matrix metalloproteinase-1 expression, Exp Mol Med 44 (2012) 387-393.
[123] D. Zhang, Z.G. Chen, S.H. Liu, Z.Q. Dong, M. Dalin, S.S. Bao, Y.W. Hu, F.C. Wei, Galectin-3 gene silencing inhibits migration and invasion of human tongue cancer cells in vitro via downregulating beta-catenin, Acta Pharmacol Sin 34 (2013) 176-184.
[124] L. Qiao, N. Liang, J. Xie, H. Luo, J. Zhang, G. Deng, Y. Li, Gene silencing of galectin-3 changes the biological behavior of Eca109 human esophageal cancer cells, Mol Med Rep 13 (2016) 160-166.
[125] K.L. Wu, E.Y. Huang, E.W. Jhu, Y.H. Huang, W.H. Su, P.C. Chuang, K.D. Yang, Overexpression of galectin-3 enhances migration of colon cancer cells related to activation of the K-Ras-Raf-Erk1/2 pathway, J Gastroenterol 48 (2013) 350-359.
[126] A. Lagana, J.G. Goetz, P. Cheung, A. Raz, J.W. Dennis, I.R. Nabi, Galectin binding to Mgat5-modified N-glycans regulates fibronectin matrix remodeling in tumor cells, Mol Cell Biol 26 (2006) 3181-3193.
[127] J.G. Goetz, B. Joshi, P. Lajoie, S.S. Strugnell, T. Scudamore, L.D. Kojic, I.R. Nabi, Concerted regulation of focal adhesion dynamics by galectin-3 and tyrosine-phosphorylated caveolin-1, J Cell Biol 180 (2008) 1261-1275.
[128] C. Boscher, I.R. Nabi, Galectin-3- and phospho-caveolin-1-dependent outside-in integrin signaling mediates the EGF motogenic response in mammary cancer cells, Mol Biol Cell 24 (2013) 2134-2145.
[129] C. Saravanan, F.T. Liu, I.K. Gipson, N. Panjwani, Galectin-3 promotes lamellipodia formation in epithelial cells by interacting with complex N-glycans on alpha3beta1 integrin, J Cell Sci 122 (2009) 3684-3693.
[130] F.H. Melo, D. Butera, S. Junqueira Mde, D.K. Hsu, A.M. da Silva, F.T. Liu, M.F. Santos, R. Chammas, The promigratory activity of the matricellular protein galectin-3 depends on the activation of PI-3 kinase, PLoS One 6 (2011) e29313.

[131] K. Jiang, C.R. Rankin, P. Nava, R. Sumagin, R. Kamekura, S.R. Stowell, M. Feng, C.A. Parkos, A. Nusrat, Galectin-3 regulates desmoglein-2 and intestinal epithelial intercellular adhesion, J Biol Chem 289 (2014) 10510-10517.
[132] C. Boscher, Y.Z. Zheng, R. Lakshminarayan, L. Johannes, J.W. Dennis, L.J. Foster, I.R. Nabi, Galectin-3 protein regulates mobility of N-cadherin and GM1 ganglioside at cell-cell junctions of mammary carcinoma cells, J Biol Chem 287 (2012) 32940-32952.
[133] J. Hirabayashi, T. Hashidate, Y. Arata, N. Nishi, T. Nakamura, M. Hirashima, T. Urashima, T. Oka, M. Futai, W.E. Muller, F. Yagi, K. Kasai, Oligosaccharide specificity of galectins: a search by frontal affinity chromatography, Biochim Biophys Acta 1572 (2002) 232-254.
[134] Y. Levy, R. Arbel-Goren, Y.R. Hadari, S. Eshhar, D. Ronen, E. Elhanany, B. Geiger, Y. Zick, Galectin-8 functions as a matricellular modulator of cell adhesion, J Biol Chem 276 (2001) 31285-31295.
[135] Y. Levy, D. Ronen, A.D. Bershadsky, Y. Zick, Sustained induction of ERK, protein kinase B, and p70 S6 kinase regulates cell spreading and formation of F-actin microspikes upon ligation of integrins by galectin-8, a mammalian lectin, J Biol Chem 278 (2003) 14533-14542.
[136] H.Y. Chen, F.T. Liu, R.Y. Yang, Roles of galectin-3 in immune responses, Arch Immunol Ther Exp (Warsz) 53 (2005) 497-504.
[137] A. Dhirapong, A. Lleo, P. Leung, M.E. Gershwin, F.T. Liu, The immunological potential of galectin-1 and -3, Autoimmun Rev 8 (2009) 360-363.
[138] G.A. Rabinovich, L.G. Baum, N. Tinari, R. Paganelli, C. Natoli, F.T. Liu, S. Iacobelli, Galectins and their ligands: amplifiers, silencers or tuners of the inflammatory response?, Trends Immunol 23 (2002) 313-320.
[139] G.A. Rabinovich, M.A. Toscano, Turning 'sweet' on immunity: galectin-glycan interactions in immune tolerance and inflammation, Nat Rev Immunol 9 (2009) 338-352.
[140] H. Sano, D.K. Hsu, L. Yu, J.R. Apgar, I. Kuwabara, T. Yamanaka, M. Hirashima, F.T. Liu, Human galectin-3 is a novel chemoattractant for monocytes and macrophages, J Immunol 165 (2000) 2156-2164.
[141] B. Vray, I. Camby, V. Vercruysse, T. Mijatovic, N.V. Bovin, P. Ricciardi-Castagnoli, H. Kaltner, I. Salmon, H.J. Gabius, R. Kiss, Up-regulation of galectin-3 and its ligands by Trypanosoma cruzi infection with modulation of adhesion and migration of murine dendritic cells, Glycobiology 14 (2004) 647-657.
[142] I. Kuwabara, F.T. Liu, Galectin-3 promotes adhesion of human neutrophils to laminin, J Immunol 156 (1996) 3939-3944.
[143] F.T. Liu, G.A. Rabinovich, Galectins as modulators of tumour progression, Nat Rev Cancer 5 (2005) 29-41.
[144] E.A. Partridge, C. Le Roy, G.M. Di Guglielmo, J. Pawling, P. Cheung, M. Granovsky, I.R. Nabi, J.L. Wrana, J.W. Dennis, Regulation of cytokine receptors by Golgi N-glycan processing and endocytosis, Science 306 (2004) 120-124.
[145] D.M. Villa-Verde, E. Silva-Monteiro, M.G. Jasiulionis, D.A. Farias-De-Oliveira, R.R. Brentani, W. Savino, R. Chammas, Galectin-3 modulates carbohydrate-dependent thymocyte interactions with the thymic microenvironment, Eur J Immunol 32 (2002) 1434-1444.
[146] W. Savino, D.A. Mendes-Da-Cruz, S. Smaniotto, E. Silva-Monteiro, D.M. Villa-Verde, Molecular mechanisms governing thymocyte migration: combined role of chemokines and extracellular matrix, J Leukoc Biol 75 (2004) 951-961.

[147] B.N. Stillman, D.K. Hsu, M. Pang, C.F. Brewer, P. Johnson, F.T. Liu, L.G. Baum, Galectin-3 and galectin-1 bind distinct cell surface glycoprotein receptors to induce T cell death, J Immunol 176 (2006) 778-789.
[148] H.G. Joo, P.S. Goedegebuure, N. Sadanaga, M. Nagoshi, W. von Bernstorff, T.J. Eberlein, Expression and function of galectin-3, a beta-galactoside-binding protein in activated T lymphocytes, J Leukoc Biol 69 (2001) 555-564.
[149] S. Dong, R.C. Hughes, Galectin-3 stimulates uptake of extracellular Ca2+ in human Jurkat T-cells, FEBS Lett 395 (1996) 165-169.
[150] M. Nachtigal, Z. Al-Assaad, E.P. Mayer, K. Kim, M. Monsigny, Galectin-3 expression in human atherosclerotic lesions, Am J Pathol 152 (1998) 1199-1208.
[151] R.I. Zuberi, D.K. Hsu, O. Kalayci, H.Y. Chen, H.K. Sheldon, L. Yu, J.R. Apgar, T. Kawakami, C.M. Lilly, F.T. Liu, Critical role for galectin-3 in airway inflammation and bronchial hyperresponsiveness in a murine model of asthma, Am J Pathol 165 (2004) 2045-2053.
[152] W. Peng, H.Y. Wang, Y. Miyahara, G. Peng, R.F. Wang, Tumor-associated galectin-3 modulates the function of tumor-reactive T cells, Cancer Res 68 (2008) 7228-7236.
[153] M.R. Zubieta, D. Furman, M. Barrio, A.I. Bravo, E. Domenichini, J. Mordoh, Galectin-3 expression correlates with apoptosis of tumor-associated lymphocytes in human melanoma biopsies, Am J Pathol 168 (2006) 1666-1675.
[154] K. Nabeshima, H. Iwasaki, K. Koga, H. Hojo, J. Suzumiya, M. Kikuchi, Emmprin (basigin/CD147): matrix metalloproteinase modulator and multifunctional cell recognition molecule that plays a critical role in cancer progression, Pathol Int 56 (2006) 359-367.
[155] U.H. Weidle, W. Scheuer, D. Eggle, S. Klostermann, H. Stockinger, Cancer-related issues of CD147, Cancer Genomics Proteomics 7 (2010) 157-169.
[156] W. Huang, W.J. Luo, P. Zhu, J. Tang, X.L. Yu, H.Y. Cui, B. Wang, Y. Zhang, J.L. Jiang, Z.N. Chen, Modulation of CD147-induced matrix metalloproteinase activity: role of CD147 N-glycosylation, Biochem J 449 (2013) 437-448.
[157] R.L. Gundry, K. Raginski, Y. Tarasova, I. Tchernyshyov, D. Bausch-Fluck, S.T. Elliott, K.R. Boheler, J.E. Van Eyk, B. Wollscheid, The mouse C2C12 myoblast cell surface N-linked glycoproteome: identification, glycosite occupancy, and membrane orientation, Mol Cell Proteomics 8 (2009) 2555-2569.
[158] B. Wollscheid, D. Bausch-Fluck, C. Henderson, R. O'Brien, M. Bibel, R. Schiess, R. Aebersold, J.D. Watts, Mass-spectrometric identification and relative quantification of N-linked cell surface glycoproteins, Nat Biotechnol 27 (2009) 378-386.
[159] W. Tang, S.B. Chang, M.E. Hemler, Links between CD147 function, glycosylation, and caveolin-1, Mol Biol Cell 15 (2004) 4043-4050.
[160] T. Muramatsu, Basigin (CD147), a multifunctional transmembrane glycoprotein with various binding partners, J Biochem (2015).
[161] C.S. Priglinger, C.M. Szober, S.G. Priglinger, J. Merl, K.N. Euler, M. Kernt, G. Gondi, J. Behler, A. Geerlof, A. Kampik, M. Ueffing, S.M. Hauck, Galectin-3 induces clustering of CD147 and integrin-beta1 transmembrane glycoprotein receptors on the RPE cell surface, PLoS One 8 (2013) e70011.
[162] G.D. Grass, M. Bratoeva, B.P. Toole, Regulation of invadopodia formation and activity by CD147, J Cell Sci 125 (2012) 777-788.

[163] G.D. Grass, L.B. Tolliver, M. Bratoeva, B.P. Toole, CD147, CD44, and the epidermal growth factor receptor (EGFR) signaling pathway cooperate to regulate breast epithelial cell invasiveness, J Biol Chem 288 (2013) 26089-26104.
[164] T.Y. Fu, C.C. Chang, C.T. Lin, C.H. Lai, S.Y. Peng, Y.J. Ko, P.C. Tang, Let-7b-mediated suppression of basigin expression and metastasis in mouse melanoma cells, Exp Cell Res 317 (2011) 445-451.
[165] Y.L. Yong, C.G. Liao, D. Wei, Z.N. Chen, H. Bian, CD147 overexpression promotes tumorigenicity in Chinese hamster ovary cells, Cell Biol Int 40 (2016) 375-386.
[166] Z.G. Fu, L. Wang, H.Y. Cui, J.L. Peng, S.J. Wang, J.J. Geng, J.D. Liu, F. Feng, F. Song, L. Li, P. Zhu, J.L. Jiang, Z.N. Chen, A novel small-molecule compound targeting CD147 inhibits the motility and invasion of hepatocellular carcinoma cells, Oncotarget (2016).
[167] A. Papadimitropoulou, A. Mamalaki, The glycosylated IgII extracellular domain of EMMPRIN is implicated in the induction of MMP-2, Mol Cell Biochem 379 (2013) 107-113.
[168] G.L. Peterson, A simplification of the protein assay method of Lowry et al. which is more generally applicable, Anal Biochem 83 (1977) 346-356.
[169] H. Towbin, T. Staehelin, J. Gordon, Electrophoretic transfer of proteins from polyacrylamide gels to nitrocellulose sheets: procedure and some applications, Proc Natl Acad Sci U S A 76 (1979) 4350-4354.
[170] A. Krzeslak, A. Lipinska, Galectin-3 as a multifunctional protein, Cell Mol Biol Lett 9 (2004) 305-328.
[171] K.A. Mace, T.E. Restivo, J.L. Rinn, A.C. Paquet, H.Y. Chang, D.M. Young, N.J. Boudreau, HOXA3 modulates injury-induced mobilization and recruitment of bone marrow-derived cells, Stem Cells 27 (2009) 1654-1665.
[172] D.K. Hsu, R.Y. Yang, Z. Pan, L. Yu, D.R. Salomon, W.P. Fung-Leung, F.T. Liu, Targeted disruption of the galectin-3 gene results in attenuated peritoneal inflammatory responses, Am J Pathol 156 (2000) 1073-1083.
[173] I.J. Fidler, Biological behavior of malignant melanoma cells correlated to their survival in vivo, Cancer Res 35 (1975) 218-224.
[174] A. Ranjan, S.M. Bane, R.D. Kalraiya, Glycosylation of the laminin receptor (alpha3beta1) regulates its association with tetraspanin CD151: Impact on cell spreading, motility, degradation and invasion of basement membrane by tumor cells, Exp Cell Res 322 (2014) 249-264.
[175] C.Y. Zheng, R.S. Petralia, Y.X. Wang, B. Kachar, Fluorescence recovery after photobleaching (FRAP) of fluorescence tagged proteins in dendritic spines of cultured hippocampal neurons, J Vis Exp (2011).
[176] S. Pellegrin, H. Mellor, Rho GTPase activation assays, Curr Protoc Cell Biol Chapter 14 (2008) Unit 14 18.
[177] I.J. Fidler, Selection of successive tumour lines for metastasis, Nat New Biol 242 (1973) 148-149.
[178] D.A. Lauffenburger, A.F. Horwitz, Cell migration: a physically integrated molecular process, Cell 84 (1996) 359-369.
[179] A.J. Ridley, Rho GTPases and cell migration, J Cell Sci 114 (2001) 2713-2722.
[180] E.C. McGary, D.C. Lev, M. Bar-Eli, Cellular adhesion pathways and metastatic potential of human melanoma, Cancer Biol Ther 1 (2002) 459-465.

[181] G. Poste, G.L. Nicolson, Arrest and metastasis of blood-borne tumor cells are modified by fusion of plasma membrane vesicles from highly metastatic cells, Proc Natl Acad Sci U S A 77 (1980) 399-403.
[182] E. Yamamoto, K. Ino, E. Miyoshi, K. Shibata, N. Takahashi, H. Kajiyama, A. Nawa, S. Nomura, T. Nagasaka, F. Kikkawa, Expression of N-acetylglucosaminyltransferase V in endometrial cancer correlates with poor prognosis, Br J Cancer 97 (2007) 1538-1544.
[183] M. Demetriou, I.R. Nabi, M. Coppolino, S. Dedhar, J.W. Dennis, Reduced contact-inhibition and substratum adhesion in epithelial cells expressing GlcNAc-transferase V, J Cell Biol 130 (1995) 383-392.
[184] M. Fukuda, N. Hiraoka, J.C. Yeh, C-type lectins and sialyl Lewis X oligosaccharides. Versatile roles in cell-cell interaction, J Cell Biol 147 (1999) 467-470.
[185] C.M. John, H. Leffler, B. Kahl-Knutsson, I. Svensson, G.A. Jarvis, Truncated galectin-3 inhibits tumor growth and metastasis in orthotopic nude mouse model of human breast cancer, Clin Cancer Res 9 (2003) 2374-2383.
[186] V.V. Glinsky, A. Raz, Modified citrus pectin anti-metastatic properties: one bullet, multiple targets, Carbohydr Res 344 (2009) 1788-1791.
[187] N.M. Abu-Elsaad, W.F. Elkashef, Modified citrus pectin stops progression of liver fibrosis by inhibiting galectin-3 and inducing apoptosis of stellate cells, Can J Physiol Pharmacol (2015) 1-9.
[188] S.K. More, N. Srinivasan, S. Budnar, S.M. Bane, A. Upadhya, R.A. Thorat, A.D. Ingle, S.V. Chiplunkar, R.D. Kalraiya, N-glycans and metastasis in galectin-3 transgenic mice, Biochem Biophys Res Commun 460 (2015) 302-307.
[189] M.J. Humphries, K. Matsumoto, S.L. White, R.J. Molyneux, K. Olden, Augmentation of murine natural killer cell activity by swainsonine, a new antimetastatic immunomodulator, Cancer Res 48 (1988) 1410-1415.
[190] H.R. Jiang, Z. Al Rasebi, E. Mensah-Brown, A. Shahin, D. Xu, C.S. Goodyear, S.Y. Fukada, F.T. Liu, F.Y. Liew, M.L. Lukic, Galectin-3 deficiency reduces the severity of experimental autoimmune encephalomyelitis, J Immunol 182 (2009) 1167-1173.
[191] G. Radosavljevic, I. Jovanovic, I. Majstorovic, M. Mitrovic, V.J. Lisnic, N. Arsenijevic, S. Jonjic, M.L. Lukic, Deletion of galectin-3 in the host attenuates metastasis of murine melanoma by modulating tumor adhesion and NK cell activity, Clin Exp Metastasis 28 (2011) 451-462.
[192] A.D. Chaudhari, R.P. Gude, R.D. Kalraiya, S.V. Chiplunkar, Endogenous galectin-3 expression levels modulate immune responses in galectin-3 transgenic mice, Mol Immunol 68 (2015) 300-311.
[193] G. Bozzuto, P. Ruggieri, A. Molinari, Molecular aspects of tumor cell migration and invasion, Ann Ist Super Sanita 46 (2010) 66-80.
[194] B.M. Gumbiner, Cell adhesion: the molecular basis of tissue architecture and morphogenesis, Cell 84 (1996) 345-357.
[195] T.D. Palmer, W.J. Ashby, J.D. Lewis, A. Zijlstra, Targeting tumor cell motility to prevent metastasis, Adv Drug Deliv Rev 63 (2011) 568-581.
[196] M. Vicente-Manzanares, D.J. Webb, A.R. Horwitz, Cell migration at a glance, J Cell Sci 118 (2005) 4917-4919.
[197] H. Yamaguchi, J. Wyckoff, J. Condeelis, Cell migration in tumors, Curr Opin Cell Biol 17 (2005) 559-564.

[198] T.D. Pollard, G.G. Borisy, Cellular motility driven by assembly and disassembly of actin filaments, Cell 112 (2003) 453-465.
[199] J.V. Small, K. Rottner, I. Kaverina, K.I. Anderson, Assembling an actin cytoskeleton for cell attachment and movement, Biochim Biophys Acta 1404 (1998) 271-281.
[200] J.V. Small, T. Stradal, E. Vignal, K. Rottner, The lamellipodium: where motility begins, Trends Cell Biol 12 (2002) 112-120.
[201] K.M. Yamada, M. Araki, Tumor suppressor PTEN: modulator of cell signaling, growth, migration and apoptosis, J Cell Sci 114 (2001) 2375-2382.
[202] M. Matsuo, H. Sakurai, Y. Ueno, O. Ohtani, I. Saiki, Activation of MEK/ERK and PI3K/Akt pathways by fibronectin requires integrin alphav-mediated ADAM activity in hepatocellular carcinoma: a novel functional target for gefitinib, Cancer Sci 97 (2006) 155-162.
[203] W.G. King, M.D. Mattaliano, T.O. Chan, P.N. Tsichlis, J.S. Brugge, Phosphatidylinositol 3-kinase is required for integrin-stimulated AKT and Raf-1/mitogen-activated protein kinase pathway activation, Mol Cell Biol 17 (1997) 4406-4418.
[204] S. Han, F.R. Khuri, J. Roman, Fibronectin stimulates non-small cell lung carcinoma cell growth through activation of Akt/mammalian target of rapamycin/S6 kinase and inactivation of LKB1/AMP-activated protein kinase signal pathways, Cancer Res 66 (2006) 315-323.
[205] W. Liu, D.K. Hsu, H.Y. Chen, R.Y. Yang, K.L. Carraway, 3rd, R.R. Isseroff, F.T. Liu, Galectin-3 regulates intracellular trafficking of EGFR through Alix and promotes keratinocyte migration, J Invest Dermatol 132 (2012) 2828-2837.
[206] C.J. Marshall, Specificity of receptor tyrosine kinase signaling: transient versus sustained extracellular signal-regulated kinase activation, Cell 80 (1995) 179-185.
[207] C.D. Nobes, A. Hall, Rho, rac, and cdc42 GTPases regulate the assembly of multimolecular focal complexes associated with actin stress fibers, lamellipodia, and filopodia, Cell 81 (1995) 53-62.
[208] A. Ridley, Rho GTPases. Integrating integrin signaling, J Cell Biol 150 (2000) F107-109.
[209] T. Kwon, D.Y. Kwon, J. Chun, J.H. Kim, S.S. Kang, Akt protein kinase inhibits Rac1-GTP binding through phosphorylation at serine 71 of Rac1, J Biol Chem 275 (2000) 423-428.
[210] J. Schwarz, J. Proff, A. Havemeier, M. Ladwein, K. Rottner, B. Barlag, A. Pich, H. Tatge, I. Just, R. Gerhard, Serine-71 phosphorylation of Rac1 modulates downstream signaling, PLoS One 7 (2012) e44358.
[211] L.A. Cary, D.C. Han, T.R. Polte, S.K. Hanks, J.L. Guan, Identification of p130Cas as a mediator of focal adhesion kinase-promoted cell migration, J Cell Biol 140 (1998) 211-221.
[212] R.J. Petrie, A.D. Doyle, K.M. Yamada, Random versus directionally persistent cell migration, Nat Rev Mol Cell Biol 10 (2009) 538-549.
[213] A. Ponti, M. Machacek, S.L. Gupton, C.M. Waterman-Storer, G. Danuser, Two distinct actin networks drive the protrusion of migrating cells, Science 305 (2004) 1782-1786.

Publications

Mol Cell Biochem
DOI 10.1007/s11010-016-2706-1

Galectin-3-induced cell spreading and motility relies on distinct signaling mechanisms compared to fibronectin

Shyam K. More[1] · Shubhada V. Chiplunkar[1] · Rajiv D. Kalraiya[1]

Received: 12 October 2015 / Accepted: 19 April 2016

Abstract Secreted galectin-3 often gets incorporated into extracellular matrix and is utilized by cancer cells for spreading, movement, and metastatic dissemination. Here we investigate molecular mechanisms by which galectin-3 brings about these effects and compare it with fibronectin. Imaging of cells spread on fibronectin showed stress fibers throughout cell body, however, galectin-3-induced formation of parallel actin bundles in the lamellipodial region resulting in unique morphological features. FRAP analysis showed that the actin turnover in the lamellipodial region was much higher in cells spread on galectin-3 as compared to that on fibronectin. Rac1 activation is correlated with lamellipodial organization on both the substrates. Activation of Akt and Rac1, the regulators of actin dynamics, show inverse correlation with each other on both galectin-3 and fibronectin. Activation of Erk however, remained similar. Further, inhibition of activation of Akt and Erk inhibited spreading and motility of cells on galectin-3 but not on fibronectin. The results very comprehensively demonstrate distinct signaling pathways that regulate microfilament organization, lamellipodial structures, spreading, and movement of cells plated on galectin-3 as opposed to fibronectin.

Rajiv D. Kalraiya: Deceased.

Electronic supplementary material The online version of this article (doi:10.1007/s11010-016-2706-1) contains supplementary material, which is available to authorized users.

✉ Shubhada V. Chiplunkar
schiplunkar@actrec.gov.in

[1] Advanced Centre for Treatment Research and Education in Cancer (ACTREC), Tata Memorial Centre, Sector 22, Kharghar, Navi Mumbai 410210, India

Keywords Galectin-3 · Fibronectin · Microfilaments · Lamellipodia · Cell spreading · Cell migration

Introduction

Metastasis is the major cause of deaths in cancer patients however, is still poorly understood because of its complexity and multistep nature. To disseminate, tumor cells modulate cell–cell and cell–extracellular matrix (ECM) interactions, degrade the surrounding matrix in a regulated manner and move away using the same matrix as traction, survive in circulation, and ultimately get arrested in the target organ vasculature. For arrest and extravasation the cells have to interact with and retract endothelium, degrade vascular basement membrane (BM), move into organ parenchyma, and give rise to secondary colonies if they are able to adapt to organ growth environment. The interaction of tumor cells with host microenvironment plays a key role in successful metastatic dissemination, especially interactions with the components of the ECM and BM [1, 2].

Galectin-3 a nucleocytoplasmic protein which is secreted out in a non-classical manner often gets incorporated onto the cell surface, ECM, and BM [3]. It is a member of a large family of galactose-binding lectins. Glycoproteins of cell surface, ECM, and BM that carry poly-*N*-acetyllactosamine (polyLacNAc) on N-glycans or Thomson Freudenreich antigens serve as the major ligands for galectin-3 and may all play a significant role in different metastatic processes [4]. Galectin-3 has been shown to be expressed in highest amounts in lungs, on almost all the tissue compartments including the surface of its vascular endothelium. Previously we showed that polyLacNAc-substituted N-glycans expressed on B16F10 murine melanoma cells act as high affinity ligand for galectin-3. This

Published online: 29 April 2016

galectin-3/polyLacNAc interaction not only facilitates initial adhesion to vascular endothelium, but participates in all the subsequent processes required for extravasation like cell spreading, degradation of matrix, motility, and organ colonization [5–8]. Further, the extent of organ-specific metastasis appears to be dictated by the levels expression of galectin-3 on the lungs [9].

The secreted extracellular galectin-3 exerts its cellular effects on motility-related processes both in the soluble form and as immobilized component on cells, ECM, and BM [3, 10]. The soluble galectin-3 promotes fibronectin-dependent cell spreading and motility of mammary carcinoma cells by interacting with β1, 6-branched N-linked oligosaccharides [11]. Interaction of integrin receptors with fibronectin in presence of soluble galectin-3 leads to phosphorylation of caveolin-1 which stabilizes focal adhesion kinase (FAK) in the focal adhesions (FAs) and induces its disassembly, required for cell migration [12]. Galectin-3 also regulates motogenic response of epidermal growth factor in mammary cell lines [13]. Exogenously added soluble galectin-3 has also been shown to induce lamellipodial formation in corneal epithelial cells by interacting with integrins [14]. Moreover, extracellular galectin-3 facilitates phosphatidylinositol 3-kinase (PI3K)-dependent migration of sarcoma-derived cell line on laminin 111 [15]. Down-regulation of galectin-3 in intestinal epithelial cells affects the stability of desmosomal cadherins and intercellular adhesion [16]. Binding of galectin-3 to N-cadherins has been shown to destabilize cell–cell junctions in murine mammary cancer cells which might favor cell migration [17]. However, it is not clear how immobilized galectin-3 as a component of ECM/BM promotes such complex cellular processes like spreading and movement critical for cancer cell metastasis.

The various ECM and BM components either positively or negatively regulate the cellular adhesion, spreading, and motility [18, 19]. Fibronectin is the major component of ECM but is also present in the basement membrane, although, the proportions in the two may vary. Fibronectin plays a major role in stabilizing the cellular interaction with the matrix via integrin receptors on the cells [20–22]. These receptors promote adhesion, spreading, and movement of cells in response to external cues. The fibronectin mediated cellular effects and downstream molecular events have been thoroughly researched over last three decades, and serve as a good model to explore and understand the possible mechanisms utilized for similar cellular processes on other substrates like galectin-3 [21, 23].

The organization of microfilaments dictates the lamellipodial/filopodial structures which are important determinants of patterns of cellular spreading and movement. The guanine nucleotide exchange factors (GEFs) activate RhoGTPases like Rac1 and CDC42 which regulate the formation of lamellipodia and filopodia, respectively. The GEFs are activated via activated FAK which is recruited and activated by integrin receptors upon binding to their respective ligands like fibronectin. FAK serves as the docking site for PI3K and Src. PI3K phosphorylates AKT resulting in sequential activation of GEFs and Rac1 [24, 25]. Activated FAK–Src complex also regulates spreading and movement by activating scaffolding proteins like paxillin and p130Cas, which activate GEFs for Rac1 and CDC42 [26–28]. Microfilaments are also organized via integrin through Ser925 site on activated FAK via Erk–MAPK cascade which leads to phosphorylation of myosin light-chain kinase 1 (MLCK1). This pathway is believed to be used to release the rear end of motile cell for efficient movement [26, 27, 29–31]. Apart from integrin receptors, growth factor receptors (GFRs) also participate in cellular motility. The matrix which acts as a sink provides a rich source of growth factors (GFs) [19]. GFRs independently or in combination with integrins, activate downstream signaling required for cell migration. GFRs regulate motility by influencing microfilament organization by activating GEFs via PI3K and ERK–MAPK pathways [32, 33].

In spite of enormous literature on the association of galectin-3 with ECM and BM and its role in different steps of metastasis, there is no evidence about the mechanism by which galectin-3 exerts its effects to promote processes like spreading and motility critical for metastasis. The present manuscript for the first time demonstrates the molecular mechanisms involved in cellular spreading and movement on galectin-3 as the immobilized substrate in detail. It demonstrates that the dynamics and organization of the lamellipodial structures formed and the signaling events for their formation on galectin-3 are very distinct as compared to those observed on fibronectin, the well-established ECM component involved in these processes. These studies should have a significant bearing on our understanding of organ (lung)-specific metastasis.

Materials and methods

Cell culture and reagents

B16F10 murine melanoma cell line was obtained from National Centre for Cell Science (NCCS), Pune, India. 10 % FBS in DMEM was used for culturing the cells. Fibronectin was obtained from BD Biosciences, USA. *Escherichia coli BL 21* with pET3c plasmid containing full-length coding DNA sequence of human galectin-3 was a kind gift from Dr. Hakon Leffler, Lund's University, Sweden. Glutathione–Sepharose beads and PVDF from Amersham Hybond GE Healthcare, UK. Developing

reagent Advansta from USA. Primary antibodies for Akt, pAkt, Erk, and pErk were from Cell Signaling Technology, USA while for Rac1 from Millipore, USA. Anti-Rabbit HRPO was from Santacruz, USA. Primers for amplification of actin, puromycin, polybrene, paraformaldehyde, BSA, Phalloidin-TRITC, DAPI, and primary antibody for β-Actin, GFP, and secondary Anti-Mouse HRPO antibody were purchased from Sigma Chemical Company, USA. Vectashield mounting medium was from Vector Labs, USA. Pharmacological inhibitors wortmannin (Wm), PD98059 and phosphatase, and protease inhibitor cocktail were purchased from Calbiochem, USA. Molecular cloning-related reagents were from New England Biolabs, USA. Reagents for bacterial culture were purchased from HiMedia, India, while all other chemicals were purchased locally and were of analytical grade.

Cell spreading assay

Cell spreading assay was done exactly as described in Ref. [34]. Briefly, melanoma cells were harvested and washed thrice with serum-free DMEM. 1 ml of melanoma cell suspension containing 0.5×10^6/ml in serum-free DMEM were seeded on precoated coverslips either with 75 μg/ml galectin-3 (for standardization 25, 50, 75, and 100 μg/ml) or 10 μg/ml fibronectin incubated overnight at 4 °C. (For all the experiments same concentration of galectin-3 and fibronectin was used. The volumes used for coating was 1 ml for 35 mm and 4 ml for 90 mm plates). The cells were then incubated at 37 °C for 15, 30, 45, and 60 min time points in a CO_2 incubator. Cells were seeded on uncoated coverslip incubated for 60 min served as control. After each time points, the non-adherent cells were removed by gentle washing 3–4 times with 1 ml PBS. The adherent cells were fixed, permeabilized, and stained with Phalloidin-TRITC for filamentous actin (F-actin) and mounted on glass slides in Vectashield containing DAPI which stains nuclei. The images were acquired using a Carl Zeiss Laser confocal microscope at ×63 magnification. To assess the effect of pharmacological inhibitors on cell spreading, adherent murine melanoma cells were pre-incubated for 1 h either with 500 nM wortmannin or 25 μm PD98059 in 0.1 % DMSO. Cells incubated in 0.1 % DMSO served as a vehicle control (VC). Later the cells were harvested and cell spreading assay as described above was performed.

Generation of stable cell line expressing fluorescent actin

B16F10 cell lines expressing green fluorescent actin (GFP-Actin) was successfully generated. The details for generation of this cell line is discussed in supplementary materials (Supplementary method 1).

Live cell imaging and fluorescence recovery after photobleaching (FRAP)

Live cell imaging was performed to study the kinetics of cell spreading on galectin-3 and fibronectin. The 35 mm glass bottom tissue culture dishes were coated either with 75 μg galectin-3 or 10 μg of fibronectin in 1 ml PBS and incubated overnight at 4 °C. B16F10 cells stably expressing GFP-Actin were harvested and washed thrice with serum-free DMEM devoid of phenol red and density was adjusted to 5×10^4 cells/ml in serum and phenol red-free DMEM. The coating solution was removed and 1 ml of melanoma cell suspension was seeded on these coated plates. Live cell imaging was performed for 1 h and the images were acquired in a single plane at 1 min time interval on these cells maintained at 37 °C in a 5 % CO_2 incubator, using Olympus 3i spinning disk microscope at ×60 magnification.

Actin turnover in the lamellipodial region was assessed using FRAP. As mentioned above for live cell imaging, the melanoma cells stably expressing GFP-Actin were seeded on uncoated, galectin-3 or fibronectin-coated petri dishes in serum and phenol red-free DMEM and incubated for 4 h at 37 °C in a 5 % CO_2 incubator. The bleaching is performed at the lamellipodial region using 488 nm laser at 100 % laser power and 100 % iterations in order to achieve at least 80 % bleaching. The 4 pre-bleached images were acquired and after bleaching images were acquired at 1 s time interval for up to 4 min in the bleached region using LSM780 Carl Zeiss confocal microscope at ×63 magnification. Three independent FRAP experiments were performed. In each experiment at least 10 cells were bleached. The percent recovery was calculated and plotted using Graphpad.

Rac1 activation assay

Glutathione–Sepharose beads conjugated with GST-PAK1 were used for pull-down of activated GTP-coupled Rac1. Purification of GST-PAK1 and its conjugation with Glutathione–Sepharose beads was done exactly as described in Ref. [35] and is discussed in detail in the supplementary materials (Supplementary method 2). For Rac1 activation assay, 24 h serum-starved cells were harvested, washed, and 4×10^6 cells were seeded on galectin-3/fibronectin-coated 90 mm plates for 15, 30, and 60 min time interval. At respective time points, non-adherent cells in each plate were removed and 1 ml lysis buffer (containing 50 mM Tris·Cl, pH 7.2, 1 % (w/v) Triton X-100, 500 mM NaCl, 10 mM $MgCl_2$, and protease inhibitor cocktail) was added to the plate. The cells were collected, sonicated, and centrifuged at 15,000 rpm, for 30 min at 4 °C. The protein content in these cell lysates was estimated. The cell lysed at

0 min time point served as control. Equal amount of Sepharose–PAK1 beads were incubated with 2 mg (in 1 ml of lysis buffer) protein in lysates of cells harvested at each time point on rocker for 1 h at 4 °C. The beads were washed 3 times with Tris wash buffer and the bound protein was eluted using 4× Laemelli buffer at 100 °C for 10 min. Western blotted total cell lysates and respective PAK1-bound proteins were analyzed using anti-Rac1 antibody.

Preparation of cell lysates and immunoblotting

B16F10 cells were grown for 24 h in serum-free condition and harvested using EDTA and glucose. To study the effect of pharmacological inhibitors the cells were incubated for 1 h with 500 nM wortmannin, 25 μm PD98059, 0.1 % DMSO (vehicle control (VC)) before harvesting them. The harvested cells were washed and 4×10^6 cells were seeded on galectin-3 or fibronectin-coated 90 mm plates for 15, 30, and 60 min time interval. At respective time points, non-adherent cells in each plate were removed and 1 ml lysis buffer (containing 50 mM Tris·Cl, pH 7.4, 150 mM NaCl, 1 % NP40, 1 % sodium deoxycholate, 0.1 % SDS, 1 mM EDTA, 1 mM EGTA, Phosphatase, and protease inhibitor cocktail) was added to the plate. The cells were collected, sonicated, and centrifuged at 15,000 rpm, for 30 min at 4 °C. The protein content in these cell lysates was estimated. The cell lysed at 0 min time point served as control. The equal amount of protein in each cell lysate was loaded on SDS-PAGE, transferred on PVDF membrane, and immunoblotted for Akt, pAkt, Erk, and pErk.

Wound healing assay

Wound healing assays were performed in 6-well plates coated with galectin-3 or fibronectin. Non-specific sites on the plates were blocked with 2 % BSA in PBS for 1 h at 37 °C. Uncoated culture dishes, blocked only with BSA served as control. Melanoma cells were harvested and seeded on the plates at a density of 0.6×10^6 cells in 2 ml of complete DMEM and incubated at 37 °C for 24 h in a CO_2 incubator. The cells were washed free of serum and grown under serum-free conditions for 24 h for cell synchronization and to reach 95 % confluency. A straight, uniform wound was made using a 2 μl micropipette tip. The dislodged cells were washed off and cells were maintained in serum-free DMEM. Wound closure of cells was measured for 16 h by time-lapse video imaging of at least three different positions across the length of the wound using a Carl Zeiss Inverted Microscope. Mean values of triplicate wound for each data set were analyzed using Image J software. To assess the effect of pharmacological inhibitors on cell motility, adherent murine melanoma cells were pre-incubated for 2 h before making the wound, either with 500 nM wortmannin or 25 μm PD98059 in 0.1 % DMSO. Cells incubated in 0.1 % DMSO served as a vehicle control (VC).

Statistics

All the statistical analysis was done using Graphpad prism 6 software. For comparison of two groups, student *t* test was performed and for multiple comparison either one-way ANOVA or two-way ANOVA was performed. All the error bars represent mean ± s.e.m.

Results

B16F10 melanoma cells show distinct cytoskeletal organization when allowed to spread on galectin-3 as opposed to fibronectin

Cells utilize extracellular matrix component (ECM) as the substrate for their spreading and movement. Different ECM components determine the type of cytoskeletal organization during spreading and movement of the cells. Secreted galectin-3 is known to get incorporated as a component of ECM and BM [3, 36]. The spreading of B16F10 cells was shown to be highest at 75 μg/ml galectin-3 (Supplementary Figure S1). The same concentration of galectin-3 was used for all the experiments. Comparison of the cell spreading pattern and cytoskeletal organization on galectin-3 of B16F10 melanoma cells with that of well-studied ECM component fibronectin, showed that it was very different (Fig. 1). On immobilized fibronectin cells show arborate or stellate (mesenchymal type) morphology with abundant stress fibers traversing through cell body (Fig. 1d, e, i) while on galectin-3 cells show rounded morphology with peripheral actin filament distribution (Fig. 1a, b, i). The cell spreading on uncoated coverslips served as a control (Fig. 1g, h). These morphological differences were also reflected during motility of the cells on galectin-3 (Fig. 1c) and fibronectin (Fig. 1f). Fixed and live cell imaging on immobilized galectin-3 and fibronectin was performed to see if differences in spreading kinetics are evident even at early time points.

Spreading kinetics of B16F10 melanoma cells on galectin-3 is more dynamic

Cell spreading is a post-adhesive event required for cell movement. Actin assembly and disassembly regulates the

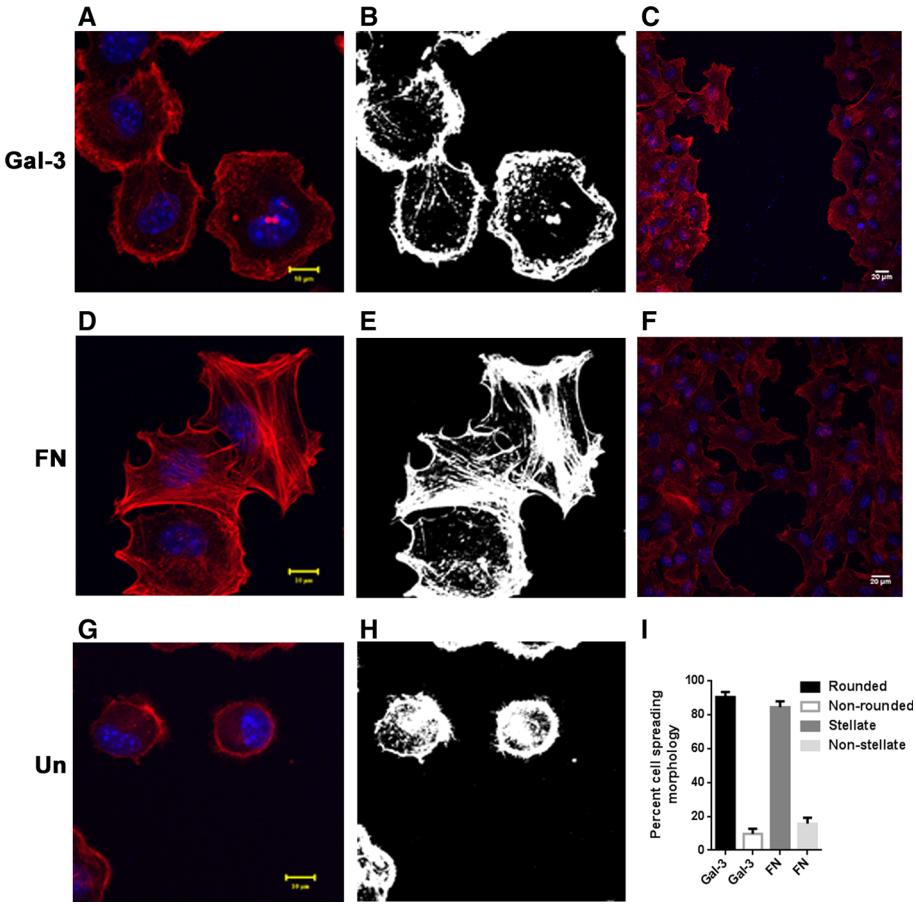

Fig. 1 Spreading pattern and actin cytoskeletal organization of cells on immobilized galectin-3 (Gal-3) and fibronectin (FN). Images represent the spreading pattern of cells on galectin-3 (**a**) and (**b**), and fibronectin (FN) (**d**) and (**e**) coated coverslips and on uncoated (Un) coverslips (**g**) and (**h**) which served as a control. **a**, **d**, and **g** are the colored confocal images while the **b**, **e**, and **h** are the threshold images of the same, respectively. The cells were fixed and stained with phalloidin-TRITC (*red*) for filamentous actin and DAPI for nucleus and images were acquired using laser confocal microscope at ×63 magnification, Scan zoom ×1.5. *Scale bar* 10 µm. The differences in lamellipodial structures in cells migrating on coverslips coated with galectin-3 (**c**) and fibronectin (**f**) to close the wound created 16 h prior. The cells were fixed and stained with phalloidin-TRITC for filamentous actin and DAPI for nucleus and images were acquired using Leica STED confocal microscope at ×40 magnification. *Scale bar* 20 µm. **i** Percent cells showing rounded or stellate morphology after spreading on galectin-3 and fibronectin. The cells were counted from three independent experiments in which minimum 50 cells were from each experiment and plotted using Graphpad

cell spreading and movement. The initiation of actin organization in various forms at initial time points of cell spreading on ECM components, is a critical event required for successful cell spreading and movement [37–40]. The cell spreading kinetics was studied on immobilized galectin-3 and fibronectin. Fixed cell imaging showed that B16F10 cells on immobilized galectin-3 start spreading early and show rounded lamellipodial morphology even at initial (15 min) time point which keeps increasing up to 30 min which was similar to that seen at 60 min (Fig. 2a). Lamellipodial structures at 15 min time point in cells plated on fibronectin were very different in appearance (stellate/arborate) to those seen on galectin-3 which progressively increase with time up to 60 min (Fig. 2b). The cell spreading on uncoated coverslips served as a control (Fig. 2c). The area of spreading of cells at each time points 15, 30, and 60 min on fibronectin was more as compared to galectin-3 (Fig. 2d).

To study the microfilament organization stable B16F10 cells expressing GFP-Actin was successfully generated (Supplementary Figure S2). Live cell imaging with these cells showed that the lamellipodial dynamics in cells plated on galectin-3 is very high even at very initial time points and the spreading of cells is stabilized by 30 min (Supplementary material Movie 1). However, in case of cells plated on fibronectin the lamellipodial dynamics is low and keeps increasing at a constant rate with time up to 60 min (Supplementary material Movie 2).

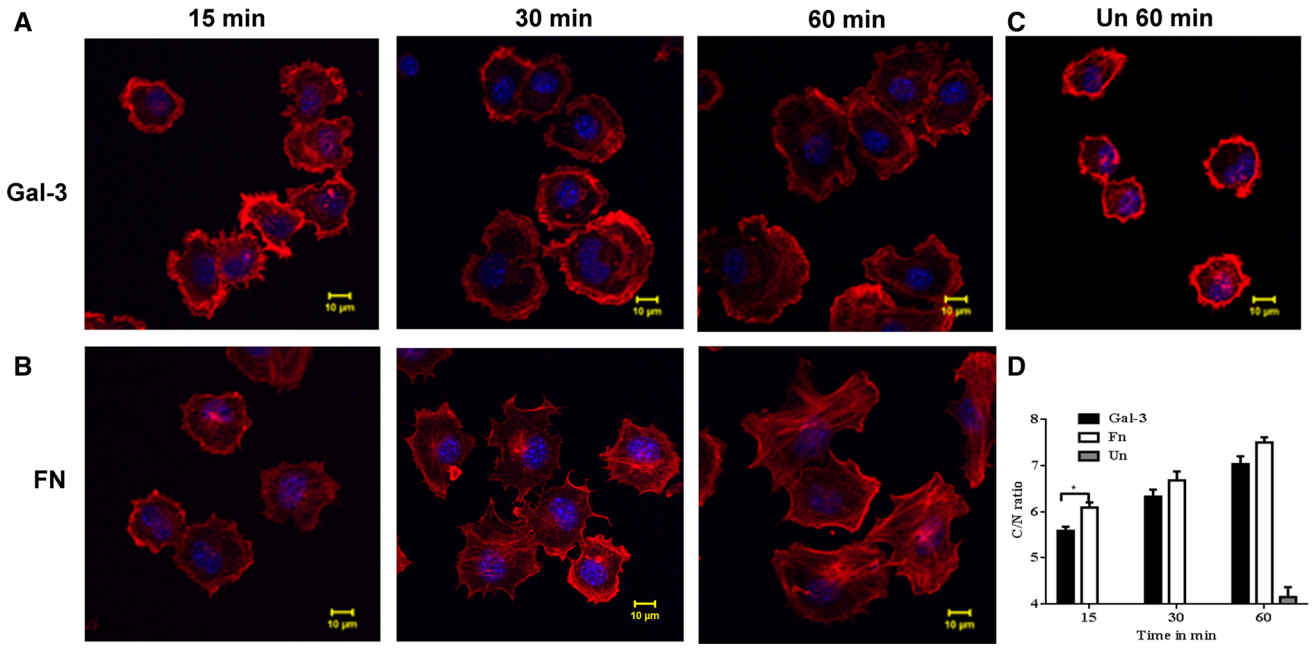

Fig. 2 Spreading kinetics of cells on galectin-3 and fibronectin assessed using fixed cell imaging. **a** and **b** represent the images of the cell spreading on immobilized galectin-3 and fibronectin, respectively fixed at 15, 30, and 60 min time points, and **c** image of cell spreading on uncoated coverslips for 60 min served as a control. The cells were stained with phalloidin-TRITC for filamentous actin and DAPI for nucleus and images were acquired using laser confocal microscope at ×63 magnification. **d** Each *bar* represents the mean ratio of cytoplasmic/nuclear area of at least 50 cells in (**a**), (**b**), and (**c**) of three independent experiments calculated using Image J software

The Rac1 is a regulator of lamellipodia formation, its activation was assessed on these substrates.

Rac1 activation is inversely regulated in cells spread on galectin-3 and fibronectin

Spatiotemporal activation of Rac1 plays an important role in the organization of actin in the lamellipodial region which in turn dictates the cell motility [41]. The levels of activated GTP-coupled Rac1 in cells spread on galectin-3 and fibronectin for different time points was assessed using Sepharose–PAK1 beads which only binds to activated Rac1 (Rac1-GTP). The levels of activated Rac1 in cells plated on galectin-3 was highest at 15 min time point which kept going down with time up to 60 min (Fig. 3a, c). However, in case of cells spread on fibronectin it was reverse. Activated Rac1 levels were lowest at 15 min and kept increasing with time, highest being at 60 min (Fig. 3b, d). The pattern of time-dependent Rac1 activation in cells spread on both the substrates (Fig. 3) is opposite to each other. However, it appears to correlate with their time-dependent spreading and lamellipodial organization (Fig. 2 and Supplementary material Movies 1 and 2) on these substrates.

The difference in cell spreading kinetics, microfilament architecture, lamellipodial organization on immobilized galectin-3 and fibronectin could be due to differential actin turnover in the lamellipodial region.

Turnover of filamentous actin in the lamellipodial region is high in cells spread on galectin-3 as compared to those on fibronectin

The continuous trade milling of actin at the lamellipodial region is required for cell spreading and movement. The actin organization in this region determines stability and dynamic nature of lamellipodia [37–40]. Actin dynamics in the lamellipodial region was assessed using fluorescence recovery after photobleaching in B16F10 cells spread on uncoated and immobilized galectin-3 and fibronectin. Percent recovery of the bleached area was significantly higher (68 %) in the cells spread on galectin-3 as compared to those spread on fibronectin (54 %). The cells spread on uncoated surfaces show lower recovery in the bleached region (46 %) (Fig. 4). These results suggest actin dynamics in the lamellipodial region in the cells spread on galectin-3 is significantly higher as compared to that seen in cells plated on fibronectin. Differences in the morphological changes and actin recovery in this region could be due to the differential regulation of molecular signaling induced by galectin-3 and fibronectin.

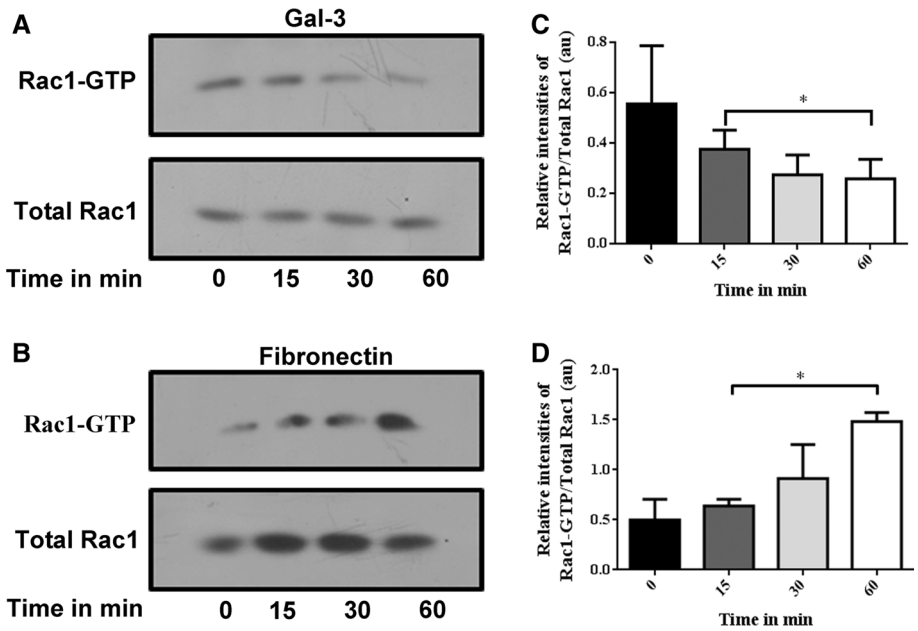

Fig. 3 Differential activation of Rac1 on immobilized galectin-3 and fibronectin. Western blotted purified activated Rac1 (as described in "Materials and methods" section) from lysates of cells allowed to spread for 0, 15, 30, and 60 min on **a** immobilized galectin-3 and **b** fibronectin, probed with anti-Rac1 antibody. Levels of total Rac1 in the cell lysates served as loading control. **c** and **d** represent the graphical quantitation using Image J of (**a**) and (**b**), respectively. Each experiment was done in duplicate. $*p < 0.05$; All *error bars* represent mean ± s.e.m

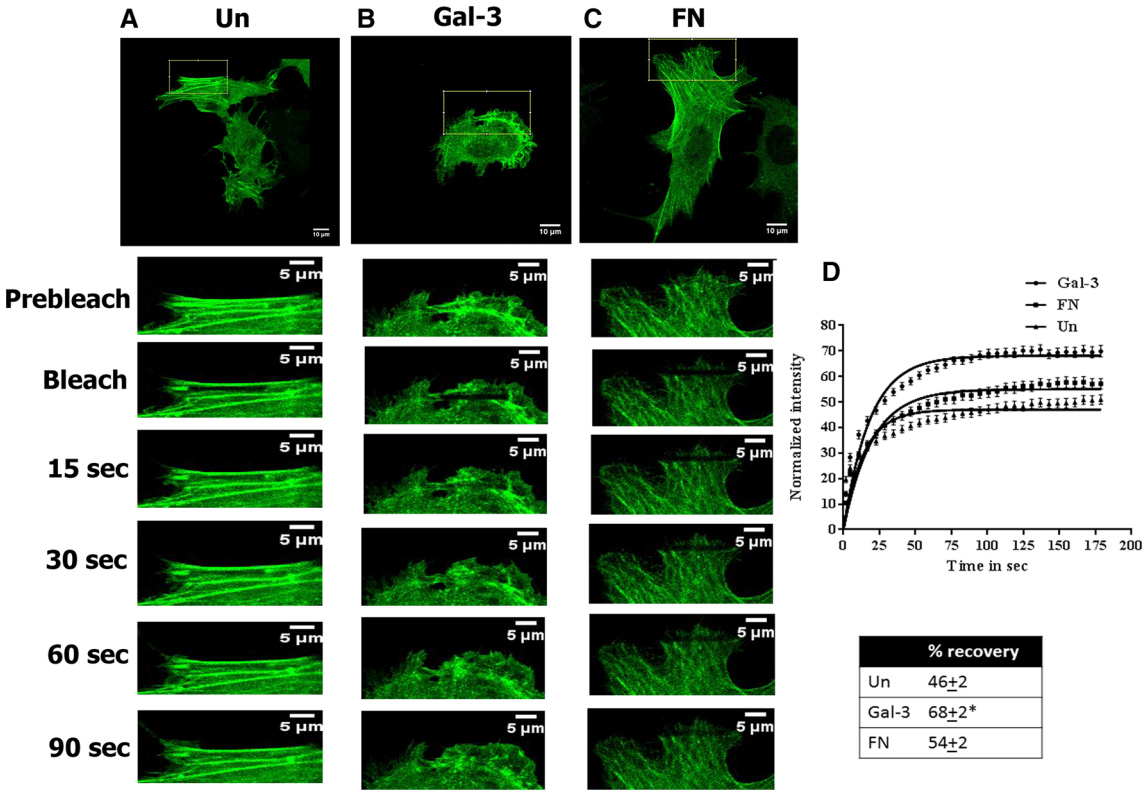

	% recovery
Un	46±2
Gal-3	68±2*
FN	54±2

Fig. 4 Actin turnover in the lamellipodial region of cells spread on galectin-3 and fibronectin. **a**, **b**, and **c** represent the fluorescence recovery after photobleaching (FRAP) analysis of GFP-actin in the lamellipodial region of B16F10 melanoma cells on uncoated, galectin-3 and fibronectin-coated surfaces, respectively. **d** Graphical representation of percent fluorescence recovery over time of GFP-actin in the lamellipodial region of cells on uncoated, galectin-3, and fibronectin-coated surfaces. FRAP values obtained from 30 cells were used to calculate the percent recovery. $*p < 0.05$, All *error bars* represent mean ± s.e.m

Akt phosphorylation is inversely regulated in cells spread on galectin-3 and fibronectin while Erk is regulated similarly in both

Different patterns of migration of cells is predominantly regulated by PI3K/Akt and/or Erk–MAPK pathways. These pathways are activated depending on the extracellular cues [25, 26, 42]. In order to investigate the signaling pathways induced by galectin-3 and fibronectin, the time-dependent activation of Akt and Erk was studied. Akt phosphorylation increases with time in cells plated on galectin-3 while it decreases when cells plated on fibronectin in a time-dependent manner. Maximum phosphorylation of Akt is observed at 60 min time point on galectin-3-plated cells while fibronectin-plated cells show maximum phosphorylation at 15 min time point (Fig. 5a, d). Phosphoryation of Akt could be completely abrogated by PI3K inhibitor wortmannin (Wm) in cells spread on both galectin-3 and fibronectin. However, PD98059, a inhibitor of MEK1/2 had no effect on Akt phosphorylation (Fig. 5b, e, c, f) suggesting that Erk–MAPK pathway has no role in the activation of Akt on both the substrates. Comparison of Erk phosphorylation in cells spread on galectin-3 and fibronectin showed that there is a time-dependent decrease in the phosphorylation of Erk in cells spread on both the substrates (Fig. 6a, d). Treatment with wortmannin only partially affected Erk phosphorylation while PD98059 completely inhibited phosphorylation of Erk in cells spread on both the substrates (Fig. 6b, c, e, f).

These differences in the regulation of signaling pathways in cells plated on substrates like galectin-3 and fibronectin could be because of activation through different cell surface receptors. The effect of upstream inhibitors wortmannin and PD98059 on spreading and motility of cells on both these substrates was assessed.

Inhibitors of Akt and Erk pathway inhibit cellular spreading and migration on galectin-3 but not on fibronectin

Standard spreading assay of B16F10 cells treated only with the vehicle (0.1 % DMSO) (VC), wortmannin (PI3K inhibitor), and PD98059 (MEK1/2 inhibitor) was performed on uncoated (Un) and galectin-3 or fibronectin-coated coverslips for 45 min at 37 °C and 5 % CO_2. Results showed that in comparison to cells plated on uncoated coverslips (Fig. 7a), those on galectin-3 (Fig. 7b) and fibronectin (Fig. 7c) spread well and show very well-

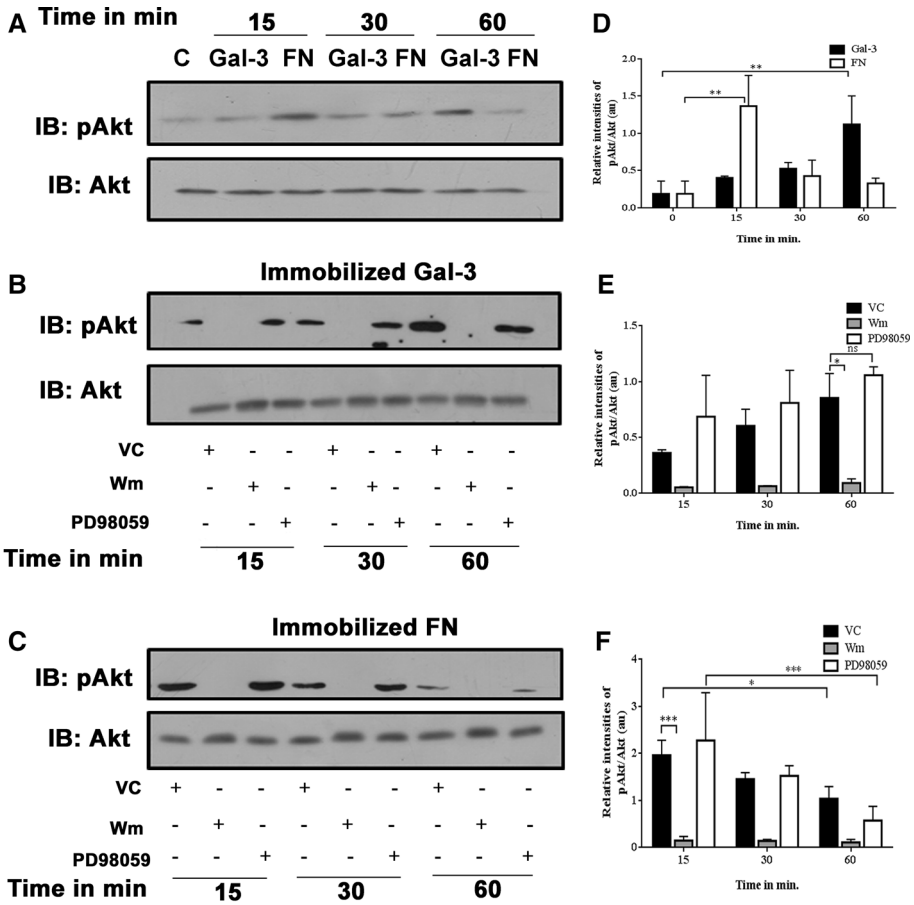

Fig. 5 Spreading of cells increases Akt phosphorylation with time on galectin-3 while decreases it on fibronectin. **a**, **b,** and **c** represent immunoblots of lysates of B16F10 cells spread on a immobilized galectin-3 and fibronectin for 0, 15, 30, and 60 min time points, $C = 0$ min control. **b** and **c** represent immunoblots of lysates of B16F10 cells grown in presence of vehicle control (VC), wortmannin (Wm) and PD98059, on **b** immobilized galectin-3 and **c** fibronectin. Each *bar* in the graphs **d**, **e,** and **f** represent the mean ratio of staining intensities with pAkt and Akt antibodies, in (**a**), (**b**), and (**c**) respectively, done in triplicate, quantitated using Image J software.*$p < 0.05$, **$p < 0.01$, and ***$p < 0.001$; All *error bars* represent mean ± s.e.m

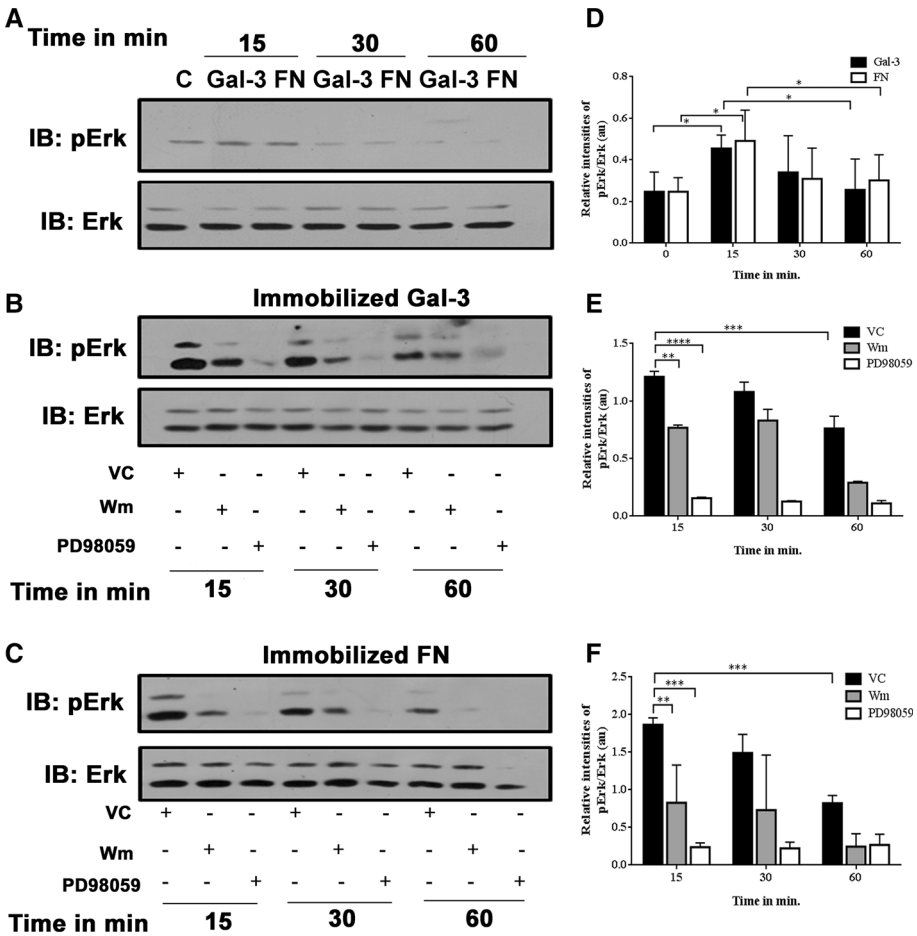

Fig. 6 Spreading of cells on galectin-3 and fibronectin decreases Erk phosphorylation with time. **a**, **b**, and **c** represent immunoblots of lysates of B16F10 cells spread on a immobilized galectin-3 and fibronectin for 0, 15, 30, and 60 min time points, $C = 0$ min control. **b** and **c** represents immunoblots of lysates of B16F10 cells grown in the presence of vehicle control (VC), Wm, and PD98059, on **b** immobilized galectin-3 and **c** fibronectin. Each *bar* in the graphs **d**, **e**, and **f** represents the mean ratio of staining intensities with pErk and Erk antibodies, in (**a**), (**b**), and (**c**), respectively, done in triplicate, quantitated using Image J software.*$p < 0.05$, **$p < 0.01$, and ***$p < 0.001$; All *error bars* represent mean ± s.e.m

organized microfilament architecture, although distinct for each substrate. This is also very evident in significantly higher ratio of cytoplasmic to nuclear area in these cells as compared to those on Un (Fig. 7d). However, treatment of cells with wortmannin and PD98059 significantly inhibited the spreading, lamellipodial structures and microfilament organization in cells plated on galectin-3, however, those plated on fibronectin largely remain unaffected. This was also evident in the bar graph depicting ratios of cytoplasmic to nuclear area of cells (Fig. 7b–d).

Spreading is an initial event that influences cellular motility. Wound healing assays were performed on cells plated on uncoated, galectin-3-, and fibronectin-coated plates in the absence or presence of vehicle, wortmannin, and PD98059. Results showed that as compared to vehicle control, wortmannin and PD98059 significantly inhibit migration of cells on galectin-3-coated plates (Fig. 7e, h), whereas, these inhibitors very marginally affect movement of cells on fibronectin (Fig. 7f, h). The lowest wound closure was observed on uncoated surfaces blocked with BSA (Fig. 7g, h). The results suggest that distinct signaling mechanisms dictate the microfilament organization, formation of lamellipodial structures, spreading, and movement of cells on galectin-3 and fibronectin.

Discussion

PolyLacNAc on cancer cells and galectin-3 on the target organ have previously been shown to promote organ-specific metastasis to the lungs by not only facilitating initial arrest on the endothelium but all the steps of extravasation [6–9]. Galectin-3, although a nucleocytoplasmic protein, gets secreted out in a non-classical manner. The secreted galectin-3 is known to get incorporated on the cell surface, ECM, and BM [3]. We showed that such immobilized galectin-3 promotes metastasis by facilitating initial arrest on the target organ vasculature and in different steps of extravasation. Like other ECM and BM components galectin-3 participates in adhesion, spreading, movement, and degradation of matrix [6]. The present investigation explores the molecular mechanisms involved in galectin-3-mediated processes, especially cellular spreading and motility by comparing it

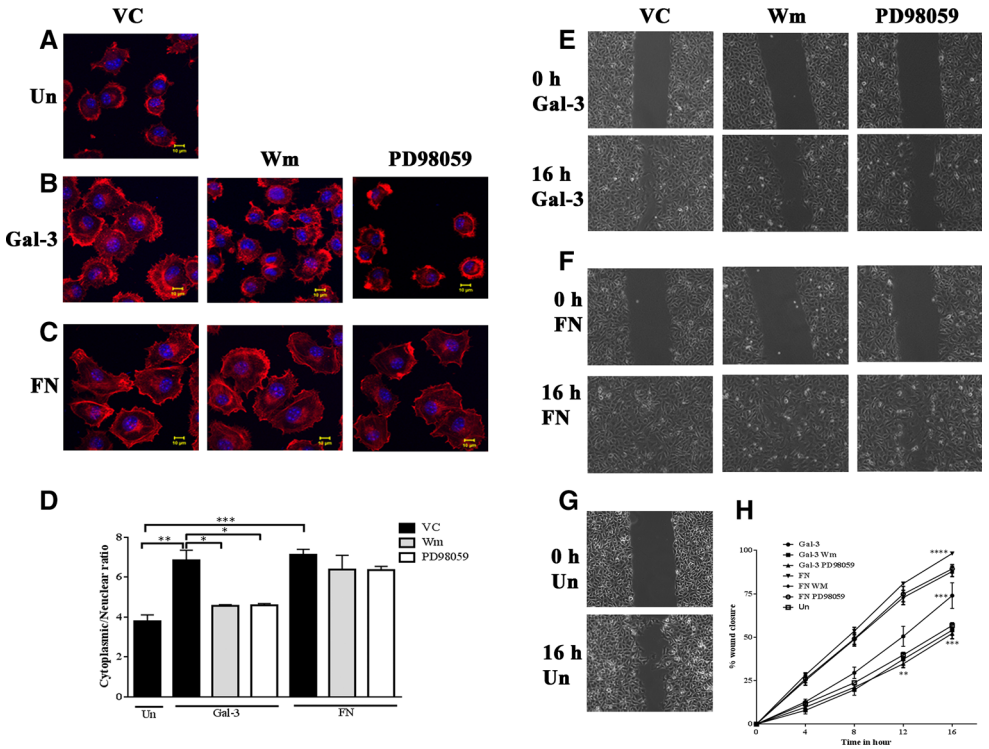

Fig. 7 Inhibitors of PI3K (Wm) and MEK1/2 (PD98059) affect cell spreading and migration on immobilized galectin-3 but not on fibronectin. **a**, **b**, and **c** represent images of the cell spreading of B16F10 treated with vehicle control (VC), Wm and PD98059, on uncoated (Un), immobilized galectin-3, and fibronectin, respectively. The cells were fixed and stained with phalloidin-TRITC for filamentous actin and DAPI for nucleus and images were acquired using laser confocal microscope at ×63 magnification. *Scale bar* 10 µm. Each *bar* in **d** represents the mean ratio of cytoplasmic/nuclear area of at least 50 cells in (**a**), (**b**), and (**c**) of three independent experiments using Image J software. **e**, **f**, and **g** are representative images of wound healing assay at 0 and 16 h time points, on, galectin-3-coated, fibronectin-coated, and uncoated surfaces respectively, of B16F10 cells treated with VC, Wm, and PD98059. **h** Represents mean percent wound closure of cells in (**e**), (**f**), and (**g**), at 4 h interval up to 16 h. Area of wound closure was measured at three different positions by Image J software from three different experiments. Two-way analysis of variance followed by Bonferroni's multiple comparison test was performed to compare significance. $*p < 0.05$, $**p < 0.01$, and $***p < 0.001$; All *error bars* represent mean ± s.e.m

with that on ECM component fibronectin which is very well studied.

Motility of cancer cells is critical for their invasiveness and metastasis. Cellular adhesion followed by spreading are crucial events that determine the pattern of cellular movement [33, 36, 43–45]. The lamellipodial organization in the cells spread on galectin-3 is typical of cells that show random motility with broad and rounded lamellipodia with parallel actin bundles along the cell periphery (Fig. 1a, b). However, cells on fibronectin expectedly show features of cells showing directional motility with classical stress fibers traversing throughout the cell body (Fig. 1d, e). The cells appear to maintain their distinct morphology even during migration on these substrates (Fig. 1c, f). Further, the kinetics of cell spreading, lamellipodial organization, and cell spreading area on each of these substrates was markedly different. The cells on galectin-3 attain the morphology and lamellipodial organization at an early time point. However, the stellate morphology, the lamellipodial structures, and the stress fibers keep growing steadily and get stabilized at a later time point in cells on fibronectin (Fig. 2, supplementary material Movies 1 and 2).

Rac1 is the major regulator of the lamellipodial organization and activation of Rac1 is required for its formation. The time-dependent increase in the levels of activated Rac1 correlated with the lamellipodial organization in cells plated on fibronectin (Fig. 3b, d). Both Rac1 activation and formation of lamellipodia keep increasing with time. However, in cells plated on galectin-3 (Fig. 3a, c) where well-formed lamellipodial structures get organized even at an early time point (15 min) the levels of activated Rac1 is highest, and keeps decreasing with time (Figs. 2, 3 and supplementary material Movie 1, 2). Organization of microfilaments is the major determinant of the type of lamellipodial structures, which in turn depends on the actin dynamics [37–40]. Actin dynamics in the lamellipodial region of cells on galectin-3 was significantly higher as compared to that on fibronectin as analyzed using FRAP (Fig. 4). This suggests that very distinct signaling mechanisms operate in the cells spread on galectin-3 and on

fibronectin which regulate microfilaments, lamellipodia formation, and spreading morphology.

The two major pathways which are known to regulate cellular spreading and motility are PI3K/Akt and Erk–MAPK. Both Akt and Erk are activated in response to extracellular cues [25, 26, 42]. Here we compared the activation status of these two regulators in cells spread on galectin-3 and fibronectin. Fibronectin being one of the best-studied ECM component acts as a substrate for various normal as well as cancer cell lines and support their adhesion-dependent motility. Fibronectin induces outside in signaling through integrin receptors while galectin-3 has myriad of cell surface receptors. Most studies have investigated the activation of signaling pathways in cells plated on fibronectin-coated plates [46–48].

The secreted extracellular galectin-3 exerts its cellular effects on motility-related processes both in the soluble and immobilized form [3, 10]. The soluble galectin-3 has been shown to modulate fibronectin, laminin 111, and EGF-dependent motogenic response by binding to their respective receptors [11–13, 15]. Soluble galectin-3 has been shown to promote movement by destabilizing cell–cell adhesion by its interaction with desmosomal- or N-cadherin [16, 17]. Exogenously added soluble galectin-3 has also been shown to induce formation of lamellipodia in corneal epithelial cells by interacting with integrins [14]. Galectin-8 which has oligosaccharide specificity very similar to galectin-3 [49] has been shown to act as a matricellular protein and modulator of cell adhesion by interacting with integrins [48, 50]. However, there is no study that investigates the signaling mechanisms in cells that use galectin-3 as the substratum for their adhesion, spreading, movement, and possibly their growth. Further, although there are a few studies that have explored the time-dependent signaling mechanisms during spreading of cells on fibronectin [30], there are no reports about the signals induced during cellular spreading mediated by immobilized galectin-3.

Comparison of the signaling pathways activated during spreading of B16F10 cells that express high levels of polyLacNAc, on fibronectin, and galectin-3 showed distinct pattern. The cells showed sustained time-dependent activation of Akt when spread on galectin-3, however, it was only transient in cells on fibronectin (Fig. 5a, d). The receptors for fibronectin are well-defined integrin receptors [20–23]. However, all the surface proteins that carry polyLacNAc-substituted β1, 6-branched N-oligosaccharides can be receptors for galectin-3, which include integrins, cell adhesion molecules (CAMs), receptor tyrosine kinases (RTKs), growth factor receptors (GFRs), and lysosomal associated membrane proteins (LAMPs) [51]. The differential activation of Akt in cells on galectin-3 and fibronectin is possibly due to the different set of receptors for each substrate which follow different pathway(s) for activation of Akt. The activation of Erk is generally transient in a migrating cell, and sustained activation leads to cellular differentiation [52]. The activation of Erk in B16F10 cells was indeed transient during spreading irrespective of the substrate used, galectin-3 or fibronectin (Fig. 6a, d). Pharmacological inhibition studies showed that Akt is activated independently of Erk–MAPK pathway while Erk activation depends on both PI3K/Akt and Erk–MAPK pathways on both galectin-3 and fibronectin (Figs. 5, 6).

Akt activation results in the regulation of the activity of RhoGTPases which play an important role in microfilament organization. Formation of lamellipodia is an important step in cellular spreading and substrate-dependent motility (haptotaxis). Rac1 is the major regulator of the lamellipodial organization and activation of Rac1 is required for its formation [24, 40, 53]. The Akt and Rac1 activation are inversely correlated with each other on both the substrates galectin-3 and fibronectin. GTP-binding activity of Rac1 is critical for the formation of lamellipodial structures and activated Akt has been shown to inhibit this activity by phosphorylating Rac1 at Ser71 [54, 55]. This explains the inverse correlation of Akt and Rac1 activation in cells on galectin-3 and fibronectin.

Although, activated Rac1 is the major regulator of lamellipodia formation and cellular spreading, it can be activated by multiple mechanisms. Spreading and motility in the presence of inhibitors of PI3K/Akt (wortmannin) and Erk–MAPK (PD98059) showed that both these pathways operate for spreading and movement on galectin-3. However, none of these inhibitors had any significant effect on these processes on fibronectin (Fig. 7), suggesting that Rac1 activation in these cells occurs via some other mechanism. FAK on activated integrin receptor for fibronectin often gets autophosphorylated at Tyr397 which serves as docking site for Src and PI3K resulting in their activation. Activated FAK–Src complex activates scaffolding proteins like p130Cas and paxillin which in turn activate GEFs for Rac1 and CDC42, the key regulators of lamellipodia and filopodia, respectively [27, 56]. The Rac1 activation and lamellipodia formation in B16F10 cells plated on fibronectin possibly act via FAK–Src/p130Cas pathway, explaining the absence of any effect of wortmannin or PD98059 on cellular spreading and motility on this substrate.

These studies clearly demonstrate that immobilized galectin-3 like other components of ECM and BM also supports spreading and movement of cells. By way of multiple receptors on the cell surface expressing high affinity ligands like polyLacNAc, galectin-3 signals distinct pathways that modulate microfilament dynamics and promote lamellipodial organization that supports spreading and movement. We demonstrate that each of these

characteristics including, lamellipodial organization, actin dynamics, signaling pathways, spreading, and movement on galectin-3 are very distinct from that seen on the classical ECM component, fibronectin.

Fibronectin supports directional motility of cells with mesenchymal phenotype which is required for almost all the stages of metastatic cascade, however, the cells do not need directional long-distance motility once they reach the target organ. The cells adopt themselves to random movement required to explore the microenvironment of the target organ. The spreading and motility pattern of cells seen on immobilized galectin-3 are typical features of random movement [57, 58]. Lungs which express highest levels of galectin-3 on almost all the tissue compartment [6–9] is apparently utilized by melanoma cells for random movement and for their establishment in the target organ as the metastatic foci. These observations together with earlier reports about the participation of galectin-3 in the initial arrest and processes involved in extravasation, clearly demonstrate its critical role in organ (lung)-specific metastasis.

Acknowledgments We dedicate this work to the memory of Late Dr. Rajiv D. Kalraiya, who was responsible for planning and supervision of this work. We acknowledge Dr. Hakon Leffler for providing *E. coli BL21* star strain expressing recombinant human galectin-3 and Dr. Sorab Dalal for providing *E. coli* strain expressing GST-PAK1 fusion protein. We acknowledge Urjita Joshi for signaling pathway experiments, Vaishali Khailaje, Tanuja Dighe, and Jairaj Kashale for help in microscopy experiments, and D. S. Chavan and A. M. Pawar for the technical help during galectin-3 purification. We thank Council of Scientific and Industrial Research (CSIR), India for providing the fellowship to Shyam K. More and Department of Biotechnology (DBT), India for funding the project.

Compliance with ethical standards

Conflict of interest The authors declare that they have no conflict of interest.

References

1. Bacac M, Stamenkovic I (2008) Metastatic cancer cell. Annu Rev Pathol 3:221–247. doi:10.1146/annurev.pathmechdis.3.121806.151523
2. Chiang AC, Massague J (2008) Molecular basis of metastasis. N Engl J Med 359(26):2814–2823. doi:10.1056/NEJMra0805239
3. Dumic J, Dabelic S, Flogel M (2006) Galectin-3: an open-ended story. Biochim Biophys Acta 1760(4):616–635. doi:10.1016/j.bbagen.2005.12.020
4. Barondes SH, Cooper DN, Gitt MA, Leffler H (1994) Galectins. Structure and function of a large family of animal lectins. J Biol Chem 269(33):20807–20810
5. Dange MC, Agarwal AK, Kalraiya RD (2015) Extracellular galectin-3 induces MMP9 expression by activating p38 MAPK pathway via lysosome-associated membrane protein-1 (LAMP1). Mol Cell Biochem 404(1–2):79–86. doi:10.1007/s11010-015-2367-5
6. Dange MC, Srinivasan N, More SK, Bane SM, Upadhya A, Ingle AD, Gude RP, Mukhopadhyaya R, Kalraiya RD (2014) Galectin-3 expressed on different lung compartments promotes organ specific metastasis by facilitating arrest, extravasation and organ colonization via high affinity ligands on melanoma cells. Clin Exp Metastasis 31(6):661–673. doi:10.1007/s10585-014-9657-2
7. Krishnan V, Bane SM, Kawle PD, Naresh KN, Kalraiya RD (2005) Altered melanoma cell surface glycosylation mediates organ specific adhesion and metastasis via lectin receptors on the lung vascular endothelium. Clin Exp Metastasis 22(1):11–24. doi:10.1007/s10585-005-2036-2
8. Srinivasan N, Bane SM, Ahire SD, Ingle AD, Kalraiya RD (2009) Poly N-acetyllactosamine substitutions on N- and not O-oligosaccharides or Thomsen-Friedenreich antigen facilitate lung specific metastasis of melanoma cells via galectin-3. Glycoconj J 26(4):445–456. doi:10.1007/s10719-008-9194-9
9. More SK, Srinivasan N, Budnar S, Bane SM, Upadhya A, Thorat RA, Ingle AD, Chiplunkar SV, Kalraiya RD (2015) N-glycans and metastasis in galectin-3 transgenic mice. Biochem Biophys Res Commun 460(2):302–307. doi:10.1016/j.bbrc.2015.03.030
10. Fortuna-Costa A, Gomes AM, Kozlowski EO, Stelling MP, Pavao MS (2014) Extracellular galectin-3 in tumor progression and metastasis. Front Oncol 4:138. doi:10.3389/fonc.2014.00138
11. Lagana A, Goetz JG, Cheung P, Raz A, Dennis JW, Nabi IR (2006) Galectin binding to Mgat5-modified N-glycans regulates fibronectin matrix remodeling in tumor cells. Mol Cell Biol 26(8):3181–3193. doi:10.1128/MCB.26.8.3181-3193.2006
12. Goetz JG, Joshi B, Lajoie P, Strugnell SS, Scudamore T, Kojic LD, Nabi IR (2008) Concerted regulation of focal adhesion dynamics by galectin-3 and tyrosine-phosphorylated caveolin-1. J Cell Biol 180(6):1261–1275. doi:10.1083/jcb.200709019
13. Boscher C, Nabi IR (2013) Galectin-3- and phospho-caveolin-1-dependent outside-in integrin signaling mediates the EGF motogenic response in mammary cancer cells. Mol Biol Cell 24(13):2134–2145. doi:10.1091/mbc.E13-02-0095
14. Saravanan C, Liu FT, Gipson IK, Panjwani N (2009) Galectin-3 promotes lamellipodia formation in epithelial cells by interacting with complex N-glycans on alpha3beta1 integrin. J Cell Sci 122(Pt 20):3684–3693. doi:10.1242/jcs.045674
15. Melo FH, Butera D, Junqueira Mde S, Hsu DK, da Silva AM, Liu FT, Santos MF, Chammas R (2011) The promigratory activity of the matricellular protein galectin-3 depends on the activation of PI-3 kinase. PLoS One 6(12):e29313. doi:10.1371/journal.pone.0029313
16. Jiang K, Rankin CR, Nava P, Sumagin R, Kamekura R, Stowell SR, Feng M, Parkos CA, Nusrat A (2014) Galectin-3 regulates desmoglein-2 and intestinal epithelial intercellular adhesion. J Biol Chem 289(15):10510–10517. doi:10.1074/jbc.M113.538538
17. Boscher C, Zheng YZ, Lakshminarayan R, Johannes L, Dennis JW, Foster LJ, Nabi IR (2012) Galectin-3 protein regulates mobility of N-cadherin and GM1 ganglioside at cell-cell junctions of mammary carcinoma cells. J Biol Chem 287(39):32940–32952. doi:10.1074/jbc.M112.353334
18. Kim SH, Turnbull J, Guimond S (2011) Extracellular matrix and cell signalling: the dynamic cooperation of integrin, proteoglycan and growth factor receptor. J Endocrinol 209(2):139–151. doi:10.1530/JOE-10-0377
19. Lu P, Weaver VM, Werb Z (2012) The extracellular matrix: a dynamic niche in cancer progression. J Cell Biol 196(4):395–406. doi:10.1083/jcb.201102147
20. Humphries JD, Byron A, Humphries MJ (2006) Integrin ligands at a glance. J Cell Sci 119(Pt 19):3901–3903. doi:10.1242/jcs.03098
21. Pankov R, Yamada KM (2002) Fibronectin at a glance. J Cell Sci 115(Pt 20):3861–3863

22. Plow EF, Haas TA, Zhang L, Loftus J, Smith JW (2000) Ligand binding to integrins. J Biol Chem 275(29):21785–21788. doi:10.1074/jbc.R000003200
23. Hynes RO (2002) Integrins: bidirectional, allosteric signaling machines. Cell 110(6):673–687
24. Welch HC, Coadwell WJ, Stephens LR, Hawkins PT (2003) Phosphoinositide 3-kinase-dependent activation of Rac. FEBS Lett 546(1):93–97
25. Xue G, Hemmings BA (2013) PKB/Akt-dependent regulation of cell motility. J Natl Cancer Inst 105(6):393–404. doi:10.1093/jnci/djs648
26. Hood JD, Cheresh DA (2002) Role of integrins in cell invasion and migration. Nat Rev Cancer 2(2):91–100. doi:10.1038/nrc727
27. Huveneers S, Danen EH (2009) Adhesion signaling—crosstalk between integrins, Src and Rho. J Cell Sci 122(Pt 8):1059–1069. doi:10.1242/jcs.039446
28. Ridley A (2000) Rho GTPases. Integrating integrin signaling. J Cell Biol 150(4):F107–F109
29. Harburger DS, Calderwood DA (2009) Integrin signalling at a glance. J Cell Sci 122(Pt 2):159–163. doi:10.1242/jcs.018093
30. Schlaepfer DD, Jones KC, Hunter T (1998) Multiple Grb2-mediated integrin-stimulated signaling pathways to ERK2/mitogen-activated protein kinase: summation of both c-Src- and focal adhesion kinase-initiated tyrosine phosphorylation events. Mol Cell Biol 18(5):2571–2585
31. Schlaepfer DD, Mitra SK (2004) Multiple connections link FAK to cell motility and invasion. Curr Opin Genet Dev 14(1):92–101. doi:10.1016/j.gde.2003.12.002
32. Sieg DJ, Hauck CR, Ilic D, Klingbeil CK, Schaefer E, Damsky CH, Schlaepfer DD (2000) FAK integrates growth-factor and integrin signals to promote cell migration. Nat Cell Biol 2(5):249–256. doi:10.1038/35010517
33. Wells A (2000) Tumor invasion: role of growth factor-induced cell motility. Adv Cancer Res 78:31–101
34. Agarwal AK, Srinivasan N, Godbole R, More SK, Budnar S, Gude RP, Kalraiya RD (2015) Role of tumor cell surface lysosome-associated membrane protein-1 (LAMP1) and its associated carbohydrates in lung metastasis. J Cancer Res Clin Oncol. doi:10.1007/s00432-015-1917-2
35. Pellegrin S, Mellor H (2008) Rho GTPase activation assays. Curr Protoc Cell Biol Chapter 14:Unit 14 8. doi:10.1002/0471143030.cb1408s38
36. Gumbiner BM (1996) Cell adhesion: the molecular basis of tissue architecture and morphogenesis. Cell 84(3):345–357
37. Lauffenburger DA, Horwitz AF (1996) Cell migration: a physically integrated molecular process. Cell 84(3):359–369
38. Pollard TD, Borisy GG (2003) Cellular motility driven by assembly and disassembly of actin filaments. Cell 112(4):453–465
39. Small JV, Rottner K, Kaverina I, Anderson KI (1998) Assembling an actin cytoskeleton for cell attachment and movement. Biochim Biophys Acta 1404(3):271–281
40. Small JV, Stradal T, Vignal E, Rottner K (2002) The lamellipodium: where motility begins. Trends Cell Biol 12(3):112–120
41. Ridley AJ (2001) Rho GTPases and cell migration. J Cell Sci 114(Pt 15):2713–2722
42. Yamada KM, Araki M (2001) Tumor suppressor PTEN: modulator of cell signaling, growth, migration and apoptosis. J Cell Sci 114(Pt 13):2375–2382
43. Bozzuto G, Ruggieri P, Molinari A (2010) Molecular aspects of tumor cell migration and invasion. Annali dell'Istituto superiore di sanita 46(1):66–80. doi:10.4415/ANN_10_01_09
44. Vicente-Manzanares M, Webb DJ, Horwitz AR (2005) Cell migration at a glance. J Cell Sci 118(Pt 21):4917–4919. doi:10.1242/jcs.02662
45. Yamaguchi H, Wyckoff J, Condeelis J (2005) Cell migration in tumors. Curr Opin Cell Biol 17(5):559–564. doi:10.1016/j.ceb.2005.08.002
46. Han S, Khuri FR, Roman J (2006) Fibronectin stimulates non-small cell lung carcinoma cell growth through activation of Akt/mammalian target of rapamycin/S6 kinase and inactivation of LKB1/AMP-activated protein kinase signal pathways. Cancer Res 66(1):315–323. doi:10.1158/0008-5472.CAN-05-2367
47. King WG, Mattaliano MD, Chan TO, Tsichlis PN, Brugge JS (1997) Phosphatidylinositol 3-kinase is required for integrin-stimulated AKT and Raf-1/mitogen-activated protein kinase pathway activation. Mol Cell Biol 17(8):4406–4418
48. Levy Y, Ronen D, Bershadsky AD, Zick Y (2003) Sustained induction of ERK, protein kinase B, and p70 S6 kinase regulates cell spreading and formation of F-actin microspikes upon ligation of integrins by galectin-8, a mammalian lectin. J Biol Chem 278(16):14533–14542. doi:10.1074/jbc.M207380200
49. Hirabayashi J, Hashidate T, Arata Y, Nishi N, Nakamura T, Hirashima M, Urashima T, Oka T, Futai M, Muller WE, Yagi F, Kasai K (2002) Oligosaccharide specificity of galectins: a search by frontal affinity chromatography. Biochim Biophys Acta 1572(2–3):232–254
50. Levy Y, Arbel-Goren R, Hadari YR, Eshhar S, Ronen D, Elhanany E, Geiger B, Zick Y (2001) Galectin-8 functions as a matricellular modulator of cell adhesion. J Biol Chem 276(33):31285–31295. doi:10.1074/jbc.M100340200
51. Przybylo M, Martuszewska D, Pochec E, Hoja-Lukowicz D, Litynska A (2007) Identification of proteins bearing beta1-6 branched N-glycans in human melanoma cell lines from different progression stages by tandem mass spectrometry analysis. Biochim Biophys Acta 1770(9):1427–1435. doi:10.1016/j.bbagen.2007.05.006
52. Marshall CJ (1995) Specificity of receptor tyrosine kinase signaling: transient versus sustained extracellular signal-regulated kinase activation. Cell 80(2):179–185
53. Nobes CD, Hall A (1995) Rho, rac, and cdc42 GTPases regulate the assembly of multimolecular focal complexes associated with actin stress fibers, lamellipodia, and filopodia. Cell 81(1):53–62
54. Kwon T, Kwon DY, Chun J, Kim JH, Kang SS (2000) Akt protein kinase inhibits Rac1-GTP binding through phosphorylation at serine 71 of Rac1. J Biol Chem 275(1):423–428
55. Schwarz J, Proff J, Havemeier A, Ladwein M, Rottner K, Barlag B, Pich A, Tatge H, Just I, Gerhard R (2012) Serine-71 phosphorylation of Rac1 modulates downstream signaling. PLoS One 7(9):e44358. doi:10.1371/journal.pone.0044358
56. Cary LA, Han DC, Polte TR, Hanks SK, Guan JL (1998) Identification of p130Cas as a mediator of focal adhesion kinase-promoted cell migration. J Cell Biol 140(1):211–221
57. Petrie RJ, Doyle AD, Yamada KM (2009) Random versus directionally persistent cell migration. Nat Rev Mol Cell Biol 10(8):538–549. doi:10.1038/nrm2729
58. Ponti A, Machacek M, Gupton SL, Waterman-Storer CM, Danuser G (2004) Two distinct actin networks drive the protrusion of migrating cells. Science 305(5691):1782–1786. doi:10.1126/science.1100533

Biochemical and Biophysical Research Communications 460 (2015) 302–307

Contents lists available at ScienceDirect

Biochemical and Biophysical Research Communications

journal homepage: www.elsevier.com/locate/ybbrc

N-glycans and metastasis in galectin-3 transgenic mice

Shyam K. More [a, 1], Nithya Srinivasan [a, 1], Srikanth Budnar [b], Sanjay M. Bane [a], Archana Upadhya [c], Rahul A. Thorat [a], Arvind D. Ingle [a], Shubhada V. Chiplunkar [a], Rajiv D. Kalraiya [a, *]

[a] Advanced Centre for Treatment Research and Education in Cancer (ACTREC), Tata Memorial Centre, Sector 22, Kharghar, Navi Mumbai 410210, India
[b] Division of Molecular Cell Biology, Institute for Molecular Bioscience, The University of Queensland, St. Lucia, Brisbane, Queensland 4072, Australia
[c] SPP School of Pharmacy & Technology Management, SVKM's NMIMS, Mumbai, India

ARTICLE INFO

Article history:
Received 12 February 2015
Available online 17 March 2015

Keywords:
Galectin-3
Organ specific metastasis
Galectin-3 transgenic mice

ABSTRACT

Poly-N-acetyl-lactosamine (polyLacNAc) on N-glycans facilitate lung specific metastasis of melanoma cells by serving as high affinity ligands for galectin-3, expressed in highest amounts in the lungs, on almost all its tissue compartments including on the surface of vascular endothelium. PolyLacNAc not only aids in initial arrest on the organ endothelium but in all the events of extravasation. Inhibition of polyLacNAc synthesis, or competitive inhibition of its interaction with galectin-3 all inhibited these processes and experimental metastasis. Transgenic galectin-3 mice, viz., gal-$3^{+/+}$ (wild type), gal-$3^{+/-}$ (hemizygous) and gal-$3^{-/-}$ (null) have been used to prove that galectin-3/polyLacNAc interactions are indeed critical for lung specific metastasis.

Gal-$3^{+/-}$ mice which showed <50% expression of galectin-3 on the lungs also showed proportionate decrease in the number of B16F10 melanoma metastatic colonies affirming that galectin-3 and polyLacNAc interactions are indeed key determinants of lung metastasis. However, surprisingly, the number and size of metastatic colonies in gal-$3^{-/-}$ mice was very similar as that seen in gal-$3^{+/+}$ mice. The levels of lactose binding lectins on the lungs and the transcripts of other galectins (galectin-1, -8 and -9) which are expressed on lungs and have similar sugar binding specificities as galectins-3, remain unchanged in gal-$3^{+/+}$ and gal-$3^{-/-}$ mice. Further, inhibition of N-glycosylation with Swainsonine (SW) which drastically reduces metastasis of B16F10 cells in gal-$3^{+/+}$ mice, did not affect lung metastasis when assessed in gal-$3^{-/-}$ mice. Together, these results rule out the possibility of some other galectin taking over the function of galectin-3 in gal-$3^{-/-}$ mice. Chimeric mice generated to assess if absence of any effect on metastasis is due to compromised tumor immunity by replacing bone marrow of gal-$3^{-/-}$ mice with that from gal-$3^{+/+}$ mice, also failed to impact melanoma metastasis. As galectin-3 regulates several immune functions including maturation of different immune cells, compromised tumor immunity could be the major determinant of melanoma metastasis in gal-$3^{-/-}$ mice and warrants thorough investigation.

1. Introduction

Metastasis is the major cause of deaths in cancer patients, yet the underlying molecular mechanisms are poorly understood, possibly, because of complexity and multistep nature of the disease [1]. To successfully metastasize the cancer cells must complete a sequential series of events which include separation from the primary tumor, invasion through surrounding tissues and basement membranes, entry and survival in the circulation and arrest in a distant target organ vasculature, extravasation and adaptation to the new organ growth environment [1–3].

Tumors often metastasize regionally to organs in the anatomic vicinity like those receiving the afferent blood vessel from the primary or the draining lymph nodes. As these organs receive maximum number of cells, some of these cells may get mechanically trapped in the fine vasculature and get adapted to the new organ environment and give rise to metastatic colonies. Colon cancers metastasizing to liver and several tumors colonizing lymph nodes are classical examples of this pattern of metastasis proposed by Ewing Ref. [2]. However, many cancers bypass several

* Corresponding author.
E-mail address: rkalraiya@actrec.gov.in (R.D. Kalraiya).
[1] Indicates that both the author have contributed equally.

http://dx.doi.org/10.1016/j.bbrc.2015.03.030
0006-291X/

organs in their blood flow path and metastasize to very specific distant organ sites. The 'seed and Soil' hypothesis was proposed by Dr. Stephen Paget in 1889 to explain the phenomenon of organ specificity of metastasis based on the autopsy studies of >700 breast cancer patients. He compared the organ microenvironment with soil and tumor cells with seeds and explained that like seeds cancer cells although get dispersed to all the organs, but survive and give rise to metastatic colonies only in the organs that can support their growth [2,4]. Apart from the organ microenvironment, adhesive interactions, chemokines and their receptors have also been shown to be the key participants in organ specific metastasis [2,5,6].

Tumor cells show several cell surface modifications associated with the metastatic phenotype. One of the frequently observed modifications is the altered expression of β1, 6 branched N-oligosaccharides on cell surface glycoproteins. These oligosaccharides have been strongly associated with the invasive and metastatic phenotype of tumor cells [7,8]. The expression of these types of oligosaccharides on human tumors correlated with the disease progression [9–12]. Majority of the cancer cell lines expressing these oligosaccharides metastasize either to lungs or to liver. The E-Selectin expressed on the liver acts as a receptor for β1,6 branched N-oligosaccharides terminally substituted with Lewis antigen on tumor cell surface and facilitate liver metastasis [13–15]. Previously we showed that poly-N-acetyl lactosamine (polyLacNAc) substituted β1,6 branched N-oligosaccharides expressed on B16F10 cells promote lung specific metastasis via galectin-3 which is expressed in highest amounts on the lungs [16,17]. Galectin-3/PolyLacNAc pair not only facilitates initial arrest but also participates in all the subsequent steps of extravasation and organ colonization. Inhibition of polyLacNAc synthesis or competitive inhibition of their interaction has been shown to inhibit all these processes and metastasis. Galectin-3 transgenic mice used to confirm their participation in the metastatic process has thrown some very intriguing but interesting results, further pointing towards the complexity of the entire process.

2. Materials and methods

2.1. All the reagents used in this study are described in supplementary method 1

2.1.1. Cell culture and experimental metastasis assay

B16F10 murine melanoma cell line was obtained from National Centre for Cell Sciences, Pune, India. Melanoma cells were routinely cultured in Dulbecco's Modified Eagle's medium (DMEM), with or without glycosylation inhibitor SW (2 μg/ml) and metastasis assays were performed as described in Ref. [17].

2.1.2. Genotyping of galectin-3 transgenic mice by PCR

Propagation of transgenic mice is described in supplementary method 2. Galectin-3 status of the littermates was determined by PCR using genomic DNA obtained from the tails of the 3–4 week mice. PCR was performed using 1 μg genomic DNA and primers: PRIMER 1 (a primer annealing to the neo cassette region) 5′GGCTGACCGCTTCCTCGTGCTTTACGG3′, PRIMER 2 (a primer annealing to the non -disrupted region of intron 4 of intact galectin-3 gene) 5′GTAGGTGAGAGTCACAAGCTG GAGGCC3′ and PRIMER 3 (a common downstream primer annealing to EXON 5) 5′CACTCTCAAAGGGGAAGGCTGACTGTC3'. PCR was carried out and the product was analyzed on 2% agarose gel by electrophoresis followed by ethidium bromide staining. Gal-$3^{+/+}$ mice give an amplicon of 450 bp, gal-$3^{+/-}$ mice give 2 amplicons of 450 bp and 300 bp while gal-$3^{-/-}$ mice give an amplicon of 300 bp [18].

2.1.3. Preparation of total cell lysates and Western blotting

Preparation of total cell lysates and analysis of Western blotted proteins was done exactly as described in Ref. [16].

2.1.4. Detection of galectin-3 expression in mouse lungs by western blotting

Lungs of 6–8 week old mice of gal-$3^{+/+}$, gal-$3^{+/-}$ and gal-$3^{-/-}$ group were excised and subsequently homogenized in 1× Laemmli's Sample buffer, Western blotted and probed with rat anti mouse galectin-3 antibody as a probe.

2.1.5. Flow cytometric analysis

For flow cytometry, melanoma cells were first fixed by overnight incubation with 1.5% gluteraldehyde in PBS (pH 7.4). Analysis of surface expression of polyLacNAc on melanoma cells was performed using biotinylated L-PHA exactly as described in Ref. [17].

2.1.6. Real time PCR

Total RNA from the lungs of gal-$3^{+/+}$, gal-$3^{+/-}$ and gal-$3^{-/-}$ transgenic mice was extracted using TRIzol reagent and the cDNA synthesized and used as a template for real time PCR. The primer pair sequences of galectin-1, galectin-8, galectin-9 and RPL4 were obtained from Ref. [19]. Real time PCR was performed as described in Ref. [20].

2.1.7. Generation of chimeric mice

Chimeric mice were generated exactly as described by Mace et al. [21]. Briefly, the bone marrow in irradiated gal-$3^{-/-}$ mice was replaced, in group 1 with that from gal-$3^{-/-}$ mice which served as control, while in group 2 with that from gal-$3^{+/+}$ mice. Chimerism was confirmed by genotyping of these mice using tail and blood genomic DNA by PCR as described by Hsu et al. [18].

2.1.8. Statistical analysis

All data are represented as mean ± SE unless stated. Student's t-test was employed for calculating significance across different groups. (p value < 0.05 was considered significant).

3. Results

3.1. Characterization of gal-$3^{+/+}$, gal-$3^{+/-}$ and gal-$3^{-/-}$ transgenic mice

Galectin-3 transgenic mice were characterized using tail genomic DNA as the template for PCR. The amplicon size for gal-$3^{+/+}$ and gal-$3^{-/-}$ mice was 450 bp and 300 bp, respectively. However, the two amplicons 450 bp and 300 bp were obtained for gal-$3^{+/-}$ mice (Fig. 1A). These results indicate that the mice were successfully propagated and maintained.

3.2. Comparison of the levels of expression of galectin-3 in galectin-3 transgenic mice

Tissue extracts of lungs of transgenic mice was analyzed by Western blotting for the presence of galectin-3. As expected, the gal-$3^{+/+}$ mice show the expression of galectin-3 while there is absence of galectin-3 in gal-$3^{-/-}$ mice. Since the gal-$3^{+/-}$ mice have one mutated allele, show >50% reduction in the expression of galectin-3 as compared to that of gal-$3^{+/+}$ mice (Fig. 1B).

3.3. Expression of galectin-3 in lungs dictates the extent of metastasis of melanoma cells

Experimental metastasis assay using B16F10 cells in gal-$3^{+/+}$ and gal-$3^{+/-}$ mice showed that the levels of galectin-3 expression

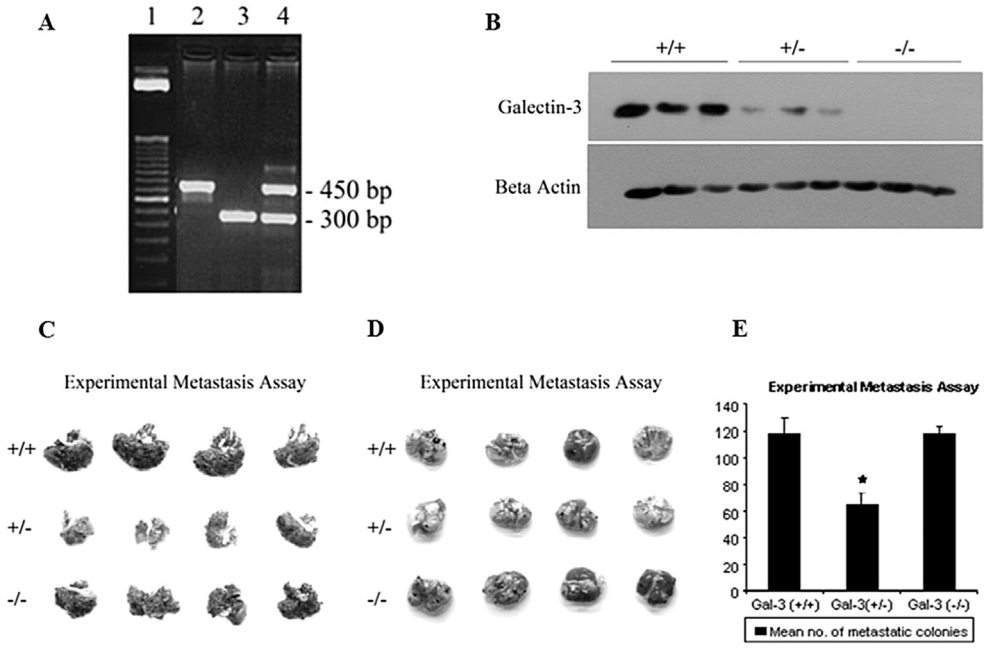

Fig. 1. Expression of galectin-3 in the lungs dictates the metastatic potential of B16F10 cells. (A) Assessment of galectin-3 status of mouse using PCR and utilizing genomic DNA as template and primers specific for galectin-3. Lane 1 represents 50 bp DNA ladder. Lane 2–4 represent PCR products using DNA from gal-$3^{+/+}$, gal-$3^{-/-}$ and gal-$3^{+/-}$ mice respectively. (B) Western blotting of 100 μg of lung lysates from gal-$3^{+/+}$, gal-$3^{+/-}$ and gal-$3^{-/-}$ mice using anti-galectin-3 antibody. Beta actin served as loading control. (C and D) Comparison of melanoma colonies in lungs of gal-$3^{+/+}$ (lane1), gal-$3^{+/-}$ (lane 2) and gal-$3^{-/-}$ (lane 3) mice, after injection with 0.18 million (C) and 0.075 million (D) B16F10 cells under experimental metastasis assay conditions. (E) Graphical representation of mean values of number of lung colonies of the three groups of mice under experimental metastasis assay conditions. Significance obtained by performing student's T-test is denoted by *, p value <0.05.

indeed dictates the metastatic outcome. Gal-$3^{+/-}$ mice which express significantly lower levels of galectin-3 in the lungs as compared to gal-$3^{+/+}$ mice, also showed corresponding decrease in lung metastasis. However, the gal-$3^{-/-}$ mice which show no galectin-3 on the lungs surprisingly showed same level of lung metastatic colonies as gal-$3^{+/+}$ mice. This pattern was always consistent even when tested by injecting different cell numbers (Fig. 1C and D).

Galectin-3 being a member of a large family of lectins the possibility of some other galectins taking over the role of galectin-3 was investigated.

3.4. Comparison of the expression of transcripts of galectin-1, -8 and -9 and lactose binding lectins in the lungs of transgenic mice

Galectin-1, -8 and -9 have similar carbohydrate binding specificities as galectin-3 and have also been shown to be expressed on the lungs [22]. In the absence of galectin-3 it is possible that one of these members takes over its function and thus may be overexpressed on the lungs. However, analysis of the transcript levels of these galectins showed insignificant difference between gal-$3^{+/+}$, gal-$3^{+/-}$ and gal-$3^{-/-}$ mice as assessed by real time PCR (Table 1).

Further, comparison of the total lactose binding lectins from the lungs of gal-$3^{+/+}$ and gal-$3^{-/-}$ mice were very similar except for the presence of galectin-3 in the fraction from lungs of gal-$3^{+/+}$ mice (Data not shown). These results appear to indicate that no other member of galectin family takes over the function of galectin-3 in facilitating metastasis. This raised the possibility that the metastasis in these mice may be due to some other mechanism and may not involve lectin-carbohydrate interaction. In such a scenario inhibition of N-oligosaccharides may not inhibit metastasis.

Table 1
Transcript levels of different galectin members in lungs of galectin-3 transgenic mice as compared to that in gal-$3^{+/+}$ mice.

Galectin-3 status in mice	Galectin-1	Galectin-8	Galectin-9
Gal-$3^{+/-}$ mice	1.5 fold increase	1.16 fold increase	1.05 fold increase
Gal-$3^{-/-}$ mice	1.244 fold increase	1.18 fold increase	1.04 fold increase

3.5. Inhibition of N-oligosaccharides on B16F10 melanoma cells does not impact metastasis when assayed in gal-$3^{-/-}$ mice

Inhibition of addition of polyLacNAc either by inhibiting synthesis of N-oligosaccharides using SW or using shRNA for enzymes that synthesize polyLacNAc, results in the loss of metastasis of B16F10 cells in gal-$3^{+/+}$ type C57BL/6 mice. However, inhibition of N-oligosaccharides using SW had no effect on experimental metastasis when assessed in gal-$3^{-/-}$ mice (Fig. 2A). The inhibition of expression of β1,6 branched N-oligosaccharides in SW treated B16F10 cells was confirmed using lectin blotting and flow cytometry using L-PHA as the probe (Fig. 2B and C). These results suggest that in absence of galectin-3 in mice, even carbohydrates on cancer cells become redundant for cancer cell metastasis. Galectin-3 is an important protein that is present in majority of the cells of immune system and performs a variety of regulatory functions. Complete absence of galecetin-3 possibly compromises the anti-tumor immunity and thus increased lung metastasis in gal-$3^{-/-}$ mice.

3.6. Generation of chimeric mice by replacing bone marrow of gal-$3^{-/-}$ mice with that of gal-$3^{+/+}$ mice does not impact metastasis of B16F10 cells

To test if absence of galectin-3 in some way alters the tumor immunity and thus metastatic outcome of cells in gal-$3^{-/-}$ mice,

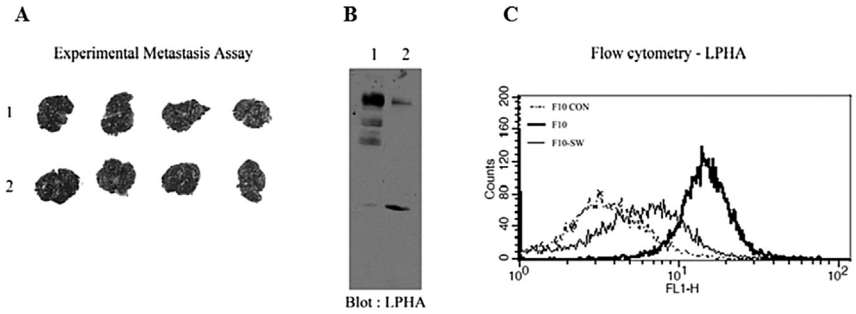

Fig. 2. Inhibition of N-oligosaccharides has no effect on the metastatic potential of melanoma cells in gal-3$^{-/-}$ mice. (A) Comparison of melanoma colonies in lungs of gal-3$^{-/-}$ mice after injecting 0.15 million (1) untreated and (2) Swainsonine treated B16F10 cells, under experimental metastasis assay conditions. The inhibition of N-oligosaccharides by SW was confirmed by (B) Western blotting and (C) flow cytometry using biotin labeled L-PHA. B16F10 cells treated only with avidin FITC served as control (B16F10 CON).

chimeric mice were generated. Replacement of bone marrow of gal-3$^{-/-}$ mice with that from gal-3$^{+/+}$ mice was confirmed by analyzing the tail and blood genomic DNA as a template for PCR. The bands at 300 bp in both the groups obtained with the tail genomic DNA confirmed their gal-3$^{-/-}$ phenotype (Fig. 3A). Further, the appearance of only 300 bp band in group 1 and bands of both 300 and 450 bp obtained with blood genomic DNA in group 2 confirms gal-3$^{-/-}$ phenotype in group 1 and successful chimerism in group 2 (Fig. 3B). However, generation of chimeric mice had no effect on the metastatic outcome of B16F10 cells in the lungs (Fig. 3C).

4. Discussion

Previous work in the lab very clearly demonstrated the role of high affinity ligands in the form of polyLacNAc on N-glycans on melanoma cells in mediating lung metastasis. By demonstrating the presence of galectin-3 in highest amounts on lungs and its constitutive expression on vascular endothelium and by using dominant negative and competitive inhibitors, galectin-3 was shown to be the potential polyLacNAc receptor that mediates metastasis on the lungs [16,20]. To prove that the galectin-3/polyLacNAc interaction is indeed indispensable for lung metastasis galectin-3 transgenic mice were used.

The three subpopulations of galectin-3 transgenic mice successfully genotyped and characterized provide an important tool to investigate the role of galectin-3 in metastatic process (Fig. 1A and B). The gal-3$^{+/-}$ mice in which the expression of galectin-3 was <50% as compared to gal-3$^{+/+}$, also showed correspondingly reduced lung metastasis, indicating that galectin-3 on the lungs is indeed an important determinant of metastatic outcome. Surprisingly, however, the gal-3$^{-/-}$ mice which lacked galectin-3 on the lungs showed almost similar extent of metastasis as the gal-3$^{+/+}$ mice (Fig. 1C and D).

Galectins are a family of β-galactoside binding lectins which often exhibit functional redundancy. Besides galectin-3, other members including galectin-1, -8 and -9 have been shown to be expressed on the lungs and have very similar oligosaccharide specificity [22]. However, analysis of the transcripts of these galectins (Table 1), or comparison of the lactose binding proteins (data not shown) in the lungs from gal-3$^{+/+}$ and gal-3$^{-/-}$ mice did not show any significant difference. Although, the results do not completely rule out the possibility of some other galectin taking over the function of galectin-3, it weakens this possibility. An alternative approach was devised to test this. While inhibition of N-oligosaccharides significantly inhibits metastasis of B16F10 cells in gal-3$^{+/+}$ mice, their inhibition should also inhibit metastasis in the gal-3$^{-/-}$ mice, in case other galectins take over galectin-3 function. However, SW treatment failed to have any effect on the metastatic properties of these cells in gal-3$^{-/-}$ mice (Fig. 2), pointing towards an alternate mechanism.

Almost a million tumor cells are believed to be in circulation in a patient diagnosed with cancer; however, only a few of them metastasize. Experimentally it has been shown that, although, > 95% of the B16F10 cells injected via tail vein can be recovered from the lungs of mice within 2 min of injection, majority of them are cleared by 24 h. Only about 2% of the injected cells remain in the lungs by 24 h [23]. Even of these 2% arrested cells, only those that are able to interact with the host organ environment are possibly able to survive and grow as 100-150 metastatic colonies. Interactions between molecules like polyLacNAc on cancer cells and galectin-3 on the organs like lungs would assume importance at this stage. However, host immune competence would play a key

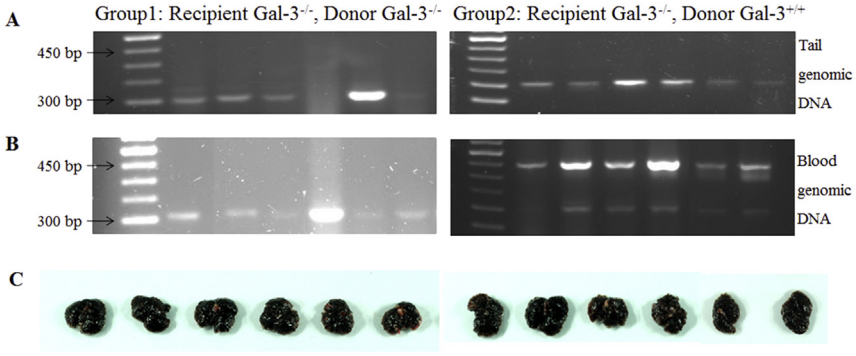

Fig. 3. Experimental metastasis assay using chimeric mice. (A) Agarose gel image showing PCR amplification band at 300 bp using tail genomic DNA. (B) Agarose gel image showing the PCR amplification band at 300 bp and 450 bp using blood genomic DNA as a template. (C) Represents the lung images taken after experimental metastasis assay.

role in clearing majority of the cells from the target organ. Agents which augment NK cell activity in mice have indeed been shown to be very efficient in inhibiting metastasis, which was ineffective in beige mice which lack NK cells or in mice where NK cells were depleted [23]. Are gal-3$^{-/-}$ mice not competent enough immunologically?

Galectin-3 plays an important role in regulating different functions of innate and adaptive immune systems [24–27]. Almost all types of immune cells express galectin-3 [24]. As galectin-3 is present in the nucleus, cytoplasm and on the cells surface and as part of Extracellular matrix ((ECM), its function varies depending on its subcellular localization. Galectin-3 in the cytoplasm is anti-apoptotic while nuclear galectin-3 is pro-apoptotic whereas that on the cell surface or on ECM/Basement membrane (BM) performs very different functions [28–30]. As a result galectin-3 influences immune response in a variety of ways which are often conflicting.

Galectin-3 influences innate immunity by modulating adhesion and migration of monocytes, macrophages and dendritic cells. It promotes adhesion of neutrophils to laminin and regulates neutrophil traversing through BM at sites of inflammation. Galectin-3 also, regulates T-cell signaling, activation, cytokine secretion, apoptosis and regulatory T-cell proliferation. Galectin-3 deficiency results in increased frequency of immune suppressor cells such as CD4^{+}CD25^{+}FOXP3^{+}T$_{reg}$ cells [24,25,27]. In contrast, galectin-3 induces apoptosis in CD8^{+}T cells in mouse model of colorectal cancer [27]. Although, gal-3$^{-/-}$ mice are viable, they have a distinct phenotype in terms of their immune functions related to autoimmunity, and responses to allergy, inflammation and infectious diseases. However, a unified picture of galectin-3 mediated effects on host immunity and thus metastasis is yet to emerge clearly. It is very likely that the gal-3$^{-/-}$ mice are defective in their critical immune function which may positively or negatively influence metastatic outcome.

In such a scenario, analogous to the beige mice which lack NK cell activity, the gal-3$^{-/-}$ mice would also have much higher burden of mechanically arrested melanoma cells in the lungs. If they are not cleared efficiently, some of these possibly give rise to metastatic colonies, especially because the high metastatic B16F10 cells have been selected specifically for lung colonization by serial in vitro and in vivo passaging of B16F1 cells. Some of these would be able to adapt to the growth environment of the lungs even in absence of polyLacNAc and galectin-3. This would be very similar to what is proposed for anatomical/mechanical mode of metastatic spread. However, a recent report on experiments with B16F1 cells using gal-3$^{+/+}$ and gal-3$^{-/-}$ mice has suggested that the gal-3$^{-/-}$ mice may be more competent in terms of their anti-tumor immunity as compared to gal-3$^{+/+}$ mice via their enhanced NK-cell activity [31]. In contrast to these, our preliminary experiments with B16F1 cells in these mice did not give statistically significant variation in the number of metastatic colonies, mainly because the total number of metastatic colonies of B16F1 cells in the lungs as such, was very low.

Generating chimeric mice by replacing the bone marrow of gal-3$^{-/-}$ mice with that of gal-3$^{+/+}$ mice may possibly restore immunity and thus should inhibit metastasis. Although, chimeric mice could be successfully generated, metastasis of B16F10 cells in the lungs could not be inhibited in these mice (Fig. 3). Galectin-3 also appears to be required for maturation of several immune cells like the maturation of plasma cells into memory B cells and the selection of CD4^{+}T and CD8^{+}T cells in the thymus [32]. These results suggest that in the absence of galectin-3, even after replacing the bone marrow, the gal-3$^{-/-}$ mice may not achieve an effective anti-tumor immunity.

In conclusion, by employing gal-3$^{+/+}$ and gal-3$^{+/-}$ transgenic mice and lung homing high metastatic B16F10 cells, the present investigation very clearly demonstrates that specific interactions between molecules on the tumor cells and on the target organ indeed play an important role in facilitating organ specific metastasis. By utilizing gal-3$^{-/-}$ mice, it also demonstrates the importance of host immunity in controlling metastasis and the complex manner in which it is regulated. This warrants a thorough investigation.

Conflict of interest

None.

Acknowledgments

We thank Prof. Fu Tong Liu (University of California at Davis, USA) for galectin-3 knock out mice via Consortium for Functional Glycomics, USA and National Centre for Cell Science, Pune for the melanoma cell lines. We acknowledge the technical help from Mr. Chavan and breeding of transgenic animals from Mr. Thackerey. We acknowledge the financial assistance received from Department of Bio-Technology, Government of India and Senior Research Fellowship to Mr. Shyam More and Ms. Nithya Srinivasan from Council for Scientific and Industrial Research, Government of India.

Appendix A. Supplementary data

Supplementary data related to this article can be found at http://dx.doi.org/10.1016/j.bbrc.2015.03.030.

Transparency document

Transparency document related to this article can be found online at http://dx.doi.org/10.1016/j.bbrc.2015.03.030.

References

[1] G.P. Gupta, J. Massague, Cancer metastasis: building a framework, Cell 127 (2006) 679–695.
[2] I.J. Fidler, The pathogenesis of cancer metastasis: the 'seed and soil' hypothesis revisited, Nat. Rev. Cancer 3 (2003) 453–458.
[3] P.S. Steeg, Tumor metastasis: mechanistic insights and clinical challenges, Nat. Med. 12 (2006) 895–904.
[4] S. Paget, The distribution of secondary growths in cancer of the breast. 1889, Cancer Metastasis Rev. 8 (1989) 98–101.
[5] A. Ben-Baruch, Organ selectivity in metastasis: regulation by chemokines and their receptors, Clin. Exp. Metastasis 25 (2008) 345–356.
[6] A.F. Chambers, A.C. Groom, I.C. MacDonald, Dissemination and growth of cancer cells in metastatic sites, Nat. Rev. Cancer 2 (2002) 563–572.
[7] R.D. Cummings, S. Kornfeld, Characterization of the structural determinants required for the high affinity interaction of asparagine-linked oligosaccharides with immobilized Phaseolus vulgaris leukoagglutinating and erythroagglutinating lectins, J. Biol. Chem. 257 (1982) 11230–11234.
[8] R.D. Cummings, I.S. Trowbridge, S. Kornfeld, A mouse lymphoma cell line resistant to the leukoagglutinating lectin from Phaseolus vulgaris is deficient in UDP-GlcNAc: alpha-D-mannoside beta 1,6 N-acetylglucosaminyltransferase, J. Biol. Chem. 257 (1982) 13421–13427.
[9] J.W. Dennis, M. Granovsky, C.E. Warren, Glycoprotein glycosylation and cancer progression, Biochim. Biophys. Acta 1473 (1999) 21–34.
[10] B. Fernandes, U. Sagman, M. Auger, M. Demetrio, J.W. Dennis, Beta 1-6 branched oligosaccharides as a marker of tumor progression in human breast and colon neoplasia, Cancer Res. 51 (1991) 718–723.
[11] R. Takano, M. Nose, T. Nishihira, M. Kyogoku, Increase of beta 1-6-branched oligosaccharides in human esophageal carcinomas invasive against surrounding tissue in vivo and in vitro, Am. J. Pathol. 137 (1990) 1007–1011.
[12] H. Yamamoto, J. Swoger, S. Greene, T. Saito, J. Hurh, C. Sweeley, J. Leestma, E. Mkrdichian, L. Cerullo, A. Nishikawa, Y. Ihara, N. Taniguchi, J.R. Moskal, Beta1,6-N-acetylglucosamine-bearing N-glycans in human gliomas: implications for a role in regulating invasivity, Cancer Res. 60 (2000) 134–142.
[13] L. Biancone, M. Araki, K. Araki, P. Vassalli, I. Stamenkovic, Redirection of tumor metastasis by expression of E-selectin in vivo, J. Exp. Med. 183 (1996) 581–587.
[14] B.W. Weston, K.M. Hiller, J.P. Mayben, G.A. Manousos, K.M. Bendt, R. Liu, J.C. Cusack Jr., Expression of human alpha(1,3)fucosyltransferase antisense sequences inhibits selectin-mediated adhesion and liver metastasis of colon carcinoma cells, Cancer Res. 59 (1999) 2127–2135.

[15] N. Yamada, Y.S. Chung, S. Takatsuka, Y. Arimoto, T. Sawada, T. Dohi, M. Sowa, Increased sialyl Lewis A expression and fucosyltransferase activity with acquisition of a high metastatic capacity in a colon cancer cell line, Br. J. Cancer 76 (1997) 582–587.
[16] V. Krishnan, S.M. Bane, P.D. Kawle, K.N. Naresh, R.D. Kalraiya, Altered melanoma cell surface glycosylation mediates organ specific adhesion and metastasis via lectin receptors on the lung vascular endothelium, Clin. Exp. Metastasis 22 (2005) 11–24.
[17] N. Srinivasan, S.M. Bane, S.D. Ahire, A.D. Ingle, R.D. Kalraiya, Poly N-acetyllactosamine substitutions on N- and not O-oligosaccharides or Thomsen-Friedenreich antigen facilitate lung specific metastasis of melanoma cells via galectin-3, Glycoconj. J. 26 (2009) 445–456.
[18] D.K. Hsu, R.Y. Yang, Z. Pan, L. Yu, D.R. Salomon, W.P. Fung-Leung, F.T. Liu, Targeted disruption of the galectin-3 gene results in attenuated peritoneal inflammatory responses, Am. J. Pathol. 156 (2000) 1073–1083.
[19] H.B. Guo, A. Nairn, K. Harris, M. Randolph, G. Alvarez-Manilla, K. Moremen, M. Pierce, Loss of expression of N-acetylglucosaminyltransferase Va results in altered gene expression of glycosyltransferases and galectins, FEBS Lett. 582 (2008) 527–535.
[20] M.C. Dange, N. Srinivasan, S.K. More, S.M. Bane, A. Upadhya, A.D. Ingle, R.P. Gude, R. Mukhopadhyaya, R.D. Kalraiya, Galectin-3 expressed on different lung compartments promotes organ specific metastasis by facilitating arrest, extravasation and organ colonization via high affinity ligands on melanoma cells, Clin. Exp. Metastasis 31 (2014) 661–673.
[21] K.A. Mace, T.E. Restivo, J.L. Rinn, A.C. Paquet, H.Y. Chang, D.M. Young, N.J. Boudreau, HOXA3 modulates injury-induced mobilization and recruitment of bone marrow-derived cells, Stem Cells 27 (2009) 1654–1665.
[22] J. Hirabayashi, T. Hashidate, Y. Arata, N. Nishi, T. Nakamura, M. Hirashima, T. Urashima, T. Oka, M. Futai, W.E. Muller, F. Yagi, K. Kasai, Oligosaccharide specificity of galectins: a search by frontal affinity chromatography, Biochim. Biophys. Acta 1572 (2002) 232–254.
[23] M.J. Humphries, K. Matsumoto, S.L. White, R.J. Molyneux, K. Olden, Augmentation of murine natural killer cell activity by swainsonine, a new antimetastatic immunomodulator, Cancer Res. 48 (1988) 1410–1415.
[24] H.Y. Chen, F.T. Liu, R.Y. Yang, Roles of galectin-3 in immune responses, Arch. Immunol. Ther. Exp. Warsz. 53 (2005) 497–504.
[25] A. Dhirapong, A. Lleo, P. Leung, M.E. Gershwin, F.T. Liu, The immunological potential of galectin-1 and -3, Autoimmun. Rev. 8 (2009) 360–363.
[26] G.A. Rabinovich, L.G. Baum, N. Tinari, R. Paganelli, C. Natoli, F.T. Liu, S. Iacobelli, Galectins and their ligands: amplifiers, silencers or tuners of the inflammatory response? Trends Immunol. 23 (2002) 313–320.
[27] G.A. Rabinovich, M.A. Toscano, Turning 'sweet' on immunity: galectin-glycan interactions in immune tolerance and inflammation, Nat. Rev. Immunol. 9 (2009) 338–352.
[28] S. Califice, V. Castronovo, F. Van Den Brule, Galectin-3 and cancer (Review), Int. J. Oncol. 25 (2004) 983–992.
[29] J. Dumic, S. Dabelic, M. Flogel, Galectin-3: an open-ended story, Biochim. Biophys. Acta 1760 (2006) 616–635.
[30] A. Fortuna-Costa, A.M. Gomes, E.O. Kozlowski, M.P. Stelling, M.S. Pavao, Extracellular galectin-3 in tumor progression and metastasis, Front. Oncol. 4 (2014) 138.
[31] G. Radosavljevic, I. Jovanovic, I. Majstorovic, M. Mitrovic, V.J. Lisnic, N. Arsenijevic, S. Jonjic, M.L. Lukic, Deletion of galectin-3 in the host attenuates metastasis of murine melanoma by modulating tumor adhesion and NK cell activity, Clin. Exp. Metastasis 28 (2011) 451–462.
[32] B.N. Stillman, D.K. Hsu, M. Pang, C.F. Brewer, P. Johnson, F.T. Liu, L.G. Baum, Galectin-3 and galectin-1 bind distinct cell surface glycoprotein receptors to induce T cell death, J. Immunol. 176 (2006) 778–789.

Clin Exp Metastasis
DOI 10.1007/s10585-014-9657-2

RESEARCH PAPER

Galectin-3 expressed on different lung compartments promotes organ specific metastasis by facilitating arrest, extravasation and organ colonization via high affinity ligands on melanoma cells

Manohar C. Dange · Nithya Srinivasan · Shyam K. More · Sanjay M. Bane · Archana Upadhya · Arvind D. Ingle · Rajiv P. Gude · Rabindranath Mukhopadhyaya · Rajiv D. Kalraiya

Received: 21 November 2013 / Accepted: 14 May 2014

Abstract Interactions between molecules on the surface of tumor cells and those on the target organ endothelium play an important role in their arrest in an organ. Galectin-3 on the lung endothelium and high affinity ligands poly-*N*-acetyllactosamine (polyLacNAc) on N-oligosaccharides on melanoma cells facilitate such interactions. However, to extravasate and colonize an organ the cells must stabilize these interactions by spreading to retract endothelium, degrade exposed basement membrane (BM) and move into parenchyma and proliferate. Here, we show that galectin-3 is expressed on all the major compartments of the lungs and participates in not just promoting adhesion but also in spreading. We for the first time demonstrate that both soluble and immobilized galectin-3 induce secretion of MMP-9 required to breach vascular BM. Further, we show that immobilized galectin-3 is used as traction for the movement of cells. Downregulation of galactosyltransferases-I and -V resulted in significant loss in expression of polyLacNAc and thus reduced binding of galectin-3. This was accompanied with a loss in adhesion, spreading, MMP-9 secretion and motility of the cells on galectin-3 and thus their metastasis to lungs. Metastasis could also be inhibited by blocking surface polyLacNAc by pre-incubating cells with truncated galectin-3 (which lacked oligomerization domain) or by feeding mice with modified citrus pectin in drinking water. Overall, these results unequivocally show that polyLacNAc on melanoma cells and galectin-3 on the lungs play a critical role in arrest and extravasation of cells in the lungs and strategies that target these interactions inhibit lung metastasis.

Keywords Organ specific metastasis · Lungs · Galectin-3 · Extravasation · Poly-*N*-acetyllactosamine · β1,6 branched N-oligosaccharides

Introduction

In spite of being the major cause of mortality in cancer patients; the underlying molecular mechanisms of metastasis are still poorly understood possibly due to the complexity of this multistep process [1]. To metastasize, tumor cells must break free from the primary site, create space for their movement, get into and survive in circulation [2]. Once in circulation, they are able to reach almost all organ sites. However, some metastasize in the anatomic vicinity, while others bypass several organs and colonize very specific organ sites [3]. The patterns of circulation and mechanical factors appear to dictate the regional spread [4]. However, organ specific metastasis is believed to be facilitated by specific interactions between the molecules on the tumor cells and the target organ, growth environment and chemotactic factors released from the target organ [3, 5–7].

Manohar C. Dange, Nithya Srinivasan have contributed equally to this work

Electronic supplementary material The online version of this article (doi:10.1007/s10585-014-9657-2) contains supplementary material, which is available to authorized users.

M. C. Dange · N. Srinivasan · S. K. More · S. M. Bane · A. D. Ingle · R. P. Gude · R. Mukhopadhyaya · R. D. Kalraiya (✉)
Kalraiya Lab, KS 131, Advanced Centre for Treatment Research and Education in Cancer (ACTREC), Tata Memorial Centre, Sector 22, Kharghar, Navi Mumbai 410210, India
e-mail: rkalraiya@actrec.gov.in

A. Upadhya
Shobhaben Pratapbhai Patel School of Pharmacy & Technology Management, SVKM's NMIMS, Mumbai, India

Published online: 21 June 2014

Vascular endothelium is the first barrier that a tumor cell must overcome to colonize an organ. Organ endothelium also provides specific receptors/ligands for organ specific homing of cancer cells [8, 9]. Extravasation of leucocytes at the inflamed site has provided useful clues to the overall process of extravasation which involves rolling, adhesion and extravasation [10]. Selectins and their ligands promote rolling and retard the movement of leucocytes. Firm endothelial adhesion is facilitated by activated integrins and their counter receptors. This is followed by diapedesis which involves endothelial retraction, degradation of vascular basement membrane (BM) and movement into organ parenchyma [10, 11].

Tumor cells are also believed to utilize similar mechanisms for extravasation and each of these steps could be rate limiting [12, 13]. The vascular endothelium has been shown to express specific set of surface molecules on different organs [14]. Tumors reportedly adhere preferentially to the endothelial cells or the 'outside out' endothelial cell membrane vesicles, derived from their metastatic site [15]. VE-cadherin, integrins, Ig class of cell adhesion molecules, selectins, carbohydrates and their lectin receptors are among the major class of molecules on the endothelial cells and on the cancer cells, which are believed to aid adhesion of cancer cells to the target organ [7, 16–19]. Constitutive expression of E-selectin on vessels of the bones or on inflamed organ endothelium has been shown to facilitate organ homing of cells expressing specific E-selectin ligands [10, 20].

However, the participation of E-selectins and its ligand in promoting metastasis in the lungs appears remote. Extravasation occurs predominantly in the micro-vascular capillaries in pulmonary circulation, which are too small to allow rolling [21, 22]. Lung colonizing cancer cells have been shown to get redirected to liver upon forced expression of ligands for E-selectin on hepatic cells [23]. Other receptors/ligands implicated in lung specific interactions include dipeptidyl peptidase IV (DPP-IV), Lu-ECAM1, VCAM-1, CLCA2 on the lung endothelium and their counter receptors like fibronectin; CXCR4, β4 integrin on tumor cells [24–26]. Galectin-3 on the organ endothelium has also been implicated in promoting organ homing [27, 28]. It is a nucleo-cytoplasmic β-galactoside specific lectin that gets secreted out in a non classical manner and gets incorporated onto the cell surface and as part of the matrix and BM [29]. In mice, lungs were shown to express highest amounts of galectin-3 and express it constitutively on its vascular endothelium [27]. Several reports implicate T/Tn antigens on tumor cells in mediating both homophilic interactions and heterophilic interactions with endothelial cells via galectin-3 [19, 30, 31]. Apart from these interactions, galectin-3 in the host may also facilitate melanoma metastasis by modulating immune response, in particular innate antitumor immunity [32, 33].

Using low and high metastatic variants of B16 melanoma cells, previous work by our group has shown that polyLacNAc substituted β1,6 branched N-oligosaccharides on cancer cells may serve as very high affinity, easily accessible form of ligands for galectin-3 [27, 28]. Galectin-3 shows >200-fold higher affinity towards polyLacNAc as compared to T/Tn antigens [34]. Galectin-3 on the lung microvascular endothelium appeared to promote lung metastasis by serving as an anchor to arrest circulating tumor cells carrying polyLacNAc substituted β1,6 branched N-oligosaccharides [27, 28]. Under flow conditions galectin-3 has been shown to bind to the glycoproteins carrying its ligands with high affinity as compared to the selectins to their ligands (Kd of 1 vs. 100–300 μM for selectins and is comparable to the interactions mediated by integrins) [35, 36]. However, just adhesion to vascular endothelium is not enough to establish metastatic foci.

The tumor cells need to displace endothelium, interact with and degrade the exposed vascular BM, move into organ parenchyma and proliferate within for effective metastasis [5, 7]. This was elegantly demonstrated by monitoring adhesive interactions with organ microvasculature and invasion by intra-vital microscopy of colon cancer cell lines differing in their metastatic potential. Although, adhesion occurred in micro-vasculatures of metastatic target organ only, their migration into organ parenchyma correlated with metastatic potential [12].

In the present communication, we demonstrate that galectin-3 present on all the major compartment of the lungs participates not just in promoting adhesion to vascular endothelium but also in all the subsequent events of extravasation. Further, we show that polyLacNAc substituted N- and not O-oligosaccharides participate in all these processes. Inhibition of expression of polyLacNAc or competitive inhibition of their interaction with the host galectin-3 both inhibited all these processes and thus metastasis.

Materials and methods

Reagents

TRIzol and Superscript TM amplification system for RT-PCR and Calcein AM were from Invitrogen, USA. Anti-mouse galectin-3 rat antibody was from R&D Biosystems, USA, and anti-Rat HRPO, anti-Goat HRPO from Santa Cruz Biotechnology, USA. *E. coli* BL 21 with pET3C plasmid containing a full-length human galectin-3 was a kind gift from Prof. Hakon Leffler, Lund University, Sweden. Biotinylated lectin *Lycopersicon esculentum* lectin (LEA), avidin–peroxidase, and streptavidin–FITC, were either from Sigma Chemical Company, USA or Vector

Labs, USA. Power SYBR Green PCR Master Mix was from Applied Biosystems. Anti-MMP-9 antibody, Primers for RT-PCR, Primers for real time PCR and for shRNA amplification, Phalloidin TRITC, Phalloidin FITC, DAPI, Pectin from citrus peel, Polybrene were purchased from Sigma Chemical Company. Dulbecco modified essential medium (DMEM) and fetal bovine serum (FBS) was purchased from Gibco, Invitrogen. All other chemicals were purchased locally and were of analytical grade. For experimental metastasis assay, inbred strain of C57BL/6 mice was used.

Cell lines

B16F1(F1) and B16F10 (F10) murine melanoma cell lines [37] were obtained from National Centre for Cell Sciences, Pune, India. The cell lines were expanded and frozen aliquots were stored in liquid nitrogen. Each aliquot was used only up to five passages in vitro. The metastatic potential of F10 cells is maintained by culturing melanoma colonies on the lungs obtained by performing experimental metastasis assay in C57BL/6 mice. Cell lines were routinely characterized for (C57BL/6) mouse specific origin and mycoplasma free status as described in supplementary methods.

Immunohistochemical detection of galectin-3 in mouse lungs

Immunohistochemical staining for galectin-3 was performed on 3-μm paraffin embedded sections as described in [27]. Sections were stained with rat anti-mouse galectin-3 monoclonal antibody followed by anti-rat horse radish peroxidase (HRPO) conjugate and developed with diaminobenzidine containing H_2O_2 as the substrate. Instead of the primary antibody, the control lung sections were treated with rat IgG in the concentration similar to the primary antibody. The slides were later counter stained with hematoxylin.

Purification of recombinant human galectin-3

Galectin-3 was purified as described in [38].

Adhesion assays

For Adhesion assays, either calcein AM labeled or tritiated thymidine labeled melanoma cells were used and were performed in 96 well plates coated overnight with galectin-3 (50 μg/ml) as described previously [39]. For labeling with calcein, melanoma cells were incubated with DMEM medium containing 3 μg/ml calcein. Fluorescence was measured in 96 well plate reader from Berthold Mithras LB-940 machine (Excitation filter-485 nm and Emission filter-535 nm). The percentage adhesion was calculated by considering F10 cells bound to galectin-3 as 100 %.

Cell spreading assay

Melanoma cells were harvested, washed free of serum and 0.5 million cells were seeded in serum free DMEM on the coverslips coated overnight with 50 μg/ml galectin-3 in serum free DMEM at 4 °C. The cells were incubated for 45 min in a CO_2 incubator. Coverslips treated with serum free DMEM only, served as control. Bound cells were fixed in 4 % paraformaldehyde, permeabilized with 0.5 % Triton X 100 for 15 min and stained with 2 μg/ml Phalloidin TRITC or Phalloidin FITC staining solution made in PBS for 15 min at 37 °C. Nuclei were stained with 5 μg/ml of 4′,6′-diamidino-2-phenylindole dihydrochloride (DAPI) in PBS for one minute. The stained cells were mounted and images were acquired using LSM510 software on a Carl Zeiss Laser confocal Microscope at 63× magnification. The ratio of cytoplasmic/nuclear (C/N) area of approximately 100 cells was measured using Image J software to quantitate cell spreading.

Detection of MMPs by zymography and Western blotting

Melanoma cells seeded at a density of 15,000 cells in 100 μl of complete DMEM were grown in 96 well plates for 24 h at 37 °C. Cells were subjected to serum starvation for additional 24 h in absence or presence of different concentrations (0.25 μg–0.75 μg/ml) of soluble galectin-3. To see the effect of immobilized galectin-3, wells were coated overnight with 100 μl of different concentrations of galectin-3 (10–75 μg/ml) at 4 °C in serum free DMEM. The cells were grown on immobilized galectin-3 in complete medium at 37 °C for 24 h in a CO_2 incubator followed by serum starvation for 24 h. Cells seeded on uncoated wells served as control. The serum free conditioned medium was collected from each well and analyzed by gelatin zymography on 10 % SDS-PAGE containing 0.1 % gelatin as per [40]. MMP-9 levels in culture supernatant were also detected by Western blotting with anti MMP-9 antibody.

Wound healing assay

35 mm culture dishes were coated overnight with galectin-3 (50 μg/ml) in serum free DMEM at 4 °C, followed by blocking of non-specific sites with 2 % BSA for 1 h. 0.75 million melanoma cells were seeded in coated plates and incubated at 37 °C for 24 h in a CO_2 incubator. The cells were serum starved for 24 h for cell synchronization. A straight, uniform wound (approx. 400 μm in width) was

made using a micropipette tip on the monolayer and the cells were maintained in serum free DMEM. Wound closure was measured for 20 h by time lapse video imaging of at least three different positions across the length of the wound using a Carl Zeiss Inverted Microscope at 10× magnification. Uncoated culture dishes, blocked only with BSA served as control.

Cloning of shRNA for targeting β1,4 galactosyltransferases-I and -V genes (GalTs)

Downregulation of polyLacNAc in F10 cells was performed by using short hairpin RNA (shRNA) against GalT-I and -V the genes involved in polyLacNAc synthesis, as per the guidelines outlined [41]. A 21 nucleotide sequence (5′-TGGGGCGGAGAAGATGACGAC-3′) from the open reading frame of GalT genes was chosen which is common and unique only to these two genes. The strategy for cloning shRNA into pSuperneo H1 vector is described in supplementary data.

For cloning shRNA into pTRIPz lentiviral vector, primers were designed according to pTRIPz manual (Open biosystems). Forward primer contained *Xho*I site followed by mir sequence (represented in italics), sense sequence (represented in italics bold) and loop sequence.

Forward GalT shRNA primer
5′GAACTCGAG*AAGGTATATTGCTGTTGACAGTGAG CG**TGGGGCGGAGAAGATGACGAC***TAGTGAAGCC ACAGA3′
Reverse primer contained *Eco*RI site followed by mir sequence (represented in italics), sense sequence (represented in italics bold) and loop sequence.
Reverse GalT shRNA primer
5′GTTGAATTC*CGAGGCAGTAGGCA**TGGGGCGGA GAAGATGACGAC***TACATCTGTGGCTTC3′

Using these primers shRNA sequence was amplified. The shRNA was cloned in pTRIPz lentiviral vector digested with *Eco*RI and *Xho*I sites. The ligated plasmid was purified and subsequently co-transfected with helper plasmids (pMD2.G and psPAX2) in HEK293FT cells for generating virus particles which were used for transduction of F10 cells. The clones were selected using puromycin (1 μg/ml) and subsequently maintained as separate stocks. For inducing shRNA expression cells were cultured in complete DMEM containing doxycycline (4 μg/ml) for 96 h.

Real time PCR

For detecting transcript levels of GalT-I and GalT-V genes specific primers were designed. RPL4 was used as housekeeping gene for relative quantification of transcript levels [42].

The real time PCR reaction was carried out in 7900HT system (ABI Prism) and for detecting amplicons Power SYBR green was used. The data represents mean of three different experiments carried out in duplicates with different batches of cDNA. The Ct values obtained were normalized to RPL4 values. Analysis was performed using $2^{-\Delta\Delta C_t}$ method [43].

Flow cytometric analysis

For flow cytometry, cells were either fixed overnight in 1.5 % glutaraldehyde or 1 % paraformaldehyde in PBS (pH 7.4) and were analyzed for surface expression of polyLacNAc using biotinylated galectin-3 (0.75 μg/ml) and biotinylated LEA (2 μg/ml) as described previously [28].

Cloning, expression and purification of mouse truncated galectin-3 (mtGal-3)

The coding DNA sequence of C-terminal carbohydrate binding domain of galectin-3 was cloned into the pET3a bacterial expression vector using forward 5′ATAGTCATCA TATCATCATAGTCGATCATATGGTGCCC3′ and reverse 5′GGTGGATCCTTAGATCATGGCGTGGTTAGC3′ primers. The total cDNA obtained from F10 cells served as a template. The *Nde*I and *Bam*HI restriction sites were incorporated in forward and reverse primers respectively to clone the amplified product into pET3a plasmid vector. The sequence of the positive clones was confirmed. This construct was transformed into *E. coli BL21* (*DE3*) strain and expression of mtGal-3 was induced by IPTG (1 mM). The expressed protein was of 15.4 kDa (amino acid sequence 130–264 of full length galectin-3). The mtGal-3 protein was purified using lactose sepharose column as described in [38].

Preparation of modified citrus pectin (MCP)

MCP was prepared from citrus pectin exactly as described in [44].

Experimental metastasis assay

Melanoma cells were routinely cultured in DMEM as described in [28], with or without glycosylation inhibitors Swainsonine (SW, 2 μg/ml) and benzyl-α-*N*-acetylgalactosamine (BG, 2 mM). For injecting GalT clones, mice were fed with doxycycline (1 mg/ml) in 5 % sucrose solution 24 h prior to injection and continued until sacrificed.

For injecting F10 cells treated with murine truncated galectin-3 (mtGal-3, carrying only CRD), 0.1 million F10 cells were pre-incubated with 0.1 ml of 500 μg/ml of mtGal-3 for 1 h on ice. The mice that received pre-treated

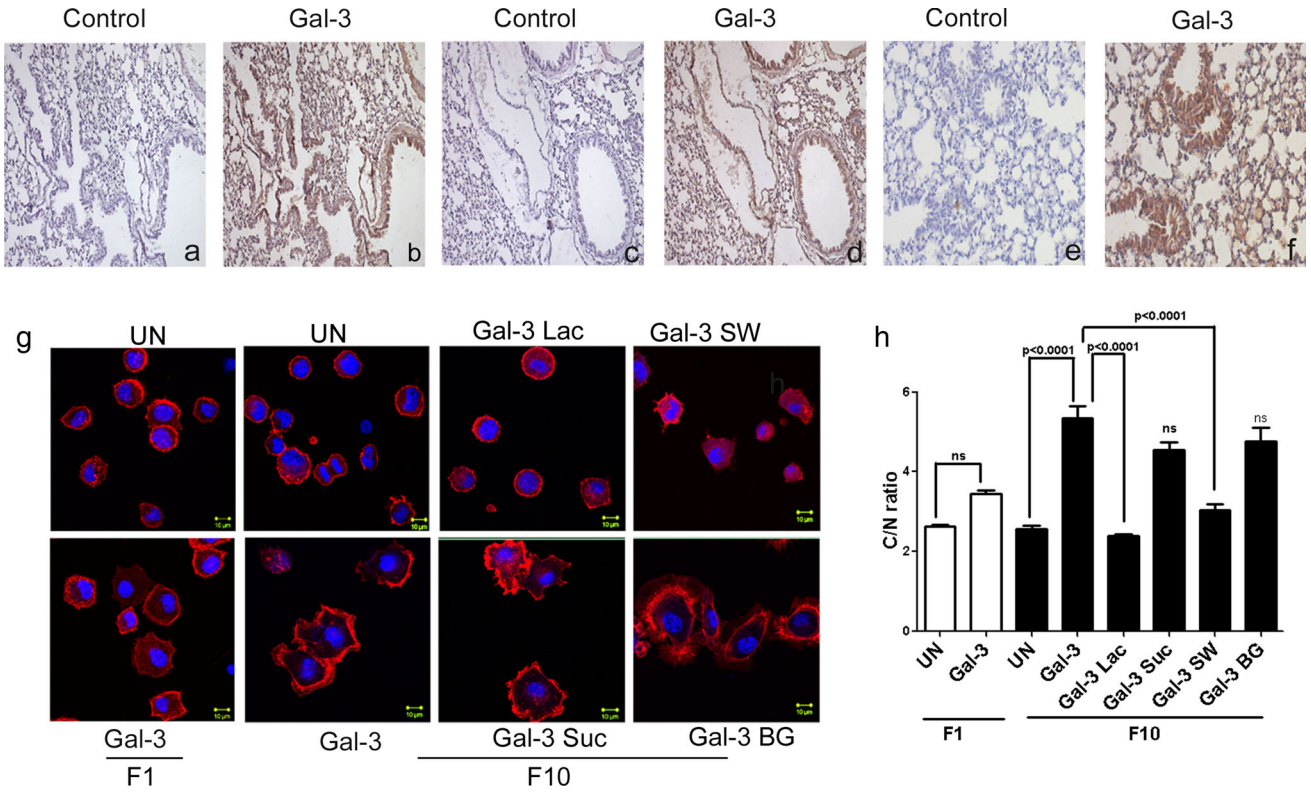

Fig. 1 Galectin-3 is expressed in all the major compartments of lungs and it facilitates spreading of melanoma cells. **a**–**f** Immuno-histochemical staining of mouse lung sections treated with rat anti-mouse galectin-3 antibody at ×10, ×20 and ×40 magnifications, respectively. The control sections were treated with pre-immune rat IgG. **g** Cell spreading of F1 and F10 cells on uncoated (UN) and galectin-3 (Gal-3) coated coverslips as assessed by Phalloidin-TRITC staining. DAPI was used to stain the nuclei (*blue*). Spreading of F10 cells was also seen on galectin-3 coated coverslips in presence of lactose (Gal-3 Lac) and sucrose (Gal-3 Suc), and after treatment with either SW (Gal-3 SW) or BG (Gal-3 BG). *Scale bar* 10 µm. **h** *Each bar* represents ratio of cytoplasmic to nuclear (C/N) area for around 100 cells from two different experiments. (Color figure online)

cells also received injections of mtGal-3 (250 µg in 0.1 ml, via intra muscular injection) on day 1 (2 h before and after injection of cells) and once on day 2.

For injecting F10 cells treated with MCP, 0.1 million F10 cells were resuspended in medium with and without MCP (0.05 %) and mice which received cells with MCP were on drinking water containing 1.5 % MCP from 5 days prior to injection till the day of sacrifice.

Statistical analysis

All the data is represented as mean ± SE unless stated. For comparison of two groups in case of cell spreading, cell adhesion, experimental metastasis assay student's *t* test was employed and multiple groups were compared by one way ANOVA. For wound-healing assays, 2-way ANOVA with the Bonferroni posttest was conducted. All the statistical analysis was performed using GraphPad Prism 5. $P < 0.05$ was considered significant.

The details of cloning of shRNA in pSupeneo H1, sequences of primers used for real time and semi quantitative RT-PCR have been described in supplementary methods. Total cell lysate, Protein estimation, SDS-PAGE and Western blotting were performed as described in [27].

Results

Galectin-3 is localized in all the major compartments of mouse lungs

In mice, lungs have previously been shown to express highest levels of galectin-3 and express it constitutively on the surface of its vascular endothelium. Immunohistochemistry results showed that not just endothelium, galectin-3 is localized in all the major tissue compartments of the lungs, including epithelia of bronchioles, alveoli and on the surface of vascular endothelium (Fig. 1a–f) and possibly thus may participate in different processes of organ colonization.

Galectin-3 facilitates spreading of melanoma cells in a metastasis and N-glycosylation dependent manner

Ability of cells to spread on immobilized galectin-3 was analyzed to see if it stabilizes the interactions of the cells

adhered on the vascular endothelium. F1 cells spread poorly with diffused organization of actin, on both uncoated and galectin-3 coated cover slips (Fig. 1g). In contrast, F10 cells showed significant spreading on galectin-3 as compared to uncoated cover slips, as characterized by organization of F-actin in lamellipodial projections and significantly increased C/N ratio (Fig. 1g, h). Like adhesion [28], the extent of spreading was also dependent on the metastatic potential of the cells which was inhibited by specific disaccharide lactose and not sucrose, and by inhibitor of N- but not O-glycosylation (Fig. 1g, h, Gal-3 Lac/Suc and Gal-3 SW/BG).

Galectin-3 induces secretion of proteases and motility in melanoma cells, thereby aiding invasion

Degradation of Basement membrane/Extracellular matrix (BM/ECM) and movement are the next major event required during extravasation. Assays were performed to see if soluble and immobilized galectin-3 promotes any of these processes. Zymography of the conditioned media collected from cells grown in the absence or presence of either soluble or immobilized galectin-3, showed that galectin-3 induces secretion of matrix degrading enzyme, MMP-9 in a dose and metastatic potential dependent manner (Fig. 2a–c).

For F10 cells, the highest induction with soluble galectin-3 was seen at 0.5 μg/ml (data not shown), whereas with immobilized galectin-3, it was 2.5 μg/well of a 96 well plate (Fig. 2a). The concentrations higher than these appeared to inhibit the induction of MMP-9 secretion. Comparison of the melanoma variants clearly showed that induction is dependent on the metastatic potential (Fig. 2b, c). No gelatin clear bands (as a result of MMP-9 activity) could be visualized in F1 lanes on 24 h incubation of the gel in renaturation buffer (Fig. 2b) whereas prolonged incubation resulted in saturation in F10 lanes due to substrate limitation (Fig. 2c). Since expression of polyLacNAc on N-glycans is also dependent on the metastatic potential of melanoma cells, the galectin-3 mediated induction of MMP-9 could be via polyLacNAc.

Movement of extravasated cells towards organ parenchyma is also a key event for metastatic establishment. Wound healing assays showed that galectin-3 is indeed used as traction by these cells for their movement. This again, was dependent on the metastatic potential and the N-glycosylation status of cells (Fig. 2d–f). O-glycosylation inhibitor BG had no effect on any of these cellular properties or on metastasis [28]. This reaffirmed our earlier observation that galectin-3 ligands only on N-oligosaccharides participate in these processes.

Downregulation of GalT-I and -V enzymes in F10 cells leads to significant reduction in the expression of polyLacNAc

Although, using Swainsonine, a broad range N-glycosylation inhibitor, we confirmed that N-glycans play an important role in metastasis of F10 cells; we needed to confirm that it is via polyLacNAc on them. PolyLacNAc is synthesized by the concerted action of the enzymes that sequentially add *N*-acetylglucosamine (β1,3 *N*-acetylglucosaminyltransferases or β3GnTs) and galactose (β1,4 galactosyltransferases—GalTs) [45]. Among the seven members of the GalT family GalT-VII adds galactose only onto proteins with proteoglycan core [46]. Comparison of transcripts of the remaining six members by semi-quantitative PCR showed up regulation of GalT-I and -V in the higher metastatic variant (Supplementary Fig. S1A). Both β4GalT-I and β4GalT-V reportedly promote addition of polyLacNAc preferentially on N-oligosaccharides [47, 48].

Both these genes were down-regulated using shRNA targeting a sequence common to both of them, using plasmid (pSuperneo H1) as well as inducible lentiviral (pTRIPz) vectors for cloning shRNA in F10 cells. The functional effects of downregulation were confirmed by in vitro as well as in vivo assays. The two F10 cell clones, sh3 and sh6, generated in pSuperneo H1 vector which constitutively expresses shRNA showed downregulation of transcripts and polyLacNAc on the cell surface. (Supplementary Fig. S1b, c).

The inducible lentiviral vector system (pTRIPz) allowed tight temporal control of target gene knock down with minimal off-target and deleterious effects on cells. The two F10 clonal cell lines (clone I and II) expressing the inducible GalT-I and -V shRNA were established. Simultaneously, clones of F10 cells expressing the inducible non-targeting shRNA (NT) were also established. Upon doxycycline induction, clone I and II showed significant reduction in the transcript levels of GalT-I and -V as compared to clone expressing non targeting sequence of shRNA (Fig. 3a, b). In contrast to NT clone, both the clones expressing specific shRNA showed significant reduction in the surface levels of polyLacNAc as assessed by flow cytometry, using biotinylated LEA and galectin-3, after doxycycline induction (Fig. 3c, d).

Downregulation of polyLacNAc results in decreased adhesion, spreading, MMP-9 secretion and motility of F10 cells on galectin-3 together with reduced experimental metastasis

Reduced expression of polyLacNAc in the induced clone I and II was associated with significantly decreased

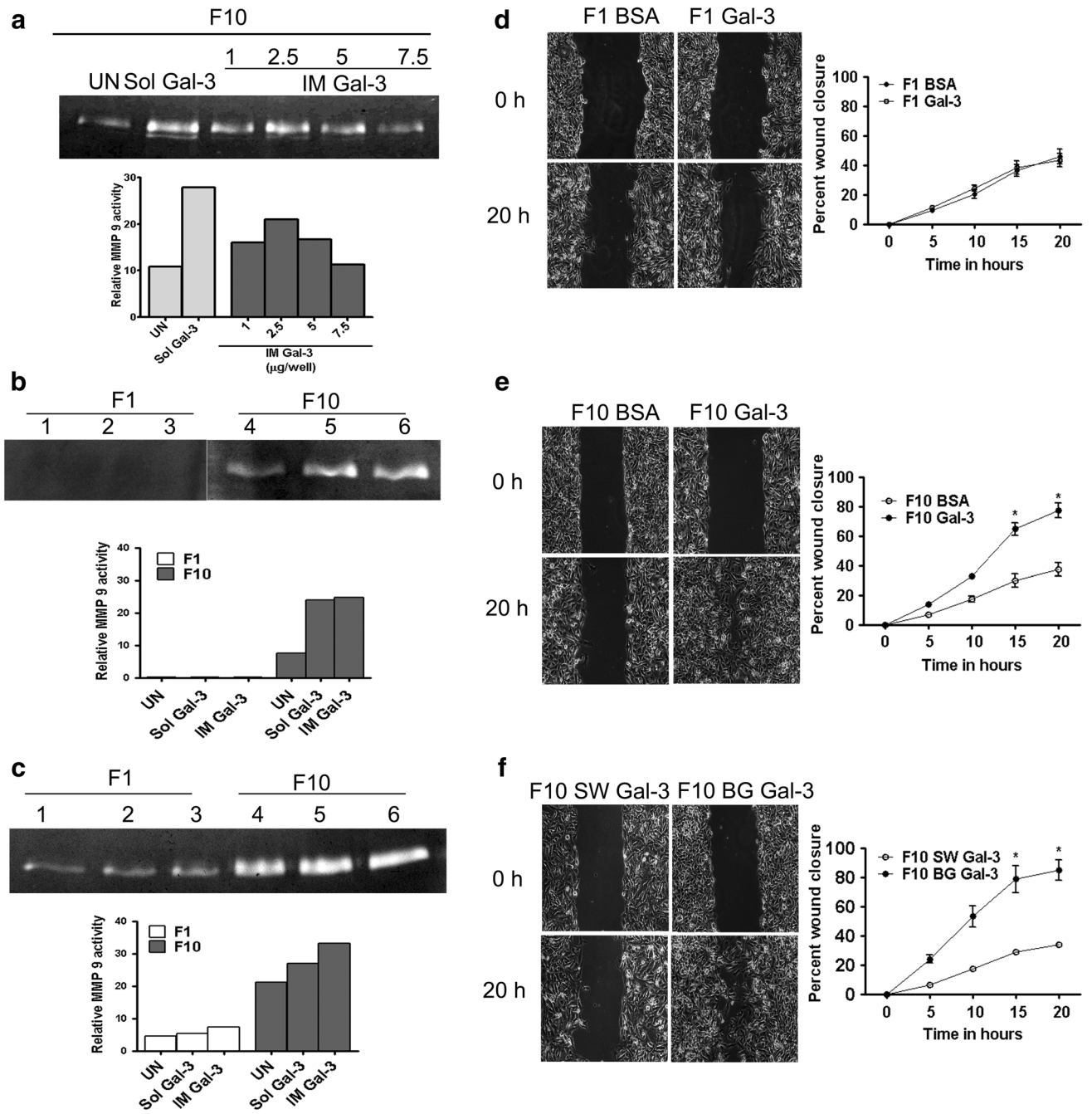

Fig. 2 Galectin-3 in both soluble (Sol Gal-3) as well as immobilized (IM Gal-3) form induces secretion of MMP-9 and IM Gal-3 promotes motility of melanoma cells. **a** Conditioned media of F10 cells grown on uncoated wells was compared with those grown in presence of 0.5 μg/ml sol gal-3 or on different amounts of IM gal-3 (0.1 ml/well of 10, 25, 50 and 75 μg/ml in 96 well plate). **b**, **c** Represent data comparing levels of MMPs in conditioned media of F1 and F10 cells grown on uncoated (UN, *lanes 1*, *4*) or in presence of soluble (Sol Gal-3, 0.5 μg/ml) (*lanes 2*, *5*) and immobilized (IM Gal-3, 0.1 ml/well of 50 μg/ml) (*lanes 3*, *6*) galectin-3. **b** The data from gels incubated for 24 h, and **c** from gels incubated for 48 h in renaturation buffer. For quantification, densitometry analysis was performed and is represented in *bar graphs* below **a**, **b**, and **c**, respectively. **d**–**f** Represent time lapse video microscopy images at 0 and 20 h of wound closure on 2 % BSA and on IM Gal-3. *Right panel* depicts graphical representation of percent wound closure of d–f at 5 h interval. Mean values of triplicate for each position of the wound width of each image frame from two different experiments, was analysed using Metamorph software. * indicates $P < 0.05$ which was considered significant

adhesion on galectin-3 (Fig. 3e). Downregulation of polyLacNAc also appeared to reduce their spreading on galectin-3 as compared to that of NT cells, as seen by microscopy images and C/N ratio (Fig. 3f, g). Similarly, induction of shRNA expression affected MMP-9 secretion by these clones on galectin-3 coated plates as compared

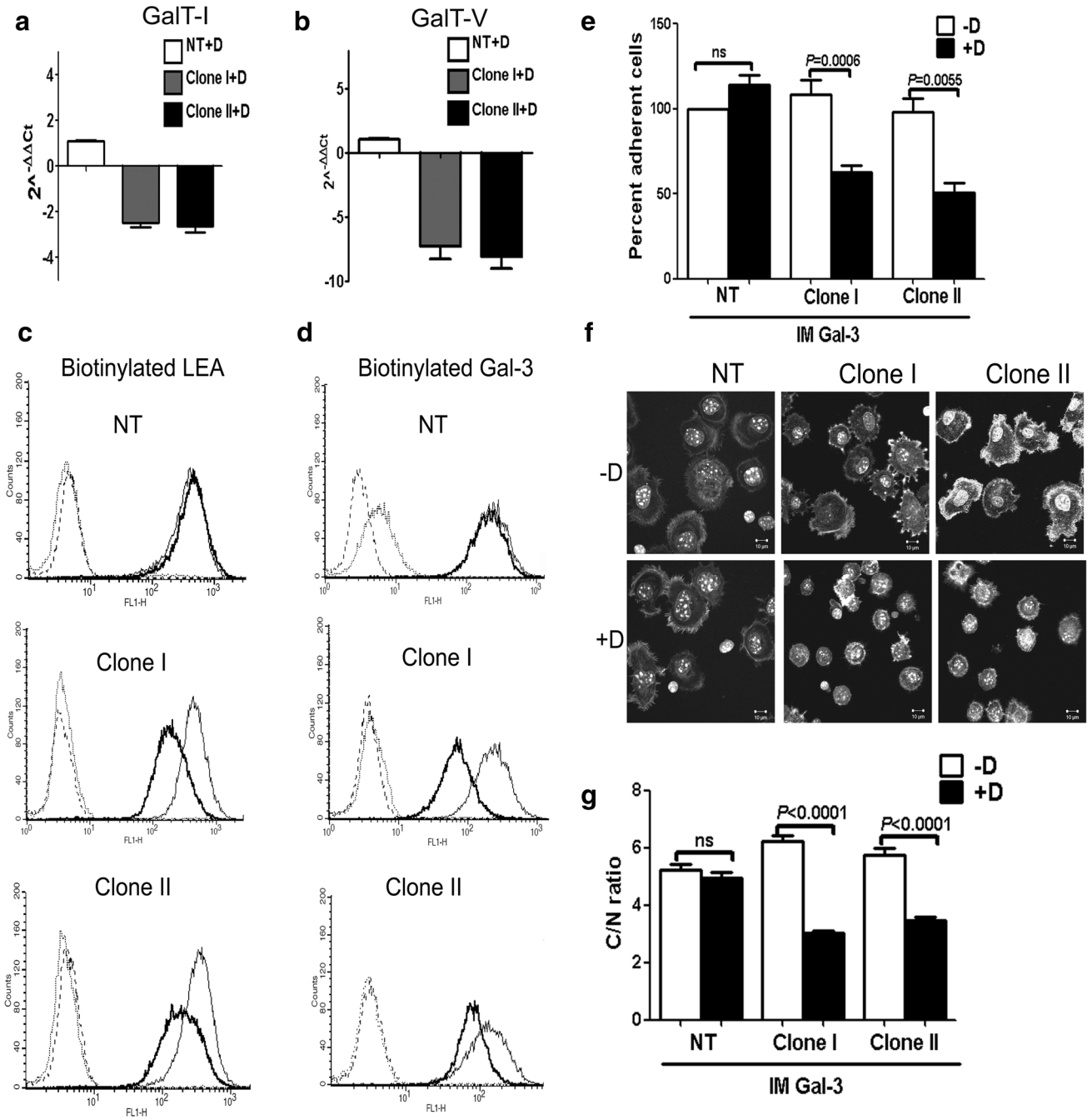

Fig. 3 Validation of down regulation of GalT-I and -V genes in clones and its effect on polyLacNAc expression, cell adhesion and spreading. **a**, **b** Represents transcript levels of beta 1,4 GalT-I and GalT-V in clones I and II respectively, after doxycycline induction by real time PCR. *NT* non targeting was used as the vector control. **c**, **d** Expression of polyLacNAc on the cell surface of clones I and II under doxycycline treated and untreated conditions by flow cytometry using biotinylated LEA and galectin-3 respectively. Cells treated with ExtraAvidin FITC only served as control, −doxycycline (*dotted line*), +doxycycline (*dashed line*). Test samples treated with doxycycline are represented as (*thick line*) and untreated samples as (*thin line*). **e** Adhesion of clones I, II and NT in presence or absence of doxycycline on galectin-3 coated plates. Values are mean ± SE of two independent experiments. **f** Spreading of NT, clone I and II on galectin-3 coated coverslips in presence or absence of doxycycline. *Scale bar* 10 μm. **g** Each *bar* represents ratio of cytoplasmic to nuclear (C/N) area for around 100 cells from two different experiments

to NT clone (Fig. 4a, b). The motility of clones I and II on galectin-3 was also significantly reduced on induction of shRNA expression (Fig. 4c–h).

These altered cellular properties as a result of loss of polyLacNAc had a major impact on the experimental metastasis of these clones as compared to non transduced

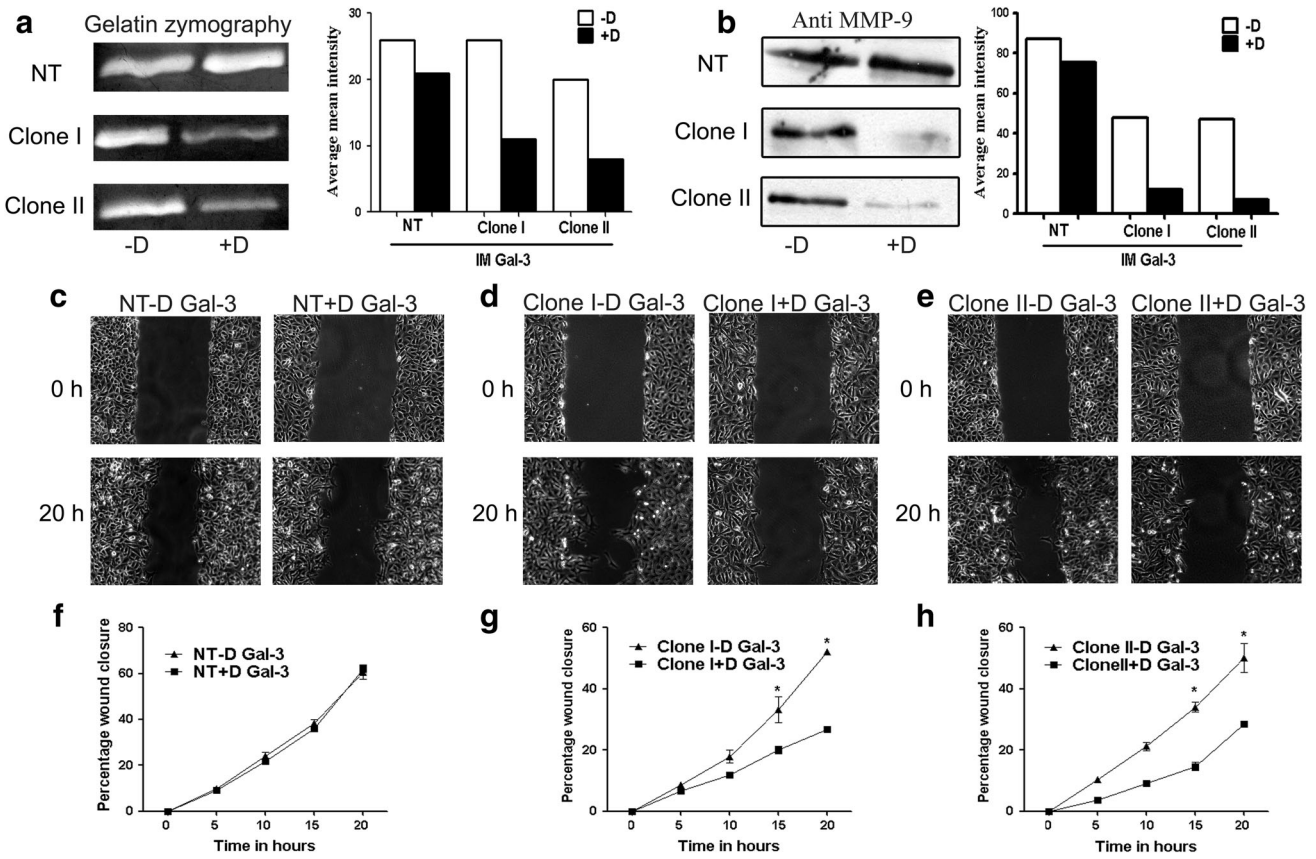

Fig. 4 Effect of polyLacNAc downregulation on secretion of MMP-9 and migration. **a** Levels of MMP-9 in culture supernatants of NT, clone I and II grown in presence and absence of doxycycline on immobilized galectin-3 as detected by zymography and **b** Western blotting. The adjacent right panel of **a**, **b** represent densitometry analysis. **c**–**e** Represent time lapse video microscopy images at 0 and 20 h of wound closure on immobilized galectin-3 of NT, clone I and II under doxycycline treated and untreated conditions, respectively. The data in **f**–**h** represents mean percent wound closure at 5 h interval. Area of wound closure was measured by Image J software and each image from two different experiments, was analyzed at three different positions. * indicates $P < 0.05$ which was considered significant

F10 cells or NT clones induced with doxycycline (Fig. 5a). This was also observed in the sh3 and sh6 clones generated by plasmid mediated constitutive shRNA expression. Reduced polyLacNAc levels affected galectin-3 mediated cell adhesion (Supplementary Fig. S1d), spreading and MMP-9 secretion (data not shown) resulting in significantly reduced metastatic potential of both sh3 and sh6 clones (Supplementary Fig. S1e, f).

These results collectively highlight that polyLacNAc on N-glycans on melanoma cells regulate key cellular processes that are critical for lung metastasis.

Effect of dominant negative inhibitor and the competitive sugar to galectin-3 on metastasis of F10 melanoma cells to the lungs

To confirm the role of galectin-3 as the major polyLacNAc binding lectin responsible for mediating lung specific colonization, two approaches were adopted. In the first case, all the available galectin-3 binding sites on melanoma cells were blocked using truncated galectin-3 which lacks oligomerization domain [49] and in second approach, we tried to block all the endogenous galectin-3 in mice by feeding them with MCP [44]. Both MCP and recombinant murine truncated galectin-3 (mtGal-3) were found to inhibit galectin-3 mediated spreading of F10 cells (Supplementary Fig. S2a, b). Blocking galectin-3 binding sites with excess mtGal-3 significantly reduced the metastatic potential of F10 cells (Fig. 5b). Similarly, injection of F10 cells into mice fed continuously with MCP resulted in profound decrease in their lung metastasis. MCP apparently competes with polyLacNAc on melanoma cells for binding to galectin-3 on the lungs thereby impacting metastasis (Fig. 5c).

Discussion

Interaction of specific molecules on organ endothelium and on the tumor cells is a major determinant of organ specific

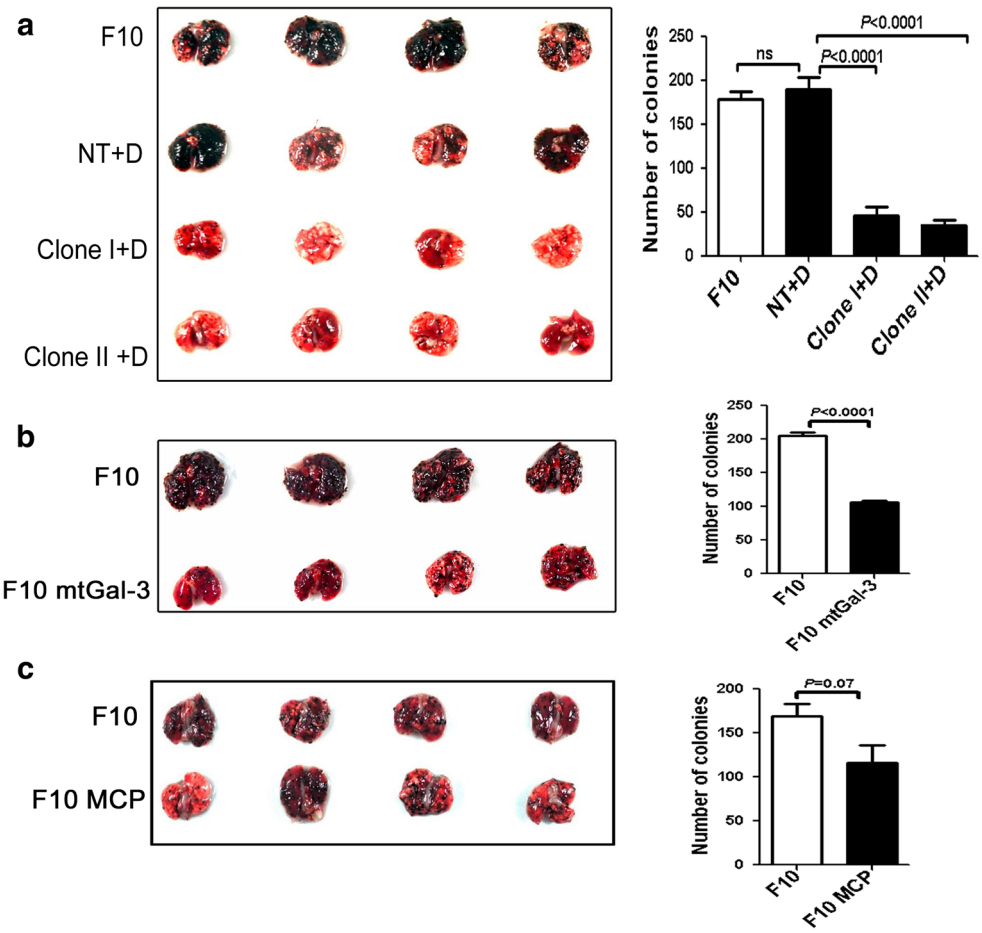

Fig. 5 Galectin-3/polyLacNAc pair plays an important role in lung metastasis. Experimental metastasis assay for **a** NT, clone I and II cells, **b**, **c** F10 cells treated with mtGal-3 and with MCP respectively (as described in "Materials and methods" section). Untreated F10 cells served as control. The *left panel* shows the lungs images while *right panel* is the graphical representation of the number of metastatic lung colonies

metastasis [3, 50]. The strength of these interactions, ability to invade the vascular BM, entry into organ parenchyma and survival in response to organ growth environment are the other key factors that determine the organ specificity of tumor cells [3, 7]. Constitutive expression of galectin-3 on the lung endothelium apparently aids arrest of tumor cells expressing high affinity easily accessible ligands in the form of polyLacNAc on *N*-oligosaccharides [27]. Lungs in mice have previously been shown to express highest levels of galectin-3 [27]. Here, we demonstrate that galectin-3 is expressed not just on the endothelial cells but on all the tissue compartments of the lungs including alveolar epithelium, bronchioles and on most pulmonary tissue spaces (Fig. 1a–f).

Galectin-3 is a multifunctional nucleo-cytoplasmic protein which is involved in different cellular functions. It can interact with transcription factors in the nucleus to regulate gene expression and also can perform anti or pro-apoptotic functions depending on its cytoplasmic or extracellular localization [29]. The secreted galectin-3 often gets incorporated on the cell surface, ECM or the BM by virtue of its ability to bind to the glycoprotein ligands and oligomerise/form lattices on cell surface [51, 52]. These studies investigated if galectin-3, present in abundance in all the major compartments of the lungs, has any role in establishing metastatic foci of cells expressing high levels of polyLacNAc on N-glycans on their surface. The interactions mediated by galectin-3 are much stronger than those via selectins and are comparable to those mediated by integrins [35, 36, 53]. However, the cells adhered to the organ endothelium via galectin-3 would need to stabilize these interactions to prevent them from being flown off under hemodynamic flow conditions and to initiate processes like vascular retraction, required to extravasate. This can be achieved by initiating the spreading of adhered cells [7].

Members like galectin-8 of the galectin family in their immobilized form have earlier been shown to regulate spreading of cells [54, 55]. We for the first time demonstrate that galectin-3 in the immobilized form induces the formation of membrane protrusions in melanoma cells which can be inhibited specifically via inhibitors of N- and not O-oligosaccharides (Fig. 1e, f).

The next barrier for effective organ colonization is the exposed vascular BM. MMPs play a major role in degradation of underlying BM and facilitate tumor cell entry into

organ parenchyma [56]. Overexpression of galectin-3 in the cytoplasmic/nuclear compartments of cells has been shown to regulate expression/secretion of MMPs, especially MMP-1, MMP-2 and MMP-9 and promote invasion. Nuclear galectin-3 in gastric cancer cells was shown to interact with AP-1 transcription factor and regulate the expression of MMP-1 [57]. Further, silencing the expression of galectin-3 in human tongue carcinoma and pancreatic cell lines affected β-catenin levels which in turn correlated with reduced levels of MMP-2 and MMP-9 [58, 59]. Galectin-3 has collagenase like repeats adjacent to its N-terminal domain which can act as a cleavage site for MMPs and cleaved form appears to serve as a marker for cancer progression [60]. Lungs express galectin-3 in highest amounts [27] which may be present in both soluble and immobilized form in different tissue compartments including vascular BM. We show that both immobilised as well as soluble forms of galectin-3 induce secretion of MMP-9 in a dose dependent manner (Fig. 2a–c). Secretion of MMP-9 by melanoma cells correlated with their metastatic potential (Fig. 2b, c). Ours is the first study which reports that extracellular galectin-3 induces the secretion of MMP-9 in melanoma cells, most likely via the polyLacNAc on N-glycans. MMP-9 mediates degradation of ECM but it has to be coupled with movement for effective extravasation of tumor cells.

Galectin-3 expressed in various compartments has been associated with motility of wide range of cell types. In the soluble form, it has been shown to induce reorganization of cytoskeleton which in turn facilitates motility of corneal epithelial cells [61]. Cell surface galectin-3 localises in lipid raft and its absence affects the formation of membrane ruffles and lamellipodia [62]. Overexpression of galectin-3 in cytoplasm of oral tongue squamous carcinoma cells (OTSCC) enhanced motility via wnt/beta-catenin signalling pathway [63]. Also, at low concentrations galectin-3 can act as chemoattractant, for monocytes and macrophages [64].

Using wound healing assays, we demonstrate that immobilised galectin-3 which often gets incorporated as part of ECM and BM can itself be used as traction for forward motility of melanoma cells. The dependence of cellular motility on the metastatic potential of the cells and their N- and not O-glycosylation status confirmed that it is indeed mediated by N-oligosaccharides on surface glycoproteins (Fig. 2d–f). Although, other members like galectin-8 have been shown to facilitate movement of cells in a similar manner [65], here we demonstrate that even immobilized galectin-3 can facilitate haptotactic motility. Galectin-3 mediated motility would be important for cells to move into lung parenchyma.

Beta 1,6 branched expressed on N-oligosaccharides of cell surface proteins is the preferred site for further substitution of polyLacNAc. Several proteins that carry β1,6 branched N-oligosaccharides may also carry polyLacNAc. Some of the possible carrier proteins include integrin subunits (α3, α5, αv and β1), growth factor receptors like EGFR and others like CD-44 (hyaluronate receptors) and lysosome associated membrane proteins (LAMPs) [66, 67]. The cancer cells most possibly use surface receptors expressing polyLacNAc on N-oligosaccharides for motility. Galectin-3 may also promote proliferation by sustained signalling via growth factor receptors by restricting them in the lattices and preventing their internalization [68, 69].

PolyLacNAc is synthesized by the sequential addition of *N*-acetylglucosamine and galactose by the enzymes β1,3 *N*-acetylglucosaminyltransferases or β3GnTs and β1,4 galactosyltransferases—GalTs [45]. Among the six possible enzymes that add galactose, the expression of GalT-I and -V correlated with metastatic potential of B16 melanoma cells (Supplementary Fig. 1a). Downregulation of these two genes by shRNA mediated plasmid and inducible lentiviral vectors, showed marked reduction in polyLacNAc expression (Fig. 3a, b, Supplementary Fig. 1b, c). This was accompanied with inhibition of all the galectin-3 mediated processes like adhesion, spreading, movement and induction of MMP-9 secretion (Fig. 3e–g, Supplementary Fig. 1d, 4a–h). Inhibition of experimental metastasis as a result of inhibition of all the galectin-3 mediated processes highlighted the importance of polyLacNAc and galectin-3 pair in facilitating lung colonization (Fig. 5a) (Supplementary Fig. 1e, f).

Galectin-3 is a monomeric lectin that forms oligomers on binding to its ligand via its N-terminal domain. Truncated galectin-3 devoid of the N-terminal domain has been shown to act as a dominant negative inhibitor of galectin-3. Truncated galectin-3 affected growth and lymph node metastasis of breast cancer cell line on sustained treatment [49]. Pre-incubation of B16F10 cells with truncated galectin-3 inhibited lung metastasis apparently by blocking polyLacNAc on melanoma cells making it unavailable for binding to galectin-3 on the lung vascular endothelial cells (Fig. 5b). MCP has been shown to affect several galectin-3 mediated processes including metastasis [70]. Inhibition of experimental metastasis in mice fed with MCP indicated that MCP in circulation possibly competes with polyLacNAc on melanoma cells for binding to endothelial cells (Fig. 5c). However, the contribution of galectin-3 as an immunomodulating agent also, cannot be ruled out in facilitating melanoma metastasis [32].

Our studies very clearly demonstrate the importance of galectin-3 and polyLacNAc in not just mediating adhesion to lung endothelium but also in several downstream processes critical for lung homing. It would be interesting to study the molecular pathways activated downstream of

galectin-3/polyLacNAc interactions which regulate the successive events involved in metastasis. We expect that confirmation of existence of similar mechanisms in lung metastasis of human tumors would open up several interesting avenues to explore and would also be crucial in developing effective strategies to prevent metastasis.

Acknowledgments This work was supported by Department of Biotechnology, Government of India and Senior Research Fellowship to Ms. Nithya Srinivasan, Manohar C. Dange and Shyam K. More was offered by Council for Scientific and Industrial Research, Government of India. We thank, Prof. Hakon Leffler, Lund University, Sweden, for the for rhGalectin-3 expression vector. We acknowledge the expert help extended by, Mrs. Sharda Sawant for immuno-histochemistry experiments, Ms. Rekha Santani and Shamal Vetale for Flow Cytometry, Ms. Vaishali Kailaje and Ms. Tanuja Dighe for Laser confocal microscopy, Mr. D.S. Chavan and A.M. Pawar for technical help.

Conflict of interest No potential conflicts of interest were disclosed.

References

1. Brooks SA et al (2010) Molecular interactions in cancer cell metastasis. Acta Histochem 112(1):3–25
2. Gupta GP, Massague J (2006) Cancer metastasis: building a framework. Cell 127(4):679–695
3. Nicolson GL (1988) Organ specificity of tumor metastasis: role of preferential adhesion, invasion and growth of malignant cells at specific secondary sites. Cancer Metastasis Rev 7(2):143–188
4. Weiss L (1992) Comments on hematogenous metastatic patterns in humans as revealed by autopsy. Clin Exp Metastasis 10(3):191–199
5. Nicolson GL (1991) Tumor and host molecules important in the organ preference of metastasis. Semin Cancer Biol 2(3):143–154
6. Paget S (1989) The distribution of secondary growths in cancer of the breast. 1889. Cancer Metastasis Rev 8(2):98–101
7. Zetter BR (1990) The cellular basis of site-specific tumor metastasis. N Engl J Med 322(9):605–612
8. Konstantopoulos K, Thomas SN (2009) Cancer cells in transit: the vascular interactions of tumor cells. Annu Rev Biomed Eng 11:177–202
9. Mierke CT (2008) Role of the endothelium during tumor cell metastasis: is the endothelium a barrier or a promoter for cell invasion and metastasis? J Biophys 2008:183516
10. Strell C, Entschladen F (2008) Extravasation of leukocytes in comparison to tumor cells. Cell Commun Signal 6:10
11. Ley K et al (2007) Getting to the site of inflammation: the leukocyte adhesion cascade updated. Nat Rev Immunol 7(9):678–689
12. Schluter K et al (2006) Organ-specific metastatic tumor cell adhesion and extravasation of colon carcinoma cells with different metastatic potential. Am J Pathol 169(3):1064–1073
13. Gassmann P et al (2010) In vivo tumor cell adhesion in the pulmonary microvasculature is exclusively mediated by tumor cell–endothelial cell interaction. BMC Cancer 10:177
14. Belloni PN, Tressler RJ (1990) Microvascular endothelial cell heterogeneity: interactions with leukocytes and tumor cells. Cancer Metastasis Rev 8(4):353–389
15. Haier J et al (2003) An intravital model to monitor steps of metastatic tumor cell adhesion within the hepatic microcirculation. J Gastrointest Surg 7(4):507–514 discussion 514–515
16. Voura EB, Sandig M, Siu CH (1998) Cell–cell interactions during transendothelial migration of tumor cells. Microsc Res Tech 43(3):265–275
17. Orr FW, Wang HH (2001) Tumor cell interactions with the microvasculature: a rate-limiting step in metastasis. Surg Oncol Clin N Am 10(2):357–381, ix–x
18. Kobayashi H, Boelte KC, Lin PC (2007) Endothelial cell adhesion molecules and cancer progression. Curr Med Chem 14(4):377–386
19. Glinskii OV et al (2005) Mechanical entrapment is insufficient and intercellular adhesion is essential for metastatic cell arrest in distant organs. Neoplasia 7(5):522–527
20. Dimitroff CJ et al (2004) Rolling of human bone-metastatic prostate tumor cells on human bone marrow endothelium under shear flow is mediated by E-selectin. Cancer Res 64(15):5261–5269
21. Aird WC (2007) Phenotypic heterogeneity of the endothelium: II. Representative vascular beds. Circ Res 100(2):174–190
22. Downey GP et al (1993) Neutrophil sequestration and migration in localized pulmonary inflammation. Capillary localization and migration across the interalveolar septum. Am Rev Respir Dis 147(1):168–176
23. Biancone L et al (1996) Redirection of tumor metastasis by expression of E-selectin in vivo. J Exp Med 183(2):581–587
24. Abdel-Ghany M et al (2001) The breast cancer beta 4 integrin and endothelial human CLCA2 mediate lung metastasis. J Biol Chem 276(27):25438–25446
25. Cardones AR, Murakami T, Hwang ST (2003) CXCR4 enhances adhesion of B16 tumor cells to endothelial cells in vitro and in vivo via beta(1) integrin. Cancer Res 63(20):6751–6757
26. Elble RC, Pauli BU (1996) Lu-ECAM-1 and DPP IV in lung metastasis. Curr Top Microbiol Immunol 213(Pt 1):107–122
27. Krishnan V et al (2005) Altered melanoma cell surface glycosylation mediates organ specific adhesion and metastasis via lectin receptors on the lung vascular endothelium. Clin Exp Metastasis 22(1):11–24
28. Srinivasan N et al (2009) Poly *N*-acetyllactosamine substitutions on N- and not O-oligosaccharides or Thomsen–Friedenreich antigen facilitate lung specific metastasis of melanoma cells via galectin-3. Glycoconj J 26(4):445–456
29. Liu FT, Rabinovich GA (2005) Galectins as modulators of tumour progression. Nat Rev Cancer 5(1):29–41
30. Glinsky VV et al (2003) Intravascular metastatic cancer cell homotypic aggregation at the sites of primary attachment to the endothelium. Cancer Res 63(13):3805–3811
31. Yu LG et al (2007) Galectin-3 interaction with Thomsen–Friedenreich disaccharide on cancer-associated MUC1 causes increased cancer cell endothelial adhesion. J Biol Chem 282(1):773–781
32. Radosavljevic G et al (2011) Deletion of galectin-3 in the host attenuates metastasis of murine melanoma by modulating tumor adhesion and NK cell activity. Clin Exp Metastasis 28(5):451–462
33. Radosavljevic G et al (2012) The roles of Galectin-3 in autoimmunity and tumor progression. Immunol Res 52(1–2):100–110
34. Sparrow CP, Leffler H, Barondes SH (1987) Multiple soluble beta-galactoside-binding lectins from human lung. J Biol Chem 262(15):7383–7390
35. Mehta P, Cummings RD, McEver RP (1998) Affinity and kinetic analysis of P-selectin binding to P-selectin glycoprotein ligand-1. J Biol Chem 273(49):32506–32513
36. Sato S et al (2002) Role of galectin-3 as an adhesion molecule for neutrophil extravasation during streptococcal pneumonia. J Immunol 168(4):1813–1822
37. Fidler IJ, Nicolson GL (1976) Organ selectivity for implantation survival and growth of B16 melanoma variant tumor lines. J Natl Cancer Inst 57(5):1199–1202

38. Massa SM et al (1993) L-29, an endogenous lectin, binds to glycoconjugate ligands with positive cooperativity. Biochemistry 32(1):260–267
39. Reddy BV, Kalraiya RD (2006) Sialilated beta1,6 branched N-oligosaccharides modulate adhesion, chemotaxis and motility of melanoma cells: effect on invasion and spontaneous metastasis properties. Biochim Biophys Acta 1760(9):1393–1402
40. Heussen C, Dowdle EB (1980) Electrophoretic analysis of plasminogen activators in polyacrylamide gels containing sodium dodecyl sulfate and copolymerized substrates. Anal Biochem 102(1):196–202
41. Dykxhoorn DM, Novina CD, Sharp PA (2003) Killing the messenger: short RNAs that silence gene expression. Nat Rev Mol Cell Biol 4(6):457–467
42. Guo HB et al (2008) Loss of expression of *N*-acetylglucosaminyltransferase Va results in altered gene expression of glycosyltransferases and galectins. FEBS Lett 582(4):527–535
43. Livak KJ, Schmittgen TD (2001) Analysis of relative gene expression data using real-time quantitative PCR and the 2(−Delta Delta C(T)) method. Methods 25(4):402–408
44. Nangia-Makker P et al (2002) Inhibition of human cancer cell growth and metastasis in nude mice by oral intake of modified citrus pectin. J Natl Cancer Inst 94(24):1854–1862
45. Zhou D (2003) Why are glycoproteins modified by poly-*N*-acetyllactosamine glyco-conjugates? Curr Protein Pept Sci 4(1):1–9
46. Daligault F et al (2009) Thermodynamic insights into the structural basis governing the donor substrate recognition by human beta1,4-galactosyltransferase 7. Biochem J 418(3):605–614
47. Sato T et al (2000) Correlated gene expression between beta-1,4-galactosyltransferase V and N-acetylglucosaminyltransferase V in human cancer cell lines. Biochem Biophys Res Commun 276(3):1019–1023
48. Shirane K et al (1999) Involvement of beta-1,4-galactosyltransferase V in malignant transformation-associated changes in glycosylation. Biochem Biophys Res Commun 265(2):434–438
49. John CM et al (2003) Truncated galectin-3 inhibits tumor growth and metastasis in orthotopic nude mouse model of human breast cancer. Clin Cancer Res 9(6):2374–2383
50. Pauli BU et al (1990) Organ-preference of metastasis. The role of endothelial cell adhesion molecules. Cancer Metastasis Rev 9(3):175–189
51. Nangia-Makker P, Balan V, Raz A (2008) Regulation of tumor progression by extracellular galectin-3. Cancer Microenviron 1(1):43–51
52. Elola MT et al (2007) Galectins: matricellular glycan-binding proteins linking cell adhesion, migration, and survival. Cell Mol Life Sci: CMLS 64(13):1679–1700
53. Barboni EA, Bawumia S, Hughes RC (1999) Kinetic measurements of binding of galectin 3 to a laminin substratum. Glycoconj J 16(7):365–373
54. Diskin S et al (2012) Galectin-8 promotes cytoskeletal rearrangement in trabecular meshwork cells through activation of Rho signaling. PLoS One 7(9):e44400
55. Alge-Priglinger CS et al (2009) Inhibition of human retinal pigment epithelial cell attachment, spreading, and migration by the human lectin galectin-1. Mol Vis 15:2162–2173
56. Deryugina EI, Quigley JP (2006) Matrix metalloproteinases and tumor metastasis. Cancer Metastasis Rev 25(1):9–34
57. Kim SJ et al (2011) Galectin-3 facilitates cell motility in gastric cancer by up-regulating protease-activated receptor-1 (PAR-1) and matrix metalloproteinase-1 (MMP-1). PLoS One 6(9):e25103
58. Kobayashi T et al (2011) Transient gene silencing of galectin-3 suppresses pancreatic cancer cell migration and invasion through degradation of beta-catenin. Int J Cancer 129(12):2775–2786
59. Zhang D et al (2013) Galectin-3 gene silencing inhibits migration and invasion of human tongue cancer cells in vitro via down-regulating beta-catenin. Acta Pharmacol Sin 34(1):176–184
60. Nangia-Makker P et al (2007) Galectin-3 cleavage: a novel surrogate marker for matrix metalloproteinase activity in growing breast cancers. Cancer Res 67(24):11760–11768
61. Saravanan C et al (2009) Galectin-3 promotes lamellipodia formation in epithelial cells by interacting with complex N-glycans on alpha3beta1 integrin. J Cell Sci 122(Pt 20):3684–3693
62. Hsu DK et al (2009) Endogenous galectin-3 is localized in membrane lipid rafts and regulates migration of dendritic cells. J Invest Dermatol 129(3):573–583
63. Wang LP et al (2013) Galectin-3 accelerates the progression of oral tongue squamous cell carcinoma via a Wnt/beta-catenin-dependent pathway. Pathol Oncol Res 19(3):461–474
64. Sano H et al (2000) Human galectin-3 is a novel chemoattractant for monocytes and macrophages. J Immunol 165(4):2156–2164
65. Delgado VM et al (2011) Modulation of endothelial cell migration and angiogenesis: a novel function for the "tandem-repeat" lectin galectin-8. FASEB J 25(1):242–254
66. Dennis JW, Granovsky M, Warren CE (1999) Glycoprotein glycosylation and cancer progression. Biochim Biophys Acta 1473(1):21–34
67. Przybylo M et al (2007) Identification of proteins bearing beta1-6 branched N-glycans in human melanoma cell lines from different progression stages by tandem mass spectrometry analysis. Biochim Biophys Acta 1770(9):1427–1435
68. Lau KS et al (2007) Complex N-glycan number and degree of branching cooperate to regulate cell proliferation and differentiation. Cell 129(1):123–134
69. Rabinovich GA et al (2007) Functions of cell surface galectin–glycoprotein lattices. Curr Opin Struct Biol 17(5):513–520
70. Glinsky VV, Raz A (2009) Modified citrus pectin anti-metastatic properties: one bullet, multiple targets. Carbohydr Res 344(14):1788–1791

J Cancer Res Clin Oncol
DOI 10.1007/s00432-015-1917-2

ORIGINAL ARTICLE – CANCER RESEARCH

Role of tumor cell surface lysosome-associated membrane protein-1 (LAMP1) and its associated carbohydrates in lung metastasis

Akhil Kumar Agarwal · Nithya Srinivasan · Rashmi Godbole · Shyam K. More · Srikanth Budnar · Rajiv P. Gude · Rajiv D. Kalraiya

Received: 17 June 2014 / Accepted: 12 January 2015

Abstract
Purpose Expression of lysosome-associated membrane protein-1 (LAMP1) on the surface correlates with metastatic potential of B16 melanoma cells. Downregulation of their expression in high metastatic (B16F10) cells reduced their surface expression and metastatic potential. Present investigations explore if overexpression of LAMP1 on the surface of low metastatic (B16F1) cells augment their metastatic ability, and if so, how?
Methods B16F1 cells were transduced with lentiviral vector carrying mutant-LAMP1 (Y386A) (mutLAMP1). Surface expression of LAMP1 and carbohydrates was analyzed by flow cytometry, immunofluorescence and/or immunoprecipitation and Western blotting. Cell spreading and motility were assessed on components of extracellular matrix (ECM) (fibronectin) and basement membrane (BM) (matrigel), and galectin-3-coated coverslips/plates. Metastatic potential was assessed using experimental metastasis assay.
Results Pre-incubation with anti-LAMP1 antibodies significantly reduced lung metastasis of B16F10 cells. Overexpression of mutLAMP1 significantly increased its surface expression on B16F1 cells, resulting in increased cellular spreading and motility on fibronectin and matrigel. LAMP1 is the major carrier of poly-*N*-acetyllactosamine (polyLacNAc) on B16F10 cells. However, significantly higher expression of mutLAMP1 had no effect on galectin-3 binding on cell surface or on spreading or motility of cells on galectin-3-coated coverslips/plates. These cells also failed to show any gain in metastatic ability. This could be because LAMP1 from these cells carried significantly lower levels of polyLacNAc in comparison with B16F10 cells.
Conclusions PolyLacNAc on B16F10 cells and galectin-3 on lungs are the major participants in melanoma metastasis. Although surface LAMP1 promotes interactions with organ ECM and BM, carbohydrates on LAMP1 play a decisive role in dictating lung metastasis.

Keywords Cell surface LAMP1 · Organ-specific metastasis · β1,6 branched N-oligosaccharides · Poly-*N*-acetyllactosamine · Galectin-3 · Motility

Electronic supplementary material The online version of this article (doi:10.1007/s00432-015-1917-2) contains supplementary material, which is available to authorized users.

A. K. Agarwal · N. Srinivasan · S. K. More · R. P. Gude · R. D. Kalraiya (✉)
Advanced Centre for Treatment, Research and Education in Cancer (ACTREC), Tata Memorial Centre, Sector 22, Kharghar, Navi Mumbai 410210, India
e-mail: rkalraiya@actrec.gov.in

R. Godbole
Proteomics Lab, Biochemical Sciences Division, CSIR-National Chemical Laboratory, Pune 411008, India

S. Budnar
Division of Molecular Cell Biology, Institute for Molecular Bioscience, The University of Queensland, St. Lucia, Brisbane, QLD 4072, Australia

Introduction

Metastasis, the major cause of mortality seen in cancer patients, is a complex multistep process involving detachment from the primary, invasion and intravasation, survival in circulation, extravasation and organ homing (Valastyan and Weinberg 2011). Most of the regional spread of tumors can be explained by anatomical/mechanical

Published online: 23 January 2015

mode of metastasis (Weiss 1992). However, the distant metastasis is generally organ-specific (Fidler 2003; Gupta and Massagué 2006; Nguyen et al. 2009). This involves one or all of the following factors, viz, adhesive interactions between the molecules on the surface of tumor cells and the target organ, organ growth microenvironment and, more recently, chemokines and their receptors that have been shown to play a critical role in organ-specific metastasis (Fidler 2003; Irmisch and Huelsken 2013; Poste and Nicolson 1980). Tumors often show several metastasis-associated cell surface modifications (Brooks et al. 2010; McGary et al. 2002). Expression of lysosome-associated membrane protein-1 (LAMP1) on the cell surface is one such modification where a lysosomal protein LAMP1 gets increasingly translocated to the surface of several metastatic tumor cells. LAMP-1 is a highly glycosylated protein which decorates the luminal side of lysosomes. Owing to the presence of highly substituted oligosaccharides, it is thought to protect itself and the lysosomal membranes from intracellular proteolysis (Fukuda 1991; Kundra and Kornfeld 1999). It has been shown to be expressed on surface of human melanoma, human colon carcinoma, human fibrosarcoma, human myelomonocytic leukemia and macrophage–melanoma fusion hybrid cells (Chakraborty et al. 2001; Mane et al. 1989; Sarafian et al. 1998). Its cell surface expression has been shown to correlate with metastatic potential of human colon carcinoma and murine melanoma cell lines (Krishnan et al. 2005; Saitoh et al. 1992). In addition to metastatic tumor cells, increased expression of LAMP1 (also known as CD107a) on the surface has also been observed on cells that are involved in migratory and/or invasive functions such as activated cytotoxic T lymphocytes, natural killer cells, platelets and macrophages as well as embryonic cells (Alter et al. 2004; Betts et al. 2003; Chakraborty et al. 2001; Cohnen et al. 2013; Febbraio and Silverstein 1990; Kannan et al. 1996; McCormick et al. 1998). However, the mechanism by which cell surface LAMP1 may mediate these functions is largely unknown.

Purified LAMP1 has been shown to bind to RGD peptides, ECM components such as fibronectin and collagen type I and BM components such as laminin and collagen type IV (Laferté and Dennis 1988), suggesting that surface LAMP1 might as well interact with organ ECM and BM components. Besides, LAMP1 has also been found to be a major carrier of poly-*N*-acetyllactosamine (polyLacNAc)-substituted β1,6 branched N-glycans (Dennis et al. 1987; Fukuda 1991; Krishnan et al. 2005). A transformation-related increase in β1,6 branching observed in fibroblasts, metastatic cell line SP1 and macrophage–melanoma fusion hybrids appeared to be associated with increased LAMP1 surface expression (Chakraborty et al. 2001; Heffernan et al. 1989). LAMP1 on cell surface has been shown to provide ligands in the form of sialyl-Le^x to E-selectin (Sawada et al. 1993; Tomlinson et al. 2000) and in the form of polyLacNAc to galectin-3 (Inohara and Raz 1994; Krishnan et al. 2005; Sarafian et al. 1998). LAMP1 has also been shown to be present on unique cell surface domains involved in cell locomotion such as membrane ruffles and microspikes (filopodia) (Garrigues et al. 1994). Further, its accumulation at the edges and extensions of A2058 human metastasizing melanoma cells (Sarafian et al. 1998) hints toward its potential role in tumor cell spreading and motility possibly by serving as additional receptors for molecules on ECM, BM and endothelium.

Using low (B16F1) and high (B16F10) metastatic variants of lung colonizing B16 murine melanoma cells (Hart and Fidler 1980), polyLacNAc-substituted β1,6 branched N-oligosaccharides were shown to promote metastasis of B16F10 cells to the lungs via galectin-3. In addition, LAMP1 was found to be a major carrier of these oligosaccharides in B16 melanoma cells. It was also shown that surface translocation of LAMP1, but not LAMP2, correlated with their metastatic potential (Krishnan et al. 2005). Recently, it was further shown that downregulation of LAMP1 significantly reduced expression of LAMP1 on the surface of B16F10 cells resulting in significant loss of their metastatic potential (Agarwal et al. 2014). LAMP1 has been shown to be a ligand for galectin-3 which is present in highest amounts in mice lungs and expressed constitutively on the surface of lung vascular endothelium (Krishnan et al. 2005).

However, it remains to be elucidated whether expression of LAMP1 protein alone on the cell surface is necessary and sufficient or it also requires glycosylation on LAMP1 especially in the form of polyLacNAc-substituted β1,6 branched N-oligosaccharides for efficient metastasis. The present paper, therefore, aims to investigate the effect of overexpression of LAMP1 on the surface of low metastatic B16F1 cells (deficient in glycosylation machinery) on their spreading and movement on components of ECM and BM together with that on galectin-3, and its bearing on their lung metastasis.

Materials and methods

Cell lines and reagents

B16F1 and B16F10 murine melanoma cell lines were obtained from National Centre for Cell Science, Pune, India. Cell culture reagents were obtained from Invitrogen,

USA. *Escherichia coli* BL 21 with pET3C plasmid containing a full-length human galectin-3 was a kind gift from Dr. Hakon Leffler, Lund University, Sweden. Purified rhgalectin-3 was biotinylated as described in (Bayer and Wilchek 1990). Inbred strains of C57BL/6 mice used for the metastatic assays and other experiments were maintained in the Institute Animal House, and all the animal experiments were approved by the Institutional Animal Ethics Committee.

Cell culture and experimental metastasis assay

Melanoma cells were routinely cultured in Dulbecco's Modified Eagle's Medium (DMEM) containing 10 % fetal bovine serum (FBS), 0.03 % glutamine, 10 units/ml of Penicillin G-sodium, 10 μg/ml of streptomycin sulfate and 25 μg/ml of amphotericin B. For treatment of cells with LAMP1 antibody, melanoma cells were harvested with 0.25 % trypsin, washed in serum-free DMEM and incubated with 10 μg/ml of LAMP1 antibody for 1 h at 4 °C. For metastasis assays, it was ensured that the cells existed as single cell suspension and had greater than 95 % viability and the assay was performed exactly as described in (Reddy and Kalraiya 2006). Briefly, cells (0.1 million for F10 + anti-LAMP1 experiment and 0.15 million for F1 + mutLAMP1 experiment, contained in 100 μl) were injected intravenously (i.v.) in inbred strains of female C57BL/6 mice via the lateral tail vein. The animals were sacrificed after 21 days, and melanoma colonies on the surface of the lungs were counted using a dissecting microscope.

Generation of mutLAMP1 (Y386A) clones and their transduction in B16F1 cells

Total RNA was prepared from B16F10 cells using TRIzol reagent, and cDNA was synthesized using cDNA synthesis kit (New England Biolabs, USA) as per manufacturer's protocol. LAMP1 was amplified from cDNA using forward primer having XhoI site (represented in bold italics) followed by Flag tag (represented in bold) and mouse LAMP1 N-terminal sequence (represented in italics): 5′-TAT***CTCGAG*** ATG**GATTACAAGGATGACGATGACAAG**GAATTC*AT GGCGGCCCCCGGCGCC*-3′ and reverse primer: 5′-GGAT CCCTAGATGGTCTGATAGCCGGCGTGACTCC-3′. The lentiviral vector generated previously, pLV-K18-YFP-IRES-Puro (Sehgal et al. 2012), was digested with XhoI and NotI restriction enzymes to remove K18-YFP and was either self-ligated to obtain empty vector control or ligated to the amplified mouse LAMP1 to generate wild-type LAMP1 (wtLAMP1) vector. The wtLAMP1 vector was further used for site-directed mutagenesis of tyrosine^{386} of wtLAMP1 to alanine to get mutant-LAMP1 (mutLAMP1) vector using site-directed mutagenesis kit (Stratagene, USA) as per manufacturer's protocol. The primers used for site-directed mutagenesis included: 5′-AGGAGTCACGCCGGC GCTCAGACCATCTAGGG-3′ and 5′-CCCTAGATGGTCT GAGCGCCGGCGTGACTCCT-3′. The vector control plasmid, the wtLAMP1 plasmid and the mutLAMP1 plasmid were purified and subsequently co-transfected with helper plasmids (pMD2.G and psPAX2) in HEK293FT cells, and infectious viruses containing empty vector control, wtLAMP1 and mutLAMP1 were generated as described previously (Ranjan and Kalraiya 2013) which were used for transduction of B16F1 cells using 8 μg/ml polybrene. The clones were stably selected using puromycin (1 μg/ml). One vector control clone (VC), one wtLAMP1 clone and two mutLAMP1 clones (C1 and C11) growing in the form of isolated colonies were selected. The selected clones were maintained at a concentration of 0.5 μg/ml puromycin.

Flow cytometric analysis of galectin-3 binding and surface expression of LAMP1

For flow cytometry of LAMP1, melanoma cells were stained with LAMP1 antibody (clone 1D4B, BD Biosciences, USA) as described previously (Krishnan et al. 2005). For determination of galectin-3 binding, melanoma cells were first fixed by overnight incubation with 1 % paraformaldehyde in PBS (pH 7.4) followed by galectin-3 staining as described previously for biotinylated LPHA (Krishnan et al. 2005). Briefly, 0.5 million melanoma cells were incubated with 30 μg of biotinylated rhgalectin-3 in 40 μl of FACS buffer (PBS pH 7.4, containing 1 % FBS) followed by extra-avidin-FITC (Sigma) diluted 1:25 in FACS buffer. Cells treated with extra-avidin-FITC alone served as control. Fluorescent cells were acquired at 488 nm and analyzed on FACSCalibur using CellQuest software (BD Biosciences).

Detection of expression of LAMP1 on the cell surface by immunofluorescence staining

Immunofluorescence staining was done as described in (Ranjan et al. 2014). Briefly, melanoma cells were seeded on coverslips and grown overnight in complete medium up to 70–80 % confluency. Cells were washed thrice with PBS (pH 7.4) and fixed with 2 % paraformaldehyde at RT for 5 min. They were washed again with PBS, blocked with 3 % BSA in PBS for 1 h at RT in humidified chamber and incubated with primary antibody (LAMP1) for 1 h in humidified chamber, followed by three washes with PBS to remove excess or non-specifically bound antibody. Cells were further incubated with

fluorescence-tagged secondary antibody (anti-rat FITC) for 1 h followed by three washes with PBS. Those incubated only with fluorescence-tagged secondary antibody served as isotype control. Nuclei were stained with 5 μg/ml of 4′,6′-diamidino-2-phenylindole dihydrochloride (DAPI) in PBS for 1 min, and coverslips were mounted on slides using vectashield mounting medium. Images were acquired using a Carl Zeiss laser confocal microscope at 63× magnification.

Purification of recombinant human galectin-3

Expression and purification of recombinant human (rh) galectin-3 was carried out exactly as described previously (Krishnan et al. 2005).

Cell spreading assays

Cell spreading assays were done as per (Lagana et al. 2006). Briefly, melanoma cells were harvested, washed free of serum and seeded at a cell density of 0.5 million/ml in serum-free DMEM on the coverslips coated overnight with 75 μg/ml galectin-3, 10 μg/ml fibronectin and matrigel (BD Biosciences, USA) in serum-free DMEM at 4 °C. The cells were incubated for 45 min in a CO_2 incubator. Coverslips treated with serum-free DMEM only served as control. Bound cells were fixed in 4 % paraformaldehyde, permeabilized with 0.5 % Triton X-100 for 15 min and stained with 2 μg/ml Phalloidin-FITC staining solution made in PBS (containing 1 μg/ml of lysolecithin, 10 % methanol, 0.5 % BSA) (Lagana et al. 2006) for 15 min at 37 °C. Nuclei were stained with 5 μg/ml of DAPI in PBS for 1 min. The stained cells were mounted, and images were acquired using a Carl Zeiss laser confocal microscope at 63× magnification.

Wound-healing assays

For wound-healing assays, six well culture dishes were coated overnight with 75 μg/ml of galectin-3, 10 μg/ml of fibronectin and matrigel in serum-free DMEM at 4 °C, followed by blocking of non-specific sites with 2 % BSA for 1 h. Melanoma cells were harvested, seeded at a density of 0.5 million cells per ml of complete medium and incubated at 37 °C for 24 h in a CO_2 incubator. The cells were treated with 40 μg/ml mitomycin C (Sigma) for 3 h for inhibiting cell proliferation. A straight, uniform wound (approx. 400 μm in width) was made using a micropipette tip on the monolayer, and the cells were maintained in serum-free DMEM. Wound closure of cells in response to the immobilized galectin-3, fibronectin and matrigel was measured for 16 h by time lapse video imaging of at least three different positions across the length of the wound using a Carl Zeiss inverted microscope at 10x magnification. Uncoated wells, blocked only with BSA, served as control.

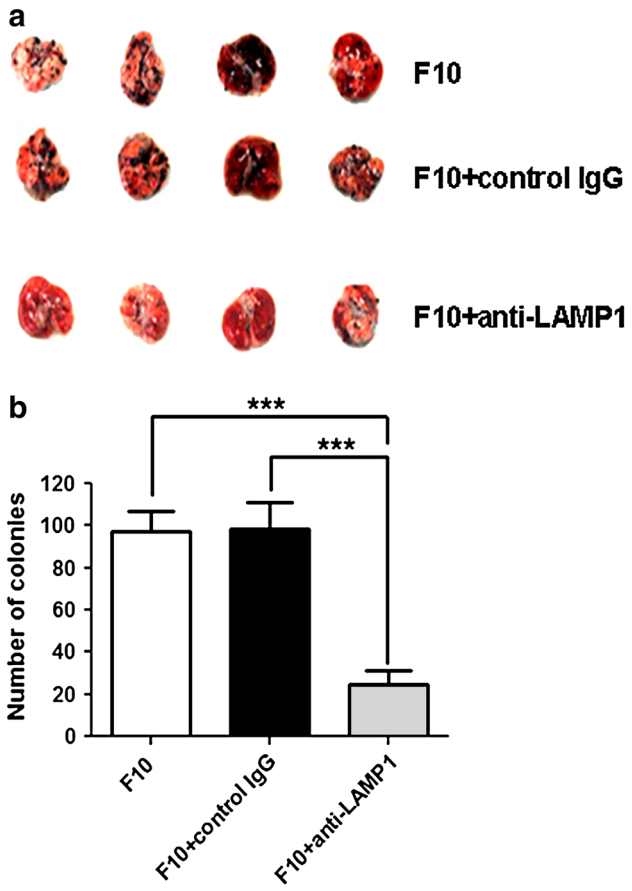

Fig. 1 Cell surface LAMP1 plays an important role in lung-specific metastasis. **a** Melanoma colonies on lungs of C57BL/6 mice injected with untreated B16F10 cells (F10), and those treated with 10 μg/ml of either control rat IgG (F10 + control IgG) or blocking antibodies to LAMP1 (F10 + anti-LAMP1). Four mice were taken in each group. **b** Graphical representation of mean number of lung colonies. One-way analysis of variance followed by Bonferroni's multiple comparison test was performed to compare significance (denoted by ***p value <0.001)

Preparation of total cell lysates, protein estimation, SDS-PAGE and Western blotting

Preparation of total cell lysates, protein estimation, SDS-PAGE and Western blotting was done exactly as described previously (Krishnan et al. 2005).

Immunoprecipitation of LAMP1

Total cell lysate (2 mg) was precleared and later incubated at RT for 2 h with 20 μg of anti-LAMP1 antibody. This was followed by addition of 200 μl of protein G

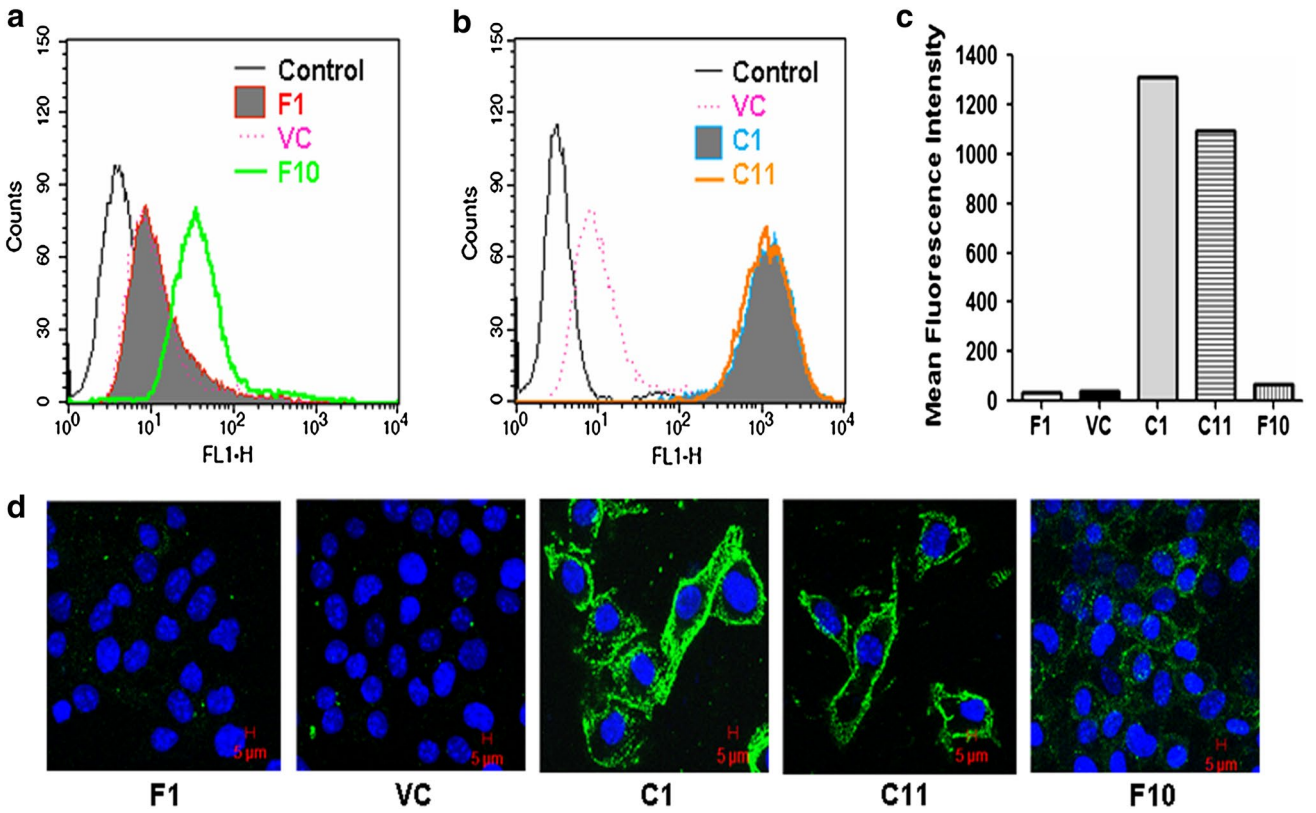

Fig. 2 Analysis of LAMP1 expression on the surface of melanoma cells. Comparison of surface expression of LAMP1 by flow cytometry, in **a** B16F1 cells (*gray shade* F1), B16F1 cells infected with viruses having empty vector control (*pink dotted lines* VC) and B16F10 cells (*green solid lines* F10) and **b** comparison of the same between vector control (*pink dotted lines* **VC**) and B16F1 clones expressing mutLAMP1 (*gray shade* C1) and (*orange solid lines* C11). Cells treated with only anti-rat FITC served as control (—). The flow cytometry overlays have been split into two for better understanding of the data. **c** Graphical representation of the mean fluorescence intensities of surface LAMP1 of the cells shown in **a** and **b**. **d** Immunofluorescence images of the cells stained with anti-LAMP1 antibody and FITC-labelled secondary antibody (*green*). Nuclei were stained with DAPI (*blue*). *Scale bar* 5 μm

Sepharose beads (50 % suspension) (GE Healthcare, Amersham, UK) and incubation overnight at 4 °C. The beads were pelleted at 2,000 rpm for 10 min and later washed five times with 1 ml of lysis buffer. The bound proteins were eluted by boiling the beads in 1× Laemmli sample buffer for 5 min, separated on SDS-PAGE, Western blotted and probed with LAMP1 antibody and with biotinylated LPHA or LEA (Vector Labs, USA) as described previously (Krishnan et al. 2005).

Statistical analysis

All the data are represented as mean ± SD unless stated. All the statistical analysis was performed using GraphPad Prism 5. For spreading and experimental metastasis assays, comparison within the group was done by performing one-way ANOVA followed by Bonferroni's multiple comparison test. For wound-healing assays, two-way ANOVA with the Bonferroni posttest was conducted. (p value <0.05 was considered significant).

Results

Blocking cell surface LAMP1 with specific antibodies inhibits lung metastasis of B16F10 cells

Expression of LAMP1 on the cell surface correlates with metastatic potential of B16 melanoma cells, and down-regulation of their expression in high metastatic B16F10 cells inhibited their metastasis. To understand how surface LAMP1 possibly participates in metastasis, B16F10 cells were pre-treated with LAMP1-specific antibodies to make it unavailable for interaction, and its effect on metastasis was assessed. Untreated cells or those treated with pre-immune IgG served as controls. Pre-treatment with anti-LAMP1 antibody significantly reduced the metastatic ability of cells as compared to controls (Fig. 1a, b) confirming that surface LAMP1 indeed plays a key role in imparting metastatic phenotype. To explore the possible mechanism by which LAMP1 facilitates interactions with molecules on lungs, B16F1 cells were transduced with mutLAMP1 (Y386A).

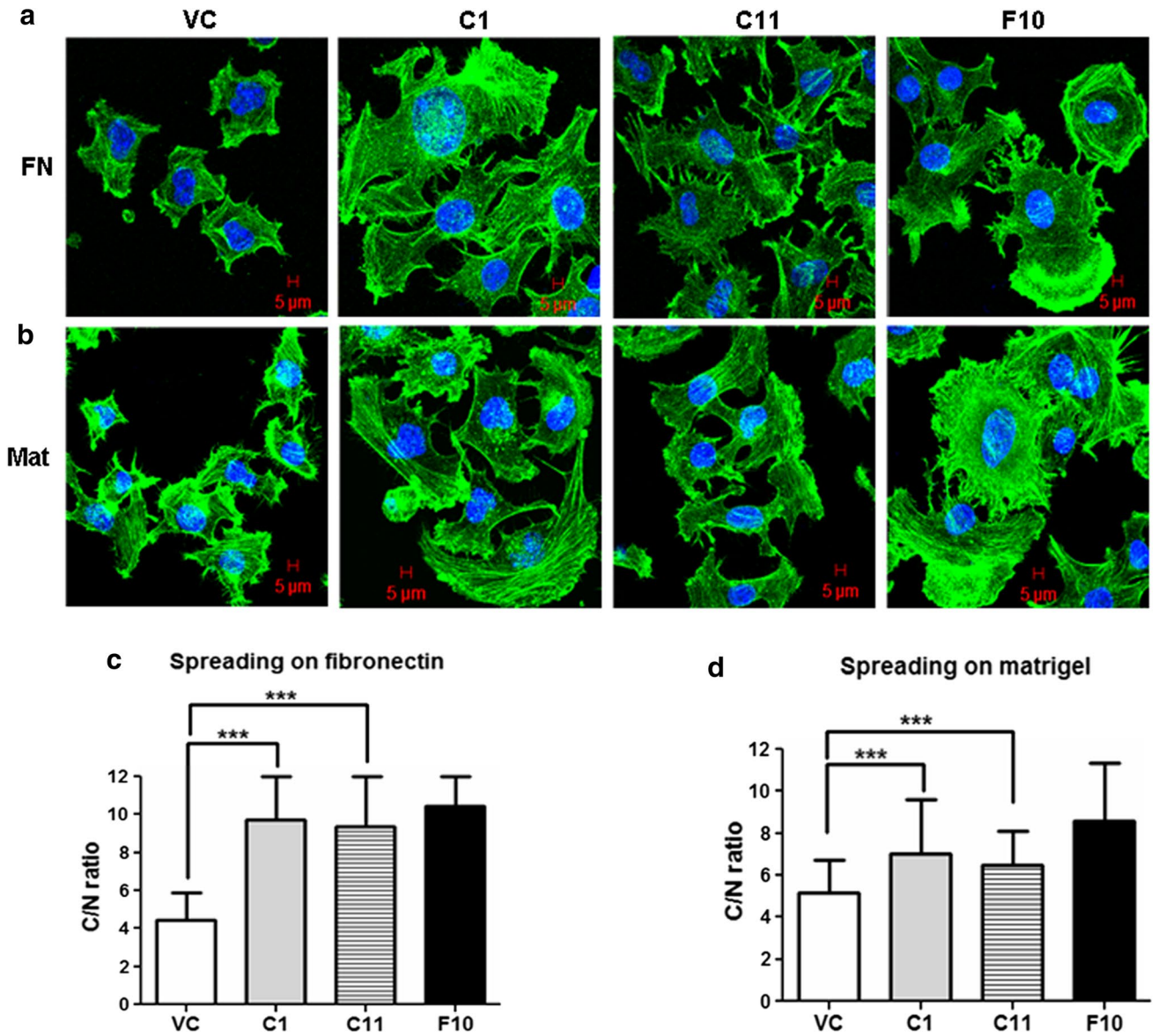

Fig. 3 Effect of increased surface expression of LAMP1 on spreading of melanoma cells on fibronectin and matrigel. Spreading of B16F1 cells infected with viruses having empty vector (VC) or those having mutLAMP1 (C1 and C11) and F10 cells on **a** fibronectin (FN) and **b** matrigel (Mat)-coated coverslips as assessed by staining with Phalloidin-FITC (*green*). DAPI was used to stain the nuclei (*blue*). *Scale bar* 5 µm. **c** Each *bar* represents ratio of cytoplasmic to nuclear (*C*/*N*) area for around 100 cells from two different experiments for spreading on fibronectin (FN) and **d** for spreading on matrigel (Mat). One-way analysis of variance followed by Bonferroni's multiple comparison test was performed to compare significance (denoted by ***p value <0.001)

Expression of mutLAMP1 (Y386A) in B16F1 cells results in elevated expression of LAMP1 on the cell surface

Mutation in a specific region (Tyr^{386}) of the cytoplasmic tail of LAMP1 has been shown to direct them to cell surface instead of lysosomes (Williams and Fukuda 1990). Stable expression of this mutLAMP1 (Tyr^{386} to Ala^{386}) by lentiviral infection of B16F1 cells resulted in significantly higher surface expression of LAMP1 in both the clones (C1 and C11) as compared to either uninfected (F1) or those infected with virus with vector alone (vector control—VC). The surface expression of LAMP1 in the clones C1 and C11 was several folds higher even when compared to B16F10 (F10) cells as observed by both flow cytometry (Fig. 2a–c) and immunofluorescence (Fig. 2d). The impact of increased surface expression of LAMP1 on the cellular properties, important from the point of view of metastasis, was explored.

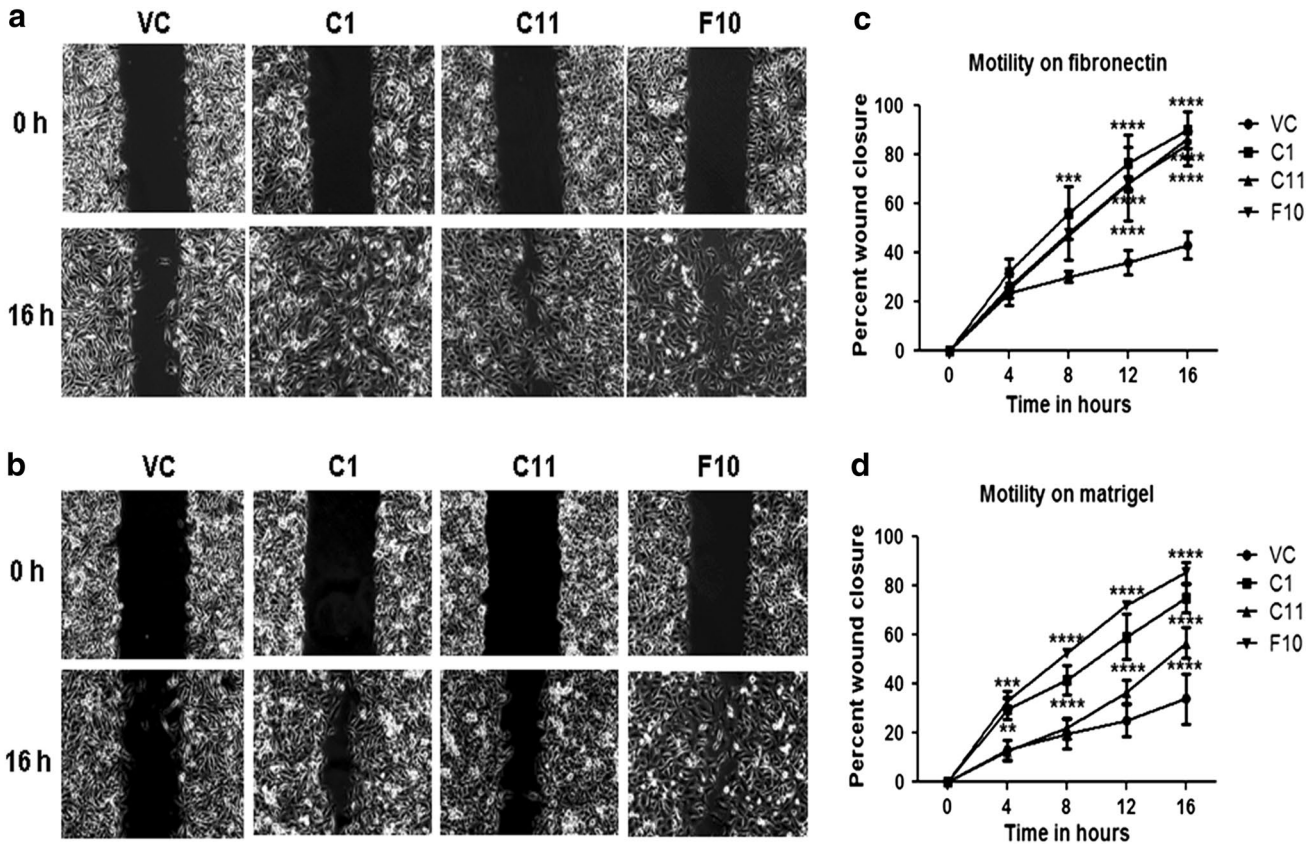

Fig. 4 Effect of increased surface expression of LAMP1 on motility of melanoma cells on fibronectin and matrigel. Motility of B16F1 cells infected with viruses having empty vector (VC) or those having mutLAMP1 (C1 and C11) and F10 cells on **a** fibronectin and **b** matrigel-coated plates as represented by time lapse video microscopy images at 0 and 16 h of wound closure. **c**, **d** Represent mean percent wound closure at 4-h interval on fibronectin and matrigel, respectively. Area of wound closure was measured by Image J software and each image from two different experiments was analyzed at three different positions. Two-way analysis of variance followed by Bonferroni's multiple comparison test was performed to compare significance from VC (denoted by ****p value <0.0001, ***p value <0.001)

Increased surface expression of LAMP1 on B16F1 cells results in significantly increased spreading and motility on fibronectin and matrigel

Purified LAMP1 has been shown to have an affinity for ECM and BM components (Laferté and Dennis 1988). It is possible that the LAMP1 overexpressed on the surface is used as an alternate receptor for these components. The clones overexpressing LAMP1 on the cell surface indeed showed significantly higher spreading on both fibronectin (ECM component) and matrigel (reconstituted BM) as compared to vector control (VC), as seen by laser confocal microscopic images (Fig. 3a, b) and by analyzing ratios of the cytoplasmic to nuclear areas (Fig. 3c, d). The clones also showed much higher motility on these substrates as measured by wound-healing assay (Fig. 4a, c for fibronectin, Fig. 4b, d for matrigel). The results strongly indicate that the increased surface LAMP1 may alter the cellular properties of cells which might eventually be important for metastasis. Wild-type LAMP1 (WT) was also overexpressed in B16F1 cells (Supplementary Fig. S1). But since its expression did neither affect the surface expression of LAMP1 (Supp Fig. S1a and b) nor affect the spreading of melanoma cells on fibronectin (Supp Fig. S1c) to a significant extent as compared to VC, it was not used for further studies.

Increased expression of LAMP1 on the surface of B16F1 cells had no effect on their spreading and motility on galectin-3

LAMP1 is a major carrier of polyLacNAc and is a known ligand for galectin-3. Secreted galectin-3 often becomes part of the ECM, BM and even the cell surface (Liu and Rabinovich 2005) and is used as a substratum for cellular adhesion, spreading and movement. Surprisingly, the increased surface expression of LAMP1 had no effect on spreading of these cells (C1 and C11) on galectin-3 as

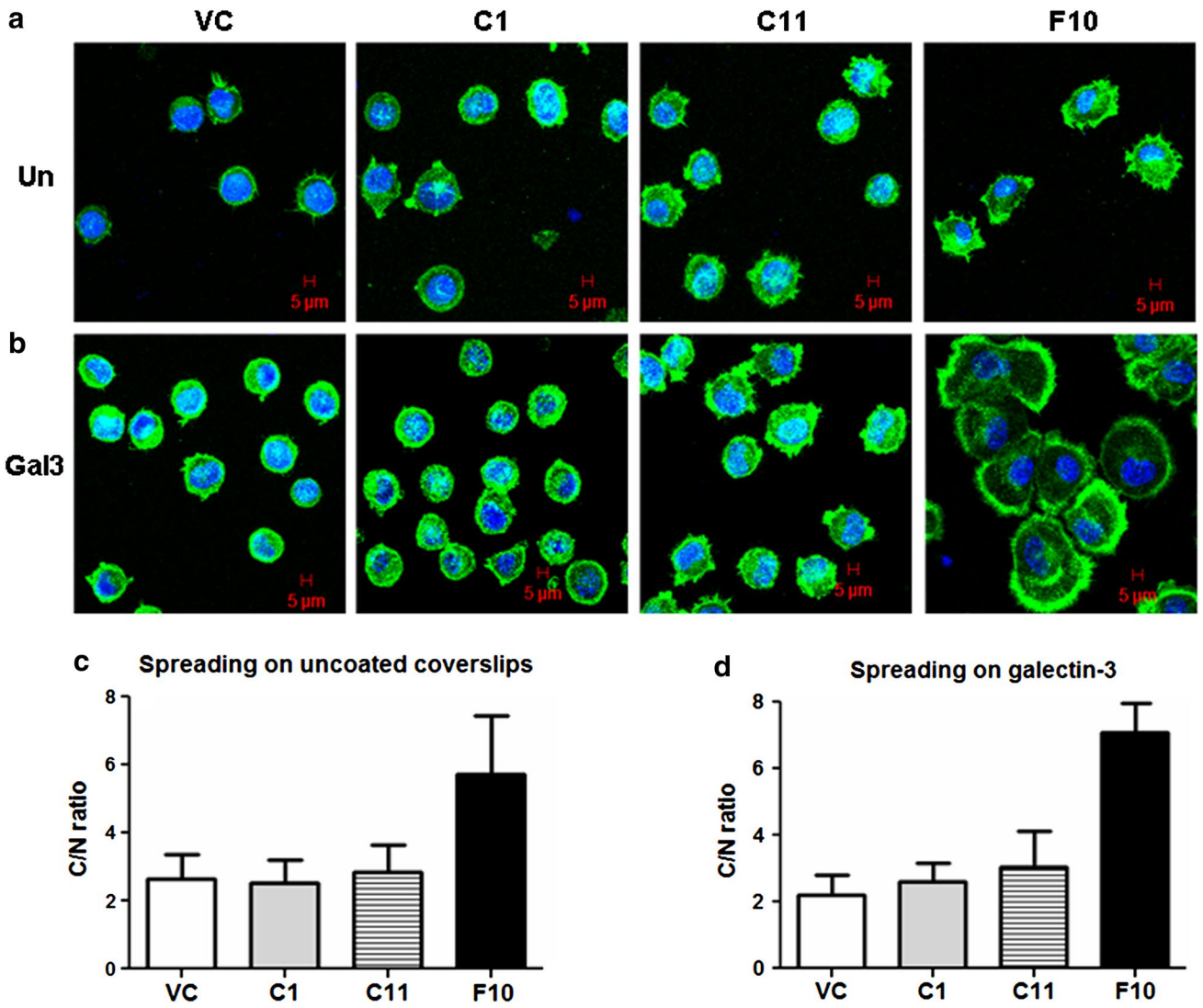

Fig. 5 Effect of increased surface expression of LAMP1 on spreading of melanoma cells on galectin-3. Spreading of B16F1 cells infected with viruses having empty vector (VC) or those having mutLAMP1 (C1 and C11) and F10 cells on **a** uncoated (Un) and **b** galectin-3 (Gal3)-coated coverslips as assessed by staining with Phalloidin-FITC (*green*). DAPI was used to stain the nuclei (*blue*). *Scale bar* 5 µm. **c**, **d** Each *bar* represents ratio of cytoplasmic to nuclear (*C/N*) area for around 100 cells from two different experiments for spreading on uncoated **c** and galectin-3-coated coverslips **d**. One-way analysis of variance followed by Bonferroni's multiple comparison test was performed to compare significance

compared to the vector control cells (VC), and the spreading was very similar to that seen on uncoated coverslips, as seen by laser confocal microscopic images (Fig. 5a, b) and quantitated by ratios of cytoplasmic to nuclear areas (Fig. 5c, d). Besides, motility of these cells (C1 and C11) was also almost similar to vector control cells (VC) in the presence of either BSA (Fig. 6a, c) or immobilized galectin-3 (Fig. 6b, d). The lack of any effect is possibly because of low levels of polyLacNAc substitutions as they have been shown to be the major participants in galectin-3-mediated processes.

Increased surface expression of LAMP1 neither increases galectin-3 binding to B16F1 cells nor increases their metastatic potential

LAMP1 is a highly glycosylated molecule and is a major carrier of polyLacNAc. In spite of >20-fold increase in expression of LAMP1 on the surface of clones C1 and C11 as compared to even B16F10 cells (Fig. 2c), it did not result in any gain of their metastatic potential as compared to the parent B16F1 cells (Fig. 7a). Moreover, the binding of galectin-3 to these cells also remained largely unaltered

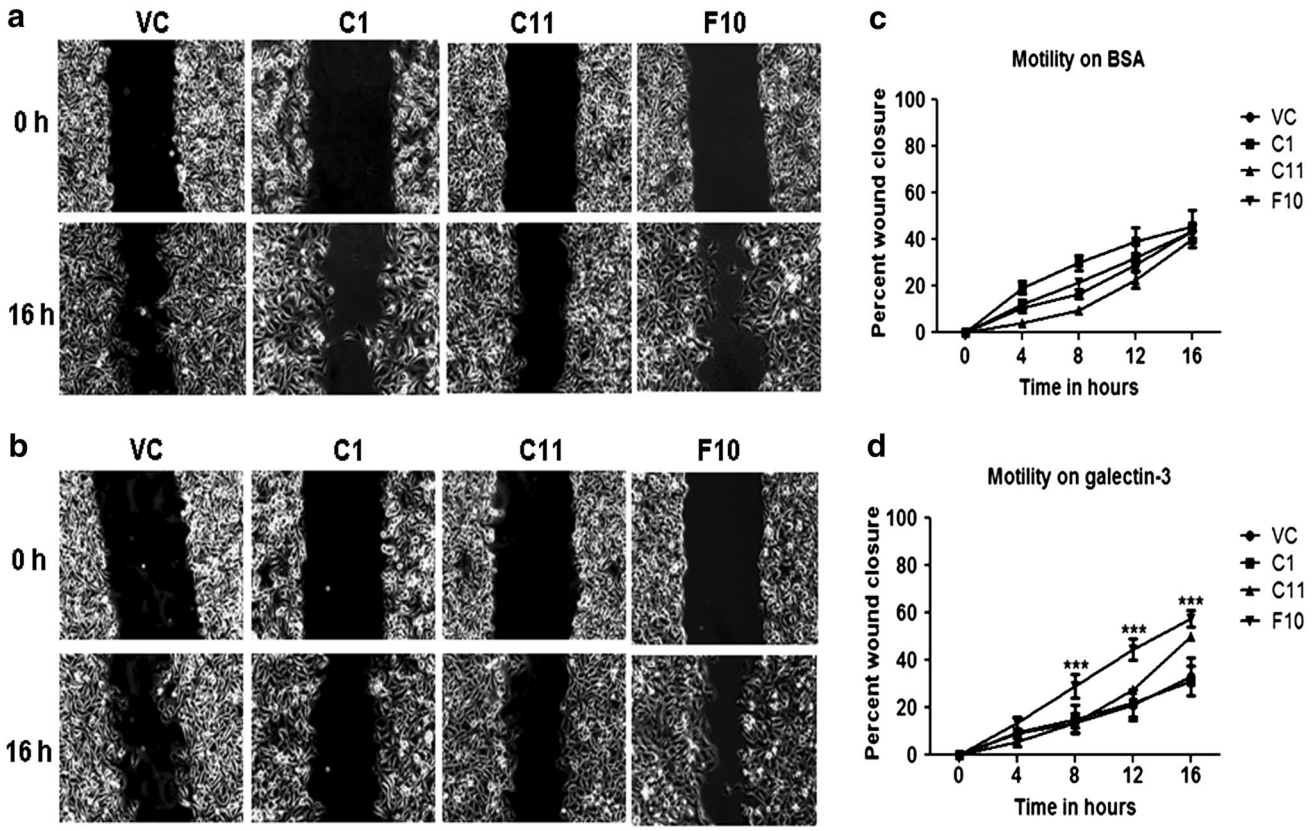

Fig. 6 Effect of increased surface expression of LAMP1 on motility of melanoma cells on galectin-3. Motility of B16F1 cells infected with viruses having empty vector (VC) or those having mutLAMP1 (C1 and C11) and F10 cells on **a** BSA and **b** galectin-3-coated plates as represented by time lapse video microscopy images at 0 and 16 h of wound closure. **c**, **d** Represent mean percent wound closure at 4-h interval on BSA and galectin-3, respectively. Area of wound closure was measured by Image J software and each image from two different experiments was analyzed at three different positions. Two-way analysis of variance followed by Bonferroni's multiple comparison test was performed to compare significance from VC (denoted by ***p value <0.001)

(Fig. 7b, c). Immunoprecipitation experiment revealed that β1,6 branched N-oligosaccharides and polyLacNAc (probed with LPHA and LEA, respectively) on LAMP1 from VC and C1 cells were comparable and were much lower as compared to that present on LAMP1 from F10 cells (Fig. 7d). This clearly suggests that carbohydrates on LAMP1 may play a crucial role in lung metastasis.

Discussion

Expression of LAMP1 on the cell surface correlates with metastatic potential of B16 melanoma cells, and down-regulation of its expression results in its decreased surface expression and concomitantly decreased metastasis (Agarwal et al. 2014; Krishnan et al. 2005). LAMP1 on the cell surface possibly facilitates metastasis by providing high density of high affinity ligands for galectin-3 expressed in highest amounts on the lungs and constitutively on its vascular endothelium, or by interacting with specific ECM/BM molecules on the lungs. Its importance in the metastatic process was further confirmed when B16F10 cells pre-incubated with LAMP1-specific antibodies showed significantly reduced metastatic potential (Fig. 1). Binding of these antibodies possibly prevented LAMP1 from interacting with such molecules on the lungs.

Although our previous results point toward the role of polyLacNAc-substituted N-oligosaccharides on LAMP1 in the metastatic process (Agarwal et al. 2014), purified LAMP1 has also been shown to have an affinity for several ECM and BM components such as fibronectin, laminin, collagen-I and IV and even RGD peptides (Laferté and Dennis 1988). On the cytoplasmic end, LAMP1 has been shown to interact with ezrin (Federici et al. 2009) which functions as a linker between the actin cortical cytoskeleton and various membrane-bound molecules (Bretscher et al. 2002; Neisch and Fehon 2011). This may influence cellular properties important for motility. It is thus possible that both LAMP1 protein and the carbohydrates on it contribute in influencing the metastatic process.

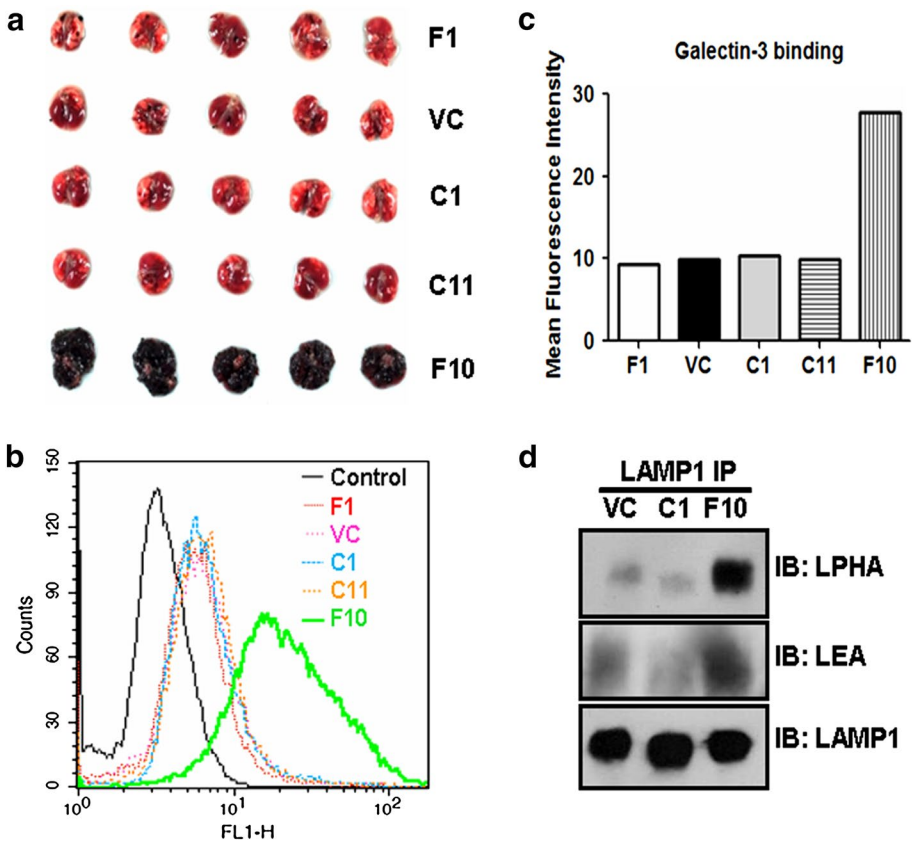

Fig. 7 Increased surface expression of LAMP1 on B16F1 cells has no effect on lung metastasis. **a** Melanoma colonies on lungs of C57BL/6 mice injected with F1, VC, C1, C11 and F10 cells. Five mice were taken in each group. **b** Comparison of galectin-3 binding by flow cytometry using biotinylated galectin-3 in uninfected B16F1 cells (*red dotted lines* F1) or those infected with viruses having empty vector as control (*pink dotted lines* VC) with B16F1 clones expressing mutLAMP1 (*blue dotted lines* C1) and (*orange dotted lines* C11) and with B16F10 cells (*green solid line* F10). Cells treated with only extra-avidin FITC (—) served as control. **c** Graphical representation of the mean fluorescence intensities of galectin-3 binding of all the cells. **d** Comparison of β1,6 branched N-oligosaccharides (LPHA) and polyLacNAc (LEA) on normalized amounts of immunoprecipitated LAMP1 from B16F10 (F10) cells and B16F1 cells having either empty vector (VC) or mutLAMP1 (C1), by Western blotting

The low metastatic B16F1 cells that express much lower levels of both surface LAMP1 and polyLacNAc-substituted β1,6 branched N-oligosaccharides provide a perfect system to investigate the role of LAMP1 and its associated oligosaccharides, in the metastatic process. Transduction of mutLAMP1 in B16F1 cells provided an ideal model to explore the mechanism by which LAMP1 may influence metastasis, as it resulted in significantly higher expression on the cell surface. These cells expressed >20-fold higher expression of LAMP1 on the cell surface as compared to even B16F10 cells (Fig. 2). Considerably increased expression of LAMP1 on cell surface resulted in significant increase in their spreading and motility on both fibronectin (ECM) and matrigel (BM) (Figs. 3, 4). Although integrins are the known receptors for such components, this is the first report which shows that LAMP1 expressed in such higher amounts on the surface could influence these cellular properties and the underlying mechanism would be worth investigating.

Alternatively, LAMP1 may also promote interactions with molecules on the target organ via high levels of glycosylated structures on it. LAMP1 is a highly glycosylated protein. More than 60 % of its weight is contributed by carbohydrates. Each LAMP1 molecule carries 17–20 N-glycosylation sites that are often substituted further with structures such as Lewis antigens and polyLacNAc (Fukuda 1991). As major portion of LAMP1 is extracellular, it may provide ligands for endogenous lectins such as selectins and galectin-3 expressed on the organ vascular endothelium, in an easily accessible manner (Häuselmann and Borsig 2014).

Lungs express highest amounts of galectin-3 and express it on all the major compartments of the lungs including constitutive expression on the surface of its vascular endothelium (Dange et al. 2014; Krishnan et al. 2005). Previously, polyLacNAc-substituted β1,6 branched N-oligosaccharides have been shown to facilitate lung metastasis by anchoring

on to galectin-3 on organ endothelium (Krishnan et al. 2005). More recently, we showed that this lectin carbohydrate pair may participate in not just anchoring, but in all the subsequent steps of extravasation such as spreading to stabilize adhesion, degradation of ECM/BM and movement into organ parenchyma (Dange et al. 2014). It has also been shown that polyLacNAc-substituted N- and not O-oligosaccharides participate in all these processes and shRNA-mediated inhibition of polyLacNAc synthesis inhibits these processes including lung metastasis (Dange et al. 2014; Srinivasan et al. 2009).

PolyLacNAc is the most preferred ligand for galectin-3, and LAMP1 was shown to be one of the major carriers of polyLacNAc on high metastatic B16F10 cells. Moreover, the levels of polyLacNAc-substituted β1,6 branched N-oligosaccharides on LAMP1 per se have been shown to correlate with the metastatic potential of melanoma cells (Krishnan et al. 2005). Further, glycosylation in these cells has also been shown to modulate the surface expression of LAMP1 (Agarwal and Kalraiya 2014). Downregulation of LAMP1 in B16F10 cells has been shown to affect the galectin-3-mediated cellular processes and their metastatic potential (Agarwal et al. 2014). Overexpression of surface LAMP1 on B16F1 cells thus may also influence galectin-3-mediated metastatic processes.

However, B16F1 clones overexpressing LAMP1 on the cell surface showed neither enhanced spreading nor motility on galectin-3-coated surfaces (Figs. 5, 6). Even the ability to metastasize to lungs remained unaltered (Fig. 7a). In spite of >20-fold higher surface expression of LAMP1, binding of galectin-3 to the clones overexpressing surface LAMP1 remained unaltered and was much lower as compared to B16F10 cells (Fig. 7b, c). Since galectin-3-mediated effects are dependent on galectin-3-polyLacNAc interactions, it was plausible to think that each LAMP1 molecule expressed on cell surface might not have adequate polyLacNAc units. Immunoprecipitation experiments indeed confirmed that there was no increase in β1,6 branched N-glycans and polyLacNAc (Fig. 7d) on LAMP1 molecules from these cells which was significantly lower as compared to that on LAMP1 from B16F10 cells. The low levels of polyLacNAc-substituted β1,6 branched N-oligosaccharides on LAMP1 in these cells could be due to limitation in availability of enzymes that add β1,6 branch and polyLacNAc in B16F1 cells (Dange et al. 2014; Srinivasan et al. 2009). Although increasing expression of such enzymes in B16F1 cells may increase their metastatic potential, it would be difficult to attribute it solely to the carbohydrates on LAMP1, as they would glycosylate several other surface proteins as well. The present study thus clearly demonstrates that although increased surface expression of LAMP1 may aid in mediating interactions with the ECM and BM components, it has no influence on melanoma metastasis to the lungs unless it carries high density of ligands (polyLacNAc) for galectin-3.

Conclusions

Metastasis being a multistep process, only cells proficient in all the steps of metastasis are able to metastasize. Cells deficient in mediating even one of these critical events are unable to metastasize, which is often referred to as metastatic inefficiency (Fidler 2003; Weiss 1990). These studies demonstrate that interaction of polyLacNAc on surface LAMP1 with galectin-3 on organ endothelium may be a critical rate-limiting step in the arrest and metastasis of melanoma cells to the lungs. In spite of gaining additional characteristics of interacting with organ ECM and BM, unless proficient in getting arrested in target organ endothelium, the cells fail to metastasize.

Acknowledgments We thank Dr. Hakon Leffler, Lund University, Sweden, for the expression vector for rhgalectin-3 and National Centre for Cell Science, Pune, for the melanoma cell lines. We acknowledge the help extended by Mrs. Vaishali Kailaje, Mrs. Tanuja Durve, Mrs. Mansi Samarth and Mr. Jayraj Kasale for laser confocal and inverted microscopy, Mrs. Rekha Gour and Ms. Shamal Vetale for flow cytometry, Mr. D. S. Chavan and Mr. A. M. Pawar for technical help and Mr. Sanjay Bane for the help in experimental metastasis and immunoprecipitation experiments. We acknowledge the financial assistance in the form of Senior Research Fellowship to Mr. Akhil Kumar Agarwal, Ms. Nithya Srinivasan and Mr. Shyam K, and more from Council for Scientific and Industrial Research (CSIR), Government of India and Department of Biotechnology (DBT), Government of India for funding the project.

Conflict of interest We declare that we have no conflict of interest.

References

Agarwal AK, Kalraiya RD (2014) Glycosylation regulates the expression of Lysosome Associated Membrane Protein-1 (LAMP1) on the cell surface. J Biosci Technol 5:556–563

Agarwal AK, Gude RP, Kalraiya RD (2014) Regulation of melanoma metastasis to lungs by cell surface Lysosome Associated Membrane Protein-1 (LAMP1) via galectin-3. Biochem Biophys Res Commun 449:332–337

Alter G, Malenfant JM, Altfeld M (2004) CD107a as a functional marker for the identification of natural killer cell activity. J Immunol Methods 294:15–22

Bayer EA, Wilchek M (1990) Protein biotinylation. Methods Enzymol 184:138–160

Betts MR, Brenchley JM, Price DA, De Rosa SC, Douek DC, Roederer M, Koup RA (2003) Sensitive and viable identification of antigen-specific CD8+ T cells by a flow cytometric assay for degranulation. J Immunol Methods 281:65–78

Bretscher A, Edwards K, Fehon RG (2002) ERM proteins and merlin: integrators at the cell cortex. Nat Rev Mol Cell Biol 3:586–599

Brooks SA, Lomax-Browne HJ, Carter TM, Kinch CE, Hall D (2010) Molecular interactions in cancer cell metastasis. Acta Histochem 112:3–25

Chakraborty AK et al (2001) Fusion hybrids with macrophage and melanoma cells up-regulate N-acetylglucosaminyltransferase V, β1-6 branching, and metastasis. Cell Growth Differ 12:623–630

Cohnen A et al (2013) Surface CD107a/LAMP-1 protects natural killer cells from degranulation-associated damage. Blood 122:1411–1418

Dange MC et al (2014) Galectin-3 expressed on different lung compartments promotes organ specific metastasis by facilitating arrest, extravasation and organ colonization via high affinity ligands on melanoma cells. Clin Exp Metastasis 31:661–673

Dennis JW, Laferte S, Waghorne C, Breitman ML, Kerbel RS (1987) Beta 1-6 branching of Asn-linked oligosaccharides is directly associated with metastasis. Science 236:582–586

Febbraio M, Silverstein R (1990) Identification and characterization of LAMP-1 as an activation-dependent platelet surface glycoprotein. J Biol Chem 265:18531–18537

Federici C et al (2009) Pleiotropic function of ezrin in human metastatic melanomas. Int J Cancer 124:2804–2812

Fidler IJ (2003) The pathogenesis of cancer metastasis: the 'seed and soil'hypothesis revisited. Nat Rev Cancer 3:453–458

Fukuda M (1991) Lysosomal membrane glycoproteins. Structure, biosynthesis, and intracellular trafficking. J Biol Chem 266:21327–21330

Garrigues J, Anderson J, Hellstrom K, Hellstrom I (1994) Anti-tumor antibody BR96 blocks cell migration and binds to a lysosomal membrane glycoprotein on cell surface microspikes and ruffled membranes. J Cell Biol 125:129–142

Gupta GP, Massagué J (2006) Cancer metastasis: building a framework. Cell 127:679–695

Hart IR, Fidler IJ (1980) Role of organ selectivity in the determination of metastatic patterns of B16 melanoma. Cancer Res 40:2281–2287

Häuselmann I, Borsig L (2014) Altered tumor-cell glycosylation promotes metastasis. Front Oncol 4:28

Heffernan M, Yousefi S, Dennis JW (1989) Molecular characterization of P2B/LAMP-1, a major protein target of a metastasis-associated oligosaccharide structure. Cancer Res 49:6077–6084

Inohara H, Raz A (1994) Identification of human melanoma cellular and secreted ligands for galectin-3. Biochem Biophys Res Commun 201:1366–1375

Irmisch A, Huelsken J (2013) Metastasis: new insights into organ-specific extravasation and metastatic niches. Exp Res 319:1604–1610

Kannan K, Stewart RM, Bounds W, Carlsson SR, Fukuda M, Betzing KW, Holcombe RF (1996) Lysosome-associated membrane proteins h-LAMP1 (CD107a) and h-LAMP2 (CD107b) are activation-dependent cell surface glycoproteins in human peripheral blood mononuclear cells which mediate cell adhesion to vascular endothelium. Cell Immunol 171:10–19

Krishnan V, Bane SM, Kawle PD, Naresh KN, Kalraiya RD (2005) Altered melanoma cell surface glycosylation mediates organ specific adhesion and metastasis via lectin receptors on the lung vascular endothelium. Clin Exp Metastasis 22:11–24

Kundra R, Kornfeld S (1999) Asparagine-linked oligosaccharides protect Lamp-1 and Lamp-2 from intracellular proteolysis. J Biol Chem 274:31039–31046

Laferté S, Dennis JW (1988) Glycosylation-dependent collagen-binding activities of two membrane glycoproteins in MDAY-D2 tumor cells. Cancer Res 48:4743–4748

Lagana A, Goetz JG, Cheung P, Raz A, Dennis JW, Nabi IR (2006) Galectin binding to Mgat5-modified N-glycans regulates fibronectin matrix remodeling in tumor cells. Mol Cell Biol 26:3181–3193

Liu F-T, Rabinovich GA (2005) Galectins as modulators of tumour progression. Nat Rev Cancer 5:29–41

Mane SM, Marzella L, Bainton DF, Holt VK, Cha Y, Hildreth JE, August JT (1989) Purification and characterization of human lysosomal membrane glycoproteins. Arch Biochem Biophys 268:360–378

McCormick PJ, Bonventre EJ, Finneran A (1998) LAMP-1/ESG p appears on the cell surface of single celled mouse embryos subsequent to fertilization. In Vitro Cell Dev Biol Anim 34:353–355

McGary EC, Lev DC, Bar-Eli M (2002) Cellular adhesion pathways and metastatic potential of human melanoma. Cancer Biol Ther 1:454–459

Neisch AL, Fehon RG (2011) Ezrin, radixin and moesin: key regulators of membrane–cortex interactions and signaling. Curr Opin Cell Biol 23:377–382

Nguyen DX, Bos PD, Massagué J (2009) Metastasis: from dissemination to organ-specific colonization. Nat Rev Cancer 9:274–284

Poste G, Nicolson GL (1980) Arrest and metastasis of blood-borne tumor cells are modified by fusion of plasma membrane vesicles from highly metastatic cells. Proc Natl Acad Sci 77:399–403

Ranjan A, Kalraiya RD (2013) α2, 6 Sialylation associated with increased β1, 6-branched N-oligosaccharides influences cellular adhesion and invasion. J Biosci 38:867–876

Ranjan A, Bane SM, Kalraiya RD (2014) Glycosylation of the laminin receptor (α3β1) regulates its association with tetraspanin CD151: impact on cell spreading, motility, degradation and invasion of basement membrane by tumor cells. Exp Cell Res 322:249–264

Reddy B, Kalraiya RD (2006) Sialilated β1, 6 branched N-oligosaccharides modulate adhesion, chemotaxis and motility of melanoma cells: effect on invasion and spontaneous metastasis properties. Biochim Biophys Acta 1760:1393–1402

Saitoh O, Wang W, Lotan R, Fukuda M (1992) Differential glycosylation and cell surface expression of lysosomal membrane glycoproteins in sublines of a human colon cancer exhibiting distinct metastatic potentials. J Biol Chem 267:5700–5711

Sarafian V et al (1998) Expression of Lamp-1 and Lamp-2 and their interactions with galectin-3 in human tumor cells. Int J Cancer 75:105–111

Sawada R, Lowe J, Fukuda M (1993) E-selectin-dependent adhesion efficiency of colonic carcinoma cells is increased by genetic manipulation of their cell surface lysosomal membrane glycoprotein-1 expression levels. J Biol Chem 268:12675–12681

Sehgal L, Budnar S, Bhatt K, Sansare S, Mukhopadhaya A, Kalraiya RD, Dalal SN (2012) Generation of HIV-1 based bi-cistronic lentiviral vectors for stable gene expression and live cell imaging. Indian J Exp Biol 50:669–676

Srinivasan N, Bane SM, Ahire SD, Ingle AD, Kalraiya RD (2009) Poly N-acetyllactosamine substitutions on N-and not O-oligosaccharides or Thomsen-Friedenreich antigen facilitate lung specific metastasis of melanoma cells via galectin-3. Glycoconj J 26:445–456

Tomlinson J, Wang JL, Barsky SH, Lee MC, Bischoff J, Nguyen M (2000) Human colon cancer cells express multiple glycoprotein ligands for E-selectin. Int J Oncol 16:347–353

Valastyan S, Weinberg RA (2011) Tumor metastasis: molecular insights and evolving paradigms. Cell 147:275–292

Weiss L (1990) Metastatic inefficiency. Adv Cancer Res 54:159–211

Weiss L (1992) Comments on hematogenous metastatic patterns in humans as revealed by autopsy. Clin Exp Metastasis 10:191–199

Williams MA, Fukuda M (1990) Accumulation of membrane glycoproteins in lysosomes requires a tyrosine residue at a particular position in the cytoplasmic tail. J Cell Biol 111:955–966